

AD-A268 592



**THE CENTRAL AMERICAN COLD SURGE:
AN OBSERVATIONAL ANALYSIS OF THE DEEP SOUTHWARD
PENETRATION OF NORTH AMERICAN COLD FRONTS**

DTIC
ELECTE
AUG 20 1993
S A D

A Thesis

by

PHILIP JOHN REDING

Submitted to the Office of Graduate Studies of
Texas A&M University ✓
in partial fulfillment of the requirements for the degree of
MASTER OF SCIENCE

This document has been approved
for public release and sale; its
distribution is unlimited.

December 1992

Major Subject: Meteorology

23 8 19 12 3

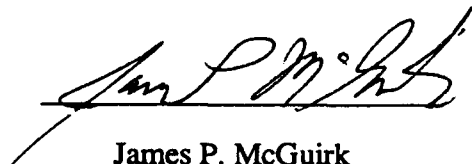
93-19413

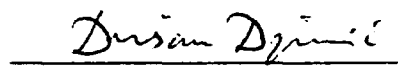
THE CENTRAL AMERICAN COLD SURGE:
AN OBSERVATIONAL ANALYSIS OF THE DEEP SOUTHWARD
PENETRATION OF NORTH AMERICAN COLD FRONTS

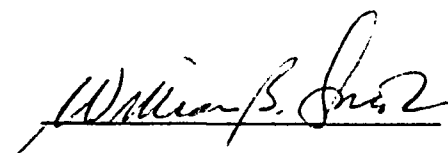
A Thesis
by
PHILIP JOHN REDING

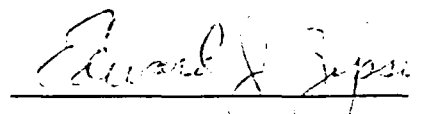
Approved as to style and content by:

Accession For	
NTIS CRA&I	✓
DTIC TAB	✓
Unannounced	✓
Justification	
By	
Distribution /	
Availability Codes	
Dist	Availability Codes Special
A-1	


James P. McGuirk
(Chair of Committee)


Dusan Djuric
(Member)


William B. Smith
(Member)


Edward J. Zipser
(Head of Department)

December 1992

ABSTRACT

**The Central American Cold Surge:
An Observational Analysis of the Deep Southward
Penetration of North American Cold Fronts. (December 1992)**

**Philip John Reding, B.S., Iowa State University
Chair of Advisory Committee: Dr. James P. McGuirk**

The occurrence and structure of the Central American Cold Surge (CACS) is quantified using surface and upper air observations, GOES satellite imagery and satellite estimates of total precipitable water (TPW) and rain rate.

A quantitative CACS definition, similar to established East Asian Cold Surge definitions, is developed and used to construct an eleven winter season climatology of CACS frequency and relative strength. Central America experiences between 11 and 21 CACS events each winter season, with a winter season average of 16 events. GOES imagery is analyzed to quantify the duration and southward penetration of CACS events. Each cold surge typically affects Central America for 3 to 6 days, but may persist for up to 13 days. The mean CACS southward penetration ranges from 12°N to 14°N, while the maximum southward penetration is approximately 7°N. Over 76% of CACS events penetrate south of 15°N and over 26% penetrate south of 10°N.

CACS onset characteristics are described from Belize City, Belize surface observations. A wind shift to the north, sharp rise in sea level pressure and increase in low-level cloud cover are the best cold surge indicators. CACS events contribute from 70% to 90% of the winter season precipitation across Central America. Temporal cross sections of upper air data are constructed to quantify the vertical structural characteristics of the pre- and post-CACS atmosphere. The most common feature is an increase in the

depth of the moist layer after frontal passage. TPW and rain rate are estimated from satellite microwave observations. The temporal and spatial structure of TPW displays distinct and consistent CACS signatures, including a surge of high TPW values into the Gulf of Mexico prior to CACS onset and a narrow band of relative TPW maxima which correspond to the position of the surface front. Minimum TPW values behind the cold surge highlight the region of strongest cold air advection.

Several case studies document the evolution and effects of CACS events as they progress through Central America. Changes in both surface variables and atmospheric vertical structure are evident at every reporting station experiencing CACS passage, indicating that the associated cold front can maintain a temperature and density discontinuity into southern Central America.

DEDICATION

**To my wife, Erika; my parents, James and Rita; and my brothers, Dave and Greg.
Without your support, this project would not have been possible.**

ACKNOWLEDGEMENTS

I acknowledge the members of my committee for their input and guidance. I especially want to express my thanks to the chair of my committee, Dr. James P. McGuirk, for his assistance, understanding, and inspiration. I also thank the scientists of NASA's WETNET program for their assistance in preparing SSM/I data.

I thank the United States Air Force for providing me with the opportunity to continue my education. I also thank my fellow graduate students for their friendship and advise. Special thanks to Mr. Hyo-Sang Chung and Mr. Tom Swanner for their invaluable assistance in creating useable surface and upper air data bases. Special thanks also to Dr. John Nielsen, Mr. Mike Nelson and Dr. (sel) Jeff Tesmer for bringing my upper air data base to life.

Finally, Erika, thank you for tolerating a husband who had to dedicate a lot of time to complete this study.

TABLE OF CONTENTS

	Page
ABSTRACT	iii
DEDICATION	v
ACKNOWLEDGEMENTS.....	vi
TABLE OF CONTENTS	vii
LIST OF TABLES	viii
LIST OF FIGURES	ix
 CHAPTER	
I INTRODUCTION	1
II PREVIOUS WORK	3
III DATA	18
IV OBJECTIVES AND PROCEDURES	22
V CACS CLIMATOLOGY	24
CACS Onset Definition	24
Annual and Monthly Statistics	27
VI CACS STRUCTURE	44
Surface Variables	45
Vertical Structure	55
Moisture Fields	61
VII CASE STUDIES	71
Case 1: 6-12 March 1984.....	72
Case 2: 20-25 November 1987	93
Case 3: 25 January - 2 February 1988	111
Cold Surge Comparison and Evolution.....	148
VIII SUMMARY AND DISCUSSION	158
REFERENCES	162
APPENDIX A	166
VTIA	177

LIST OF TABLES

Table	Page
1. List of North, Central and South American surface and upper air reporting stations	20
2. Annual and monthly CACS events	29
3. CACS event statistics for the 1979-1980 winter season.....	166
4. CACS event statistics for the 1980-1981 winter season.....	167
5. CACS event statistics for the 1981-1982 winter season.....	168
6. CACS event statistics for the 1982-1983 winter season.....	169
7. CACS event statistics for the 1983-1984 winter season.....	170
8. CACS event statistics for the 1984-1985 winter season.....	171
9. CACS event statistics for the 1985-1986 winter season.....	172
10. CACS event statistics for the 1986-1987 winter season.....	173
11. CACS event statistics for the 1987-1988 winter season.....	174
12. CACS event statistics for the 1988-1989 winter season.....	175
13. CACS event statistics for the 1989-1990 winter season.....	176

LIST OF FIGURES

Figure	Page
1. The topography of Central America	4
2. Mean winter 850 mb flow over Central America. After Whiteside (1985)	6
3. Mean annual rainfall (cm) in Central America. After Portig (1976)	7
4. The southern limit of Northers. After Snow (1976)	9
5. Model of the surface streamline (solid) and isotach (dashed) patterns associated with a shear line over a tropical oceanic area. After Palmer et al. (1955)	12
6. ESSA 9 satellite image showing the squall line associated with a Tehuantepecer on February 3, 1970. After Parmenter (1970)	14
7. Schematic movement of the Gulf of Tehuantepec squall line. After Parmenter (1970)	15
8. Number of fronts analyzed by the NMC compared to the number of fronts indicated by Belize surface data from 1 November through 31 March. After Horvath and Henry (1980)	17
9. Map of North, Central and South American reporting stations	19
10. Annual CACS events	30
11. Monthly CACS event frequency.....	30
12. Mean annual CACS temperature change at Merida, Mexico.	32
13. Mean monthly CACS temperature change at Merida, Mexico	32
14. GOES IR satellite image with MB enhancement from 21 February 1989, 1901 UTC.....	34
15. GOES IR satellite image with MB enhancement from 22 February 1989, 1901 UTC.....	35
16. GOES visible satellite image from 23 February 1989, 1731 UTC.....	36
17. GOES visible satellite image from 26 February 1989, 1731 UTC.....	37
18. GOES visible satellite image from 28 February 1989, 1831 UTC.....	38
19. Mean annual CACS event duration.....	40

LIST OF FIGURES (continued)

Figure	Page
20. Mean monthly CACS event duration.....	40
21. Mean annual CACS southward penetration	42
22. Mean monthly CACS southward penetration	42
23. Mean daily maximum and minimum temperatures (°C) during frontal passage at Belize City, Belize.....	47
24. Mean dew point (°C) at 0000 UTC and 1200 UTC during frontal passage at Belize City, Belize.....	47
25. Mean wind direction at 0000 UTC and 1200 UTC during frontal passage at Belize City, Belize.....	49
26. Mean wind speed (m/s) at 0000 UTC and 1800 UTC during frontal passage at Belize City, Belize.....	49
27. Mean sea level pressure (mb) at 0000 UTC and 1500 UTC during frontal passage at Belize City, Belize.....	52
28. Mean daily precipitation (mm) during frontal passage at Belize City, Belize	52
29. Mean cloud ceiling height (m) at 0000 UTC and 1200 UTC during frontal passage at Belize City, Belize.....	54
30. Mean percent frequency of cloud ceiling at 0000 UTC and 1200 UTC during frontal passage at Belize City, Belize.....	54
31. Vertical temporal cross section at Belize City, Belize from 9 November 1987, 0000 UTC to 13 November 1987, 1200 UTC.....	57
32. As in Fig. 31, except from 5 February 1988, 0000 UTC to 9 February 1988, 1200 UTC	59
33. As in Fig. 31, except from 18 November 1987, 0000 UTC to 22 November 1987, 1200 UTC.....	60
34. Total precipitable water (kg/m ²) field on 19 November 1987, 1800 UTC....	62
35. Total precipitable water (kg/m ²) field on 20 November 1987, 0600 UTC....	63
36. Total precipitable water (kg/m ²) field on 22 November 1987, 1800 UTC....	64

LIST OF FIGURES (continued)

Figure	Page
37. Total precipitable water (kg/m^2) field on 24 November 1987, 0600 UTC.....	65
38. Total precipitable water (kg/m^2) field on 26 November 1987, 0600 UTC.....	66
39. Rain rate (mm/h) on 19 November 1987, 0600 UTC.....	69
40. Rain rate (mm/h) on 21 November 1987, 1800 UTC.....	70
41. GOES IR satellite image with MB enhancement from 6 March 1984, 1500 UTC.....	73
42. GOES IR satellite image with MB enhancement from 7 March 1984, 1800 UTC.....	74
43. GOES IR satellite image with MB enhancement from 9 March 1984, 1800 UTC.....	75
44. Daily maximum and minimum temperatures ($^{\circ}\text{C}$) from 1-13 March 1984.....	77
45. Dew point ($^{\circ}\text{C}$) at 0000 UTC and 1200 UTC from 1-13 March 1984	78
46. Wind direction at 0000 UTC and 1200 UTC from 1-13 March 1984.....	79
47. Wind speed (m/s) at 0000 UTC and 1800 UTC from 1-13 March 1984.....	81
48. Sea level pressure (mb) at 0000 UTC and 1500 UTC from 1-13 March 1984	82
49. Cloud ceiling height (m) at 0000 UTC and 1200 UTC from 1-13 March 1984	83
50. Daily precipitation (mm) from 1-13 March 1984	85
51. Vertical temporal cross section at Belize City, Belize from 5 March 1984, 1200 UTC to 9 March 1984, 1200 UTC	86
52. As in Fig. 51, except at Guatemala City, Guatemala from 3 March 1984, 1200 UTC to 12 March 1984, 1200 UTC.....	88
53. Total precipitable water (kg/m^2) field on 3 March 1984.....	89
54. Total precipitable water (kg/m^2) field on 7 March 1984.....	91
55. Total precipitable water (kg/m^2) field on 11 March 1984	92

LIST OF FIGURES (continued)

Figure	Page
56. GOES IR satellite image with MB enhancement from 20 November 1987, 1801 UTC.....	94
57. GOES IR satellite image with MB enhancement from 22 November 1987, 1801 UTC.....	95
58. GOES IR satellite image with MB enhancement from 25 November 1987, 1801 UTC.....	97
59. Daily maximum and minimum temperatures (°C) from 14-26 November 1987.....	98
60. Dew point (°C) at 0000 UTC and 1200 UTC from 14-26 November 1987.	100
61. Wind direction at 0000 UTC and 1200 UTC from 14-26 November 1987.	101
62. Wind speed (m/s) at 0000 UTC and 1800 UTC from 14-26 November 1987.....	102
63. Sea level pressure (mb) or altimeter setting (in) at 0000 UTC and 1500 UTC from 14-26 November 1987.....	103
64. Cloud ceiling height (m) at 0000 UTC and 1200 UTC from 14-26 November 1987.....	105
65. Daily precipitation (mm) from 14-26 November 1987.....	106
66. Vertical temporal cross section at Guatemala City, Guatemala from 16 November 1987, 1200 UTC to 27 November 1987, 1200 UTC.....	108
67. As in Fig. 66, except at Tegucigalpa, Honduras from 17 November 1987, 1200 UTC to 27 November 1987, 1200 UTC.....	109
68. GOES IR satellite image with MB enhancement from 23 January 1988, 1901 UTC.....	112
69. GOES IR satellite image with MB enhancement from 24 January 1988, 1831 UTC.....	113
70. GOES IR satellite image with MB enhancement from 25 January 1988, 1831 UTC.....	114
71. GOES IR satellite image with MB enhancement from 28 January 1988, 1831 UTC.....	116

LIST OF FIGURES (continued)

Figure	Page
72. GOES IR satellite image with MB enhancement from 2 February 1988, 1831 UTC.....	117
73. Daily maximum and minimum temperatures (°C) from 20-31 January 1988.....	118
73. (Continued)	119
74. Dew point (°C) at 0000 UTC and 1200 UTC from 20-31 January 1988	121
74. (Continued)	122
75. Wind direction at 0000 UTC and 1200 UTC from 20-31 January 1988	123
75. (Continued)	124
76. Wind speed (m/s) at 0000 UTC and 1800 UTC from 20-31 January 1988.	125
76. (Continued)	126
77. Sea level pressure (mb) or altimeter setting (in) at 0000 UTC and 1500 UTC from 20-31 January 1988.....	128
77. (Continued)	129
78. Cloud ceiling height (m) at 0000 UTC and 1200 UTC from 20-31 January 1988.....	130
78. (Continued)	131
79. Daily precipitation (mm) from 20-31 January 1988.....	132
79. (Continued)	133
80. Vertical temporal cross section at Belize City, Belize from 23 January 1988, 0000 UTC to 27 January 1988, 0000 UTC	135
81. As in Fig. 80, except at Tegucigalpa, Honduras from 22 January 1988, 1200 UTC to 31 January 1988, 1200 UTC	136
82. As in Fig. 80, except at San Andres, Colombia from 22 January 1988, 1200 UTC to 31 January 1988, 1200 UTC	137

LIST OF FIGURES (continued)

Figure	Page
83. As in Fig. 80, except at San Jose, Costa Rica from 22 January 1988, 1200 UTC to 30 January 1988, 1200 UTC	139
84. Total precipitable water (kg/m^2) field on 22 January 1988, 0600 UTC	140
85. Total precipitable water (kg/m^2) field on 24 January 1988, 0600 UTC	142
86. Total precipitable water (kg/m^2) field on 29 January 1988, 1800 UTC	143
87. Rain rate (mm/h) on 21 January 1988, 0600 UTC	144
88. Rain rate (mm/h) on 28 January 1988, 1800 UTC	145
89. Rain rate (mm/h) on 30 January 1988, 0600 UTC	147
90. The Central American Cold Surge: Phase 1	151
91. The Central American Cold Surge: Phase 2	153
92. The Central American Cold Surge: Phase 3	154
93. The Central American Cold Surge: Phase 4	156

CHAPTER I

INTRODUCTION

Mid-latitude cold fronts can, and do penetrate into various regions of the global tropics. DiMego (1976) identified such events as one of the clearest examples of mid-latitude/tropical interaction. So far, most research efforts concerning intrusions of mid-latitude air into the tropics have focused on the Eastern Hemisphere, the most notable of which pertain to the East-Asian Cold Surge (EACS). In contrast, only limited attention has been paid to such events in the Western Hemisphere, specifically over Central America. Furthermore, the research that has been conducted on cold frontal intrusions into Central America has revealed many discrepancies in terms of frequency of occurrence, intensity and meridional range.

Regardless of the conflicting research results, incursions of North American polar air masses into the tropics occur with sufficient frequency to have been given regional names throughout Central America, "Nortes" (Northers) being the most common. Other colloquialisms include "Tehuantepecer" in southern Mexico (Parmenter, 1970), "Atemporalado" in Honduras (Brooks, 1987), and "Invierno de las Chicharras" (Winter of the Cicadas) in northern Venezuela (Snow, 1976). Some questions remain concerning whether these events are actually North American cold fronts which have maintained their identity well into the tropics, or if they are only shear lines associated with the remnants of old frontal boundaries that have lost their density discontinuity (Palmer et al., 1955). For purposes of clarity and in an effort to describe this phenomenon more accurately, this study will refer to all such events as the Central American Cold Surge (CACS).

The style is that of the *Monthly Weather Review*.

The intensity of CACS events is often reflected in the degree of associated weather. While many cold surge air masses are rapidly modified by the warm underlying waters of the Gulf of Mexico and Caribbean Sea, others may maintain their strength throughout Central America and even into northern South America. Portig (1958) recorded 93 kt wind gusts at 1700 m elevation in Central America during a "frontal passage". Guard (1986) reported wind gusts exceeding 60 kt throughout the mountains of Guatemala, Honduras and Nicaragua. An even more intense CACS event in 1970 released over 1100 mm of rain in twelve days along the northern coast of Venezuela, causing devastating property damage and loss of life (Henry, 1979). The potentially severe weather associated with CACS events alone warrants the conduct of further research.

The aim of this study is to quantify the occurrence and structure of cold surge events in Central America. Surface observations and GOES satellite imagery are reviewed to determine frequency, duration, meridional range, and relative strength of CACS events. Surface and upper air data, along with satellite brightness temperature data are analyzed to quantify cold surge structure. Several case studies are then reviewed to document the evolution of CACS events and help illustrate the life cycle of synoptic features associated with the CACS.

Chapter II contains a review of previous work describing the current understanding of cold frontal intrusions into the American tropics. Chapter III details the data sets used in this study. The objectives and general procedures of this research are outlined in Chapter IV. Chapter V presents a climatology of CACS events. CACS structure is described in Chapter VI, and several case studies are presented in Chapter VII. Finally, a summary and discussion are contained in Chapter VIII.

CHAPTER II

PREVIOUS WORK

Early studies by Chapel (1927) and Hurd (1929) on the effects of mid-latitude polar air mass incursions into the tropics focused primarily on the importance of associated wind direction and speed changes. Hastenrath (1967) helped validate the significance of these early research efforts by emphasizing that rainfall over Central America is largely controlled by the orientation of mountain ranges and configuration of coast lines relative to the seasonal flow patterns. With topography and wind flow patterns established as two of the most important controls in Central American weather, it is useful to understand them and their interaction before comprehending the effects of cold surges on Central American weather.

The topography of Central America can best be described as a series of meridionally oriented mountain ranges separated by valleys, with the Sierra Madres extending nearly uninterrupted from northern Mexico to western Panama (Fig. 1). The only major exceptions are the lowlands of the Yucatan peninsula, Belize and northern Guatemala, and the coastal plains of eastern Nicaragua. Together with the Rocky Mountains, the Sierra Madre chain forms a wall, or western boundary, stretching from nearly 70°N to 10°N. Atkinson (1971) and Hastenrath (1988) agree that this topography both provides a good setting for the generation of vast pools of cold air over North America and assists in the equatorward penetration of North American cold fronts.

The winter months, when cold surges are most likely to affect the tropics, are Central America's dry season, typically lasting from December through April. Pearson et al. (1987) described and contrasted the seasonal flow patterns and resulting cloud distributions over Central America. During the dry season, Central America is

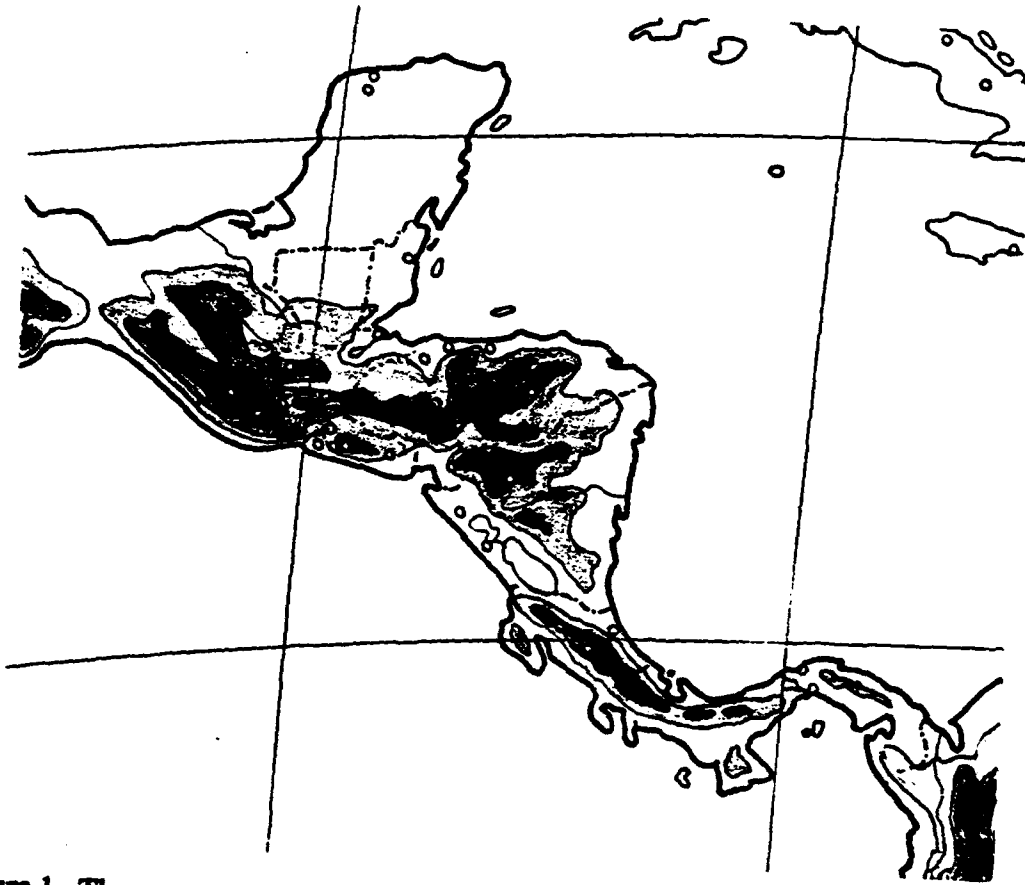


Figure 1. The topography of Central America. Light shading indicates elevations from 1000-2000 m, medium shading from 2000-3000 m and dark shading above 3000 m.

dominated by northeast tradewinds of the Atlantic subtropical high (Fig. 2). Cloud cover remains primarily scattered through the season, especially on the lee side of the mountains. Broken cloud cover and isolated rainshowers develop only occasionally along the windward mountain slopes during the afternoon. However, dry season weather is highly dependent on the strength of the tradewinds. Weak wind flow patterns generally result in scattered clouds evenly distributed across the Isthmus. Stronger winds tend to enhance cloud cover over windward mountain slopes and inhibit cloud formation on the lee side. Although cloud cover may be enhanced, the shear associated with stronger wind flow patterns tends to inhibit afternoon rainshower development. Whiteside (1985) added that the trade wind inversion is an important factor in Central America's dry season. The inversion is often strong enough to act as a cap on convection, preventing the development of rainshowers and thunderstorms which are normally common to the American tropics.

The typical dry season flow pattern and associated weather are seriously disrupted with the onset of a CACS. Hastenrath (1967) hypothesized that the polar air mass behind the surface front is strongly modified by latent and sensible heat fluxes while crossing the Gulf of Mexico and Caribbean Sea. Interaction between the invading air mass, the north-northwesterly flow behind the surface front and the Central American topography often results in dense low-level cloud cover and persistent stratiform precipitation. Hastenrath estimated that 40-60% of the annual precipitation along the northern Honduras coast falls during what is the "dry" season for the rest of Central America. Note the winter maximum in mean annual rainfall at stations 21 and 22 along the northern Honduras coast in Fig. 3. Most of this rainfall and cloud cover is a result of the CACS. In contrast, downslope winds create nearly clear skies and dryer than normal conditions during CACS episodes on the Pacific side of the Central American

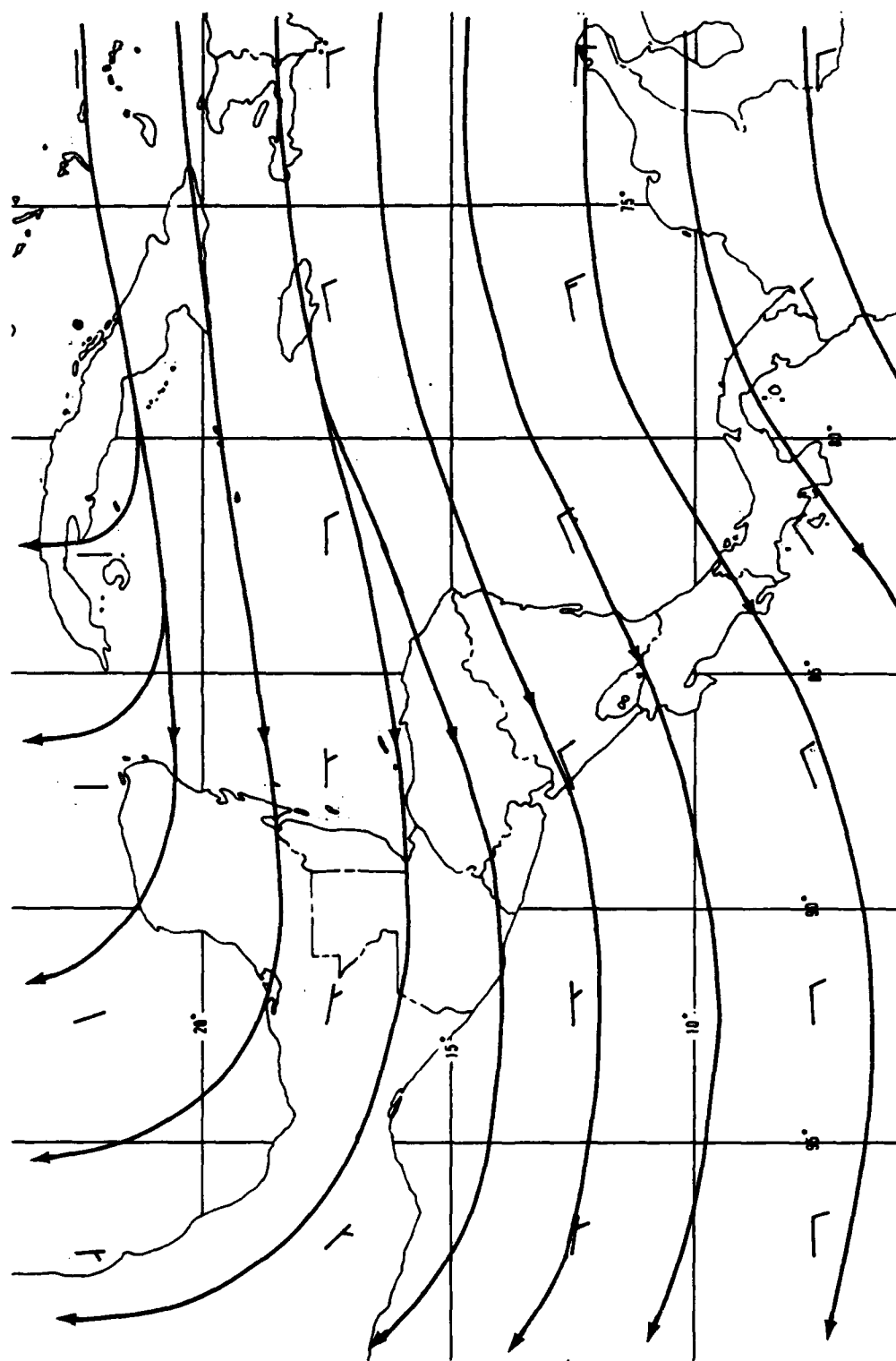


Figure 2. Mean winter 850 mb flow over Central America. After Whiteside (1985).

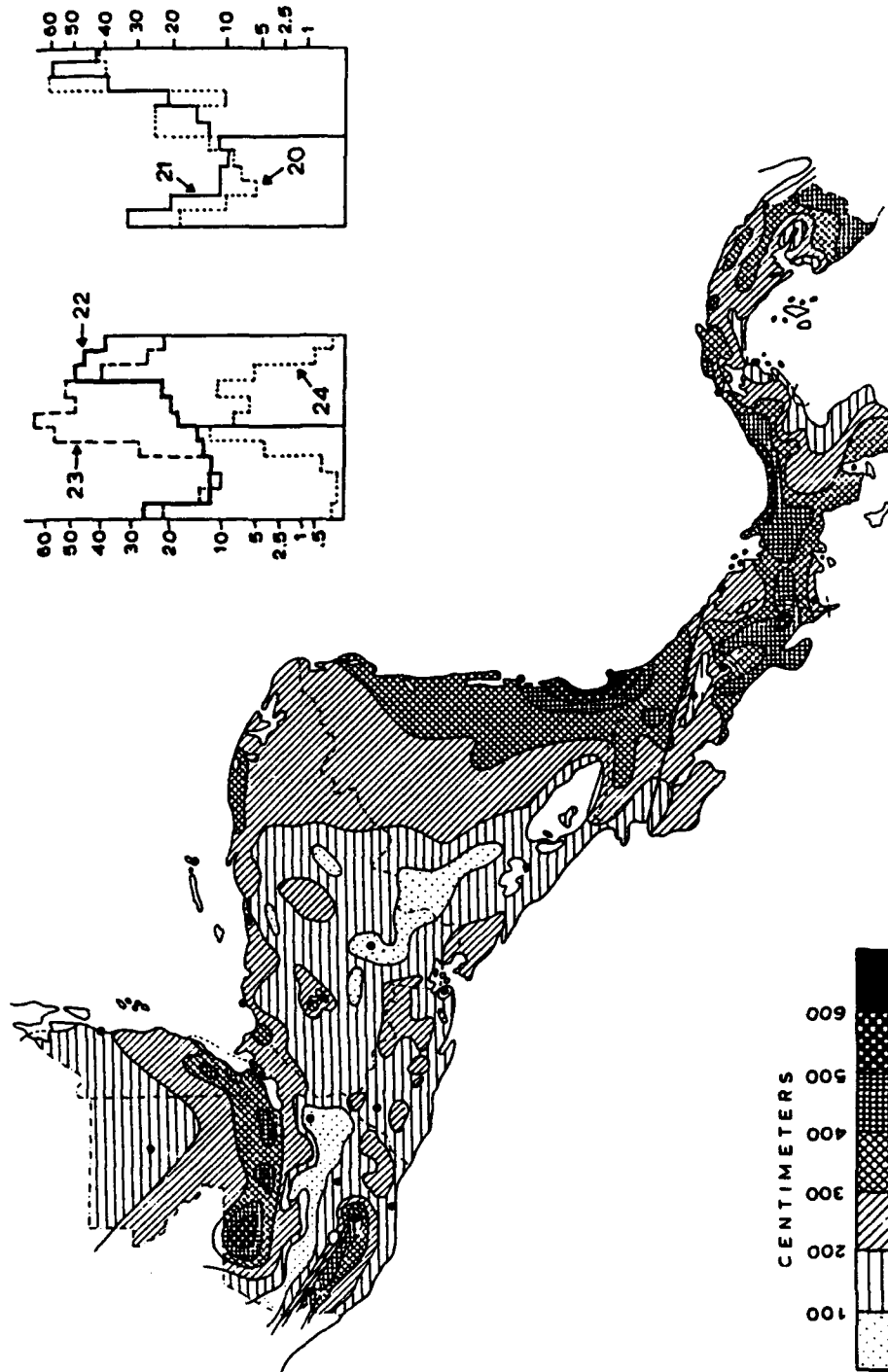


Figure 3. Mean annual rainfall (cm) in Central America. After Portig (1976).

Isthmus. Again, interaction between topography and the prevailing wind flow pattern determines the resulting weather.

Estimates of the frequency and maximum equatorward penetration of the CACS are extremely varied and strongly dependent on the research methods employed. In early studies of cold fronts in Central America, frequency estimates were ambiguous, simply ranging from rare to common. Maximum equatorward penetration estimates were more specific, but just as varied, ranging from central Nicaragua (Portig, 1976; Snow, 1976), to central Panama and northern Venezuela (Garbel, 1947) (see Fig. 4). Recently, Pearson et al. (1987) attempted to be more specific about CACS frequency, estimating an annual average of 12 occurrences between October and May, with a range from 6 to 18.

Schumann and van Rooy (1951) were among the first to present statistics on the frequency of fronts throughout the Northern Hemisphere. Schumann and van Rooy counted the number of fronts analyzed on daily synoptic surface maps in $5^{\circ} \times 5^{\circ}$ squares, allowing the frequency to depend both on the number of individual fronts and the velocity of the fronts. The most significant result, for the purposes of this study, was that the frequency of fronts in the tropics was greatest over Southeast Asia, and second greatest over Central America. Hill (1969) produced results similar to those of Schumann and van Rooy (1951) in his study of cold fronts in Mexico.

DiMego et al. (1976) produced maps of mean monthly frequency and duration of frontal incursions into the Gulf of Mexico and Caribbean Sea using methods similar to those of Schumann and van Rooy (1951). They discovered frequency maxima in the western Gulf of Mexico and over eastern Florida, with a sharp increase in frequency from September to October and a more gradual decrease in frequency during the spring. The frequency maximum over the western Gulf of Mexico corresponds to cold fronts

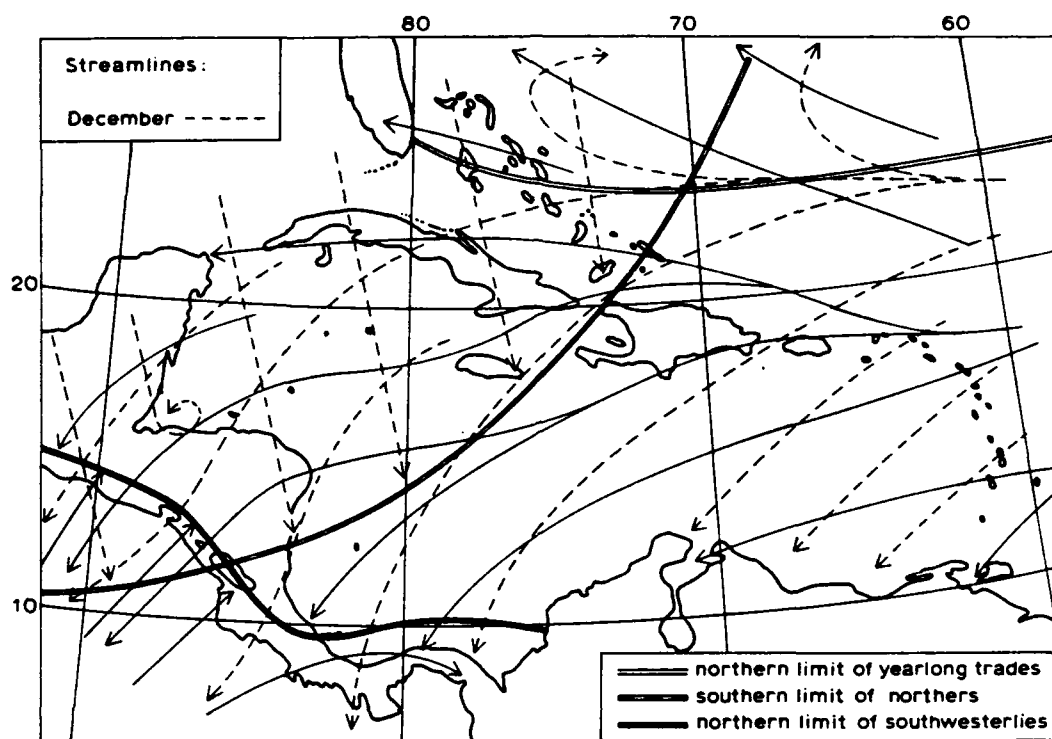


Figure 4. The southern limit of Northers. After Snow (1976).

which affect Central America. The duration maximum stretched from the Yucatan peninsula to the central Gulf of Mexico. Conditions prior to frontal passage over the Gulf of Mexico include veering wind, rising temperature, falling pressure, increasing humidity, decreasing stability, and a lifting and weakening of the trade wind inversion. All of these trends reverse abruptly after frontal passage. DiMego et al. added that the frequency and equatorward penetration of cold fronts over the Gulf of Mexico is directly related to topographic features, and the position, strength and amplitude of the middle latitude circulation.

Henry (1979) applied a different technique in determining the frequency of cold fronts in the Gulf of Mexico, following individual fronts themselves rather than using latitude-longitude squares. He also extended his analysis into Central America. Maximum frontal frequency occurred from December through March, but fronts may affect the Gulf any month of the year. Fronts may move into the Gulf of Mexico from the North American continent or from the Pacific. Although Pacific fronts were more common, North American fronts were more likely to penetrate southward into Central America. Of the fronts studied, 25% penetrated south of 15°N, with Honduras and Nicaragua experiencing about one frontal passage each month of the winter season. Only 5% of the fronts were tracked south of 10°N and all of these occurred between December and March.

Determination of accurate frontal passage indicators is a serious consideration in the analysis of frontal frequency over the Gulf of Mexico and Central America. Air mass modification can make standard temperature differential analysis difficult, if not impossible, leading to underestimates of frontal frequency and southward penetration. Other methods of analysis incorporating surface wind fields (Brooks, 1987) and satellite imagery (Atkinson, 1971) have proven beneficial. In one case, Anderson and Smith

(1969) tracked a cold front into northern Venezuela, two days after it had been dropped from the NMC analysis.

With the significant modification of polar air masses over the Gulf of Mexico and Caribbean, it is important to consider the concept of shear lines as a mechanism for deep "frontal" penetration into Central America. The *Glossary of Meteorology*, (Huschke, 1959), defines a shear line as "a line or narrow zone across which there is an abrupt change in the horizontal wind component parallel to this line; a line of maximum horizontal wind shear." Atkinson (1971) added that shear lines can be associated with the remnants of old frontal zones that have lost their temperature contrast in the barotropic environment of the tropics. Palmer et al. (1955) applied the above definitions to the case of a cold front moving into the tropics and developed a conceptual shear line model (Fig. 5). The model depicts a cold front in the surface streamline and isotach field extending northeast to southwest into a col, or saddle point, of the stream line pattern. The axis of dilatation extending southwest of the col is what Palmer et al. defined as a shear line. According to this model, the cold air mass behind the surface front is modified by the warm ocean surface and subsidence aloft. Eventually, the density discontinuity dissolves leaving a line of cyclonic shear. This shear line may persist for several days and continue to move equatorward.

Few references to shear lines are available in the standard literature sources. However, United States Air Force documents concerning tropical meteorology (Brooks, 1987 and Pearson et al., 1987) focus on shear lines as a major weather producer, generating low stratiform ceilings, continuous precipitation and strong northerly winds. Atkinson (1971) proposed that some shear lines are able to maintain a temperature discontinuity because of repeated nocturnal radiational cooling in the relatively dry air mass behind the shear line. Atkinson also noted that shear lines are easy to recognize on

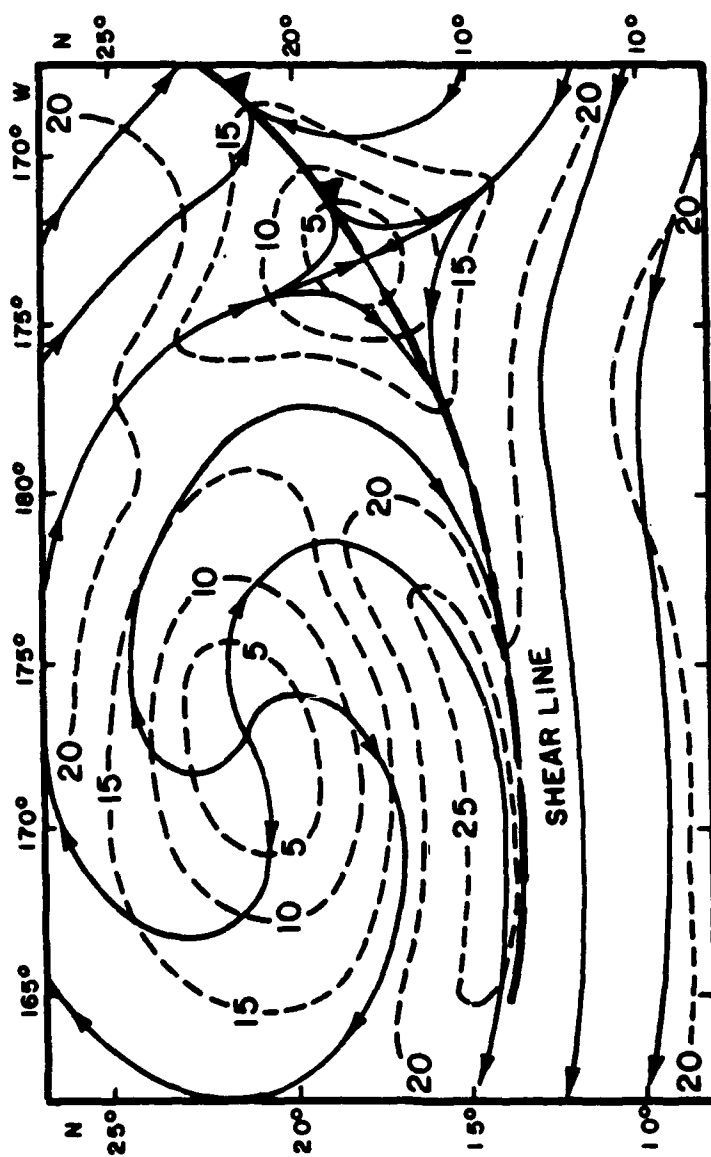


Figure 5. Model of the surface streamline (solid) and isotach (dashed) patterns associated with a shear line over a tropical oceanic area. After Palmer et al. (1955).

satellite imagery, an important point when considering the problems involved in conventional analysis of such features.

Several research efforts have been directed toward the effects of frontal passage in specific countries or areas. Hill (1969) studied the temperature variability associated with frontal passage in Mexico, Fermor (1971) analyzed frontal passage in Jamaica, DiMego (1976) concentrated on the Gulf of Mexico and Caribbean Sea, while Brooks (1987) and Ladd and Henry (1980) studied the "Atemporalado" in Honduras.

Hurd (1929) and Parmenter (1970) studied a phenomenon in southern Mexico known as the "Tehuantepecer". The Gulf of Tehuantepec is located on the Pacific coast of southern Mexico near 95°W. The area immediately north of the Gulf is the narrowest portion of the Mexican Isthmus and has some of the lowest elevations (1000-2000 ft) in the Sierra Madre chain. In effect, a natural spillway is formed. During strong cold surges, the polar air mass overflows across this spillway and rushes down the lee side of the mountains into the Gulf of Tehuantepec. Winds of 45-65 kt are characteristic both through the pass and over the Gulf. The effects normally last only a few hours, but can persist for several days. Parmenter captured this event on satellite imagery (Figs. 6 and 7). The result is a semi-circular squall line which may propagate into the Pacific for several hundred miles, followed by rapidly clearing skies, gusty northeast wind and falling temperature.

Horvath and Henry (1980) studied the effects of cold fronts in Belize. They determined that the best indicators of frontal passage were a wind shift to the north or northwest, an increase in wind speed, a decrease in equivalent temperature, and the onset of precipitation. Pre-frontal trends included fog, drizzle, rainshowers, haze and a gradual pressure rise. Horvath and Henry relied on NMC Northern Hemispheric surface analyses to grasp the synoptic situation during each event, but performed their

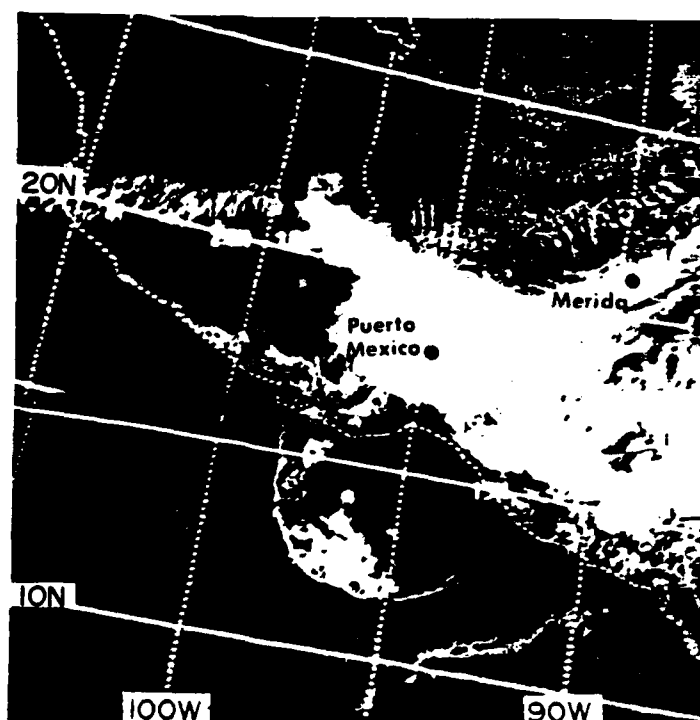


Figure 6. ESSA 9 satellite image showing the squall line associated with a Tehuantepecer on February 3, 1970. After Parmenter (1970).

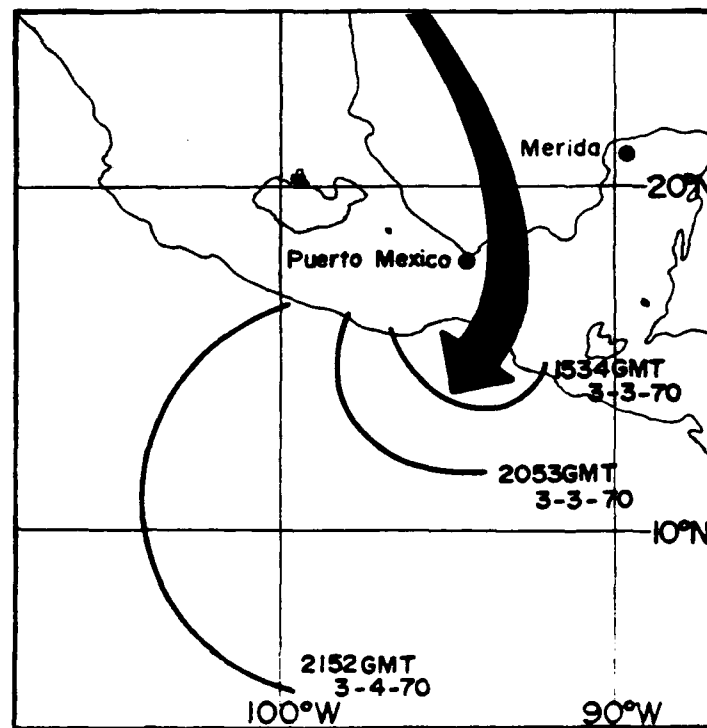


Figure 7. Schematic movement of the Gulf of Tehuantepec squall line. After Parmenter (1970).

own analyses for each event using Belize City surface observations. They discovered that nearly twice as many fronts passed through Belize as were indicated on the NMC analyses (Fig. 8). Apparently, the 1000-500 mb thickness gradient associated with the missed fronts was not strong enough to meet the NMC frontal criteria. This again raises questions concerning the proper definition of a front. Regardless if the weather systems missed by the NMC analyses were "fronts" or "shear lines", Horvath and Henry concluded that they do produce significant weather, and that they can be analyzed and forecast.

The preceding discussion illustrates that the CACS is a significant atmospheric event with potentially destructive consequences. The most comprehensive research efforts to date have been limited to individual Central American countries or have been confined to the Gulf of Mexico and Caribbean Sea. Other studies have produced only qualitative, or even conflicting results. Furthermore, detailed studies have relied almost exclusively on pre-analyzed surface maps as a data source. In effect, these studies have attempted to identify strongly modified frontal systems in the tropics by using criteria associated with mid-latitude synoptic scale cold fronts. This procedure tends to underestimate cold surge frequency, duration and extent. The purpose of this research is to expand the understanding of cold frontal intrusions into Central America by incorporating previously unexploited data sources into a quantitative analysis of CACS events spanning the entire Central American Isthmus.

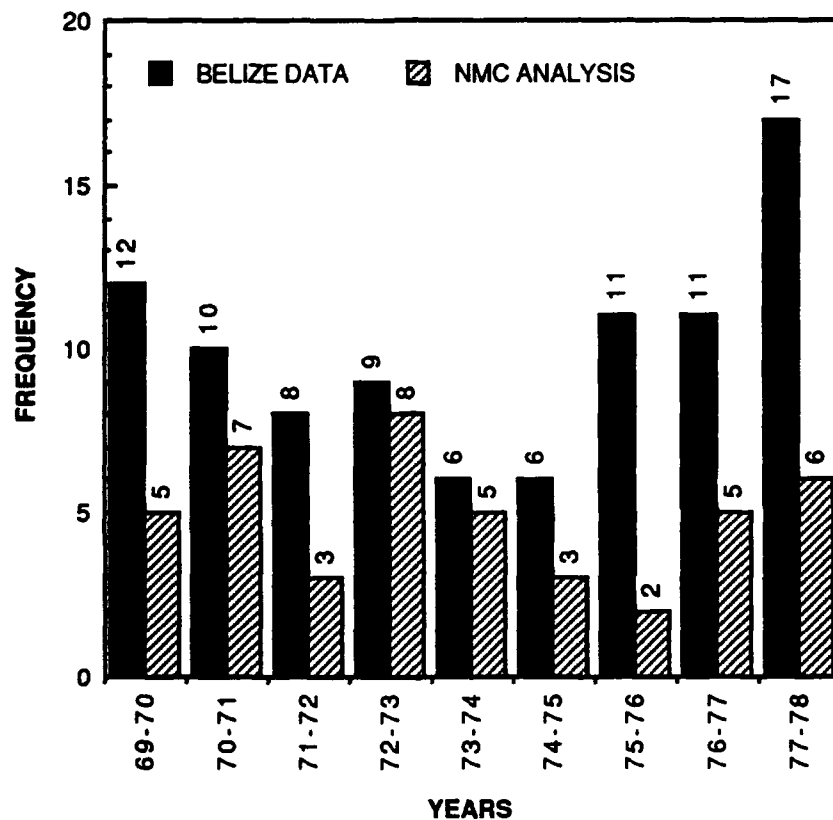


Figure 8. Number of fronts analyzed by the NMC compared to the number of fronts indicated by Belize surface data from 1 November through 31 March. After Horvath and Henry (1980).

CHAPTER III

DATA

Numerous data sources have been enlisted for this study because of the typical unavailability and/or unreliability of meteorological data in the Central American region.

The primary data set consists of hourly surface observations from sixteen North, Central and South American reporting stations, and 12-hourly upper air observations from seven Central American reporting stations. Locations and details of each station are given in Fig. 9 and Table 1. This data set spans October through March of eleven winter seasons from 1979 through 1990. The data are archived by the United States Air Force Environmental Technical Applications Center (USAFETAC), Scott Air Force Base, Illinois.

The surface data set consists of blocked variable length records in an 8-bit ASCII character format known as DATSAVII. The upper air data set consists of blocked variable length records in an 8-bit binary format known as DATSAV. The upper air data set has been converted to ASCII character format to facilitate data processing.

Another data set consists of satellite derived rain rate and total precipitable water (TPW) estimates available through NASA's WetNet program. WetNet is a NASA pilot program devoted to examining the role of a remote interactive computer network in an earth science research environment. The primary data source for the WetNet project is the Special Sensor Microwave / Imager (SSM/I) on board the polar orbiting Defense Meteorological Satellite Program (DMSP) F8 and F10 satellites. NASA's Marshall Space Flight Center disseminates derived SSM/I products, including rain rate and TPW, from pre-processed SSM/I brightness temperature data. Rain rate is estimated in mm/h, and TPW in kg/m^2 . Algorithms are detailed in the WetNet software. The primary

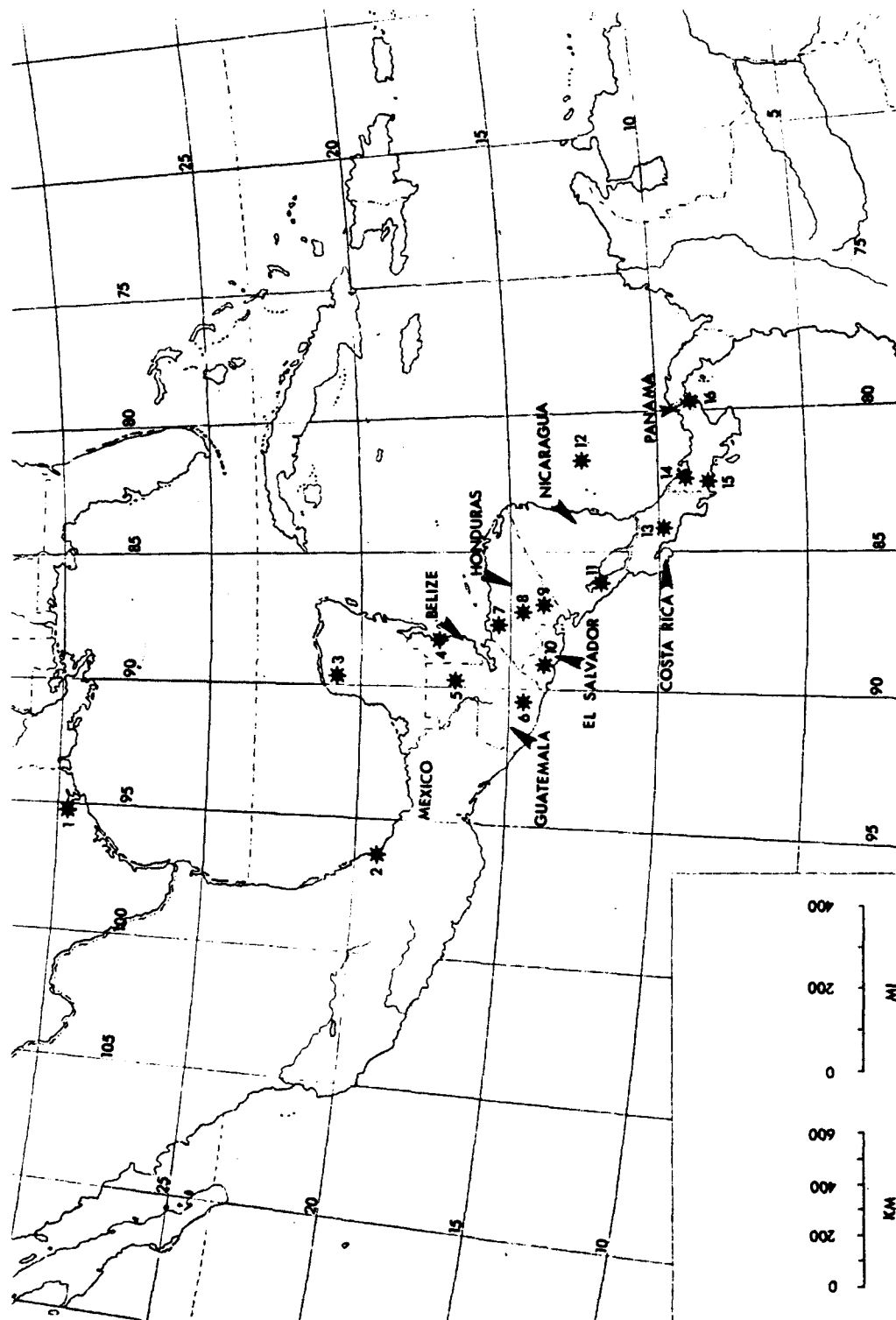


Figure 9. Map of North, Central and South American reporting stations.

Table 1. List of North, Central and South American surface and upper air reporting stations.

<u>STATION</u>	<u>LOCATION</u>	<u>ELEVATION</u>	<u>ICAO</u>	<u>WMO</u>
1. Houston, Texas	29°58'N 95°21'W	33m	KHOU	72243
2. Veracruz, Mexico	19°12'N 96°08'W	14m	MMVR	76691
3. Merida, Mexico	20°59'N 89°39'W	9m	MMMD	76644
4. Belize City, Belize	17°32'N 88°18'N	5m	MZBZ	78583 *
5. Flores, Guatemala	16°55'N 89°53'W	115m	MGFL	78615
6. Guatemala City, Guatemala	14°35'N 90°31'W	1489m	MGGT	78641 *
7. La Mesa, Honduras	15°27'N 87°56'W	31m	MHLM	78708
8. Soto Cano AB, Honduras	14°23'N 87°37'W	626m	KQIZ	78718
9. Tegucigalpa, Honduras	14°03'N 87°13'W	1007m	MHTG	78720 *
10. San Salvador, El Salvador	13°42'N 89°07'W	621m	MSSS	78663
11. Managua, Nicaragua	12°09'N 86°10'W	56m	MNMG	78741 *
12. San Andres, Colombia	12°35'N 81°43'W	6m	SKSP	80001 *
13. San Jose, Costa Rica	10°00'N 84°13'W	939m	MROC	78762 *
14. Bocas del Toro, Panama	09°15'N 82°30'W	9m	MPBO	N/A
15. David, Panama	08°24'N 82°25'W	26m	MPDA	78793
16. Howard AFB, Panama	08°55'N 79°36'W	13m	MPHO	78806 *

* RAOB reporting stations

means of data set distribution is via magneto-optical disk. The available data set is limited to October 1987 through July 1988.

TPW has also been estimated from Nimbus-7 Scanning Multi-channel Microwave Radiometer (SMMR) observations for January through March of the 1983-1984 winter season. The data domain extends from 5°S to 35°N latitude and 60°W to 110°W longitude. TPW estimates were made from 18 GHz and 21 GHz horizontally and vertically polarized channel brightness temperatures at a 60 km resolution, processed through an algorithm developed by Wilheit and Chang (1980). Details of the processing scheme are outlined by Fink (1989).

Additional data sources utilized in this study include Geostationary Operational Environmental Satellite (GOES) visible and infrared (IR) imagery, available both in hardcopy form and on the WetNet system, National Meteorological Center (NMC) Northern Hemispheric surface analyses, National Hurricane Center (NHC) tropical surface analyses, and NHC Analysis of Tropical Ocean Lower Level (ATOLL) maps.

CHAPTER IV

OBJECTIVES AND PROCEDURES

The overall goal of this research is to incorporate previously unexploited data sources into a quantitative analysis of CACS occurrence and structure spanning the entire Central American Isthmus. Three objectives have been developed to accomplish this goal. The first objective is to define and determine the frequency, duration and meridional extent of Central American Cold Surge events. The second objective is to identify and quantify the horizontal, vertical and temporal structural characteristics of cold frontal intrusions into Central America. The final objective is to document the evolution and effects of cold surge events as they propagate through Central America.

These objectives are accomplished by completing approximately nine well defined tasks.

Tasks required to accomplish the first objective include:

1. Identify periods of cold frontal activity in Central America during the 1983-1984 and 1987-1988 winter seasons through an analysis of low-level cloud features on visible and IR GOES imagery and a review of corresponding NMC/NHC surface analyses.
2. Construct a quantitative definition of CACS onset similar to definitions established for the EACS (Boyle and Chen, 1987). The definition is developed through an analysis of changes in surface variables at Merida, Mexico (20° 59'N, 89° 39'W) during the identified periods of cold frontal activity.
3. Prepare a climatology of CACS event frequency during the winter months of October 1979 through March 1990 based on the CACS onset definition. The duration and meridional extent of each identified CACS event will be determined through an analysis of low-level cloud patterns using visible and infrared GOES imagery.

Tasks required to accomplish the second objective include:

4. Isolate and quantify key surface elements associated with CACS onset at a single Central American reporting station (Belize City, Belize) ($17^{\circ} 32'N$, $88^{\circ} 18'W$). Variables to be considered include temperature, dew point, wind direction and speed, sea level pressure, low-level cloud cover and precipitation. The mean changes of each variable are computed to quantify their evolution in response to the CACS and identify those most sensitive to CACS onset.

5. Isolate and quantify the vertical structural characteristics of the pre- and post-CACS atmosphere using Belize City upper air observations. Construct temporal cross sections to evaluate stability, strength and height of both the trade wind and frontal inversions, depth of the frontal layer and evolution of the wind field.

6. Estimate total precipitable water, rain rates and their associated structure during CACS events using SMMR (1983-1984) and SSM/I (1987-1988) data sets. Identify patterns in each field typical during CACS events.

Tasks required to accomplish the third objective include:

7. Select several typical and extreme CACS events from the 1983-1984 and 1987-1988 time frames for in-depth case studies.

8. Describe the evolution of typical CACS surface variables, vertical structural characteristics, rain rate and TPW patterns, and satellite cloud signatures for each event as the cold surge propagates through Central America.

9. Based on the identified characteristics, patterns and climatology, illustrate the life cycle of a typical CACS event.

CHAPTER V

CACS CLIMATOLOGY

Previous studies have established that North American cold fronts can penetrate well into the American tropics. Several important results of these studies must be emphasized with respect to the present research effort. A fundamental conclusion is that existing mid-latitude frontal criteria seldom accurately identify fronts in the tropics (Horvath and Henry, 1980). Furthermore, cold fronts can be easily and often more accurately analyzed in the tropics using existing alternative data sources such as raw surface observations (Horvath and Henry, 1980), surface wind field analysis (Brooks, 1987) or satellite imagery (Anderson and Smith, 1969; Atkinson, 1971). This section of the study attempts to develop new criteria, which more accurately identify frontal and shear line (cold surge) activity in the tropics, based on the data sources which have been proven to be more reliable than standard surface analyses.

CACS ONSET DEFINITION

Several lists of criteria have already been proposed to define the East Asian Cold Surge (EACS), a phenomenon similar to the CACS. Most of the EACS definitions make use of changes in surface variables, such as temperature drop, wind shift or pressure gradient, at a single or pair of reporting stations during a specified time frame. This study proposes a CACS definition modeled after the established EACS definitions.

Merida, Mexico was selected as the location to define CACS onset. Merida is located on the northwest tip of the Yucatan Peninsula and therefore is one of the first stations to experience cold surge effects after the cold front crosses the Gulf of Mexico.

The lowest level of cold air behind the surface front is subject to air mass modification only from the Gulf of Mexico and will retain a greater portion of its original air mass characteristics at Merida than at more southerly reporting stations. As a result, changes in surface variables associated with CACS onset are expected to be more prominent at Merida than at more southerly stations with similar elevations. This hypothesis assumes that no frontogenesis occurs south of Merida, as this may re-intensify some CACS signatures.

The initial step was to identify periods of cold surge activity in Central America. This was accomplished through an analysis of frontally related and low-level cloud features on visible and IR GOES imagery during the 1983-1984 and 1987-1988 winter seasons. Cold fronts were initially identified over the southern United States using NMC Northern Hemispheric surface analyses. The corresponding cloud features were then tracked across the Gulf of Mexico and into Central America using hourly satellite imagery. Forty nine potential cold surges were identified. Approximate time frames for frontal passage at Merida, Mexico were recorded for each identified case during the two sample winter seasons. If satellite imagery was inconclusive due to high-level cloud cover or missing data, frontal placement on NHC tropical surface analyses and ATOLL streamline analyses were used to aid in frontal identification and placement. It is important to note that satellite imagery was the primary data source in this step. Pre-analyzed surface maps were used only to confirm the satellite analysis.

Hourly surface observations from Merida were reviewed during each of the potential cold surge time frames identified in the satellite analysis, with the initial hypothesis that temperature, pressure and wind direction and speed would display the most distinct changes during frontal passage. Daily temperature maxima and minima were analyzed separately in order to avoid contamination of the frontal temperature drop by the diurnal

temperature variations. Of the potential CACS events identified, 40 / 49, nearly 82% displayed at least a 4°C drop in daily maximum temperature within 48 h after frontal passage. A temperature change could not be established in two of the ten cases in question because of missing data. These cases were dropped from consideration. Another case occurred at Merida less than 48 h after a previous cold surge, thereby suppressing the temperature change. These two cases were counted as one cold surge event. The remaining seven cases were reanalyzed using the original satellite imagery. In each case, the cold front became stationary over the northern Yucatan Peninsula and either dissipated or returned north into the Gulf of Mexico as a warm front. These cases were not applicable to the current study because the cold fronts did not penetrate into Central America and were dropped from the analysis. In effect, 39 / 40, or nearly 98% of the remaining potential CACS events identified by satellite displayed at least a 4°C drop in daily maximum temperature within 48 h after frontal passage. The entire surface data set for the 1983-1984 and 1987-1988 winter seasons was then reviewed to identify additional temperature change events. No cases were found where the daily maximum temperature dropped 4°C within a 48 h period except during the CACS cases already identified by satellite.

Easterly surface winds dominate Merida during the dry season. The afternoon sea breeze may shift the wind to northerly, but the sea breeze is generally active only between the hours of 1700 UTC and 0400 UTC, and occurs only during periods of weak low-level trade winds. A review of Merida surface observations revealed that cold surge induced northerly flow was quite distinct from sea breeze induced northerly flow because of its duration. Surface winds from 300° to 030° were sustained for more than 24 h after frontal passage during all of the identified CACS events. In addition, many of

the cold surge events were marked by a shift to southerly or southeasterly flow at Merida prior to frontal passage.

Sea Level Pressure (SLP) at Merida generally increased 4-6 mb following frontal passage. A slow pressure rise usually accompanied the cold surge event prior to frontal passage, partially obscuring a distinct jump. The other surface variables investigated, including daily minimum temperature, dew point, wind speed, cloud cover and precipitation, displayed identifiable trends during CACS events, but the trends were not nearly as distinct or consistent as those displayed by daily maximum temperature and wind direction.

Based on the above analysis of satellite imagery and surface data, CACS onset is defined in this study by the following criteria:

- a) A decrease in daily maximum temperature greater than or equal to 4°C within 48 h at Merida, Mexico.
- b) Northerly winds (300° - 030°) sustained for more than 24 h during the same period.

ANNUAL AND MONTHLY STATISTICS

The CACS definition was applied to the entire eleven winter season surface data set to identify the onset of each cold surge event and determine the magnitude of the cold surge induced temperature change. If the temperature change could not be determined because of missing data, the event was not included in the analysis. If the magnitude of the temperature change was greater than or equal to 4°C, but the 48 h time criteria could not be confirmed because of missing data, the event was included in the analysis and the temperature change was recorded as unknown. No cases were encountered where only one of the two CACS onset criteria was met. The duration and maximum southern

penetration of each event was determined through an analysis of low-level cloud features on GOES visible and IR imagery. The details of this analysis method are discussed later in this chapter. The onset date, duration, maximum southern penetration and 48 h temperature change of each event are listed by winter season in Appendix A.

Frequency

A summary of the number of annual and monthly CACS events is presented in Table 2. A total of 177 events were identified during the eleven winter seasons, yielding an average annual CACS frequency of 16. Annual frequency ranged from a minimum of 11 during the 1988-1989 winter season to a maximum of 21 during 1982-1983 (Fig. 10). These figures are probably slight underestimates because of the problems with missing surface data at Merida, but the frequencies are still 25% higher than those estimated by Pearson et al. (1987). One of the most interesting features of Fig. 10 is the relative peaks in CACS frequency during the 1982-1983 / 1983-1984 and 1986-1987 / 1987-1988 winter seasons. The peaks roughly correspond to both warm and cold phases of El Nino, however, no inferences about the possible relationship between these two phenomena is attempted in this study.

Mean, minimum and maximum monthly CACS frequencies are displayed in Fig. 11. Maximum and minimum values (range) were chosen as a measure of variability in this chapter instead of standard deviation because they are more standard climatological parameters. The minimum frequency found was 0 events/month in October 1985 and the maximum was 6 events/month in January 1987, February 1983 and March 1983. Mean monthly frequencies increased gradually from a minimum of just over 1 event/month in October to a maximum of well over 3 events/month in January. These figures are slightly higher than, but quite similar to the results of DiMego et al. (1976).

Table 2. Annual and monthly CACS events.

YEAR	OCT	NOV	DEC	JAN	FEB	MAR	TOTAL
79-80	1	3	3	3	4	1	15
80-81	1	3	3	4	3	3	17
81-82	1	3	3	3	3	1	14
82-83	1	1	2	5	6	6	21
83-84	2	3	5	3	4	3	20
84-85	1	3	1	2	3	2	12
85-86	0	1	4	4	2	2	13
86-87	2	1	5	6	2	4	20
87-88	2	3	3	4	4	3	19
88-89	1	2	3	1	2	2	11
89-90	1	2	4	3	3	2	15
TOTAL	13	25	36	38	36	29	177

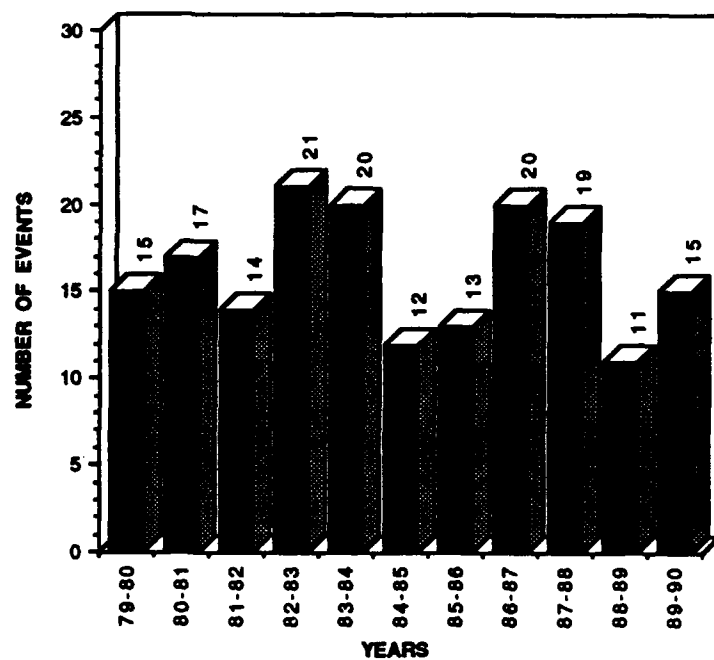


Figure 10. Annual CACS events.

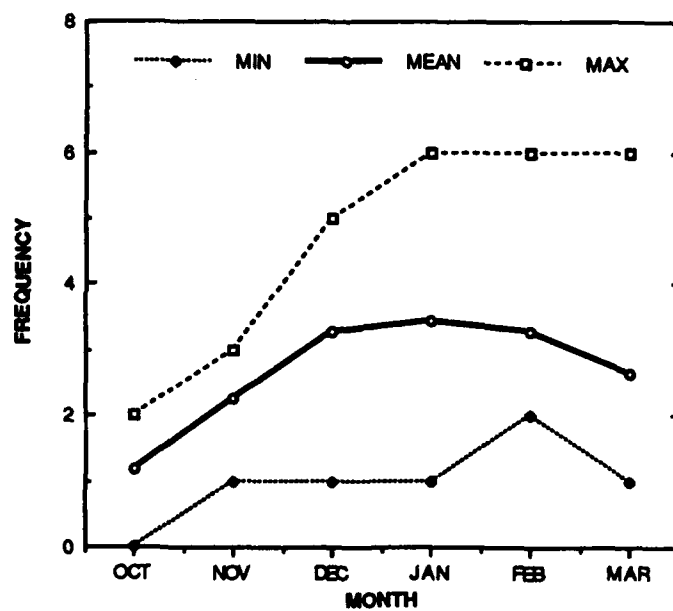


Figure 11. Monthly CACS event frequency.

Temperature

The 48 h change in daily maximum temperature was initially used as a part of the CACS definition. It has also been used in this study as a measure of the relative strength of individual cold surge events. Stronger events should generally display a more dramatic temperature drop than weaker events. Mean annual temperature drops displayed a rather random pattern during the eleven winter seasons, ranging from 4.7°C during 1987-1988 to 6.9°C during 1983-1984 and 1988-1989 (Fig. 12). The minimum temperature change was capped at 4°C because of the CACS definition, while the maximum change of 17°C occurred in March 1989. Monthly mean, minimum and maximum temperature changes are displayed in Fig. 13. Mean monthly CACS temperature drops begin at 6.1°C in October, reach a minimum of 4.8°C in November, then rise steadily to a maximum mean monthly temperature change of 7.8°C in March. The relative maximum in October may be due to the relatively higher daily maximum temperatures occurring early in the winter season. A cold front would have to be quite strong to reach as far south as Merida in October. However, in November and December, when temperatures are cooler, a greater percentage of relatively weak fronts do reach Merida, thereby decreasing the mean CACS temperature change.

Duration and Maximum Southward Penetration

Determining the duration of each CACS event and how far south the cold surge penetrated required a more subjective technique involving analysis of low-level cloud patterns on visible and IR GOES imagery. Central American weather is dominated to a large extent by the interaction of topography and mean wind flow patterns. As a result, the typical distribution of low-level cloud cover over Central America during periods when easterly - northeasterly trade winds dominate is radically different than when the

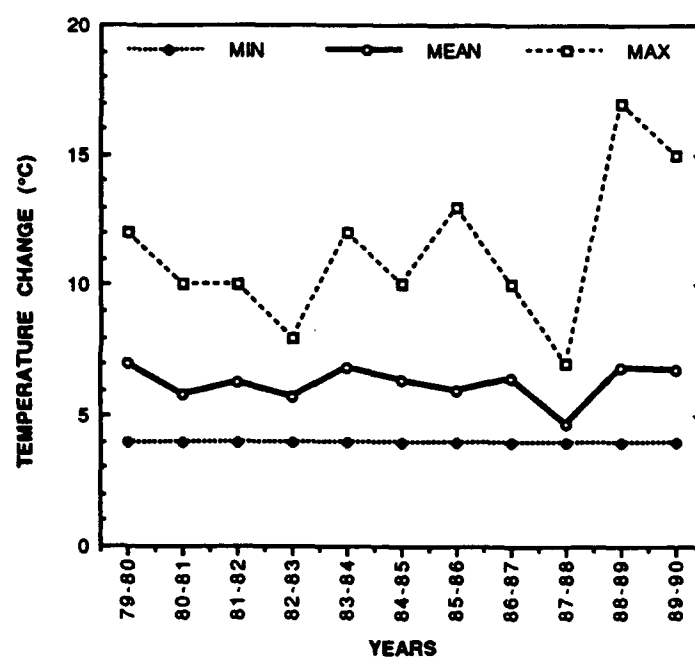


Figure 12. Mean annual CACS temperature change at Merida, Mexico.

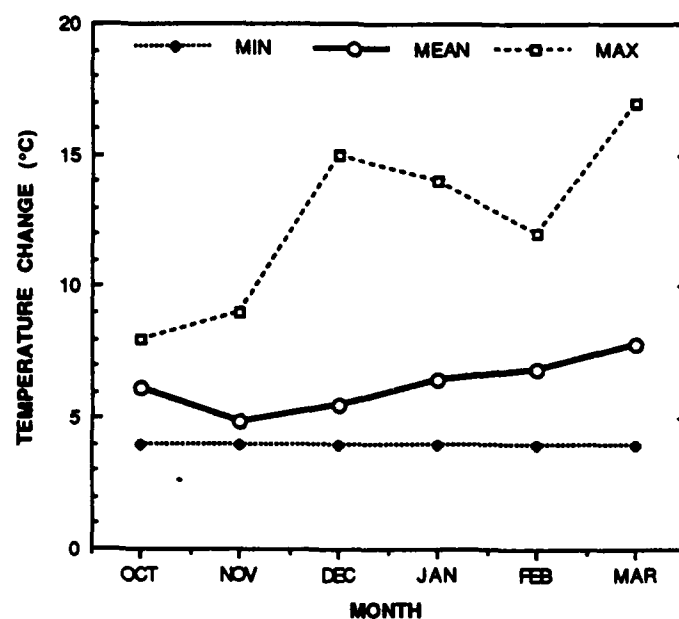


Figure 13. Mean monthly CACS temperature change at Merida, Mexico.

northerly - northwesterly low-level flow behind a cold surge dominates the region. The transition between these two wind flow regimes is also quite distinct. Although the method is subjective, cloud feature analysis provides a relatively accurate determination of CACS onset, duration and maximum southward penetration. For the purposes of this study, CACS duration is defined as the time, in days, between CACS onset at Merida and when cloud features indicate east - northeast low-level trade wind flow has regained control over all of Central America. Maximum southward penetration is defined as the southernmost location at which cloud features indicate northerly - northwesterly low-level cold surge flow is affecting the Central American land mass.

A series of visible and IR GOES imagery (Figs. 14-18) is presented to help clarify this analysis technique. A pre-cold surge situation on 21 February 1989 at 1901 UTC is depicted in Fig. 14. A mature cyclone was located over the northeastern U.S. with a cold front extending into the northern Gulf of Mexico. Note the wave developing along the front over Georgia and Alabama. Low-level cloud cover was primarily scattered and evenly distributed over Central America except over the continental divide of Costa Rica and western Panama. A sea breeze was evident along the Pacific coast of Guatemala and El Salvador. The even distribution of scattered clouds and presence of a sea breeze along the Pacific coast indicates weak easterly - northeasterly trade wind flow. By 22 February, the wave over the southeastern United States had intensified and a well defined frontal cloud band extended across southern Florida and western Cuba into central Honduras (Fig. 15). Note the broken to overcast low-level cloud cover packed up against the higher terrain features of Mexico, Guatemala and western Honduras, while nearly clear skies dominate the Pacific coastal areas of southern Mexico, Guatemala and El Salvador. This is a very clear signature of the presence of northwesterly to northeasterly low-level wind flow associated with the cold surge.

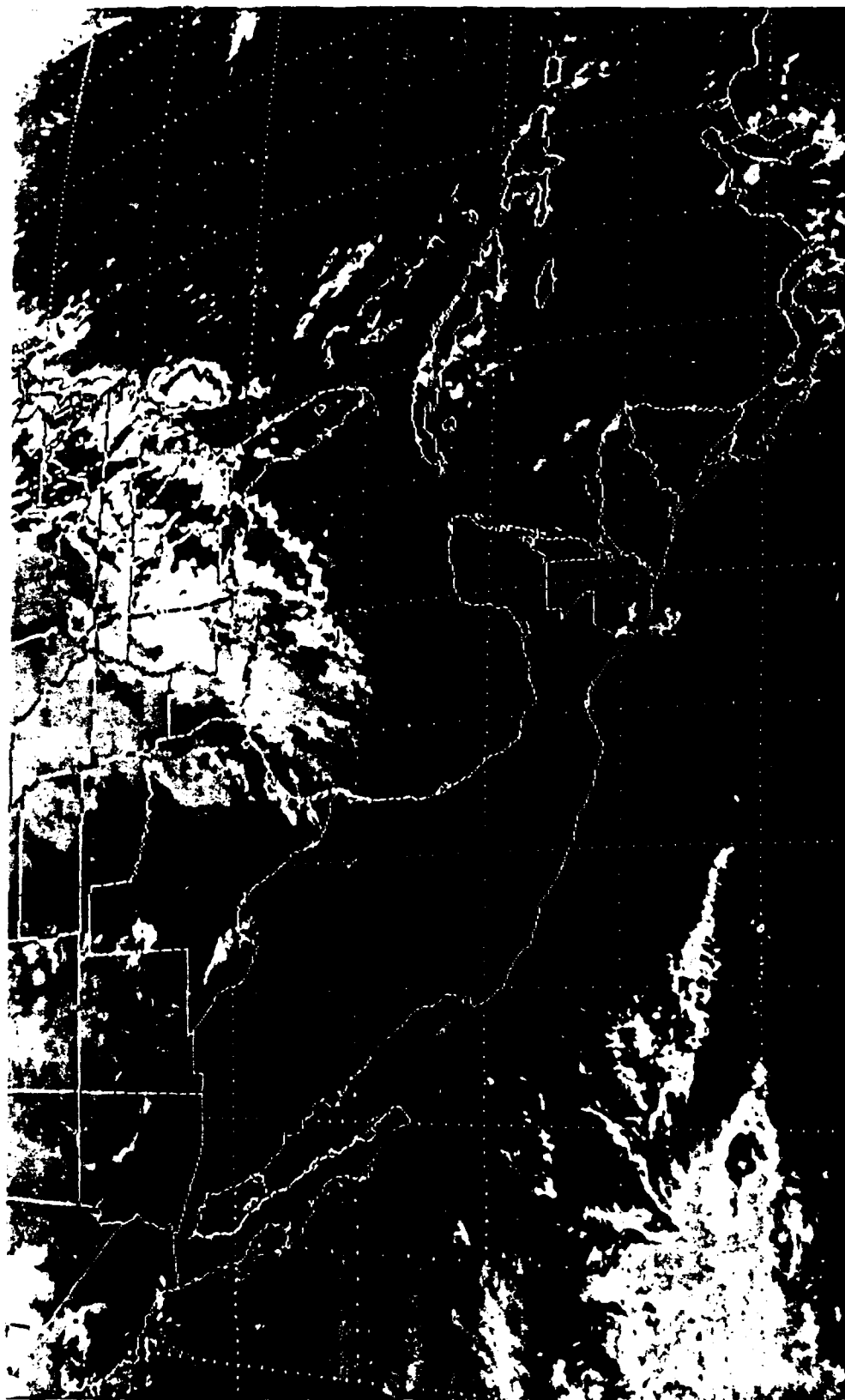


Figure 14. GOES IR satellite image with MB enhancement from 21 February 1989, 1901 UTC.

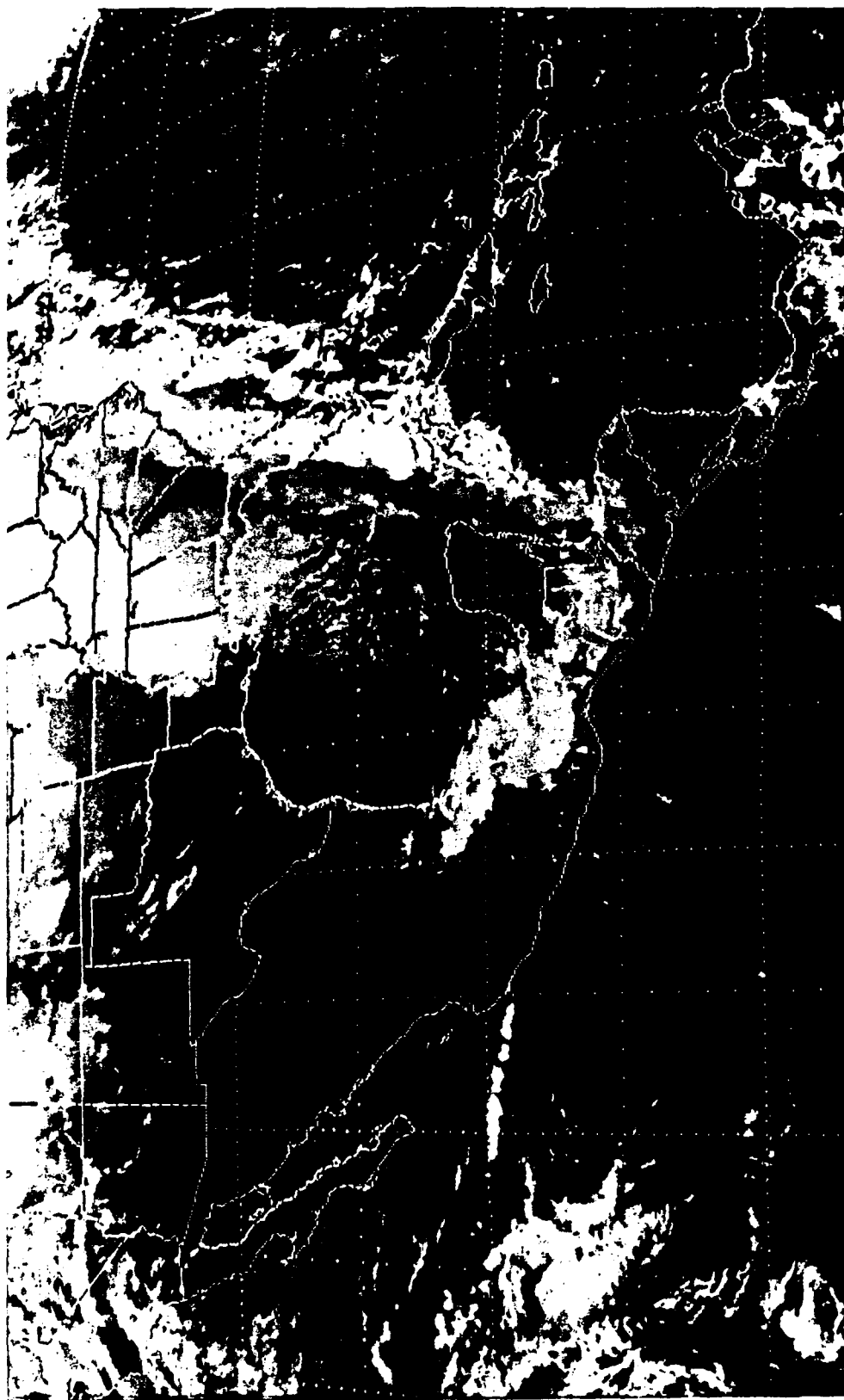


Figure 15. GOES IR satellite image with MB enhancement from 22 February 1989, 1901 UTC.

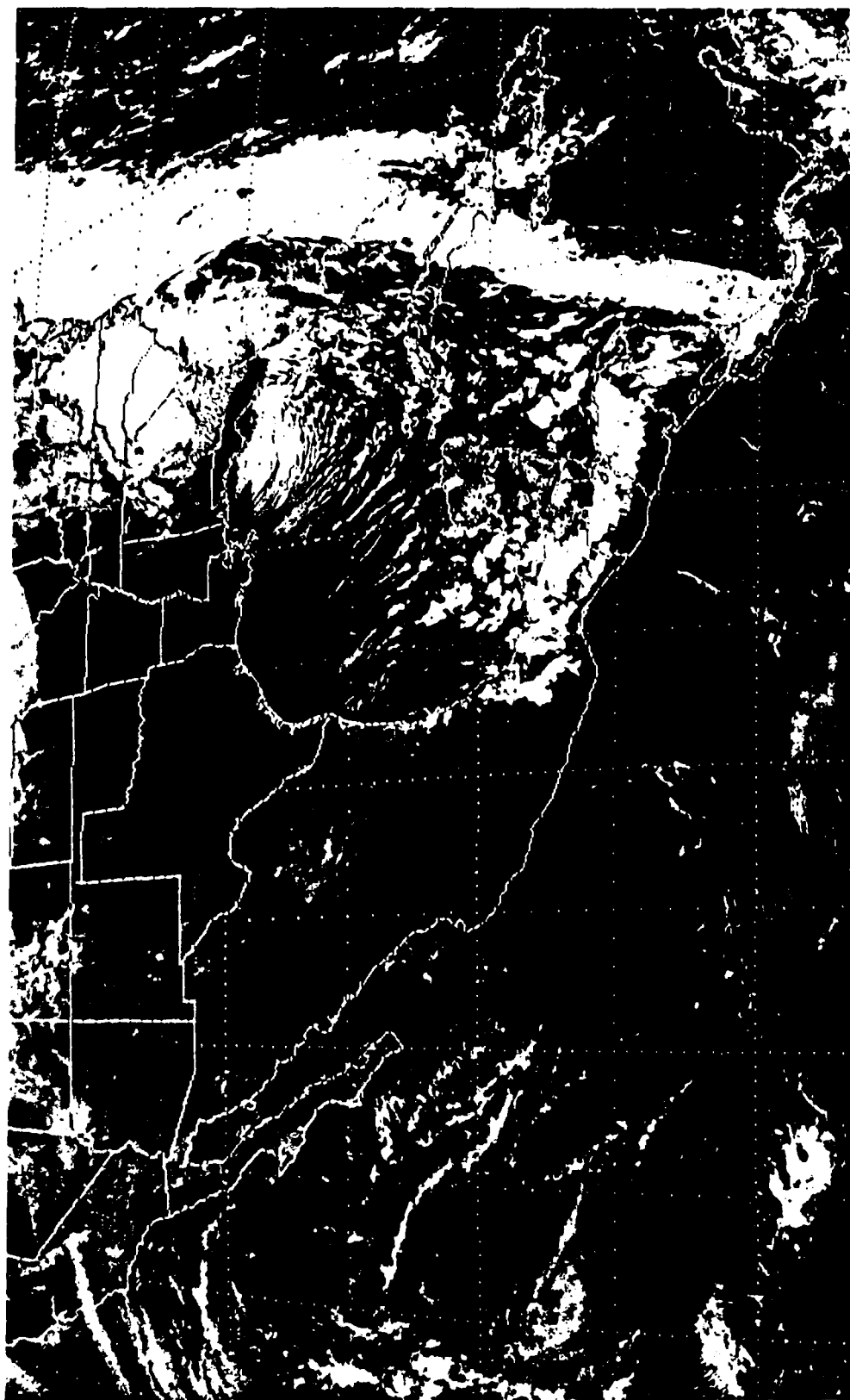


Figure 16. GOES visible satellite image from 23 February 1989, 1731 UTC.

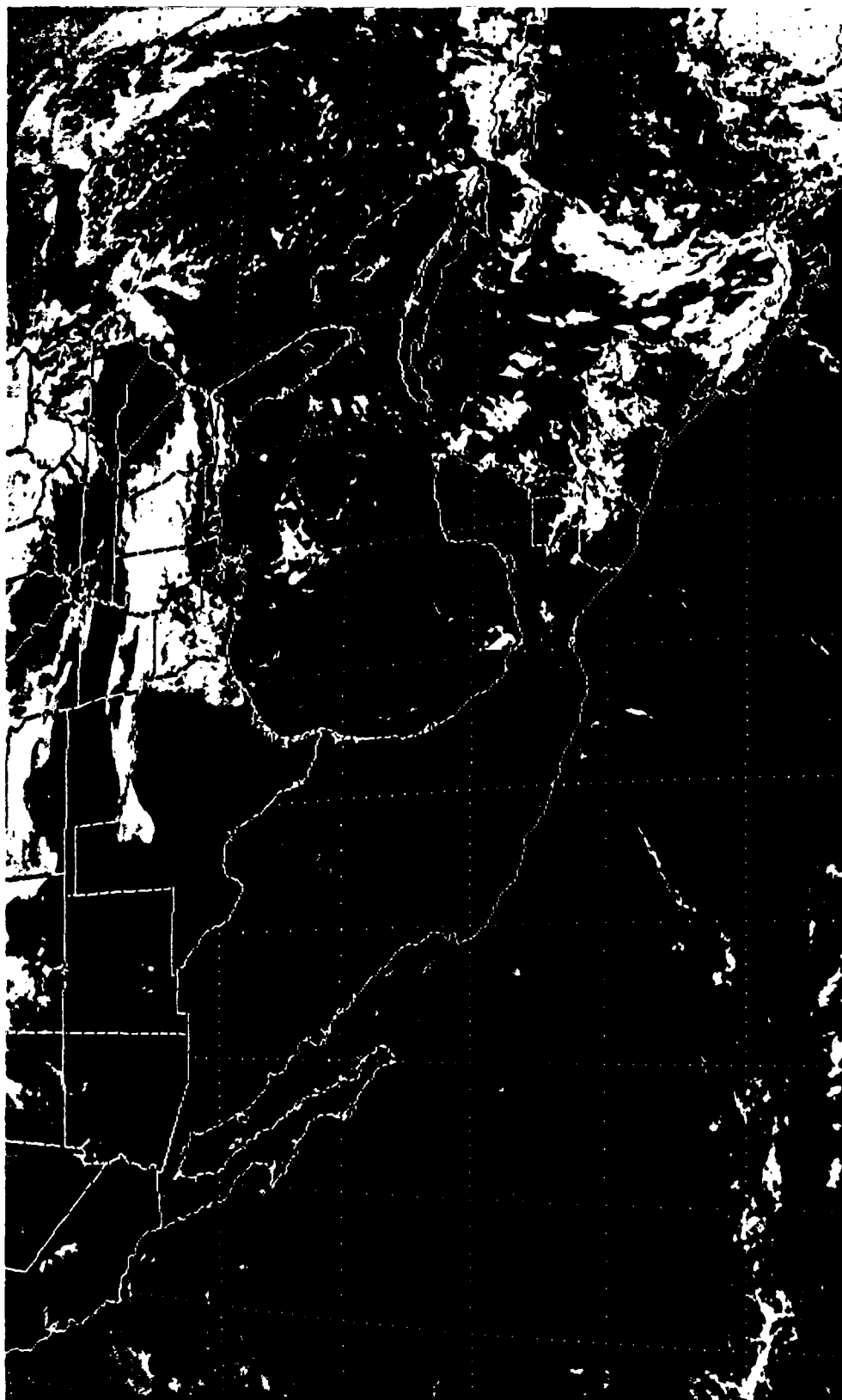


Figure 17. GOES visible satellite image from 26 February 1989, 1731 UTC.

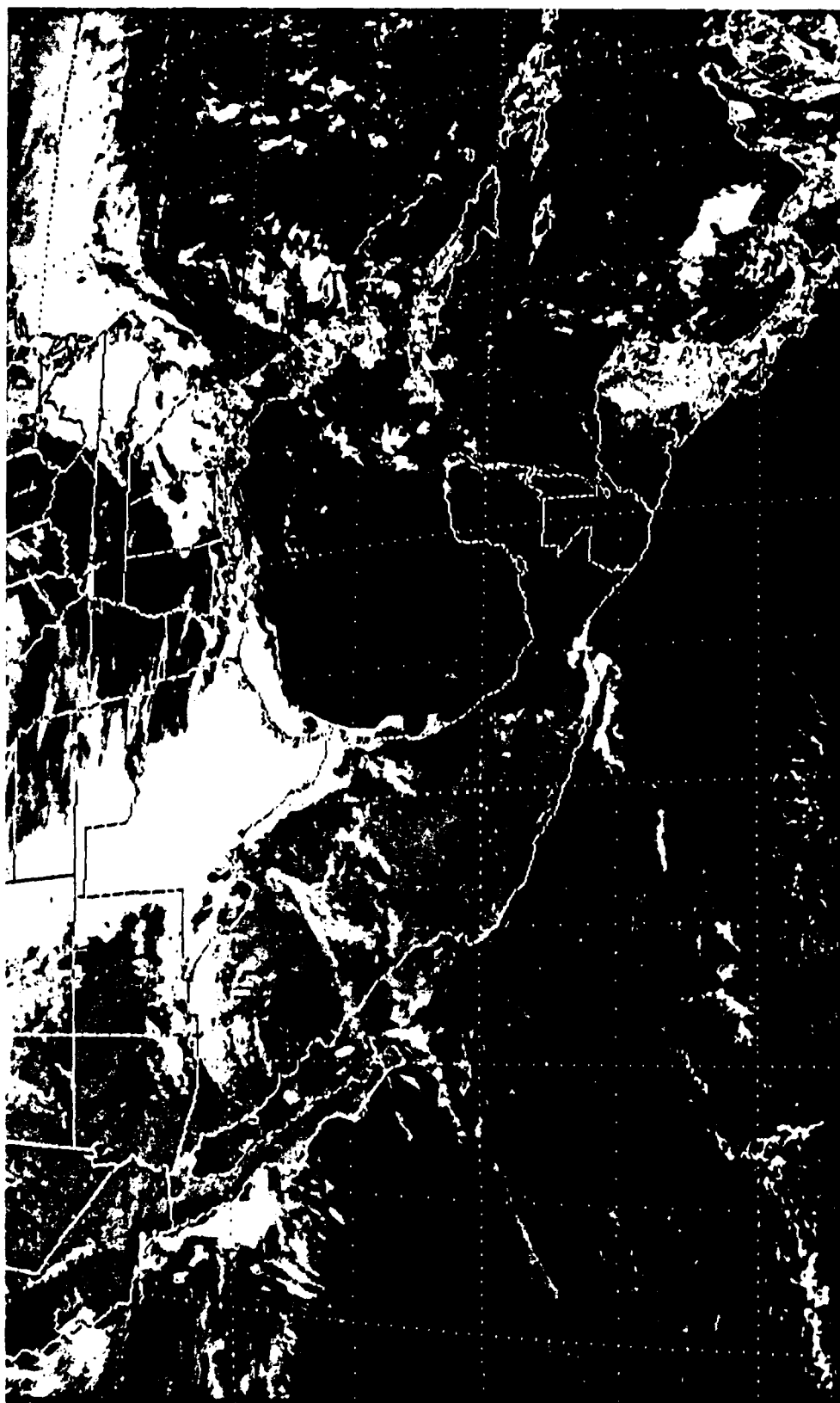


Figure 18. GOES visible satellite image from 28 February 1989, 1831 UTC.

Scattered low-level cloud cover over southeastern Honduras and Nicaragua indicates that easterly flow remained dominant ahead of the cold surge. Visible imagery from 23 February shows the cold frontal cloud band extending from the the central Atlantic United States across western Cuba and into Western Panama (Fig. 16). Cloud lines indicate that low-level flow was definitely from the northwest across the Gulf of Mexico. Broken to overcast low-level cloud cover banked up against the northern slopes of the higher terrain features from southern Mexico into western Panama further indicates that northwesterly - northeasterly flow dominated behind the cold surge. This is as far south as the front progressed, and the leading edge of the frontal cloud band extending into western Panama marks the maximum southward penetration of this CACS event. By 26 February (Fig. 17), the cold surge had weakened considerably. While the frontal cloud band was still evident from the northern Atlantic across Puerto Rico and into the southern Caribbean, it was not as well defined and the southern portion of the cloud band had begun to move back to the west. Northerly low-level flow was still apparent in the low-level cloud features over Guatemala, Honduras, Costa Rica and western Panama. The southern end of the front had completely dissipated by 28 February (Fig. 18). Note how the cloud mass over Nicaragua and eastern Honduras is now banked up against eastern slopes of the higher terrain. This indicates that easterly trade winds had regained control over the entire Central American land mass and marks the end of this CACS event.

Statistics for mean annual and mean monthly event duration are presented in Figs. 19 and 20. Mean annual duration displayed a somewhat random pattern during the eleven winter seasons, ranging from 3.6 days in 1981-1982 to 6.3 days in 1988-1989. The minimum duration recorded was one day, while the maximum was 13 days in October 1987. Monthly mean duration ranged from 4.1 days in February to 6.6 days in

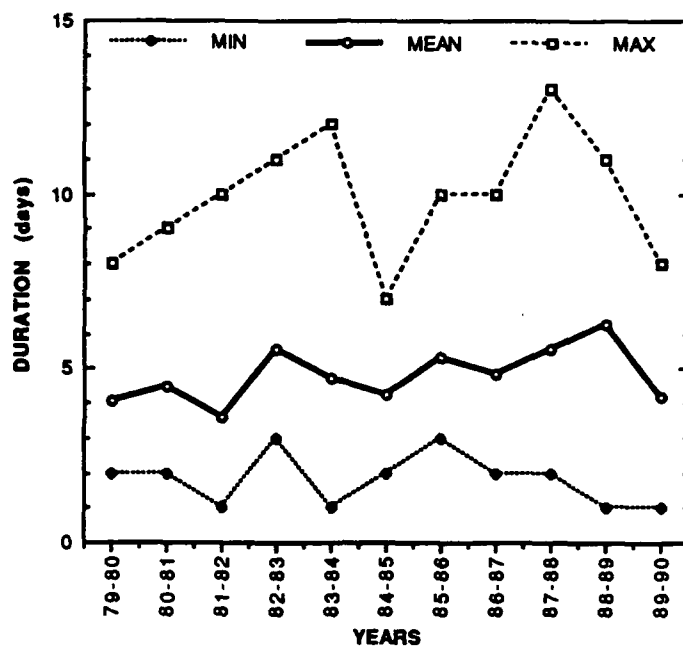


Figure 19. Mean annual CACS event duration.

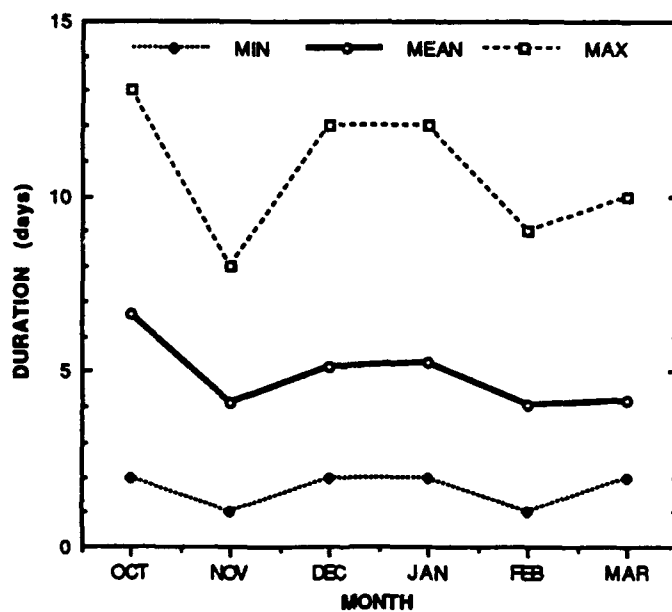


Figure 20. Mean monthly CACS event duration.

October. CACS events in October repeatedly displayed a tendency to become stationary in the Gulf of Honduras or the Yucatan gap (15°N - 20°N) and remain active for several days, while events in other months would either continue southeast into Central America and the Caribbean, return north into the Gulf of Mexico, or dissipate. This tendency is often responsible for extended periods of heavy rainfall and thunderstorms across the Yucatan Peninsula and western Cuba. Although the convection along the stalled fronts normally remains unorganized, one event actually spawned a tropical storm. A series of fronts had moved into the Gulf of Honduras, merged and stalled during late September and early October 1987. The convection associated with these fronts organized into Tropical Storm Floyd on 11 October in the Yucatan gap. Floyd moved rapidly north into the Gulf of Mexico, strengthened into Hurricane Floyd on 12 October and made landfall along the central Florida Peninsula on 13 October.

Mean annual CACS southward penetration (Fig. 21) again displayed a rather random pattern during the eleven winter seasons, ranging from a minimum of 14.7°N (northern Nicaragua) in 1989-1990 to a maximum of 11.4°N (northern Costa Rica) in 1984-1985. Monthly mean southward penetration (Fig. 22) increased slowly from 14.1°N (northern Nicaragua) in October to a maximum of 12.2°N (southern Nicaragua) in January. The minimum southward penetration recorded was 20°N (central Yucatan Peninsula), although this statistic is somewhat governed by the CACS definition. Maximum southward penetration was capped at 7°N by the Panamanian Isthmus and mountains of northern Colombia, approximately 200 km farther south than the most extreme estimate of the southern extent of cold fronts by Garbel (1947). CACS events were observed as far south as 7°N in every month but October and March and during every Winter season except 1979-1980 and 1987-1988, so is is not an uncommon occurrence. In fact, cold surges exhibit deep southward penetration much more

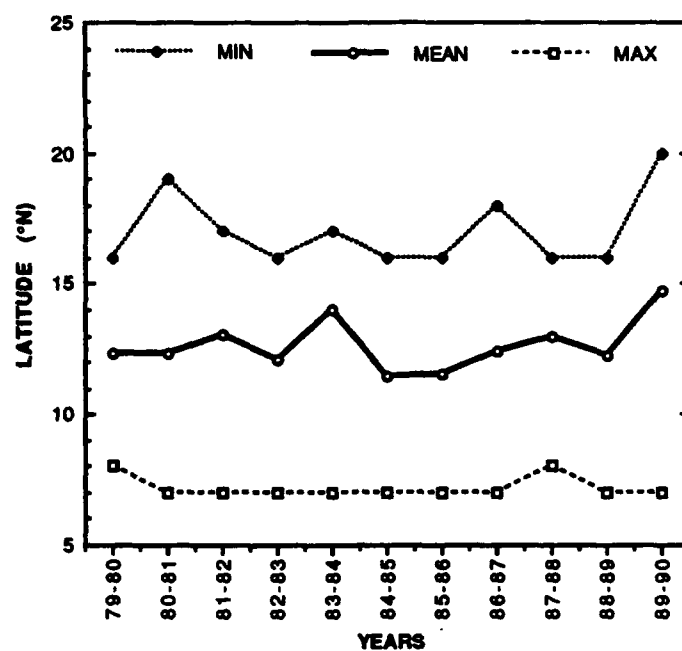


Figure 21. Mean annual CACS southward penetration.

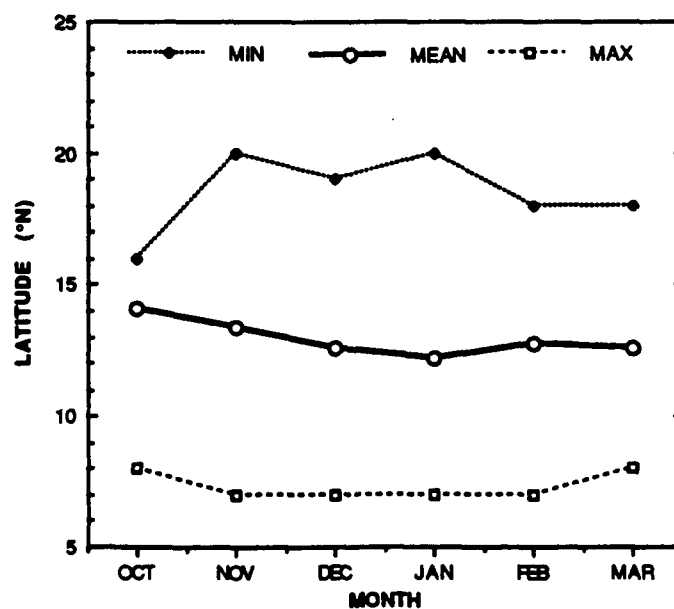


Figure 22. Mean monthly CACS southward penetration.

frequently than previously thought. Henry (1979) found that approximately 25% of the cold fronts analyzed on the NMC Northern Hemispheric surface analysis between 1967 and 1977 made it to 15°N, and less than 5% made it to 10°N. In this study, over 76% of the identified CACS events penetrated south of 15°N, and over 26% penetrated south of 10°N. Some suggestions have been made that extreme cold surge events may extend even farther south across the Central American land mass. Although some satellite imagery hints at northerly flow crossing Costa Rica and western Panama into the Pacific, no conclusive evidence was found in this study.

CHAPTER VI

CACS STRUCTURE

The response of surface variables to cold frontal passage was examined by Horvath and Henry (1980) for Belize and Ladd and Henry (1980) for coastal Honduras. The vertical structure of cold fronts over the Gulf of Mexico was briefly examined by DiMego et al. (1976). This chapter attempts a more comprehensive analysis of CACS structure by examining both the effects of cold surge passage on surface variables and the vertical structure of the pre- and post-CACS atmosphere at Belize City, Belize. Additionally, TPW and rain rate are estimated for several cases using SSM/I and SMMR brightness temperature data to evaluate the evolution of moisture fields in association with CACS events. Belize City was selected primarily because of the availability of relatively continuous hourly surface observations and 12-hourly upper air observations; however, several other important considerations were involved in the selection. Belize City is located on the Caribbean coast (elevation 5 m) with only limited terrain features to the north across the entire Yucatan Peninsula which could impede the progress or mutate the structure of advancing cold fronts. In addition, Belize City experiences both a greater frequency and more representative distribution of CACS events than more southern areas where only the strongest cold surges penetrate. Finally, a similar study of surface variables (Horvath and Henry, 1980) provides a baseline for comparison of results. Note that results in the surface variable and vertical structure sections of this chapter are based only on data from Belize City, and therefore, are probably representative of only Caribbean coastal areas of Central America.

SURFACE VARIABLES

Thirty nine CACS cases from two sample winter seasons (1983-1984 and 1987-1988) were selected for detailed analysis. These two time frames were chosen because of the availability of SMMR data for January through March of 1984 and SSM/I data for October through February of 1987-1988. Although a marked increase in CACS frequency was discovered during both seasons, all other aspects of the this sample are representative of the entire data set.

The date of frontal passage at Belize City was recorded for each case. Means and standard deviations (not shown) of daily maximum and minimum temperature, dew point, wind direction, wind speed, sea level pressure (SLP), precipitation, cloud ceiling height and cloud ceiling frequency were then calculated for a ten day period centered on the date of frontal passage. Further extension of the ten day period results in data contamination from other cold surge events.

Maximum and Minimum Temperature

Daily mean maximum temperature displayed a very distinct cold surge signature with a gradual warming trend during the four days prior to frontal passage followed by a sharp 4.2°C drop on the day of frontal passage (Fig. 23). Maximum temperature remained depressed, but made a gradual recovery toward pre-cold surge levels through the remainder of the period. Daily mean minimum temperature displayed a much more gradual drop of 2.5°C over a 72 h period during frontal passage. The standard deviation of daily maximum temperature ranged from 1.8°C to 2.8°C, while the standard deviation of daily minimum temperature ranged from 1.5°C to 2.6°C, both indicating a very low degree of variability. Horvath and Henry (1980) reported similar results. However, they analyzed 3-hourly surface observations and the frontal temperature drop was

somewhat obscured by the diurnal temperature curve. As a result, Horvath and Henry chose to analyze equivalent temperature, which displayed an impressive mean 12°K drop during a 24 h period centered at the time of frontal passage.

Dew Point

Mean dew point was calculated daily at 0000 UTC and 1200 UTC for the ten day period. In Fig. 24, mean dew point shows a gradual increase at both times during the four days prior to frontal passage, followed by a 3.1°C decrease at 0000 UTC and a 3.5°C decrease at 1200 UTC during the 48 h immediately after frontal passage. The greatest drop in mean dew point was 4.8°C, occurring between 0000 UTC on day 0 and 1200 UTC on day 1. As with mean daily maximum and minimum temperature, the mean dew point remained lower than before frontal passage, but recovered steadily through the remainder of the period. Standard deviation of dew point ranged from 1.6°C to 3.3°C, indicating slightly more variability than temperature. Horvath and Henry (1980) reported similar, but slightly less dramatic results with a 4°C drop in mean dew point during the 24 h period centered at the time of frontal passage.

Wind Direction

The inherent problems associated with averaging wind directions were addressed before initiation of this part of the study. The prevailing wind direction during the winter season at Belize City fluctuates on a diurnal basis because of land/sea breeze effects, shifting from east or southeast during the afternoon to north or northwest in the early morning (Whiteside, 1985). Wind direction is nearly constant within each of the flow regimes. However, wind direction is much more variable during transition between the two regimes. Therefore, wind direction was recorded at 0000 UTC and

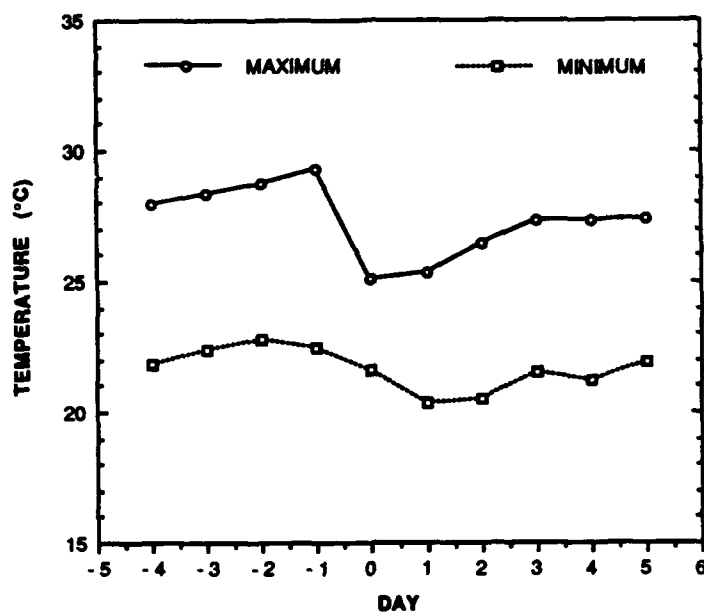


Figure 23. Mean daily maximum and minimum temperatures (°C) during frontal passage at Belize City, Belize.

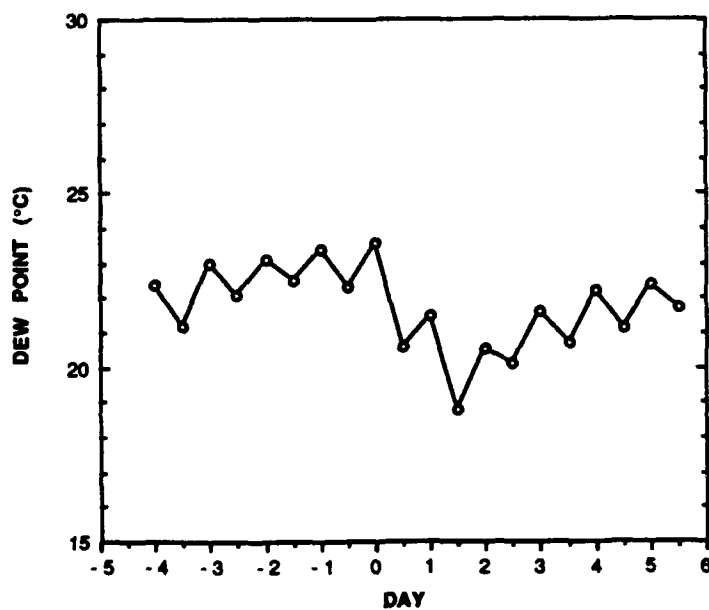


Figure 24. Mean dew point (°C) at 0000 UTC and 1200 UTC during frontal passage at Belize City, Belize.

1200 UTC, in the middle the time frame of each flow regime, and averaged separately to minimize the case to case variability. Results were strikingly similar to both the individual case studies presented in Chapter VI and the results of Horvath and Henry (1980), thus lending credibility to this method of mean wind direction analysis.

Mean wind direction prior to frontal passage exhibited a diurnal oscillation from southwesterly to east-southeasterly (Fig. 25). A very dramatic shift to westerly and then northwesterly winds was evident on the day of frontal passage. Winds remained northwesterly for three days at both 0000 UTC and 1200 UTC, followed by a return to diurnally varying southerly flow toward the end of the period. Variance in wind direction was at a minimum immediately after frontal passage, with standard deviation ranging from 30° to 60° during days 0 and 1. Standard deviation was significantly higher at the beginning and end of the period, ranging from 90° to 130° during the first four days and 90° to 140° during the last four days. This high degree of variability is probably a result of both the method of analysis and the fact that wind direction is simply more erratic during periods of normal flow than immediately after frontal passage. Consequently, results from the beginning and end of the period should be viewed with some skepticism. However, mean wind direction still displayed the most pronounced CACS signature of all the surface variables studied, both in terms of the dramatic wind shift with frontal passage and the lack of diurnal variability after the wind shift.

Wind Speed

Mean wind speed was analyzed at 0000 UTC and 1800 UTC instead of 0000 UTC and 1200 UTC primarily because it was often calm between 0600 UTC and 1500 UTC. An obvious CACS signature was not evident at either time (Fig. 26). Mean wind speed

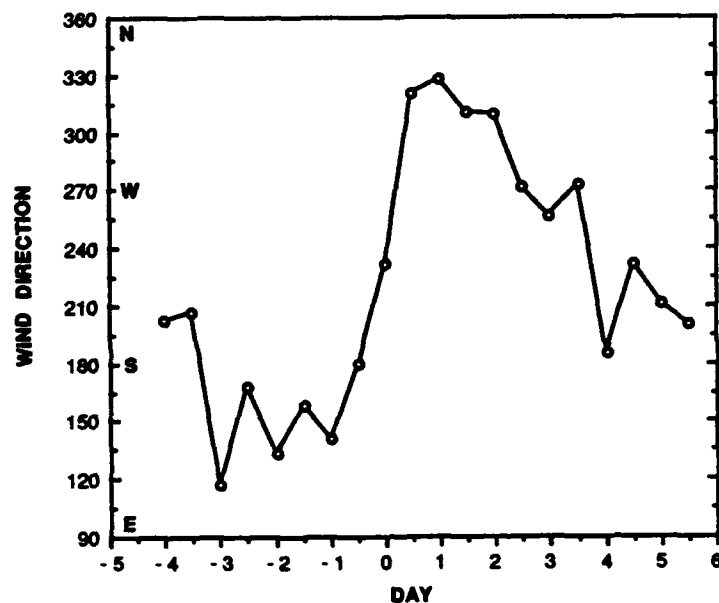


Figure 25. Mean wind direction at 0000 UTC and 1200 UTC during frontal passage at Belize City, Belize.

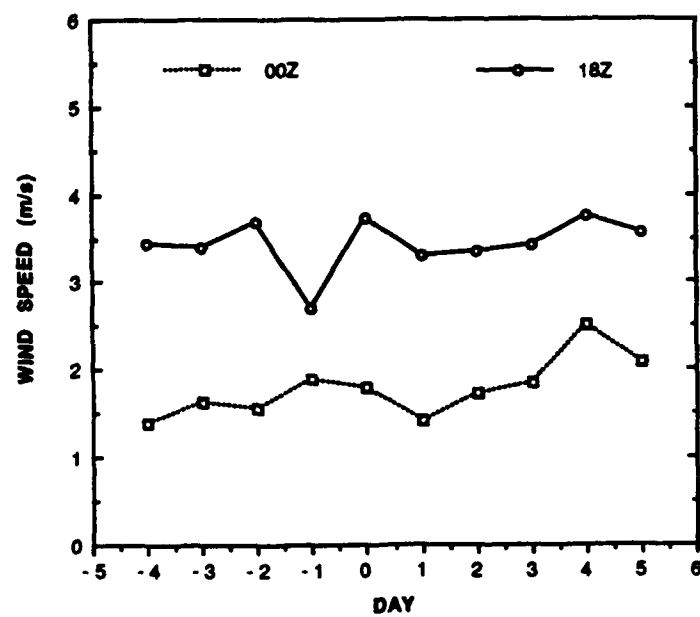


Figure 26. Mean wind speed (m/s) at 0000 UTC and 1800 UTC during frontal passage at Belize City, Belize.

was consistently higher at 1800 UTC than 0000 UTC, varying rather randomly from 1.4 m/s to 2.5 m/s at 0000 UTC and from 2.7 m/s to 3.8 m/s at 1800 UTC. Standard deviation of the wind speed was of the same magnitude as the mean at 0000 UTC, ranging from 1.2 m/s to 3.1 m/s. Standard deviation of the wind speed at 1800 UTC ranged from 1.4 m/s to 1.9 m/s. Horvath and Henry (1980) reported significantly different results, with mean wind speed increasing from calm prior to frontal passage to 10 kt after frontal passage. However, the wind speed increase was confined to 12 h after frontal passage, so the temporal spacing of observations used in this analysis was probably too coarse to reflect frontal passage, at least in the mean. An analysis of 3-hourly or 6-hourly mean wind speed trends was not attempted.

Sea Level Pressure

Mean SLP was studied at 0000 UTC (1800 local) and 1500 UTC (0900 local) for two reasons. These times were selected primarily because they approximately correspond to the times of daily maximum and minimum SLP in the diurnal pressure curve. Actual maximum and minimum values were not used because SLP was reported only on a 3-hourly basis. In addition, analyzing the two times separately will help to minimize contamination of the CACS pressure signal by the diurnal pressure curve.

A distinct cold surge signal is evident in Fig. 27, with a slight increase in SLP immediately prior to frontal passage, followed by a 48 h jump in SLP of 4.0 mb at 0000 UTC and 4.4 mb at 1500 UTC. The maximum increase was 6.1 mb, occurring between day 0 at 0000 UTC and day 1 at 1500 UTC. Standard deviation of SLP remained relatively consistent through the period, ranging from 2.5 mb to 4.1 mb at 0000 UTC and from 2.8 mb to 4.4 mb at 1500 UTC. Results from Horvath and Henry (1980)

were quite similar. A 6 mb increase in mean SLP was reported from 12 h before to 12 h after frontal passage.

Some consideration was given to the possibility that the CACS associated pressure jump was simply a reflection of the CACS temperature discontinuity and/or equatorward displacement of the front. Therefore, pressure changes were estimated for 15 CACS cases at Belize City using the Hydrostatic approximation, assuming a 1 km deep frontal layer, and Taylor's hypothesis. In each of the 15 cases, the estimated SLP change due to temperature and frontal displacement consistently accounted for less than 20% of the actual cold surge pressure jump. In addition, pressure change estimates were made for the case studies presented in Chapter VII. Similar results were found at all stations. This indicates both that the synoptic scale pressure gradient accounts for the majority of the CACS associated rise in SLP, and that this contribution is relatively independent of latitude.

Precipitation

Daily precipitation was highly variable. Rainfall during individual CACS events ranged from 0 mm to 76 mm. As a result, standard deviation was typically twice the magnitude of the mean. Despite the high degree of variability, mean daily precipitation displayed a distinct response to cold surge onset (Fig. 28). Daily rainfall of 1 mm to 2 mm was common prior to frontal passage. Mean precipitation amounts increased dramatically to 4-5 mm/d beginning on day -1 and lasting through day 2. Horvath and Henry (1980) found that precipitation typically began just before frontal passage, with a mean maximum of 10 mm falling in the hours immediately after frontal passage. No other precipitation was recorded during the 48 h period centered at the time of frontal passage.

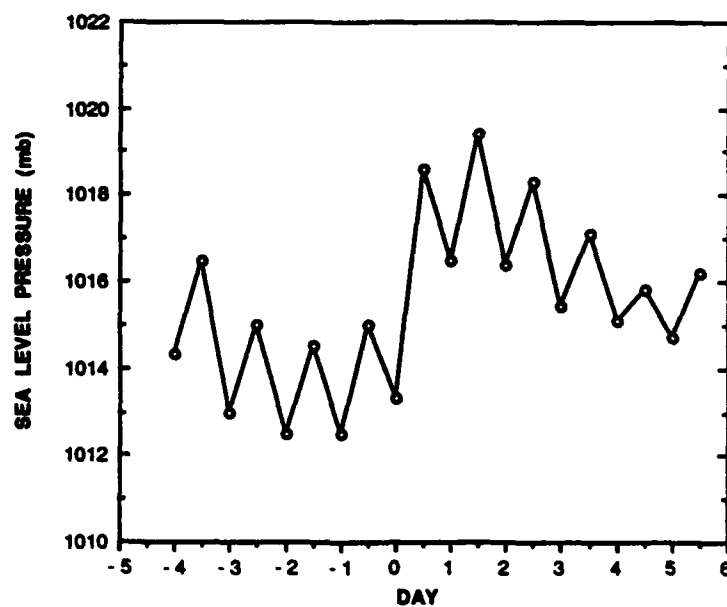


Figure 27. Mean sea level pressure (mb) at 0000 UTC and 1500 UTC during frontal passage at Belize City, Belize.

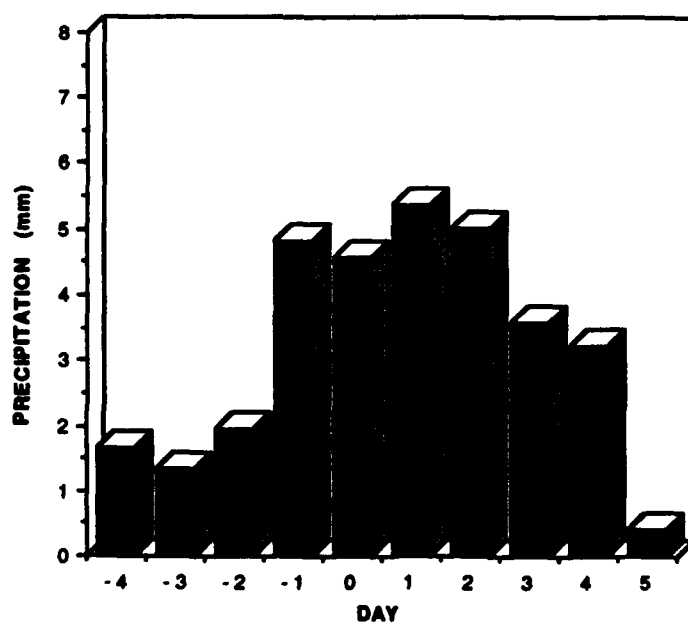


Figure 28. Mean daily precipitation (mm) during frontal passage at Belize City, Belize.

Precipitation is one of the most evident characteristics of the CACS. Hastenrath (1967) estimated that 40-60% of the annual precipitation along the northern Honduras coast falls during what is the "dry" season for the remainder of Central America. Rainfall statistics were examined for the 1983-1984 and 1986-1987 winter seasons at all reporting stations to determine how much of this dry season precipitation is a result of the CACS. At Belize City, over 70% of the winter season precipitation fell during CACS events. Flores, Guatemala, Managua, Nicaragua and San Andres, Colombia displayed similar results. Cold surges were responsible for just over 50% of the winter season precipitation at San Jose, Costa Rica, while well over 90% of the winter season rainfall at La Mesa, Honduras, Tegucigalpa, Honduras and Guatemala City, Guatemala was observed during the CACS.

Cloud Cover

Horvath and Henry (1980) investigated fluctuations in cloud cover during frontal passages by measuring total sky cover. In this study, changes in cloud cover were investigated by calculating both mean cloud ceiling height and the mean frequency of cloud ceiling occurrence at 0000 UTC and 1200 UTC. A cloud ceiling was defined as the level at which 5/8 or more of the celestial dome is covered by clouds. Results are presented in Figs. 29 and 30. A definite cold surge signature was evident in both statistics, with mean ceiling height between 3500-4000 m before frontal passage dropping to 800-2000 m afterwards, and mean ceiling frequencies increasing from 20-40% to 60-85%. Cloud cover trends during individual CACS events displayed a high degree of variability, especially before frontal passage. Standard deviation ranged from 1400-3400 m before and 700-1800 m after frontal passage.

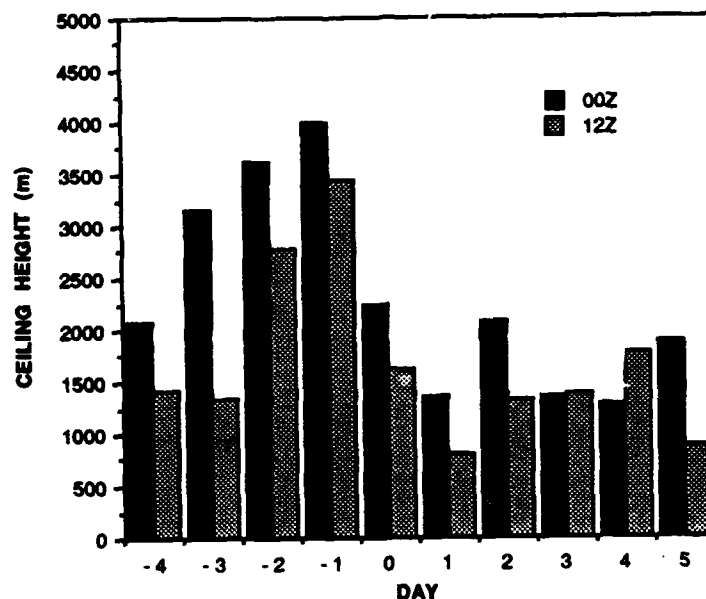


Figure 29. Mean cloud ceiling height (m) at 0000 UTC and 1200 UTC during frontal passage at Belize City, Belize.

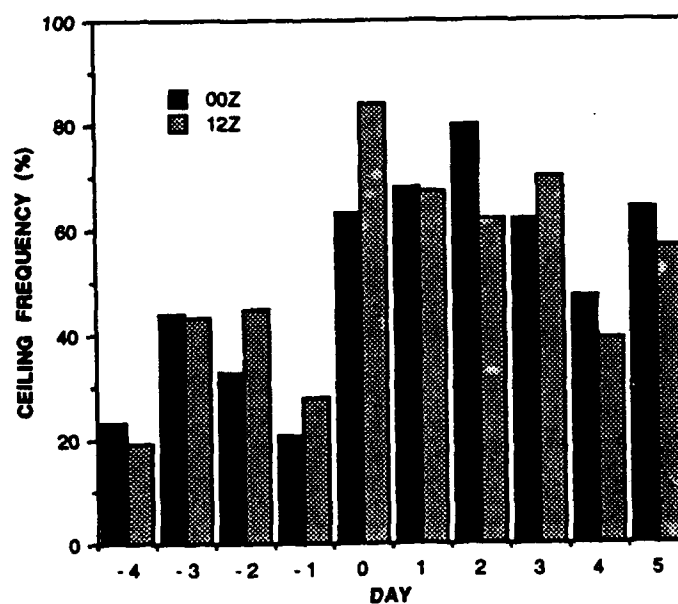


Figure 30. Mean percent frequency of cloud ceiling at 0000 UTC and 1200 UTC during frontal passage at Belize City, Belize.

VERTICAL STRUCTURE

12-hourly upper air observations were available from six Central and South American reporting stations, including Belize City, Belize, Guatemala City, Guatemala, Tegucigalpa, Honduras, Managua, Nicaragua, San Andres, Colombia and Howard AFB, Panama. In this section, CACS events were selected from the 1983-1984 and 1987-1988 sample winter seasons for detailed vertical structural analysis. If more than two consecutive observations were missing during any event, the case was not included in the analysis. Unfortunately, this criterion eliminated all but 8 of the 39 CACS events available for study. The remaining cases included two CACS events from 1984, four events from 1987 and two events from 1988.

Temporal cross sections were produced using GEMPAK, a collection of interactive FORTRAN programs developed by NASA's Goddard Space Flight Center for the retrieval and manipulation of meteorological data. Cross sections from Belize City were plotted for a five day (ten observation) period centered on the date of frontal passage. Isotherms were plotted at 4°C intervals and isodrosotherms were plotted at 5°C, 15°C and 25°C, with time increasing to the right. GEMPAK interpolated the contours where data were missing. Dew point depressions less than or equal to 5°C were shaded to highlight significant areas of moisture. Wind speed (kt) and direction was plotted at all available levels. Inversions were hand analyzed and added to the cross sections. Individual Skew-T's and 1°C interval temperature cross sections were produced to assist in the inversion analysis. The Lifted Index, K Index and Total Totals Index were also calculated for each case to evaluate atmospheric stability.

The most evident CACS-associated feature in the cross sections appeared in the moisture field. Moisture was evident through a deeper layer of the atmosphere after frontal passage in all cases. Dew point depressions less than or equal to 5°C were

generally confined below 850-700 mb before frontal passage, but extended from the surface up to 700-500 mb afterwards. Two cases in 1987 exhibited moist layers up to 300 mb immediately after frontal passage. In both cases, inversions were either weak or absent. The moist layer was capped by a subsidence inversion in the remaining six cases. A distinct trade wind inversion was apparent during only one cold surge event. Distinct frontal inversions were evident in only two of the analyzed cases. The most common inversion associated with frontal passage was normally found between 800 mb and 600 mb; however, it appeared as low as 850 mb and as high as 500 mb. This inversion was not distinctly frontal or subsidence related, but seemed to share characteristics of both. Wind profiles were highly dependent on the strength and location of the inversions in each case. In general, both a shift in wind direction from east-southeast to northwest or northeast and a slight increase in wind speed was evident below 700-500 mb after frontal passage. Above 500 mb, wind remained from the west or northwest and displayed no obvious response to frontal passage other than a gradual increase in speed through the period. The stability indices all displayed consistent trends toward decreasing stability prior to frontal passage, and then an abrupt change toward increasing stability through the remainder of the period. Magnitudes of the stability indices varied considerably from case to case. No other features were identified which adequately characterized the change of vertical atmospheric structure in response cold surge events. Each case displayed very unique features, probably because of the small sample size.

The cold surge of 10-14 November 1987 was a moderate event which penetrated into southern Nicaragua. The temporal cross section shows that moisture was confined primarily below 850 mb until frontal passage (Fig. 31). After frontal passage, a deep layer of moist air was apparent, extending up to approximately 350 mb. The most

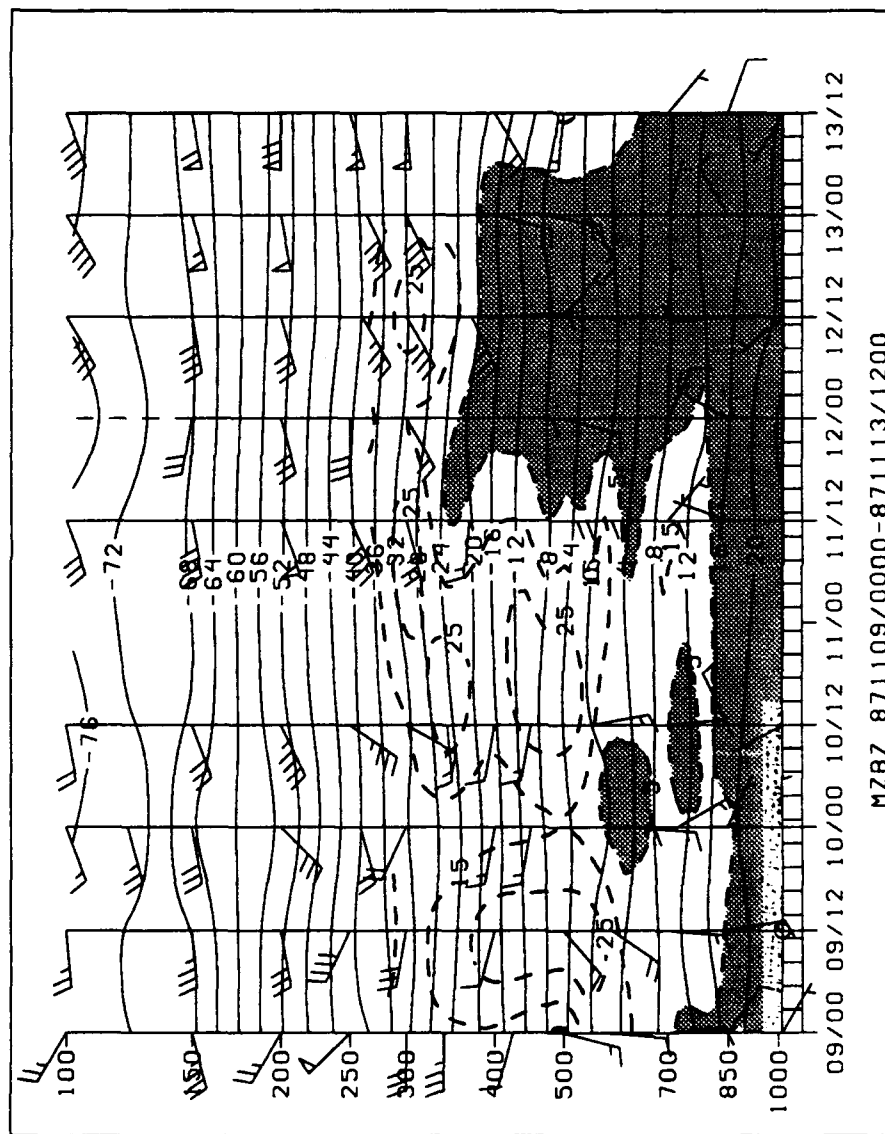
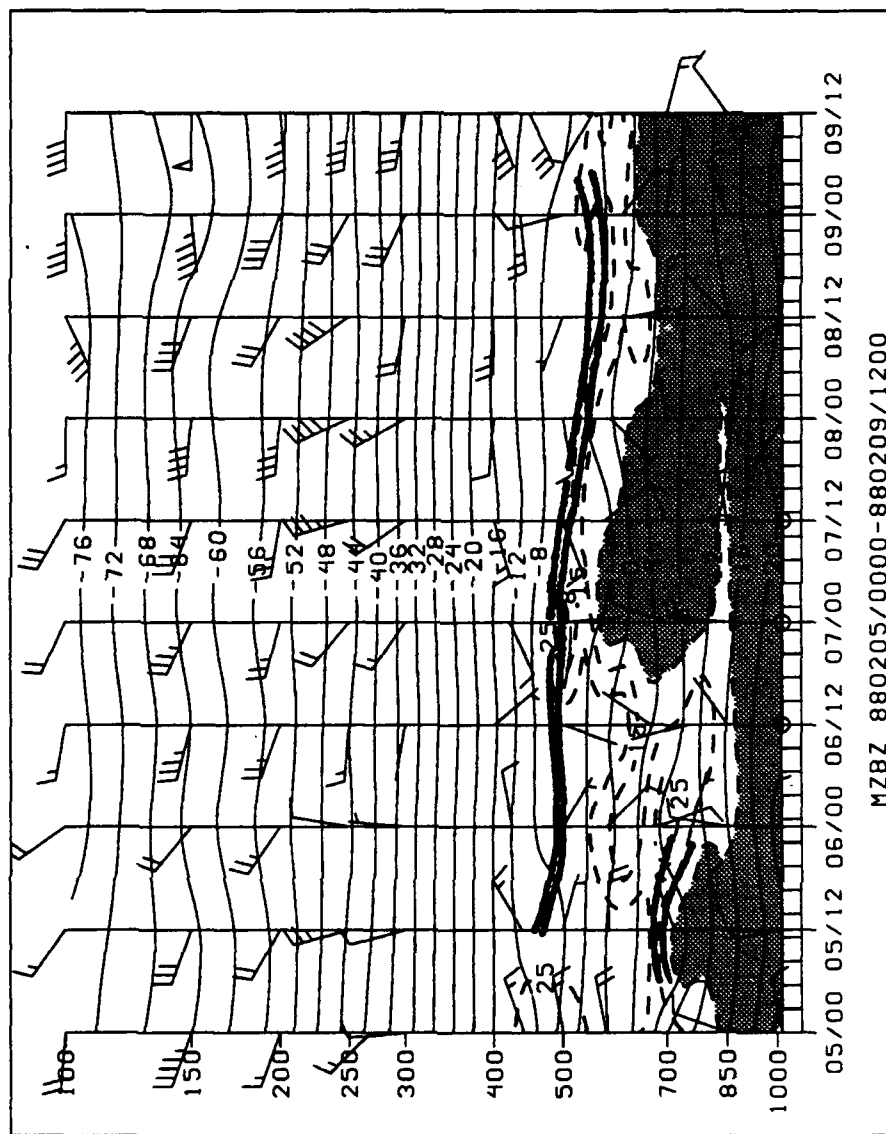


Figure 31. Vertical temporal cross section at Belize City, Belize from 9 November 1987, 0000 UTC to 13 November 1987, 1200 UTC. Isotherms (solid) are plotted at 4°C intervals and isodrosotherms (dashed) at 5°C and 25°C. Also shown are areas with dew point depression less than or equal to 5°C (shaded), wind speed (kt) and direction, and inversion layers (heavy solid).

striking feature of this event was that no inversions were evident, and the atmosphere remained relatively unstable through the entire period. In November, the subtropical high is not yet the dominant feature over Central America, and the trade wind inversion was probably not yet well established. A wind shift from south-southeast to northeast-northwest was confined below 700 mb after frontal passage. Above 400 mb, winds remained from the west, but increased by 20-40 kt after 12 November.

The cold surge of 6-9 February 1988 was another moderate case which pushed only into eastern Honduras. The most striking feature of this event was the dominant trade wind (subsidence) inversion which persisted near 500 mb through the entire period (Fig. 32). A definite frontal inversion was not evident. Moisture was confined below 700 mb by a weak subsidence inversion prior to frontal passage, and expanded up to 600 mb, near the trade wind inversion, afterwards. Surface winds shifted to the northwest after frontal passage; however, mid-level flow remained easterly through the period. The depth of upper level westerlies expanded from above 300 mb initially to near 500 mb after frontal passage. Upper level flow again displayed a gradual increase in speed after frontal passage.

The cold surge of 20-25 November 1987 was a significantly more interesting event. The moist layer was initially quite deep, extending to near 300 mb both in advance of the front and during frontal passage (Fig. 33). Moisture was confined below 600 mb by a weak subsidence inversion from 18-20 November. Another subsidence inversion capped moisture below 400 mb on 21 November, suggesting the presence of convective activity. Belize City received 4 mm of rainfall on that day. Following frontal passage, moisture was capped below 850 mb by a distinct frontal inversion. Low-level flow was primarily from the east initially. After frontal passage, northwest winds dominated below the frontal inversion and winds shifted to northeasterly from the top of the



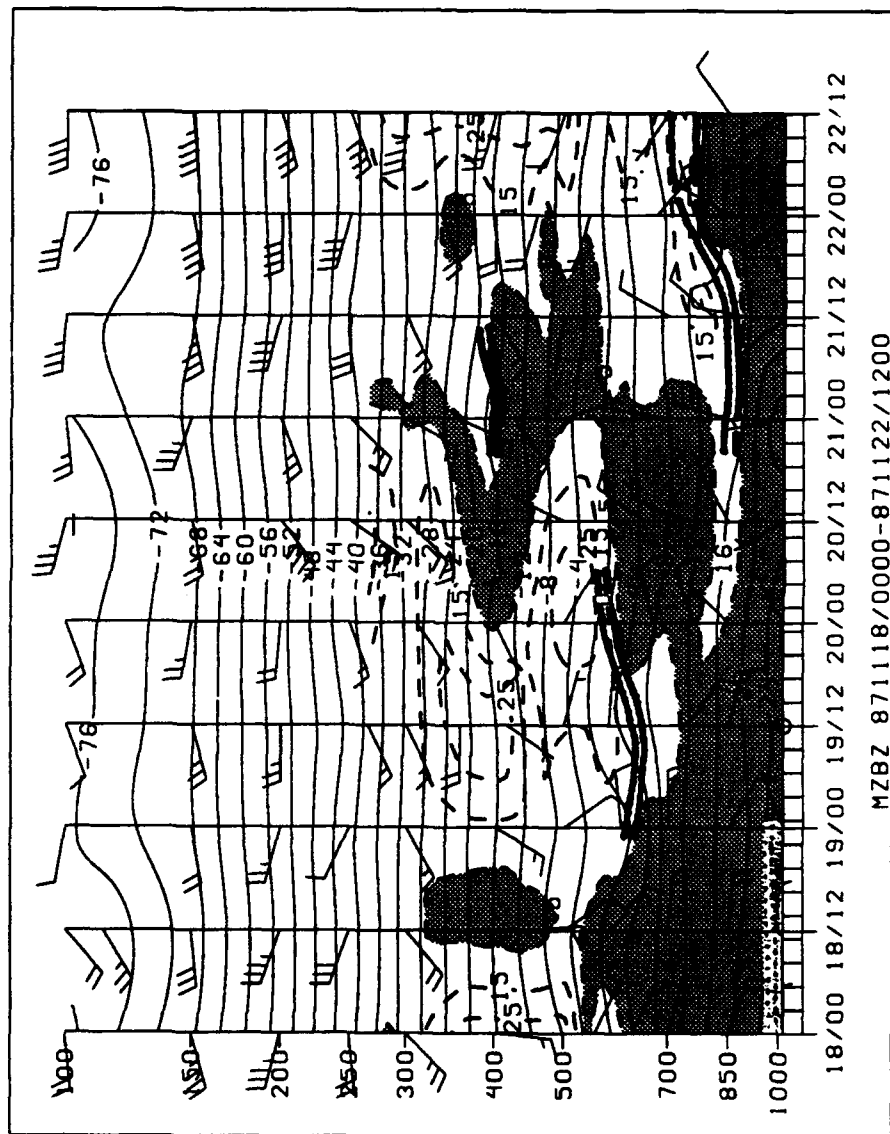


Figure 33. As in Fig. 31, except from 18 November 1987, 0000 UTC to 22 November 1987, 1200 UTC.

inversion to near 650 mb. Upper level westerly flow again gradually increased in strength after frontal passage. The diurnal temperature curve was very pronounced near the surface after frontal passage, indicating strong radiational cooling in the relatively dry air behind the front.

MOISTURE FIELDS

TPW and rain rate estimates derived from SSM/I brightness temperature data through NASA's WetNet program were analyzed for seven CACS events during the 1987-1988 winter season. Data were available from both ascending and descending passes of the DMSP satellite on a daily basis, at approximately 0600 UTC and 1200 UTC respectively, with a 60 km resolution. Data were occasionally unavailable over the Central American region because of missing or unfavorably positioned swaths. TPW estimates are displayed for values between 0 kg/m^2 and 70 kg/m^2 in 5 kg/m^2 increments above 15 kg/m^2 . Rain rate estimates are displayed for values between -0.2 mm/h and 3 mm/h during 1987 and for values between 0 mm/h and 12 mm/h during 1988. Specific levels are detailed on a data bar for each product.

In addition, TPW was estimated using SMMR brightness temperature data for January through March of the 1983-1984 Winter season. Data are available only every other day and every other swath with this sensor. As a result, sufficient information was available to estimate TPW for only one CACS event. These TPW estimates are discussed in detail as a part of the March 1984 case study in Chapter VII. Note that the results discussed in this section are based on a sample of only 8 CACS cases.

A consistent cold surge signature was evident in the TPW field during all of the analyzed cases. A series of images (Figs. 34-38) from the 20-25 November 1987 CACS case is presented to clarify the CACS TPW signature. The distribution of TPW

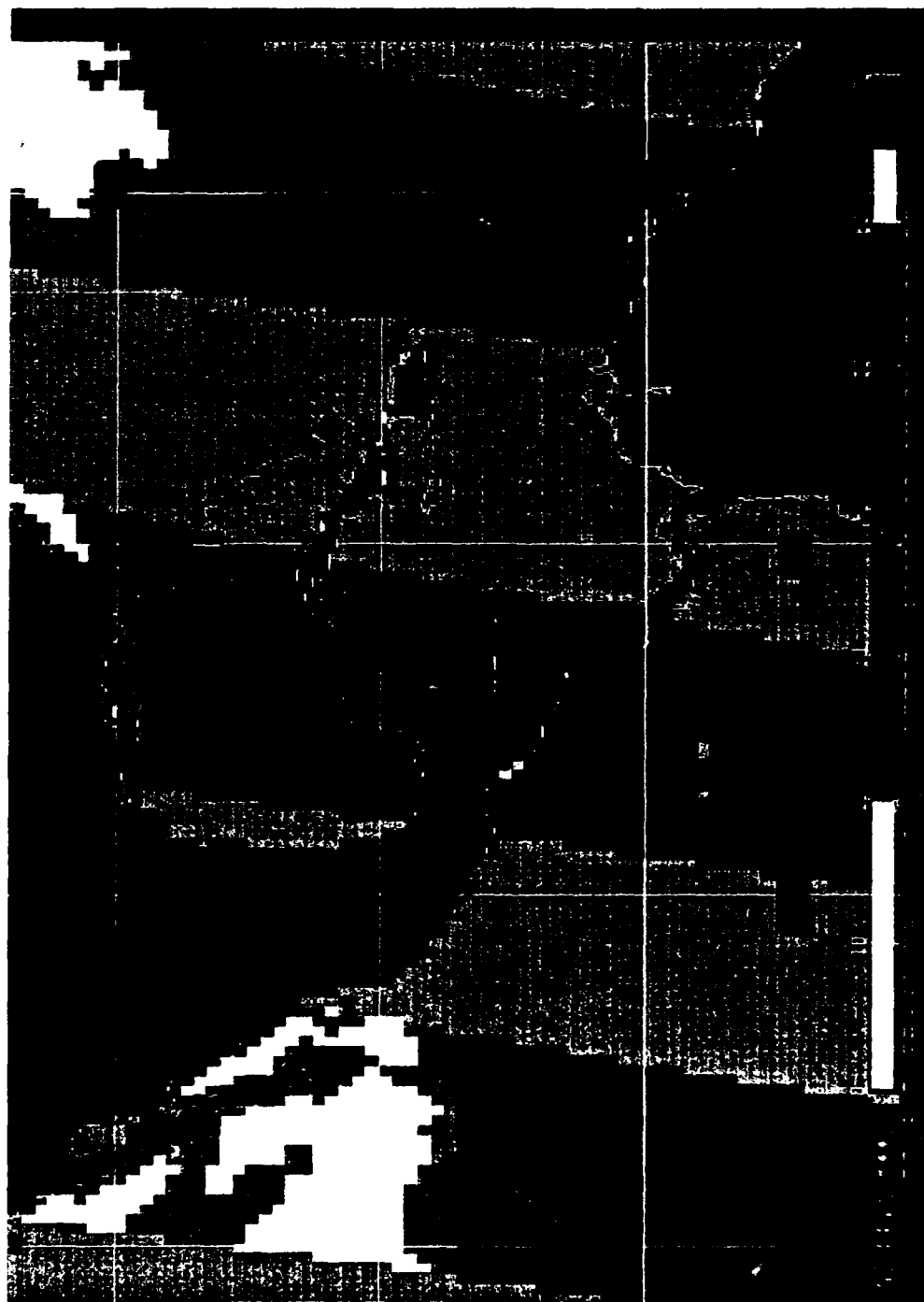


Figure 34. Total precipitable water (kg/m^2) field on 19 November 1987, 1800 UTC.

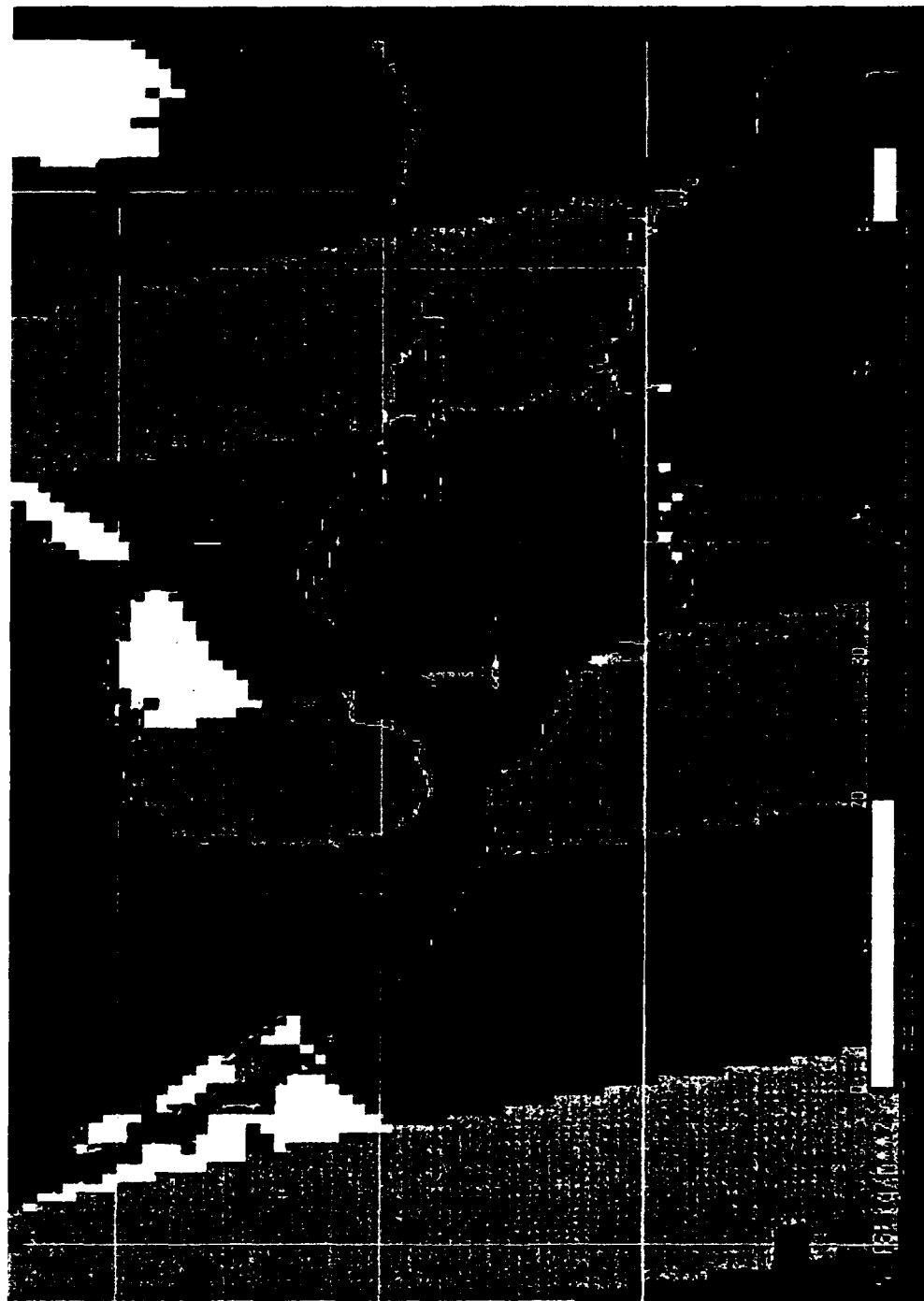


Figure 35. Total precipitable water (kg/m^2) field on 20 November 1987, 0600 UTC.



Figure 36. Total precipitable water (kg/m^2) field on 22 November 1987, 1800 UTC.

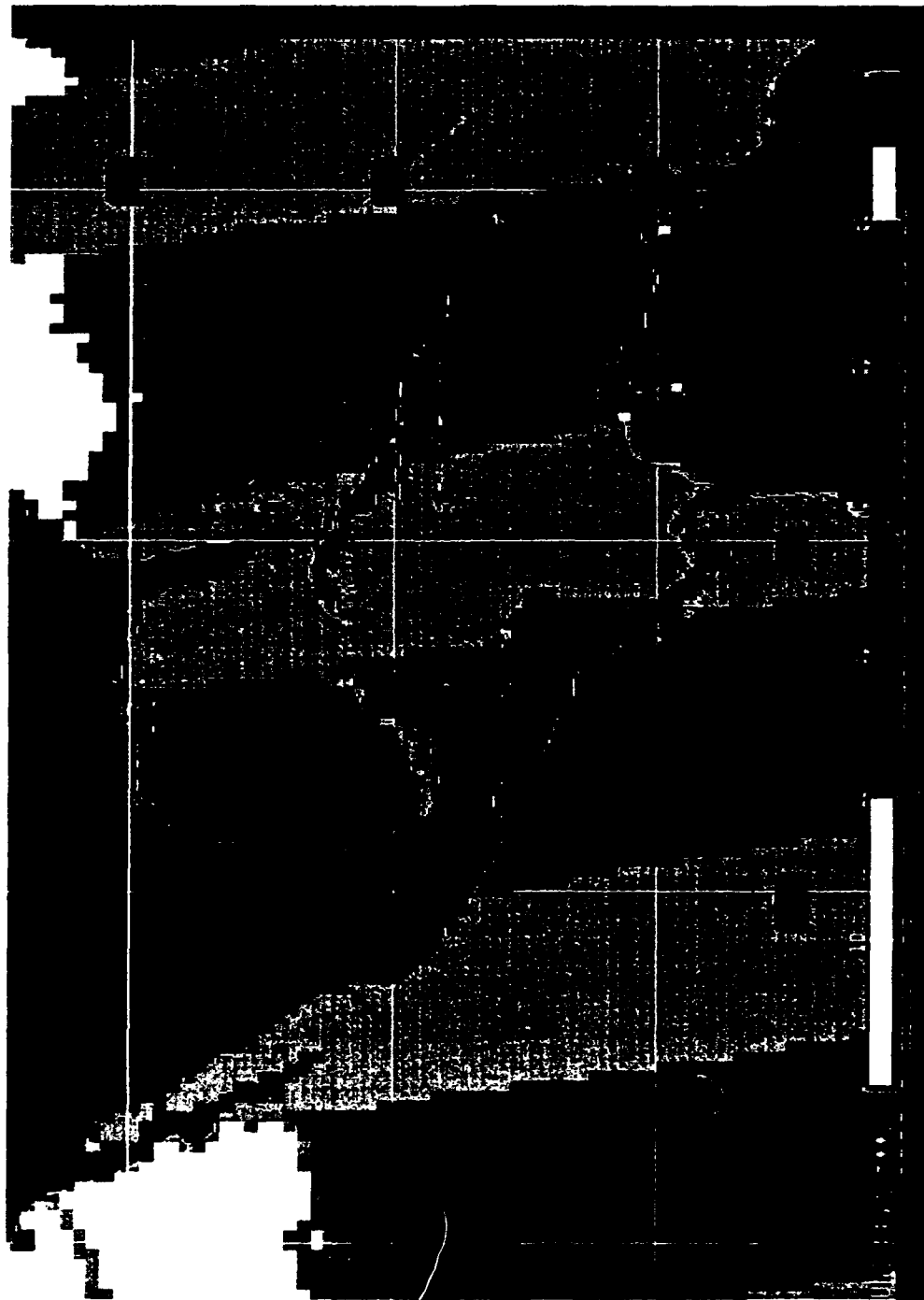


Figure 37. Total precipitable water (kg/m^2) field on 24 November 1987, 0600 UTC.



Figure 38. Total precipitable water (kg/m^2) field on 26 November 1987, 0600 UTC.

remained relatively constant during periods of trade wind flow, with a gradual poleward decrease in the magnitude of TPW from 40-60 kg/m² in the tropics to 15-30 kg/m² in the mid-latitudes. TPW values greater than 40 kg/m² were confined to areas south of 25°N in the Gulf of Mexico and south of 20°N throughout the remainder of the tropics. Imminent cold surge activity was signaled by a northward surge of TPW values greater than 45 kg/m² into the northern Caribbean east of the Yucatan Peninsula and the southern Gulf of Mexico (Fig. 34). The strongest CACS signature appeared after the surface cold front had crossed into the Gulf of Mexico. TPW values plummeted to below 20 kg/m² immediately behind the front across the northwestern 3/4 of the Gulf of Mexico (Fig. 35). The position of the surface front generally corresponded to a relative TPW maximum, on the order of 50 kg/m², extending from south of Florida across western Cuba and into the central Yucatan Peninsula. This relative TPW maximum corresponded to the position of the surface front through the duration of the cold surge. A sharp TPW gradient existed on the poleward side of the relative maximum from the southern Atlantic across central Cuba and into the Gulf of Honduras (Fig. 36). A more relaxed gradient was evident ahead of the cold surge, from Hispanola to Costa Rica, where lower TPW values of 20-40 kg/m² were apparently being advected in from the Atlantic. TPW values less than 20 kg/m² did not penetrate south of 25°N during any of the 8 CACS events studied, regardless of strength or southward penetration. This may be an indication of the strong air mass modification which takes place over the Gulf of Mexico. In addition, the location of the area of TPW values less than 20 kg/m² corresponded well to the primary focus of cold air advection behind the surface front. The relative TPW maximum gradually weakened and eventually disappeared toward the end of the cold surge (Fig. 37). A strong poleward TPW gradient remained from Cuba toward the northwest, but TPW values greater than 40 kg/m² had regained control of the

Caribbean. The poleward gradient gradually weakened through the remainder of the period (Fig. 38), while a surge of high TPW values north of the Yucatan Peninsula was again evident moving into the Gulf of Mexico in advance of the next cold surge.

Rain rate estimates also displayed a consistent pattern during all of the analyzed CACS events. Rain rate maximums were clearly confined to the immediate vicinity of the surface front through the duration of each event. The greatest rain rates (greater than 2 mm/h) were generally evident while the cold front was crossing the Gulf of Mexico (Fig. 39). Rain rate decreased steadily as each front progressed further south. More widespread areas of precipitation were evident along the northward facing coastlines of Central America, especially along the northern Honduras coast (Fig. 40), in response to orographic lifting of the cold surge induced northerly flow. Rain rate is examined in more detail in Chapter VII.

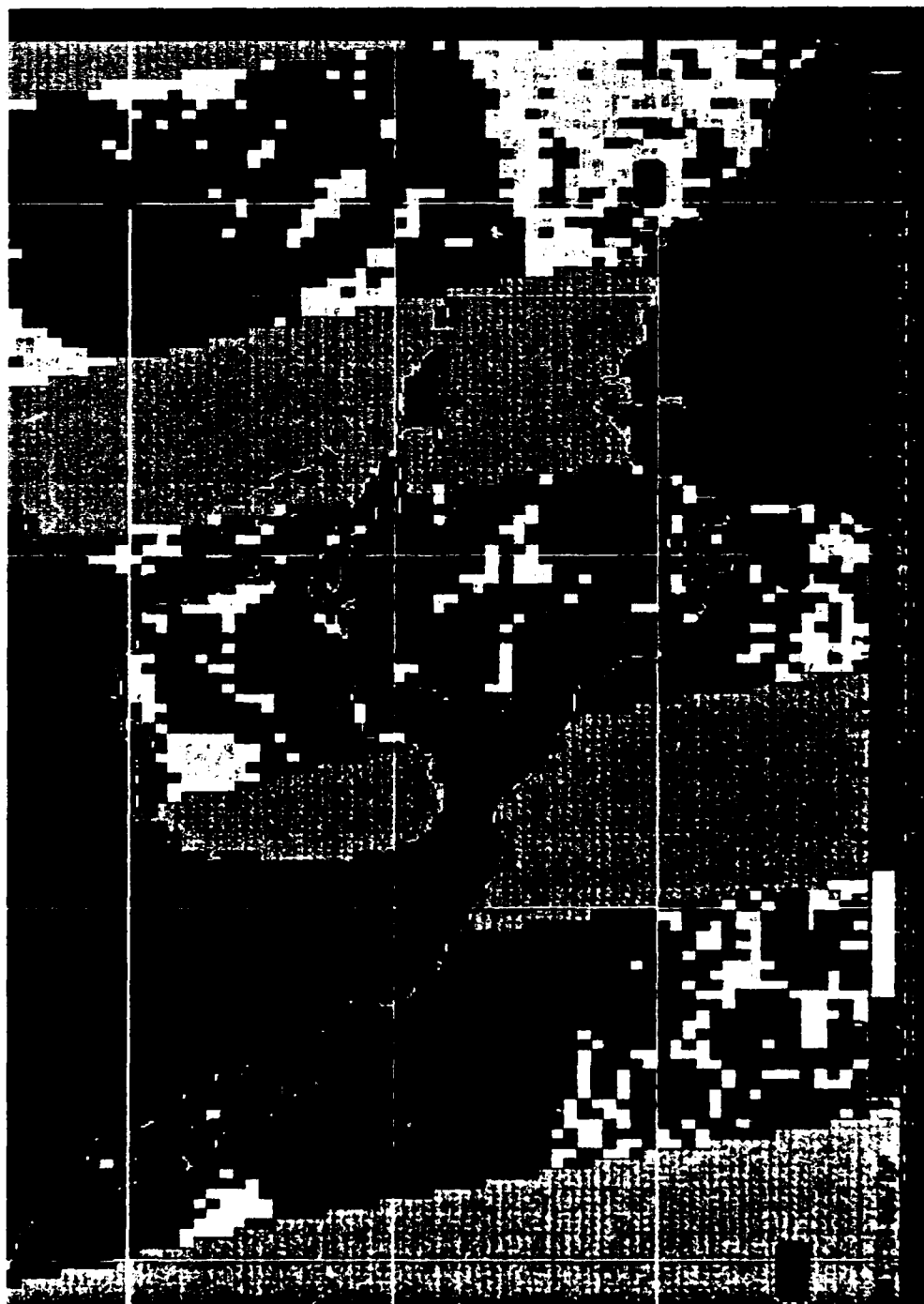


Figure 39. Rain rate (mm/h) on 19 November 1987, 0600 UTC.



Figure 40. Rain rate (mm/h) on 21 November 1987, 1800 UTC.

CHAPTER VII

CASE STUDIES

This chapter examines the life cycle of three CACS events through a detailed analysis of the evolution of the cloud features, surface variables, vertical structure and moisture fields of each cold surge as it progresses through Central America. Although no single CACS can be considered a "typical" event, these three cases were chosen because they displayed features typical of many cold surges. In addition, these cases occurred during times when consistent data were available from all remote and surface sources.

Hourly GOES IR imagery was analyzed for each case with emphasis on the development of cold surge associated cloud features. Surface variables, including daily maximum and minimum temperature, dew point, wind direction, wind speed, sea level pressure, precipitation and cloud ceiling height were examined at each station affected by the cold surge for a thirteen day period centered on the date of frontal passage at the northern most station. In this way, the time of frontal passage at each station could be visualized relative to the other stations. Temporal cross sections were produced for all upper air reporting stations affected by each cold surge to evaluate the evolution of atmospheric vertical structure. Consistent 12-hourly observations were available only for Belize City. Data at all other stations were available only at 1200 UTC, so cross sections were normally produced for an eleven day period centered on the date of frontal passage. The number of observations included in each plot varied slightly based on data availability. Evolution of the moisture field during each event was examined using SMMR TPW estimates and SSM/I TPW and rain rate estimates.

CASE 1: 6-12 MARCH 1984

Satellite Cloud Signatures

The pre-cold surge stage of this event on 4 March was characterized by a relatively weak cyclone located over southern Lake Michigan with a cold front extending southwest into Texas. Central America was dominated by weak easterly flow with minimal cloud cover evident. By 6 March, the parent cyclone had moved off the northeast coast of the United States and the cold front extended along the eastern U.S. coast into the northern Gulf of Mexico (Fig. 41). Features of the front were partially obscured by high-level cloud cover. A break in the cirrus over southern Mexico revealed stratocumulus banked up against the Sierra Madres, indicating northeasterly low-level flow was present. The cold front passed Merida later in the afternoon. Jet stream cirrus continued to obscure features of the frontal system on 7 March; however, distinct low-level cloud features became apparent from southern Mexico into Central America (Fig. 42). Northwesterly to northeasterly low-level flow was indicated by a broad band of broken to overcast stratocumulus extending across the southern half of the Gulf of Mexico. The southern edge of the cloud band clearly followed the highest terrain features from central Mexico across northern Guatemala and into western Honduras. A sea breeze was evident along the Caribbean coast of Nicaragua, indicating that low-level easterly flow remained in control over areas ahead of the cold surge. Little evidence of the surface front remained by 9 March, except a poorly defined band of low clouds extending across the southern Atlantic (Fig. 43). However, northerly low-level flow clearly remained dominant across the majority of southern Mexico and northern Central America, with broken to overcast stratus/stratocumulus extending south to the border of Honduras and Nicaragua and nearly clear skies on the Pacific side of the

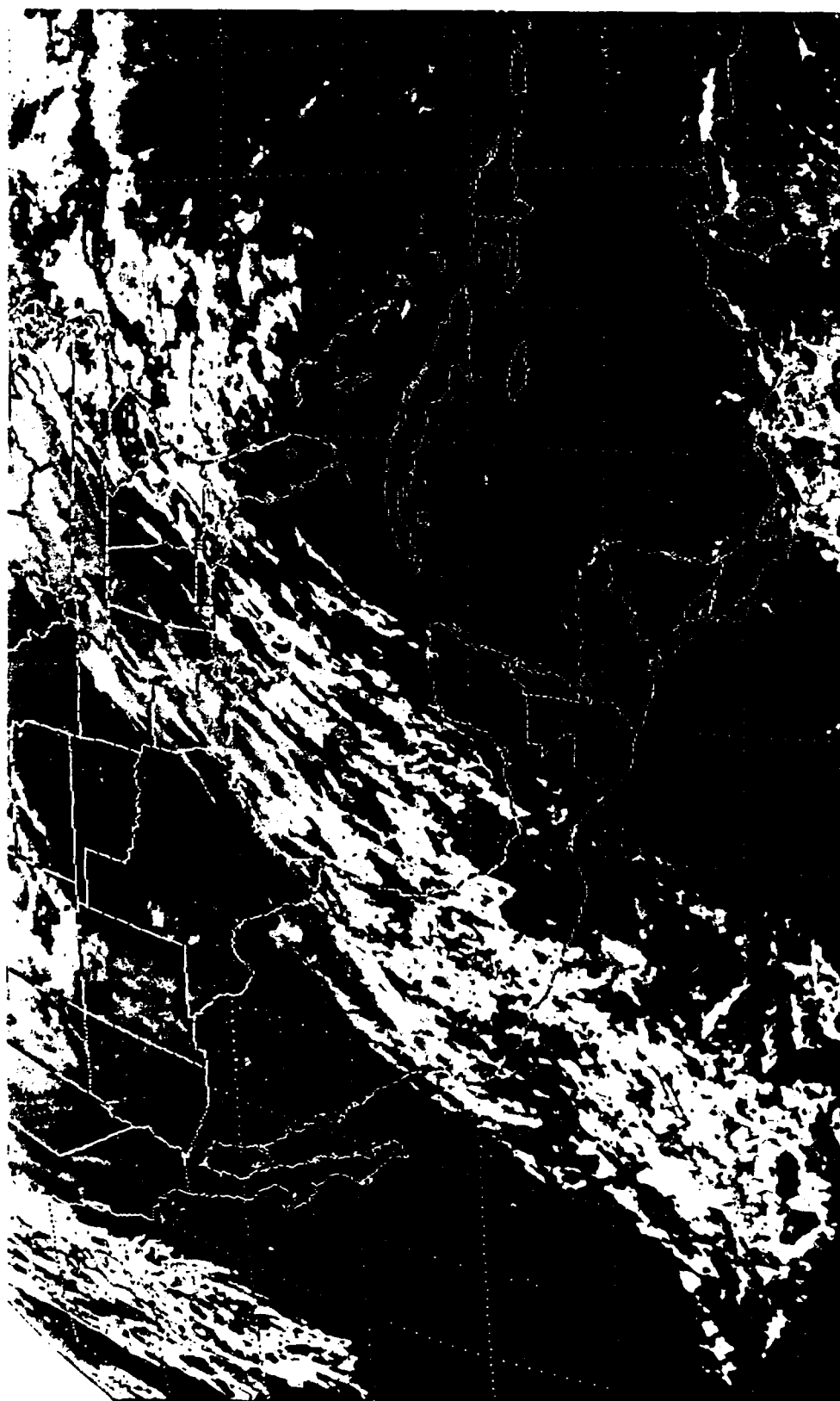


Figure 41. GOES IR satellite image with MB enhancement from 6 March 1984, 1500 UTC.

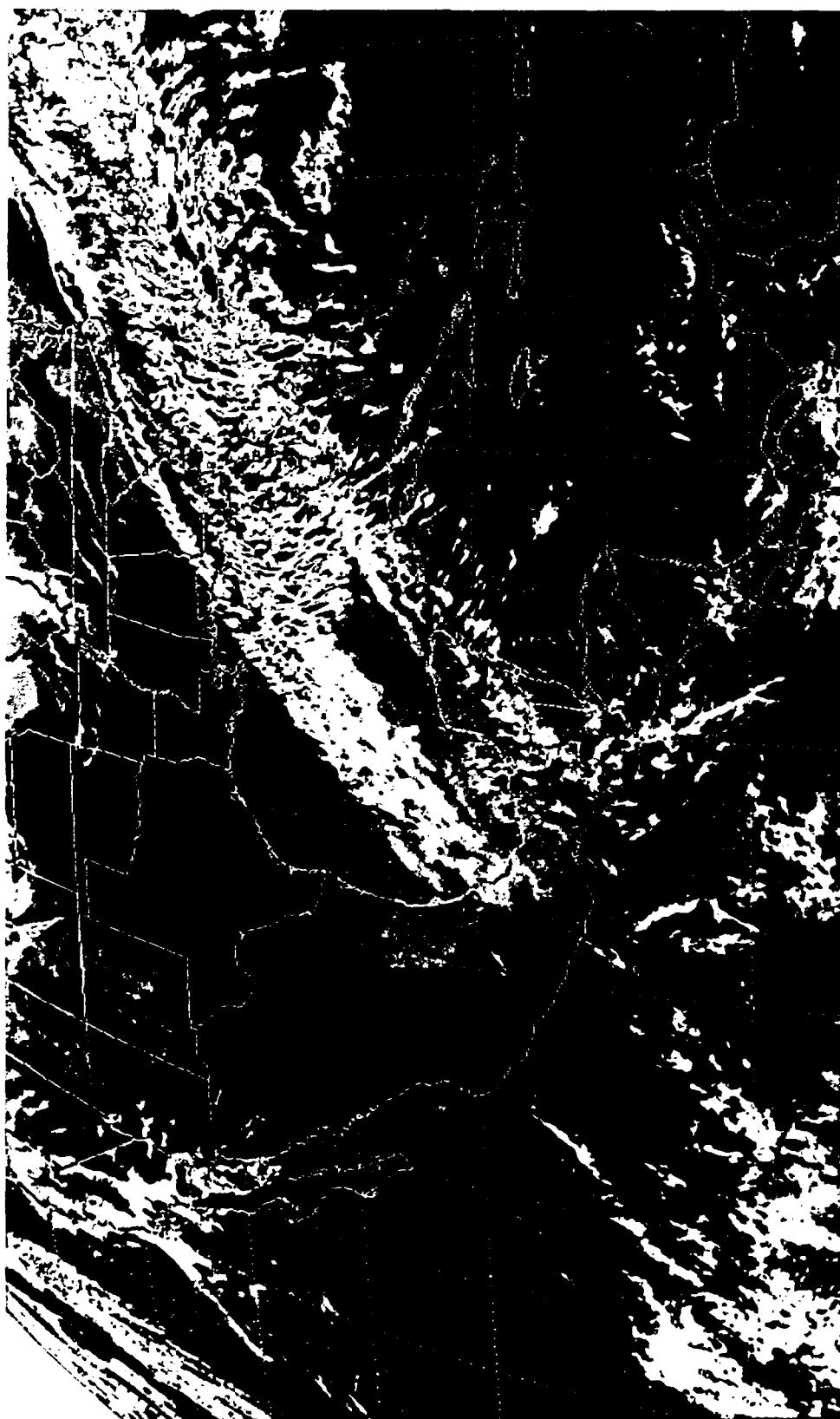


Figure 42. GOES IR satellite image with MB enhancement from 7 March 1984, 1800 UTC.

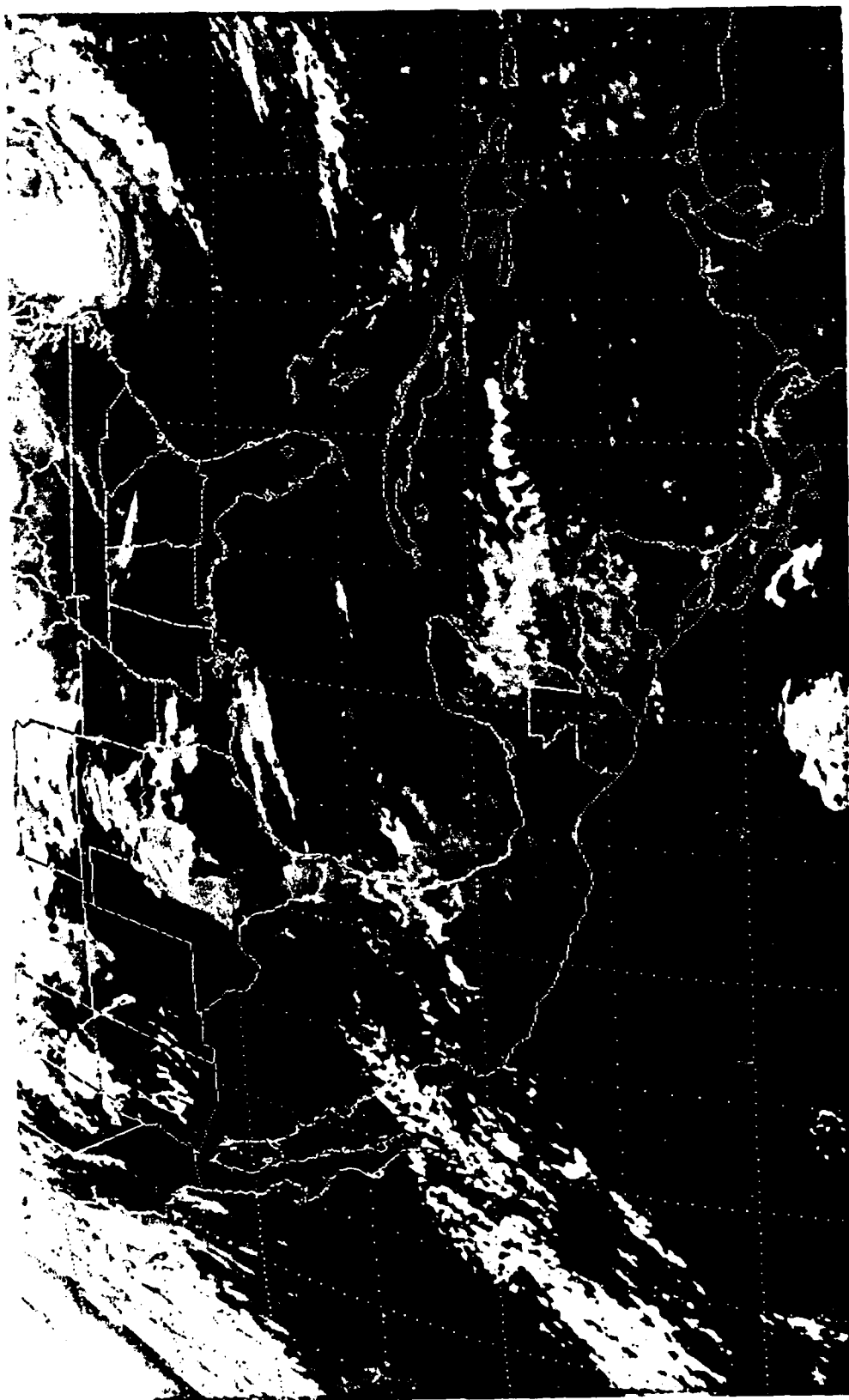


Figure 43. GOES IR satellite image with MB enhancement from 9 March 1984, 1800 UTC.

Isthmus. Although no clearly defined frontal cloud band was evident, the leading edge of the stratus over southern Honduras marked the position and maximum southward penetration of this event at 13°N. By 12 March, no evidence of the cold surge was apparent and easterly low-level flow had regained control over all of Central America.

Surface Variables

This was a moderate CACS event which lasted 6 days and produced a 12°C temperature drop at Merida. The cold surge penetrated to approximately 13°N, so Merida, Mexico, Belize City, Belize, Flores, Guatemala, Guatemala City, Guatemala, La Mesa, Honduras and Tegucigalpa, Honduras were included in the analysis. San Salvador, El Salvador was not included because of missing data. Surface variable trends were centered on the date of frontal passage at Merida (7 March) and extended from 1 March through 13 March.

Daily maximum and minimum temperature trends are presented in Fig. 44. All stations displayed a typical CACS signature, with a gradual temperature rise followed by a distinct drop in daily high temperature immediately after frontal passage. CACS signals were apparent, but much less dramatic in the daily minimum temperature trends. La Mesa, although located over 500 km south of Merida, experienced a 14°C drop in daily maximum temperature, the largest of any station.

Dew point exhibited a cold surge associated drop at all stations except Tegucigalpa (Fig. 45). The strongest CACS signature occurred at the two northern most stations, Merida and Belize City, with a 9°C drop in dew point during the first 48 h after frontal passage. Flores, Guatemala City and La Mesa experienced 4°-6°C drops in dew point after frontal passage.

Wind direction displayed the most distinct CACS signal (Fig. 46). The prevailing

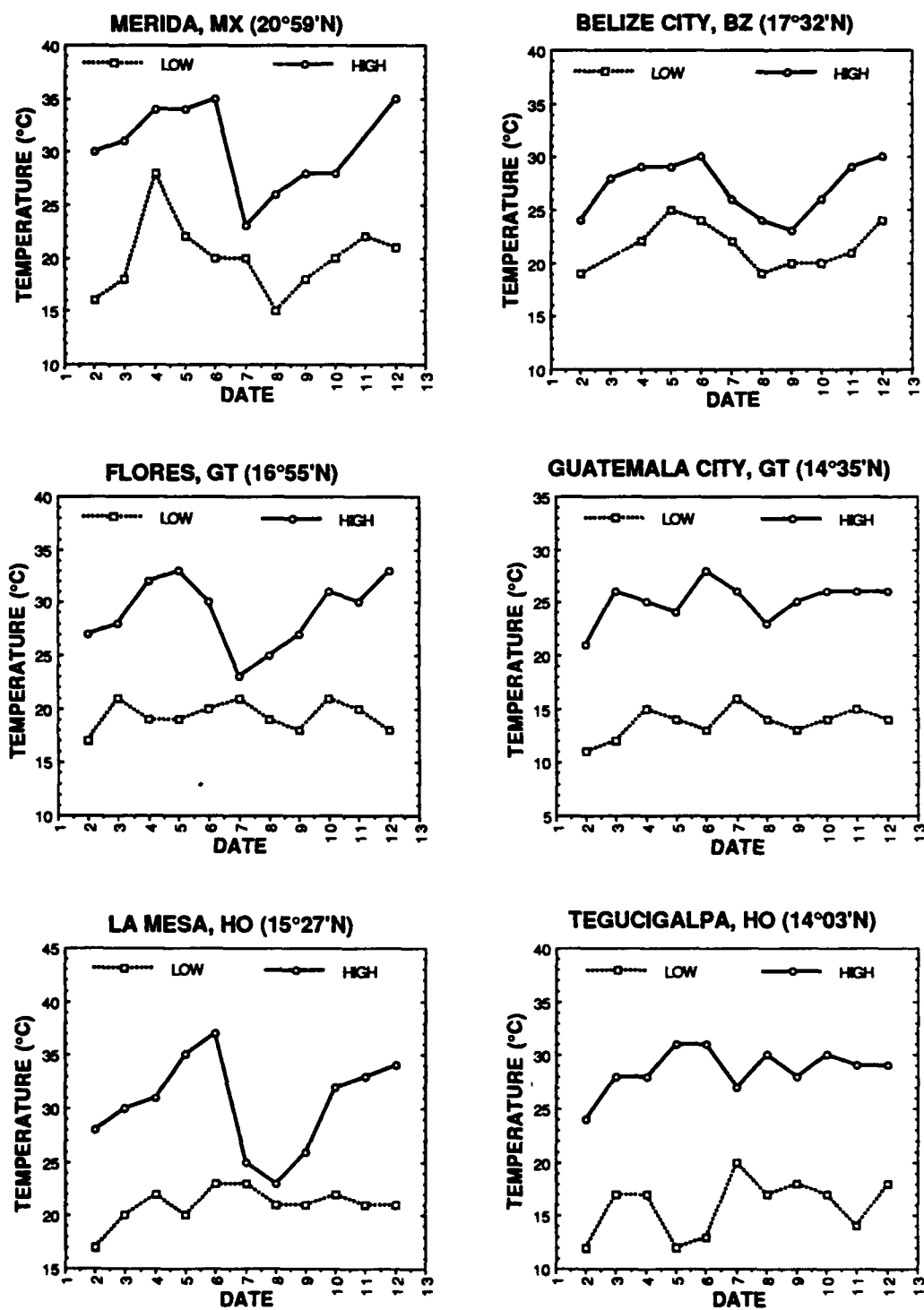


Figure 44. Daily maximum and minimum temperatures (°C) from 1-13 March 1984.

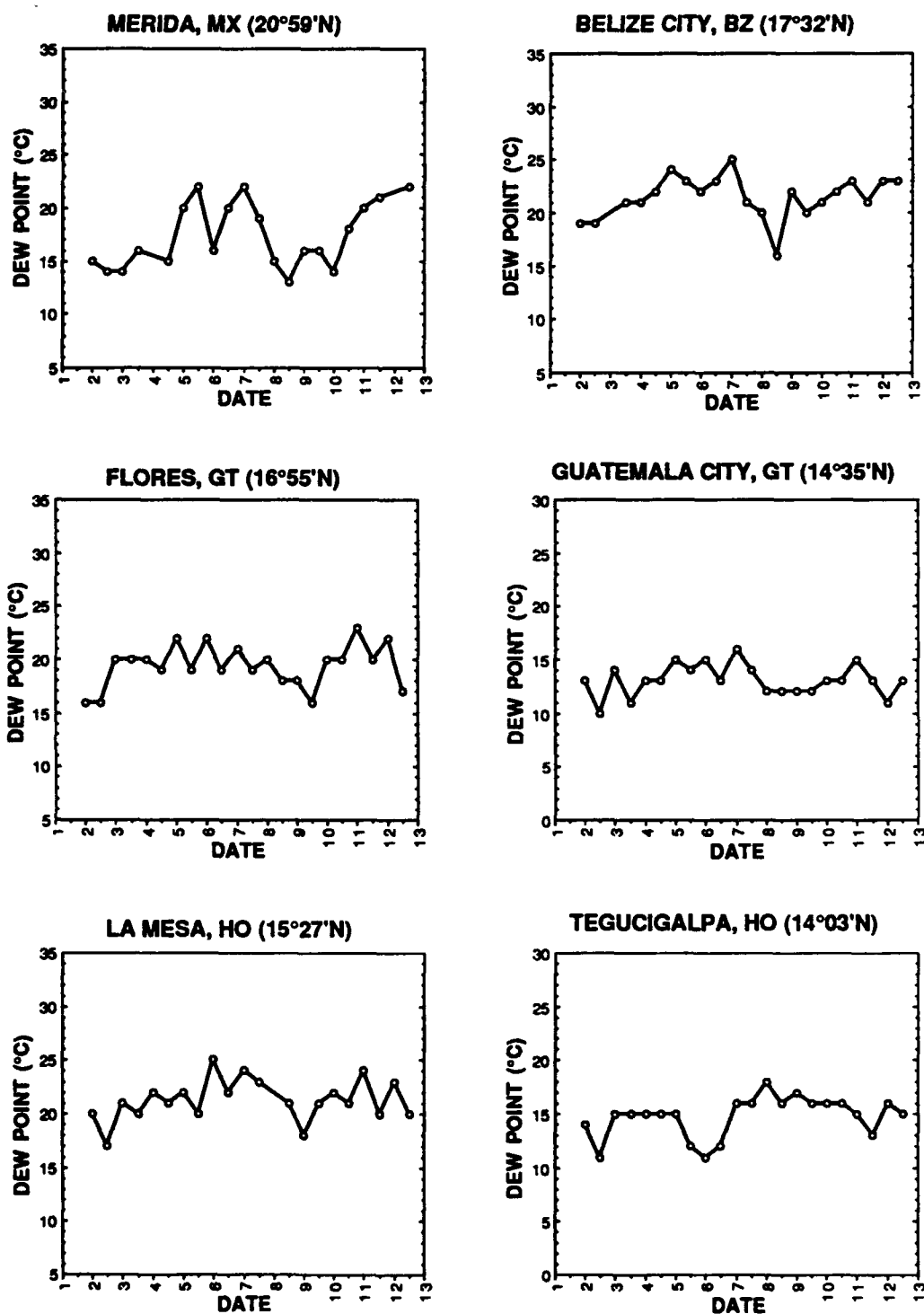


Figure 45. Dew point (°C) at 0000 UTC and 1200 UTC from 1-13 March 1984.

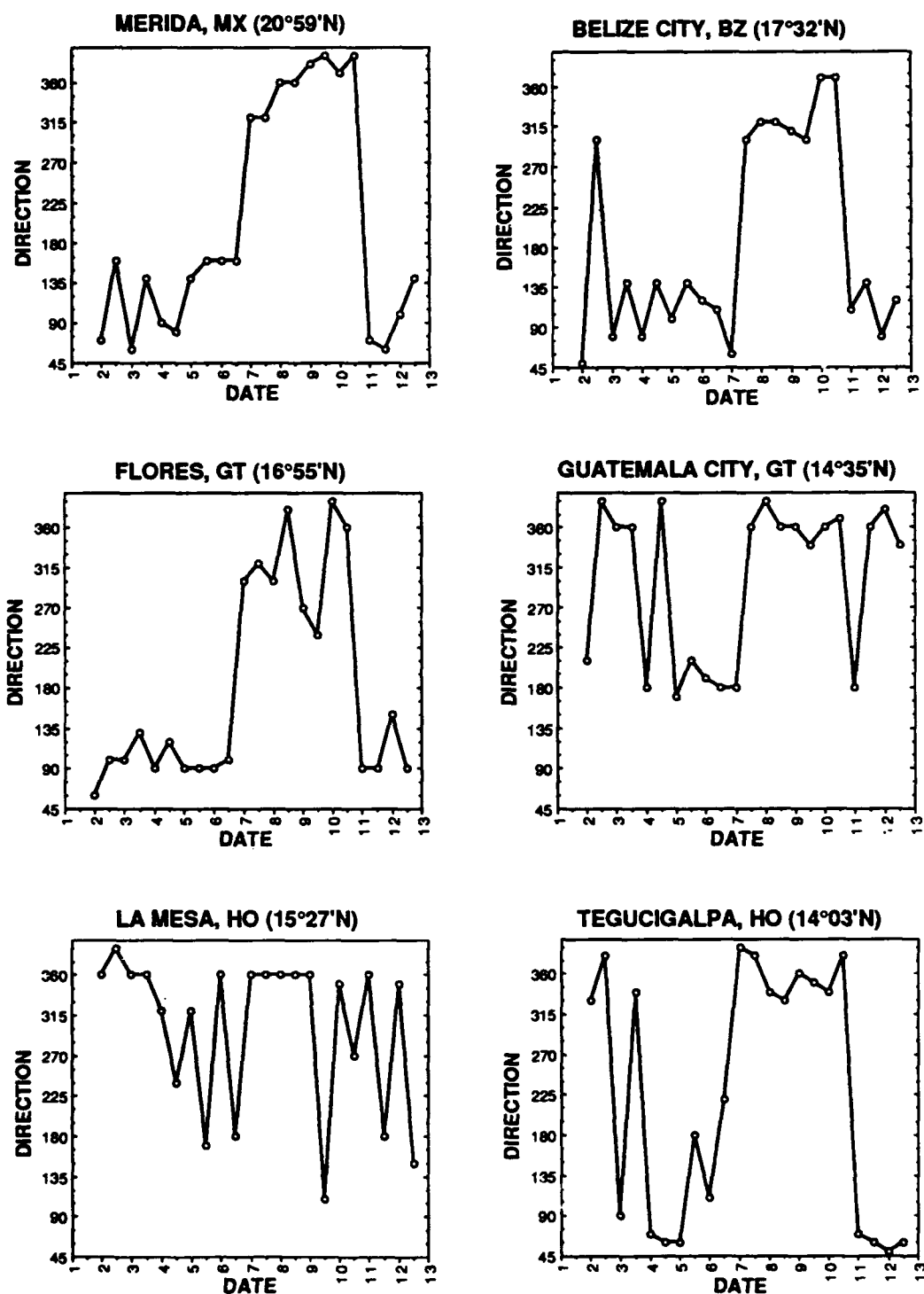


Figure 46. Wind direction at 0000 UTC and 1200 UTC from 1-13 March 1984.

low-level flow is easterly during the winter season at Merida, Belize City and Flores. Wind direction shifted from east - southeast to northwest at all three stations immediately after frontal passage and remained from the northwest until the end of the cold surge on 11 March. The low-level flow patterns at Guatemala City, La Mesa and Tegucigalpa are primarily controlled by mountain/valley breezes throughout the year, resulting in radical diurnal shifts in wind direction. Frontal passage at these stations was clearly indicated both by northerly flow and an absence of the normal diurnal fluctuation in wind direction.

As with mean wind speed at Merida, wind speed at individual stations showed very little response to frontal passage (Fig. 47). Wind speeds at Merida, Belize City, Flores and La Mesa varied randomly throughout the period. At Guatemala City and Tegucigalpa, however, wind speeds increased 5-7 m/s during the period immediately after frontal passage. Both stations are located in mountainous regions with a relatively unobstructed system of valleys extending north and east all the way to the Caribbean coast. Therefore, the cold surge associated wind speed increase was probably a result of both the shift to northerly flow behind the cold front and funnelling effects.

SLP displayed the most consistent CACS signature, with a well defined pressure jump evident at every station immediately after frontal passage (Fig. 48). The magnitude of the pressure jump generally decreased from northern stations (16.1 mb at Merida) to southern stations (7.6 mb at Tegucigalpa). However, Flores displayed the most impressive jump with SLP increasing 17.8 mb between 6 March at 0000 UTC and 8 March at 1500 UTC.

Significant changes in cloud ceiling height were evident at every station (Fig. 49). However, the signature was not as clearly defined or as consistent as the cold surge associated changes in wind direction or SLP. Clear skies or only scattered cloud cover

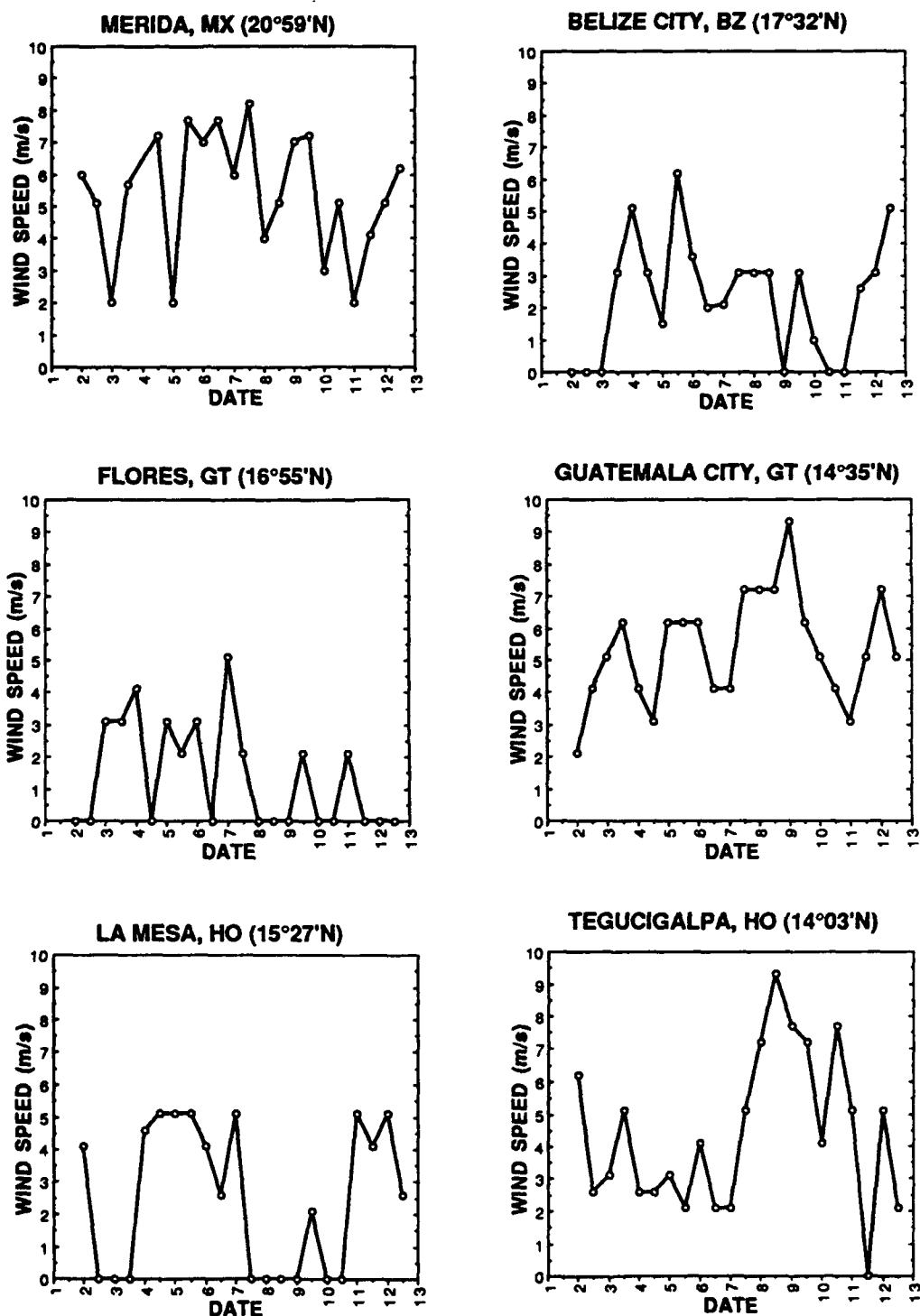


Figure 47. Wind speed (m/s) at 0000 UTC and 1800 UTC from 1-13 March 1984.

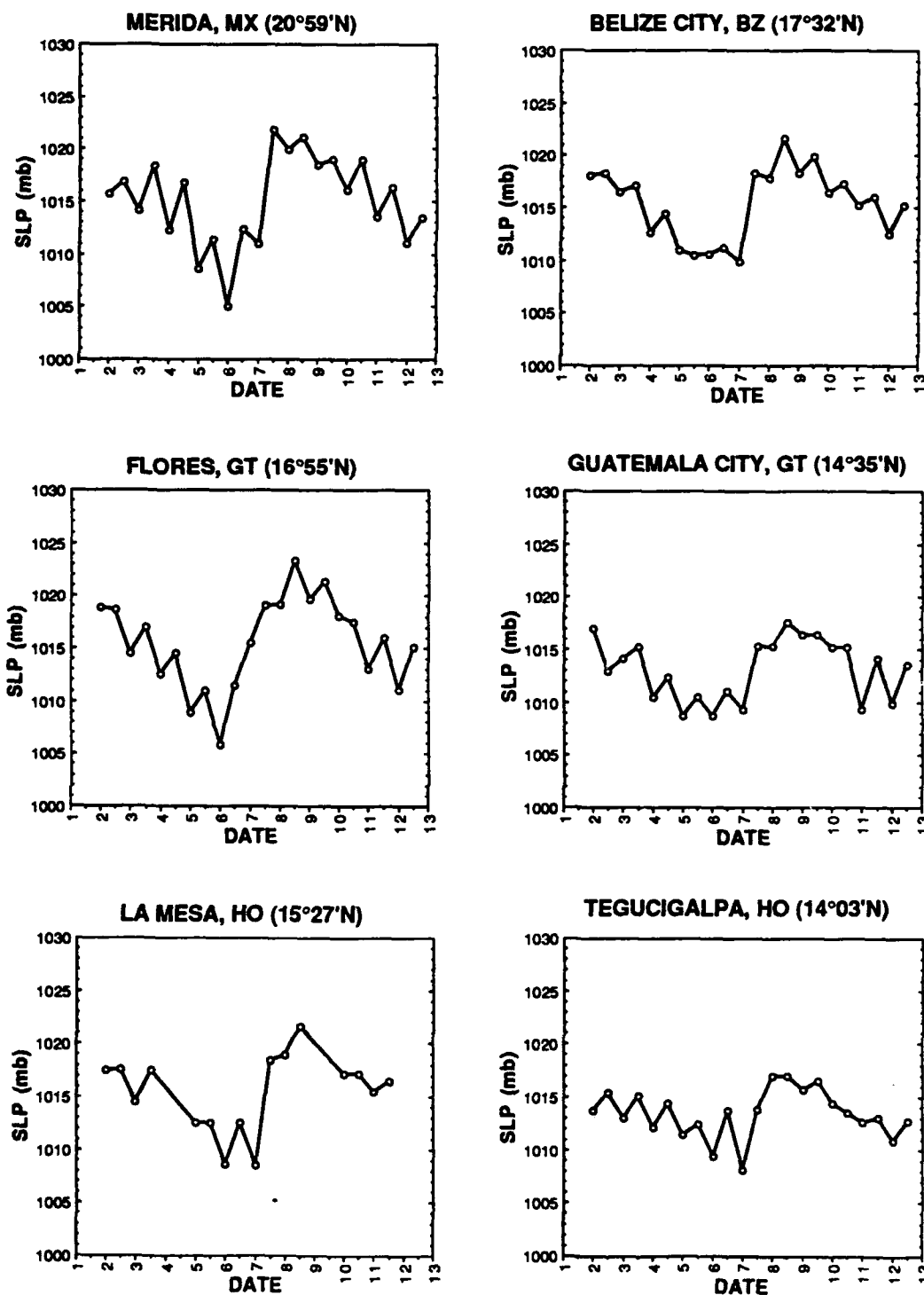


Figure 48. Sea level pressure (mb) at 0000 UTC and 1500 UTC from 1-13 March 1984.

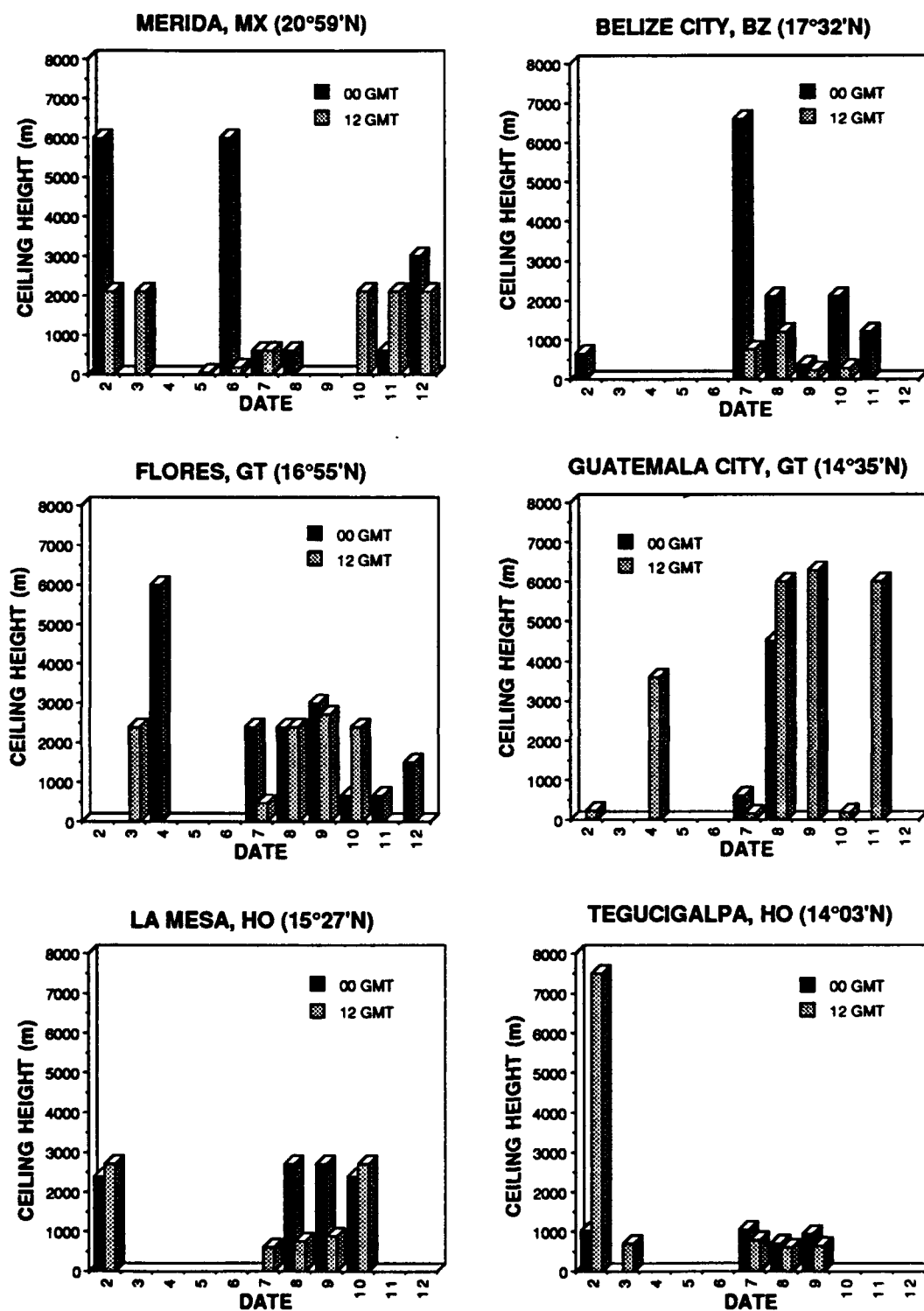


Figure 49. Cloud ceiling height (m) at 0000 UTC and 1200 UTC from 1-13 March 1984.

dominated the days prior to frontal passage. Cloud cover increased immediately before frontal passage and cloud ceiling heights generally decreased during or immediately after frontal passage. The duration of cold surge associated cloud cover and the height of the cloud ceilings varied greatly from station to station.

Precipitation was recorded with frontal passage at every station except Guatemala City (Fig. 50). Belize City and Flores received the most rainfall during the CACS event with 19 mm and 15 mm respectively.

Vertical Structure

Temporal cross sections of upper air data were generated for Belize City and Guatemala City. A cross section was not produced for Tegucigalpa because of missing data. The procedure outlined in the vertical structure section of Chapter VI was also used to produce the cross sections presented in this chapter.

The Belize City cross section included 12-hourly observations from 5 March at 1200 UTC through 9 March at 1200 UTC (Fig. 51). Moisture was initially capped near 850 mb by a weak subsidence inversion. A frontal inversion was identified between 700 mb and 600 mb from a previous cold surge event. Another inversion was evident between 800 mb and 600 mb from 7 March through 8 March at 1200 UTC. While it shared characteristics of both frontal and subsidence inversions, this layer was definitely a boundary between air masses. Surface winds shifted to the northwest after frontal passage and winds below the inversion shifted from west-northwest to east-northeast. The atmosphere above the inversion was relatively dry with prevailing westerly flow. Significant moisture was capped below the inversion where wind directions ranged from east to northwest. A weak frontal inversion was also apparent near 900 mb on 9 March. The atmosphere displayed a trend toward decreasing stability prior to frontal passage.

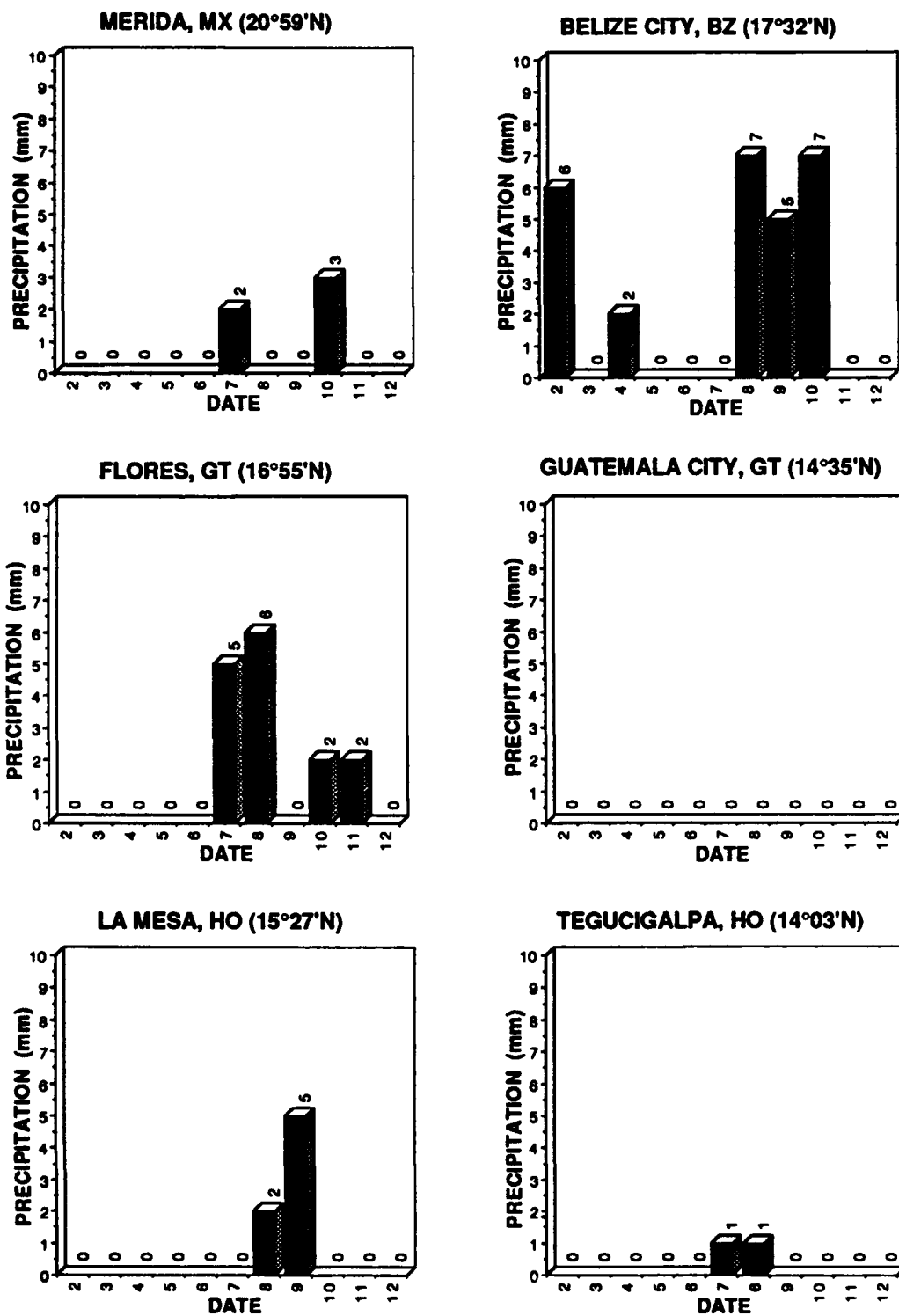


Figure 50. Daily precipitation (mm) from 1-13 March 1984.

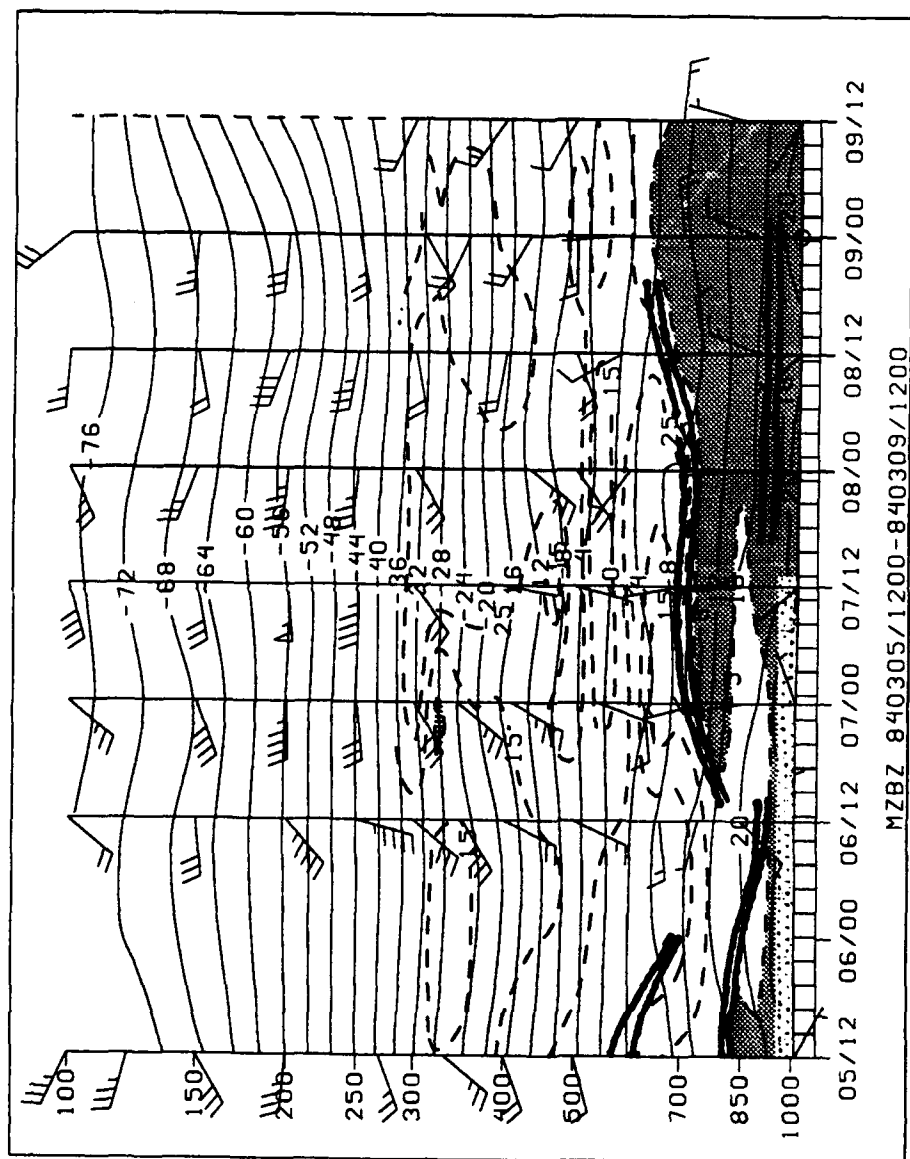


Figure 51. Vertical temporal cross section at Belize City, Belize from 5 March 1984, 1200 UTC to 9 March 1984, 1200 UTC. Isotherms (solid) are plotted at 4°C intervals and isodrosotherms (dashed) at 5°C, 15°C and 25°C. Also shown are areas with dew point depression less than or equal to 5°C (shaded), wind speed (kt) and direction, and inversion layers (heavy solid).

The maximum instability occurred immediately before frontal passage when the Lifted Index was -3.1 and the K Index was 25.3. Very stable conditions prevailed after frontal passage and through the remainder of the period. However, the majority of the rainfall at Belize occurred after the frontal passage. This highlights the fact that the majority of the precipitation associated with CACS events is stratiform, not convective.

The cross section from Guatemala City (Fig. 52) displayed very similar features. A weak frontal inversion was evident near 500 mb through 5 March from the previous cold surge, while a subsidence inversion capped moisture below 700 mb. Very little evidence of a frontal passage was apparent except for the shift to northerly flow in the low-levels on 7 March, and the shift in mid-level flow (700-300 mb) from southwest to northeast from 8-11 March. Another subsidence inversion capped moisture below 700 mb after 9 March. The atmosphere remained stable through the entire period.

Moisture Analysis

TPW was estimated using SMMR brightness temperatures for this case. Data were available every other day from 3 March through 13 March. TPW was calculated in kg/m^2 and plotted in 4 kg/m^2 increments. Data contaminated by land were not blacked out; however, it is easy to recognize on the plots as an area of abnormally low TPW with a sharp TPW gradient outlining the shape of the land mass. Analysis was complicated by the fact that the position of individual swaths varies with each pass of the satellite. Therefore, detailed analysis of features with the temporal and spatial scales of a cold surge can be challenging.

Data from 3 March are presented in Fig. 53. This was four days before CACS onset and the cold front had not yet entered the Gulf of Mexico. TPW values increased slowly from 20 kg/m^2 over the northern Gulf to 32 kg/m^2 near the Yucatan Peninsula. No

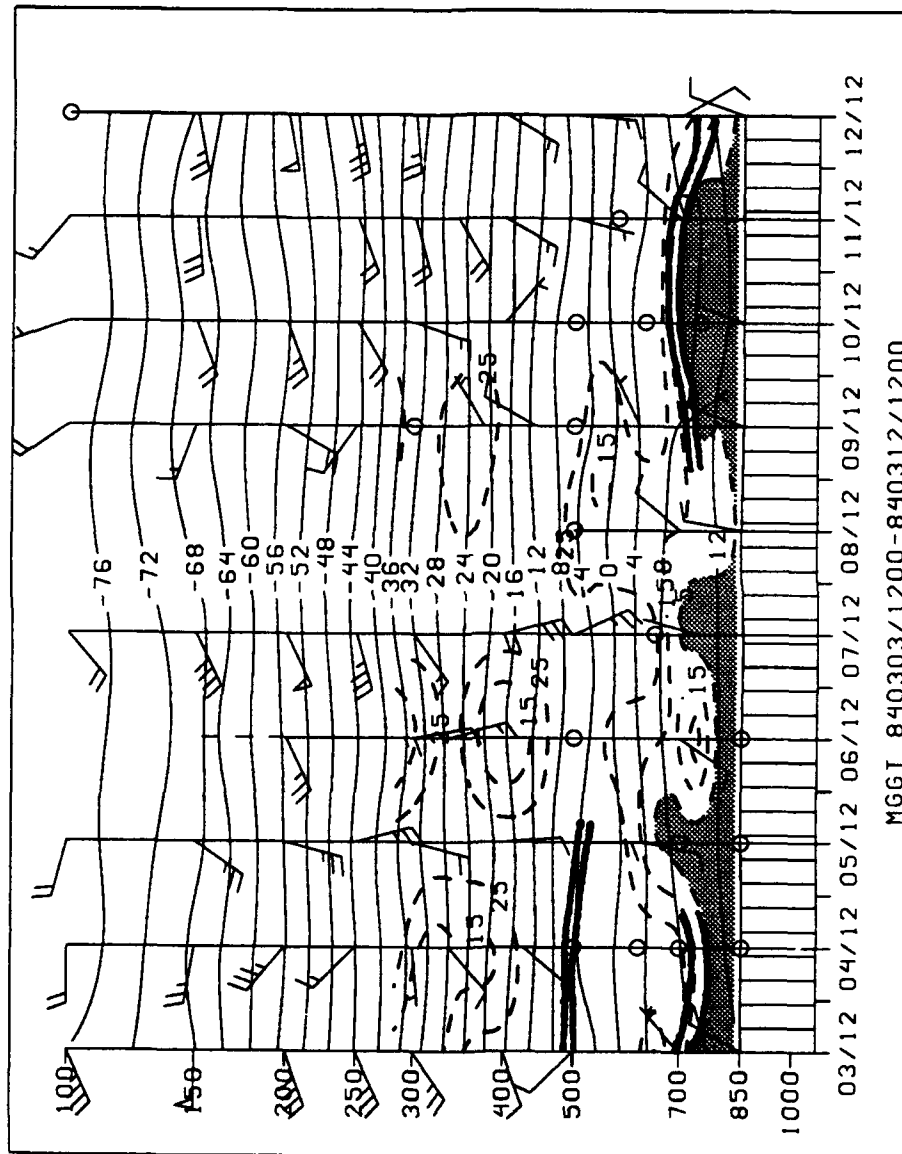


Figure 52. As in Fig. 51, except at Guatemala City, Guatemala from 3 March 1984, 1200 UTC to 12 March 1984, 1200 UTC.

specific features were evident. By 5 March, TPW values had increased to over 32 kg/m² throughout at least the western Gulf of Mexico, although the area of data coverage was too small to identify a specific trend. TPW values in the Caribbean ranged from 32 kg/m² to over 40 kg/m² south of Cuba. Data from 7 March (Fig 54) confirmed that TPW values had increased to 36–40 kg/m² ahead of the cold front over the Gulf of Mexico. TPW values had decreased slightly over the Caribbean. Data from 9 March was highly contaminated by a band of precipitation over the northern Gulf of Mexico and no useful information could be extracted from the TPW plot. TPW values over the Caribbean continued to decrease on 11 March (Fig. 55). The 32 kg/m² contour was displaced from the central Caribbean on 7 March to near the Panama and Colombia coast lines. The cold surge was over on 13 March and TPW values had returned to pre-cold surge levels throughout the Caribbean and Gulf of Mexico. An area of TPW greater than 40 kg/m² was evident north of the Yucatan Peninsula, indicating another rise in TPW over the Gulf in advance of the next cold surge.

Summary

This was a moderate cold surge, and did not appear particularly impressive on GOES imagery. However, the evolution of surface variables, especially wind direction, confirmed the satellite analysis of CACS duration (6 days) and maximum southward penetration (13°N). Surface variables at all stations displayed distinct responses to CACS onset. In general, the intensity of each response decreased equatorward, the major exception being La Mesa's 14°C drop in daily maximum temperature. Surface variable response to CACS onset also depended on station elevation and terrain, especially the response of wind direction between coastal and mountain stations. CACS vertical structure depends even more on latitude and station elevation, as the cold surge

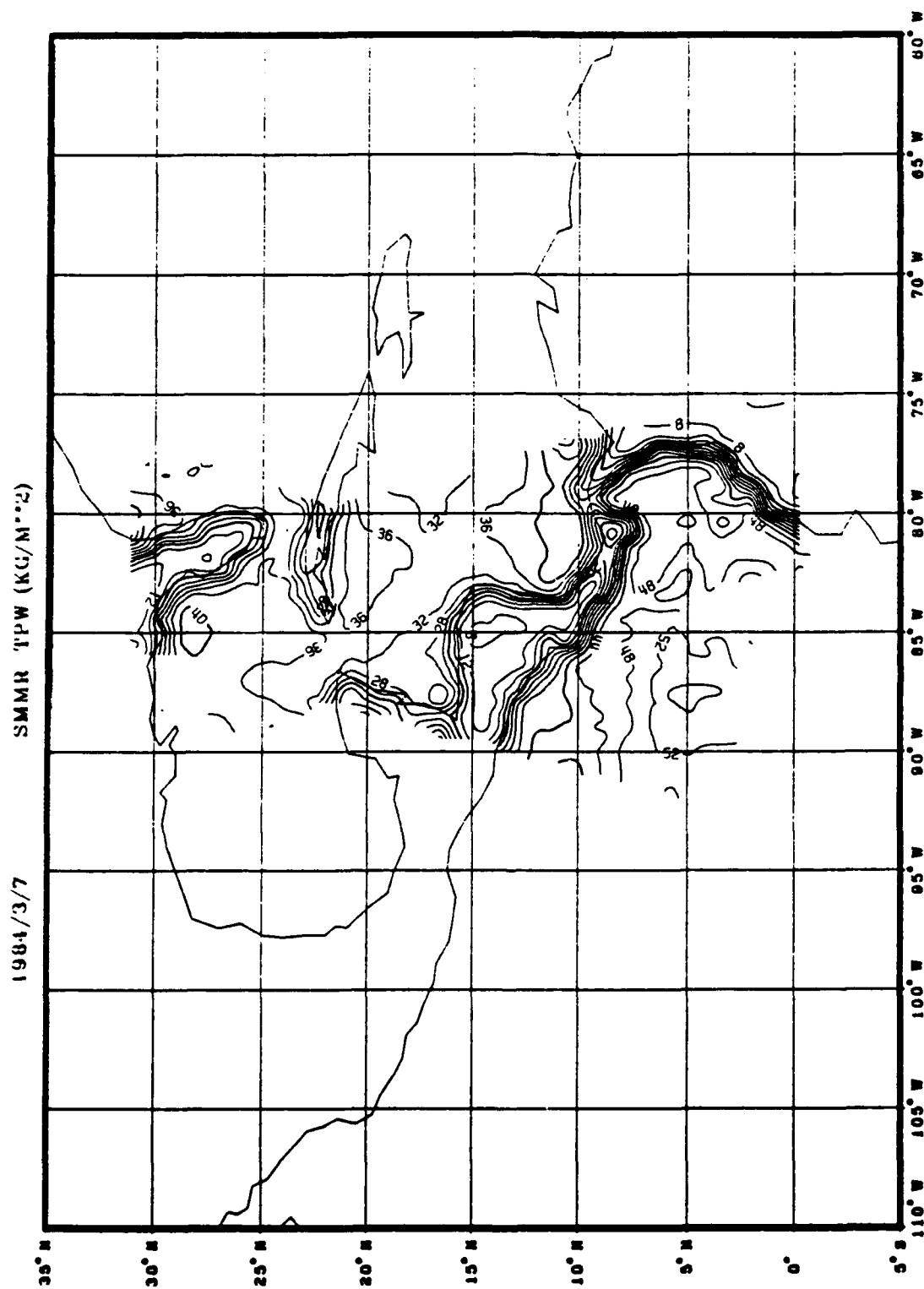


Figure 54. Total precipitable water (kg/m^2) field on 7 March 1984.

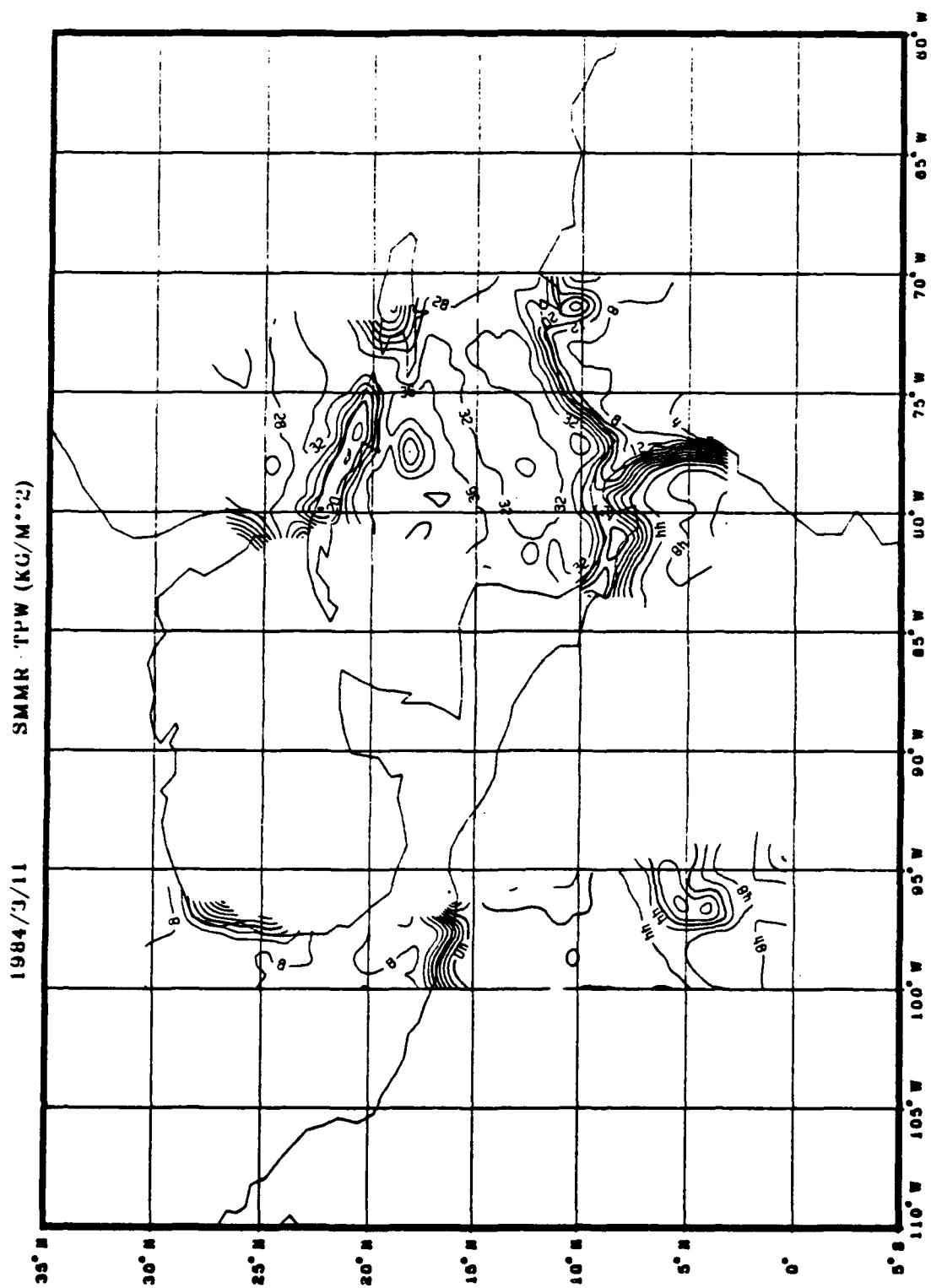


Figure 55. Total precipitable water (kg/m²) field on 11 March 1984.

appeared much weaker at Guatemala City than at Belize City. The Belize City cross section emphasized that CACS induced precipitation is primarily stratiform. Belize City received 19 mm of rainfall with a strong inversion at 700 mb and a stable atmosphere.

CASE 2: 20-25 NOVEMBER 1987

Satellite Cloud Signatures

GOES imagery from 19 November depicted a weakening cold front extending from the northern Atlantic across the southeastern U.S. and into the central Gulf of Mexico. The front had been stationary for 36-48 h, but a wave was beginning to develop along it over Georgia and South Carolina. Broken low-level cloud cover and isolated rainshowers dominated most of Central America indicating a weak easterly low-level flow pattern. November is still wet season in the American tropics and the ITCZ was active between 5°N and 10°N. The wave had rapidly developed into a mature cyclone located over the eastern Great Lakes by 20 November (Fig. 56). A well defined frontal cloud band was evident extending across central Cuba into the Gulf of Honduras and Guatemala. Cloud lines in the southwestern Gulf of Mexico and a broken to overcast stratocumulus layer closely following the terrain features in southern Mexico and Guatemala clearly indicate northerly low-level was dominant behind the cold surge. Low-level flow over the remainder of Central America was difficult to determine because of image contamination by upper level convective debris. A more stable situation dominated Central America on 22 November allowing a better view of the low-level CACS features. The parent storm continued to intensify as it moved off the northeast U.S. coast and the main thrust of the cold air was now clearly off the central Atlantic coast (Fig. 57). The southern end of the front had weakened, but was still apparent extending between Cuba and Haiti, across Jamaica and into northeast

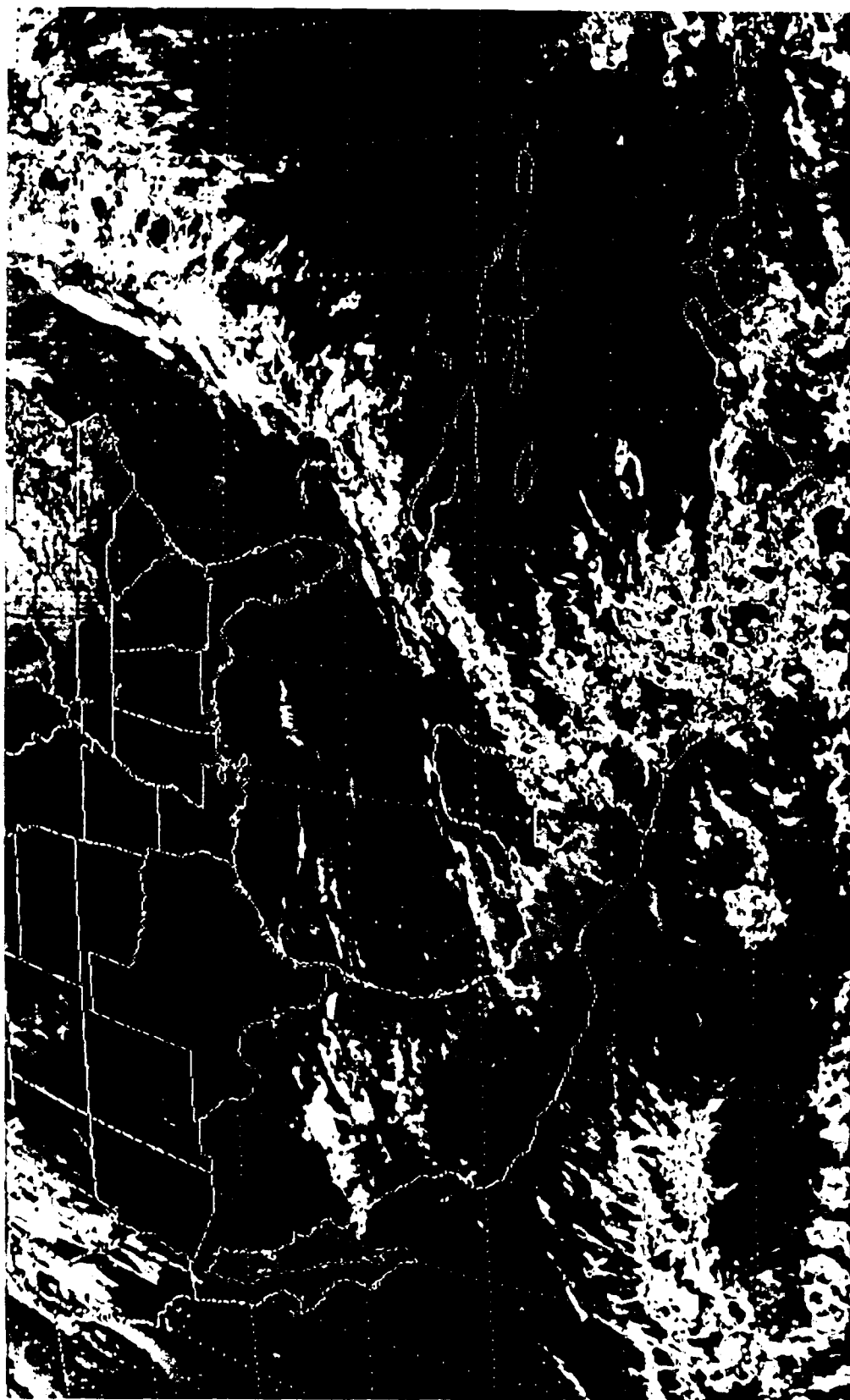


Figure 56. GOES IR satellite image with MB enhancement from 20 November 1987, 1801 UTC.

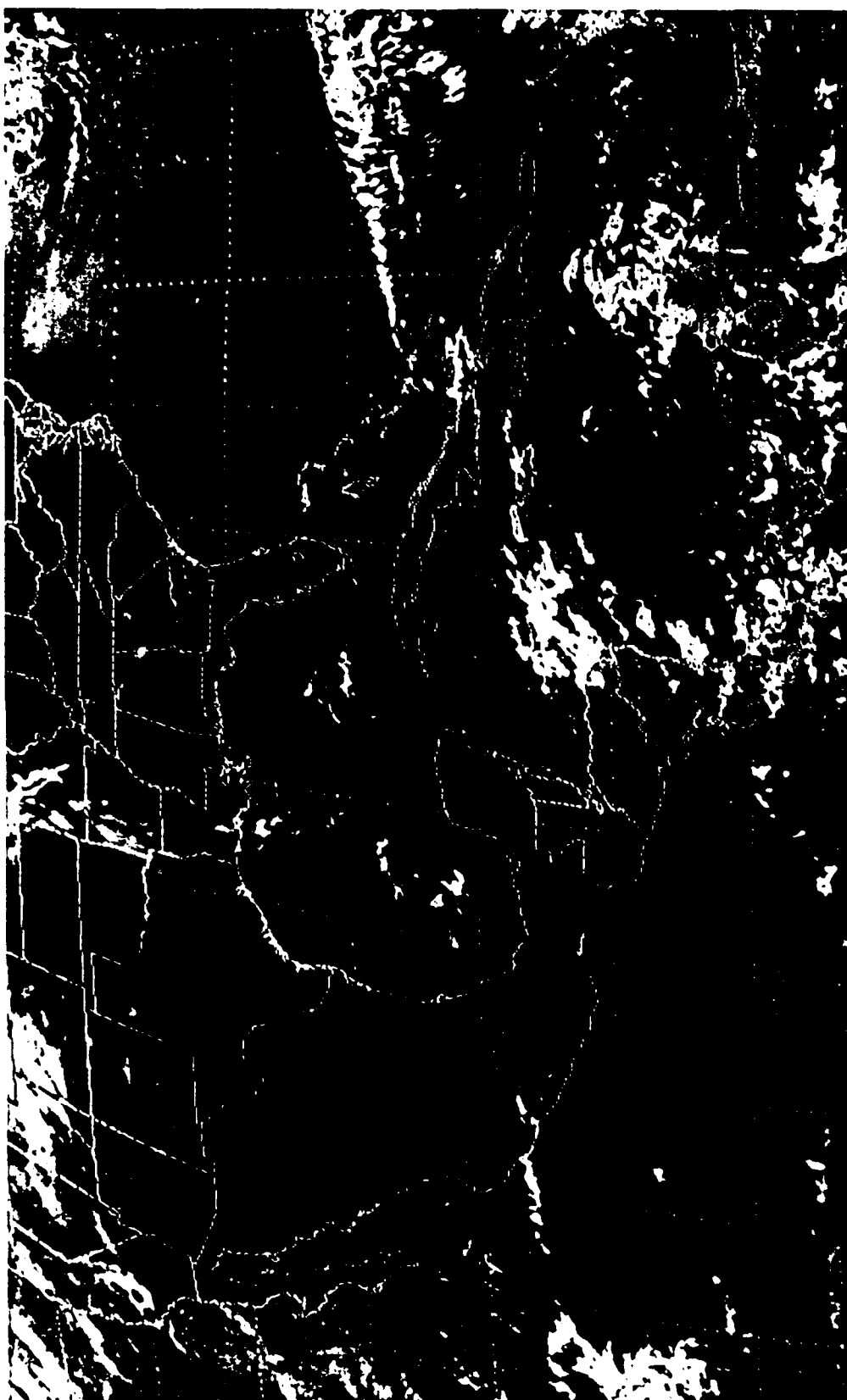


Figure 57. GOES IR satellite image with MB enhancement from 22 November 1987, 1801 UTC.

Honduras. Northerly flow had also weakened but was still in control over northern Central America with broken low-level clouds covering Belize, northern Guatemala and Honduras. The southern edge of the cloud mass over central Honduras marks the maximum southward penetration of this CACS at 14°N. The southern end of the front had dissipated by 24 November; however, northerly flow was still evident across Guatemala, Belize and Honduras. A wave in the easterlies was rapidly moving across the southern Caribbean on 25 November (Fig. 58) signaling the end of this CACS event.

Surface Variables

Like the March 1984 case, this was a moderate CACS event. It lasted 6 days, but produced only 4°C temperature drop at Merida. The maximum southward penetration of this CACS event was 14°N. Therefore, Belize City, Flores, Guatemala City, La Mesa, Soto Cano Air Base, and San Salvador were included in the analysis. Merida and Tegucigalpa were not included because of missing data. Surface variables were analyzed from 14 November through 26 November, centered on the date of frontal passage at Belize City (20 November).

Daily maximum temperature displayed a strong CACS signature, with well defined temperature drops during the 48 h after frontal passage (Fig. 59). Once again the maximum temperature change occurred at one of the southern most stations; 12°C at Soto Cano AB. The gradual pre-frontal warming trend evident in the mean analysis and the March 1984 cold surge was not apparent in this case and the post-frontal temperature recovery period was slightly shorter. Daily minimum temperature trends exhibited changes equal in magnitude to the maximum temperature changes in some cases, but they were extended over a longer period of time. The temperature drop at San Salvador

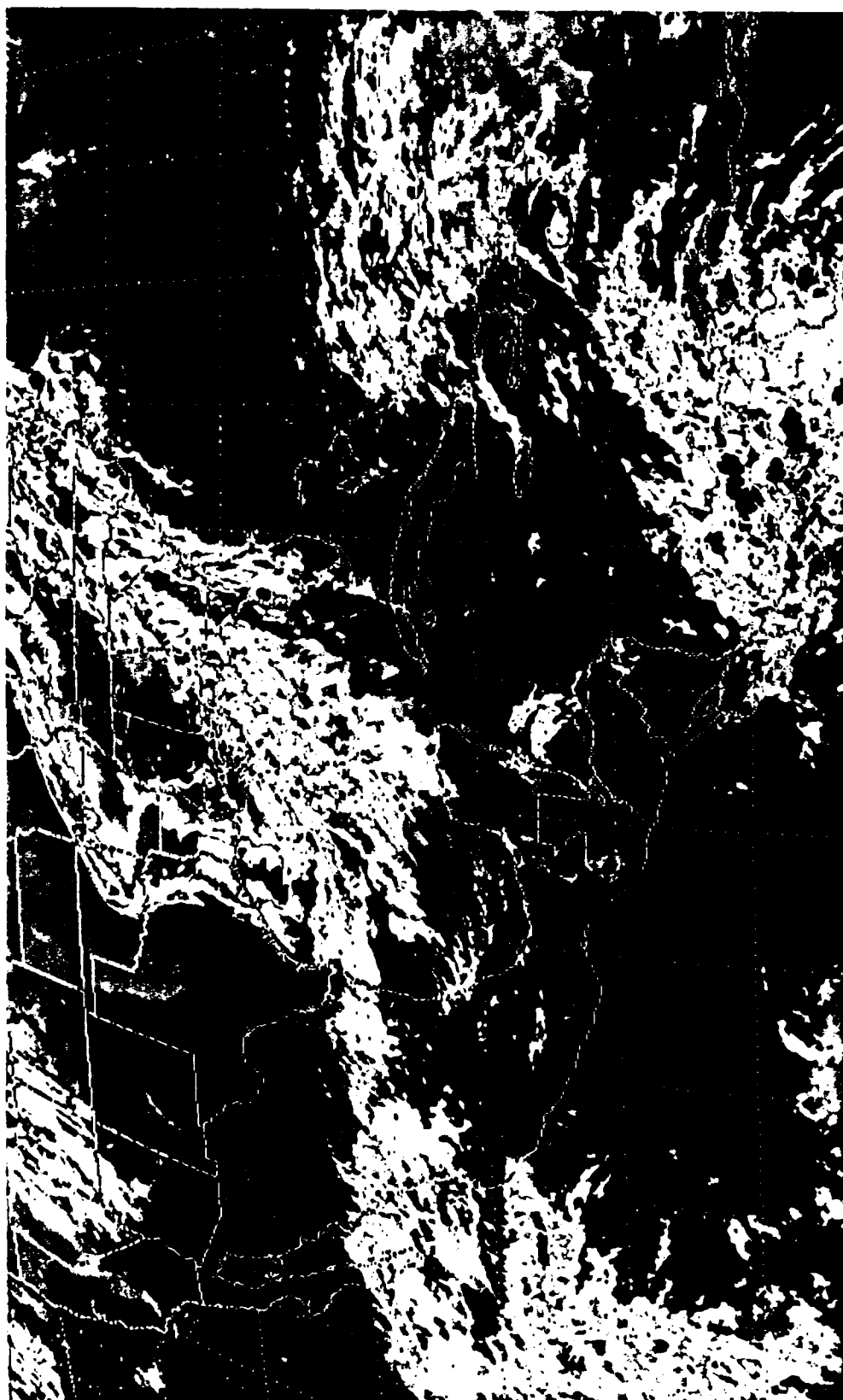


Figure 58. GOES IR satellite image with MB enhancement from 25 November 1987, 1801 UTC.

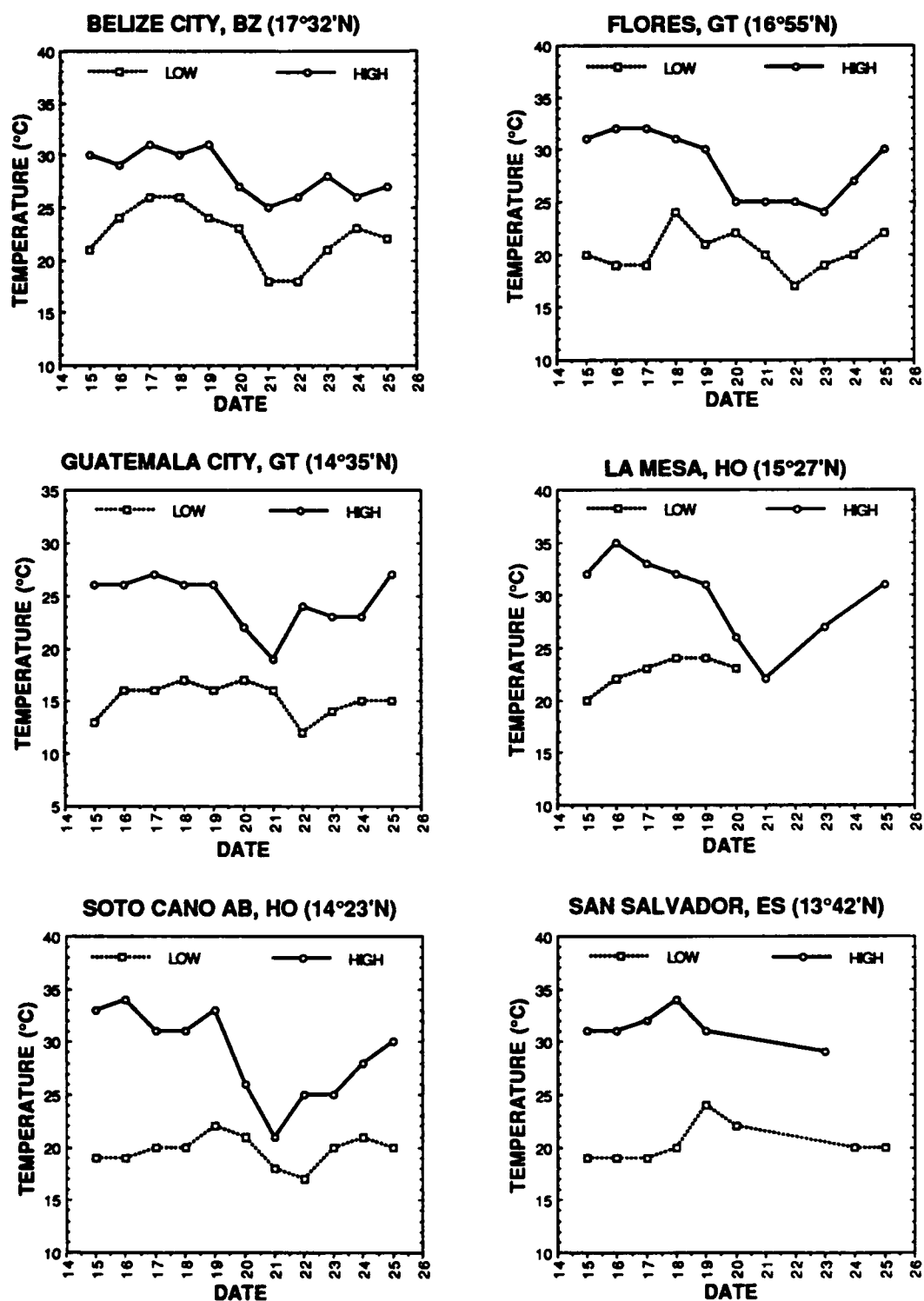


Figure 59. Daily maximum and minimum temperatures (°C) from 14-26 November 1987.

was probably not a result of the cold surge because it occurred prior to CACS onset.

Dew point displayed a more moderate but clearly evident response to the cold surge. Dew point drops ranged from 6°C at Soto Cano AB to 8°C at Belize City (Fig. 60). An accurate measurement could not be obtained from San Salvador because of missing data.

Wind direction again displayed the most prominent CACS signal. Easterly flow dominated at Belize City and Flores prior to frontal passage, followed by a well defined shift to northwesterly flow (Fig. 61). The remaining stations are located in mountainous regions where wind direction was primarily controlled by diurnally fluctuating mountain/valley breezes prior to frontal passage. Steady north-northwesterly flow dominated after frontal passage and through the remainder of the period. Even San Salvador, which experienced little cold surge induced changes in temperature or dew point, exhibited a shift to steady northerly flow. This indicates at least some CACS effects are felt on the Pacific side of the Central American continental divide.

Wind speed demonstrated no apparent CACS related fluctuations at Flores, La Mesa or San Salvador (Fig. 62). Northerly flow behind the cold front may have been enhanced by funnelling effects, increasing the wind speed at Guatemala City and Soto Cano AB after frontal passage. However, Belize City wind speed also displayed a delayed, but distinct increase after frontal passage. This indicates that the intensity of low-level flow behind the cold front may increase in at least some CACS cases.

SLP jumps were evident at all stations (Fig. 63), although they were not as defined and were of a smaller magnitude than the March 84 case. SLP was not reported at Soto Cano AB, so altimeter settings were used to illustrate cold surge induced pressure changes. The greatest SLP increase was 8.4 mb at Flores.

Ceiling height was the only variable that exhibited a stronger CACS signal than the March 1984 case. With the exception of San Salvador, all stations experienced either an

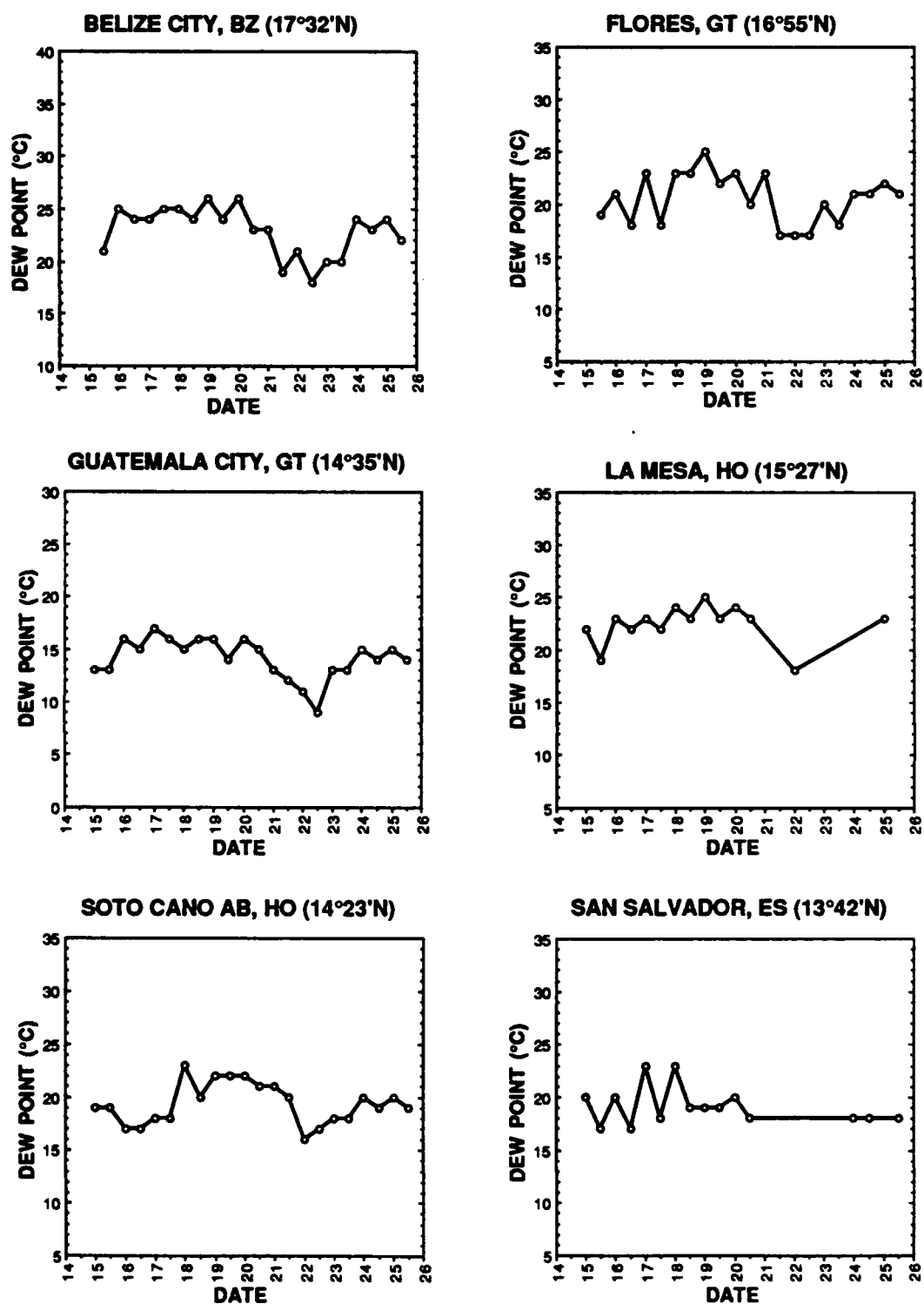


Figure 60. Dew point (°C) at 0000 UTC and 1200 UTC from 14-26 November 1987.

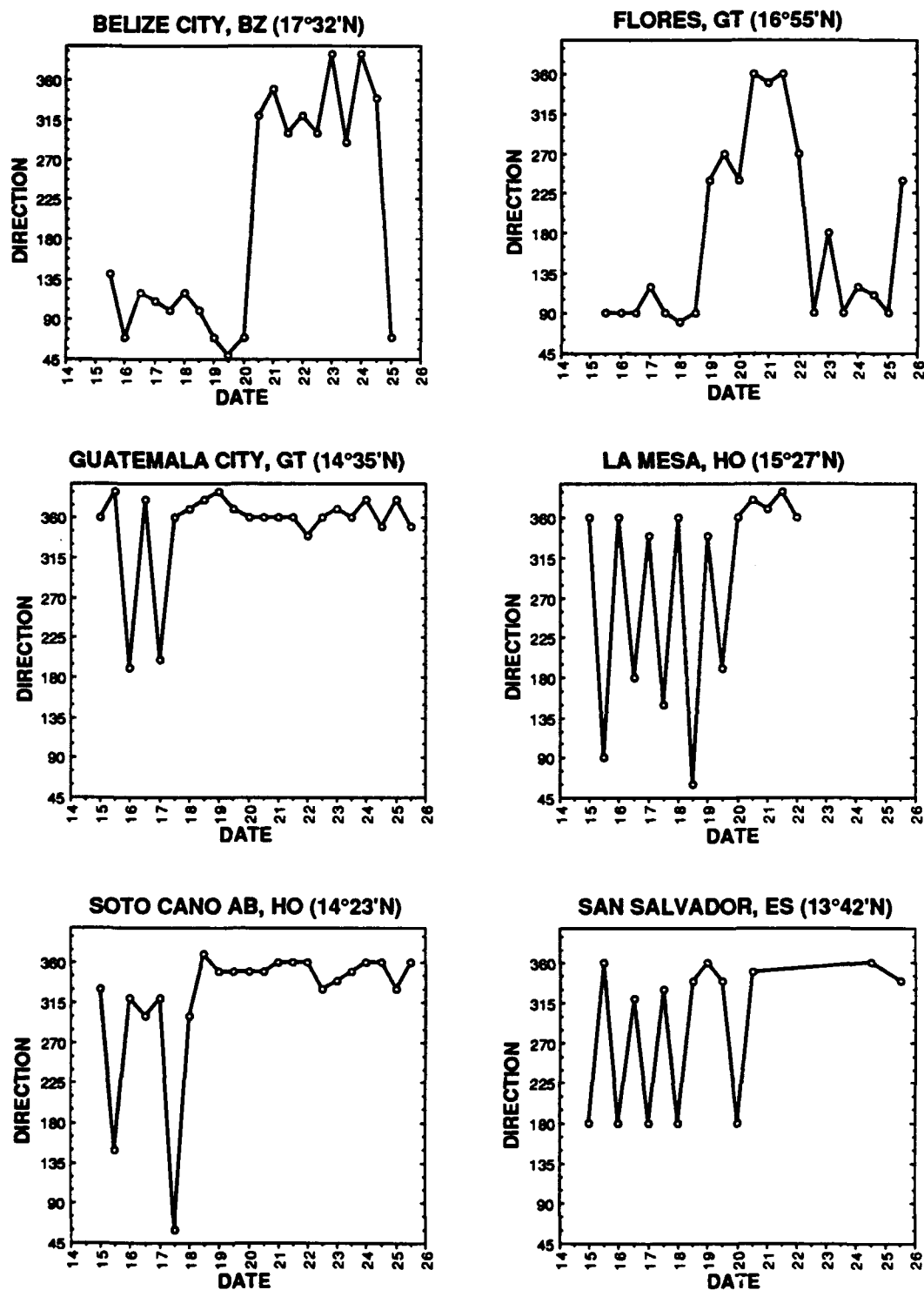


Figure 61. Wind direction at 0000 UTC and 1200 UTC from 14-26 November 1987.

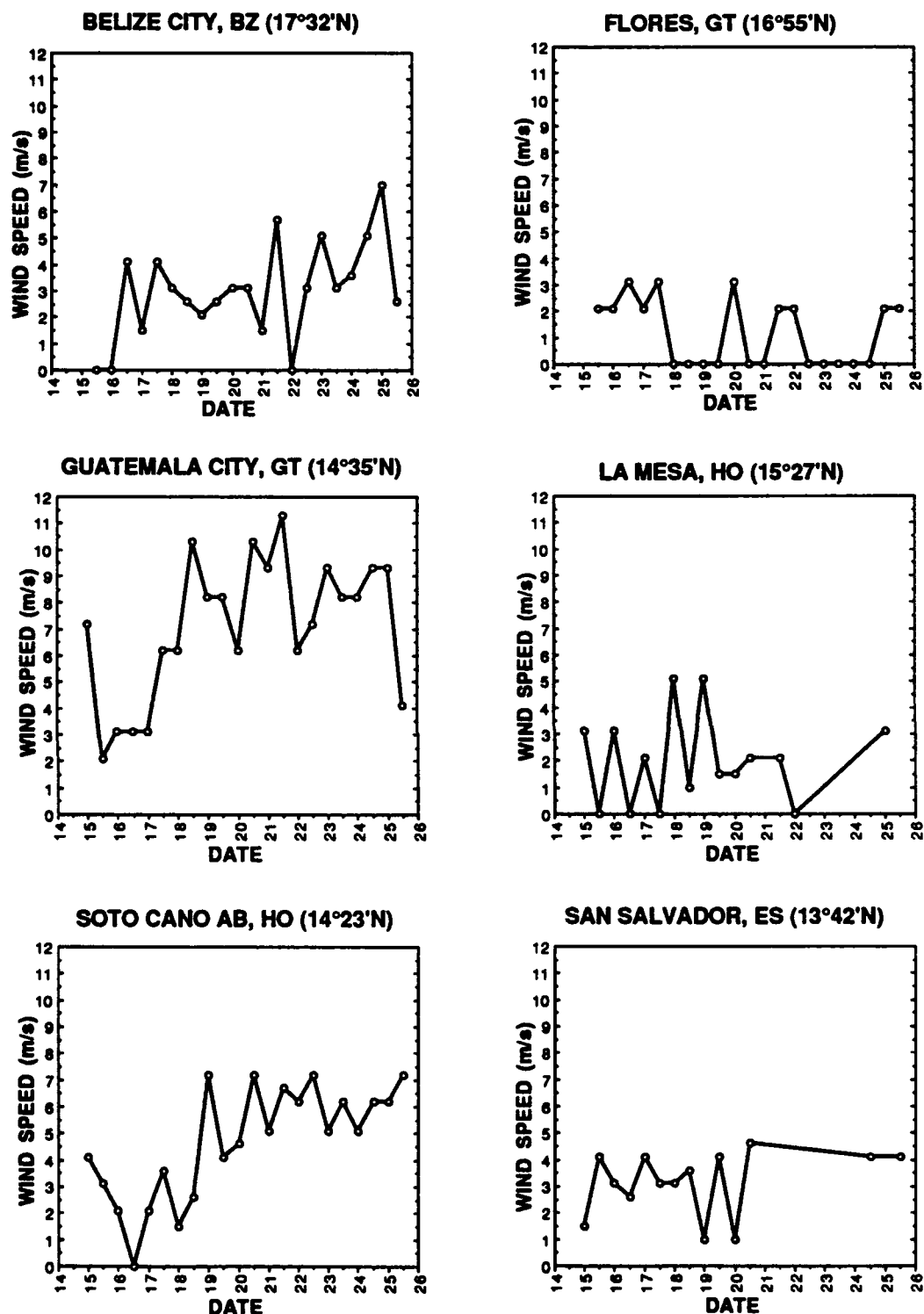


Figure 62. Wind speed (m/s) at 0000 UTC and 1800 UTC from 14-26 November 1987.

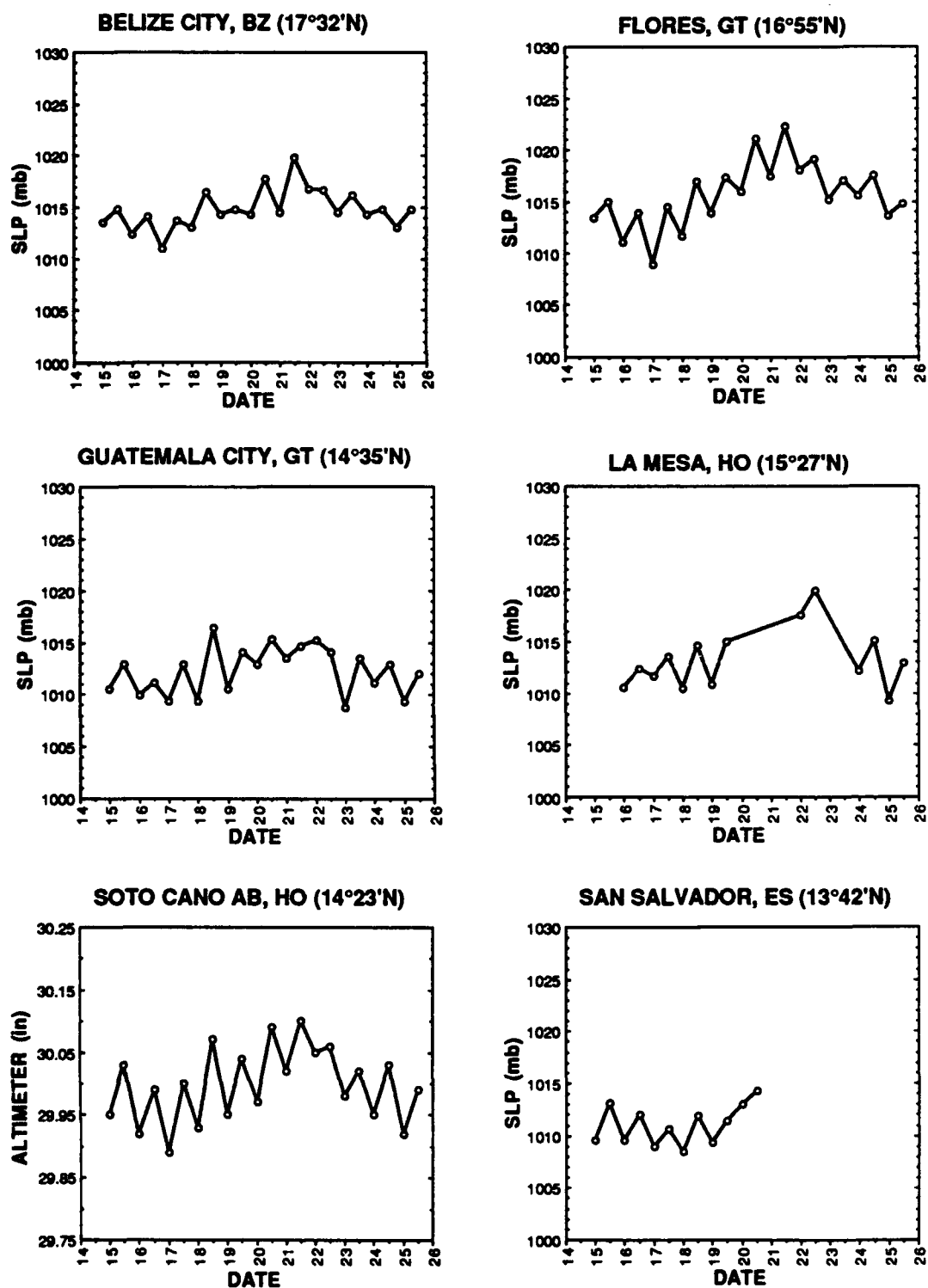


Figure 63. Sea level pressure (mb) or altimeter setting (in) at 0000 UTC and 1500 UTC from 14-26 November 1987.

increase in cloud cover, a decrease in ceiling height, or both during frontal passage (Fig. 64). San Salvador is located on the Pacific side of the continental divide and should actually experience a decrease in cloud cover after CACS onset because of adiabatic drying effects. The most dramatic cloud cover change was at La Mesa, where either scattered cloud cover or mid-level ceilings dominated initially. Cloud ceilings dropped to 540 m immediately after frontal passage and remained below 750 m for the remainder of the period.

Cold surge induced precipitation, again, varied widely from station to station (Fig. 65). Belize City recorded 37 mm of rainfall prior to frontal passage and 87 mm toward the end of the cold surge, while Guatemala City received only 10 mm of rain and San Salvador remained dry through the period. Flores recorded a total of 92 mm of rain during the cold surge, most of which was concentrated near the date of frontal passage. Precipitation was not consistently recorded at La Mesa or Soto Cano AB, but both stations experienced drizzle, rain and/or rainshowers during this CACS event.

Vertical Structure

Vertical temporal cross sections were produced for Belize City using 12-hourly upper air observations from 18 November at 0000 UTC through 22 November at 1200 UTC. Observations from Guatemala City and Tegucigalpa were available only at 1200 UTC. These time cross sections were expanded to make use of data from 16 November through 27 November. Significant amounts of data were missing at both Guatemala City and Tegucigalpa. GEMPAK appears to have done an acceptable job of interpolation in both cases. All cross sections are centered at the time of frontal passage with time increasing to the right.

The vertical cross section from Belize City was presented in Fig. 33. A deep layer

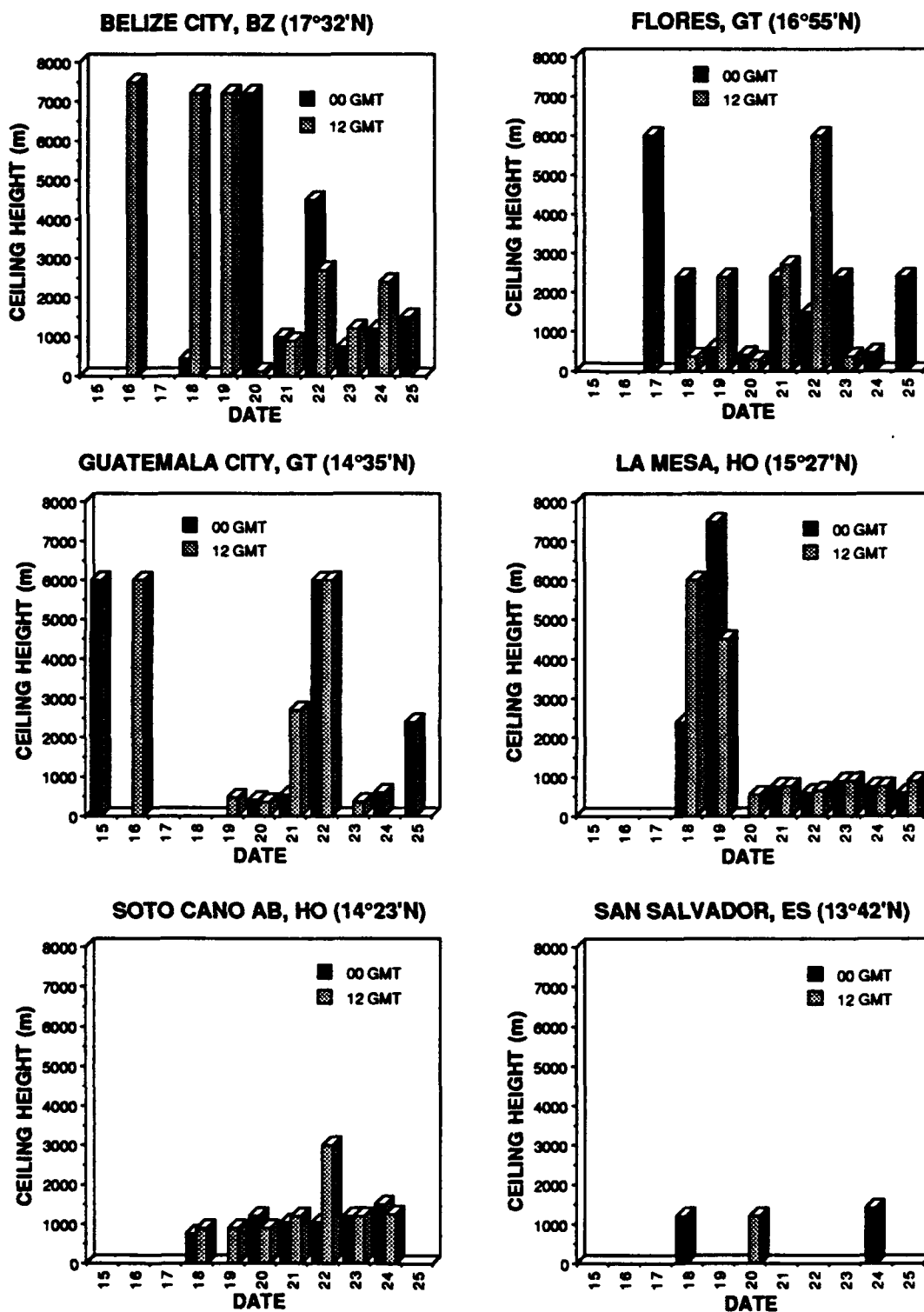


Figure 64. Cloud ceiling height (m) at 0000 UTC and 1200 UTC from 14-26 November 1987.

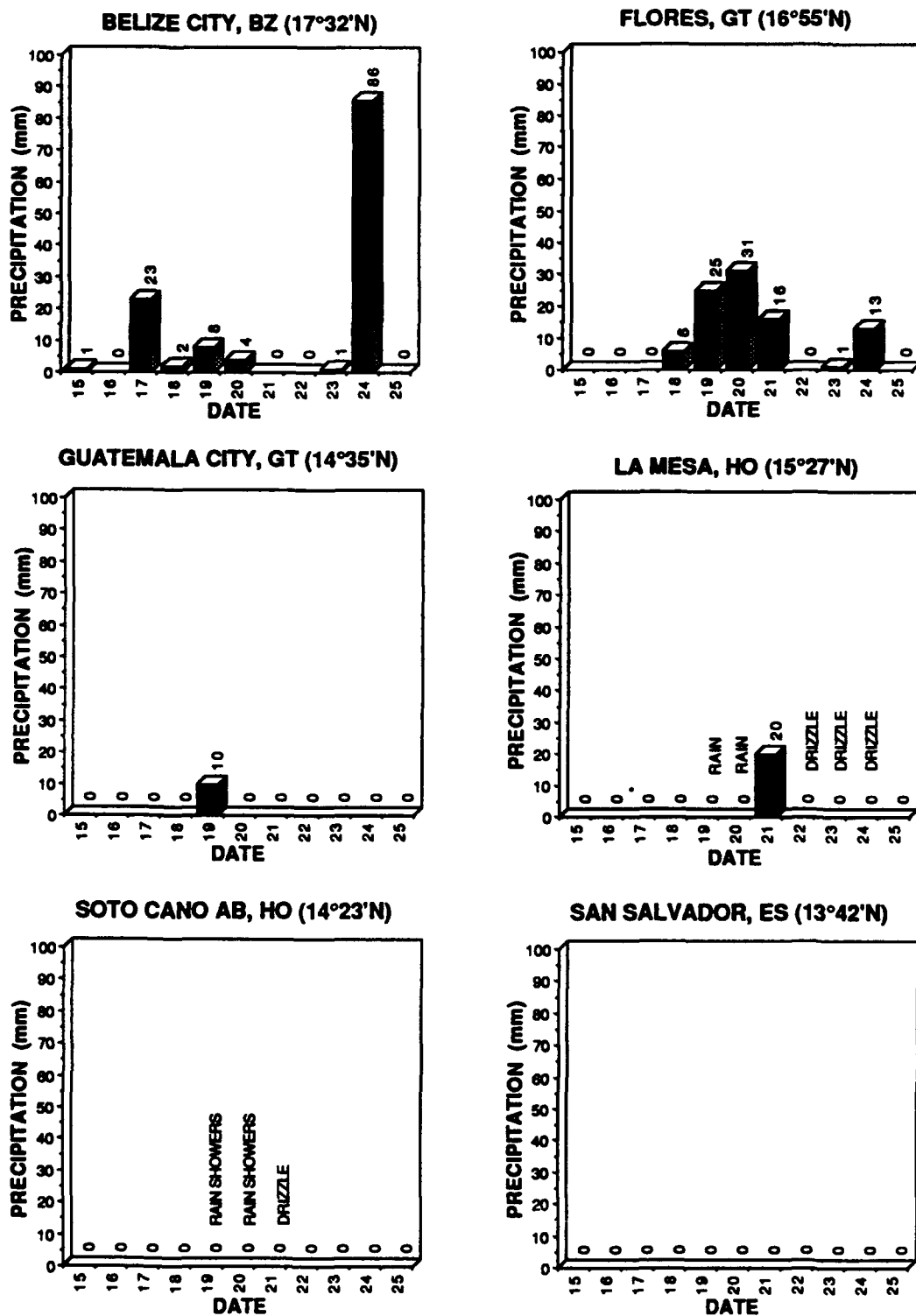


Figure 65. Daily precipitation (mm) from 14-26 November 1987.

of moisture was evident extending to near 300 mb during the beginning of the period and immediately after frontal passage. Moisture was capped below 500 mb by a weak subsidence inversion from 18 November through 20 November. Low-level flow prior to frontal passage was primarily from the east up to 500 mb. Frontal passage was best characterized by a distinct frontal inversion between 850 mb and 700 mb which persisted through the remainder of the period. Low-level wind flow displayed an abrupt shift to northerly directions immediately after frontal passage. The diurnal temperature curve was very pronounced after frontal passage, indicating strong radiational cooling in the relatively dry air behind the front. The atmosphere was generally unstable prior to frontal passage, with the Lifted Index ranging from -3.5 to -6.8 and the K Index ranging from 39.3 to 45.3. Stability increased dramatically after frontal passage.

The Guatemala City cross section is displayed in Fig. 66. Moisture was generally confined below 700 mb through the period. Weak subsidence inversions were evident prior to frontal passage near 700 mb and 550 mb, and near 500 mb after frontal passage. No frontal inversion was apparent. Low-level wind flow demonstrated little variation through the period, however, flow between 700 mb and 500 mb shifted from east-southeast to north-northwest from 21-25 November. All stability indices displayed only a gradual trend toward increasing stability after frontal passage. The most significant cold surge indicator was a distinct cooling below 700 mb immediately after frontal passage.

Upper air observations for Tegucigalpa were plotted from 17 November through 27 November. Significant amounts of data were missing during the period. The most impressive feature identified was a strong trade wind inversion which persisted through the entire period near 500 mb (Fig. 67). As a result, the atmosphere was stable through the entire period. Winds below the inversion were generally from the east or northeast,

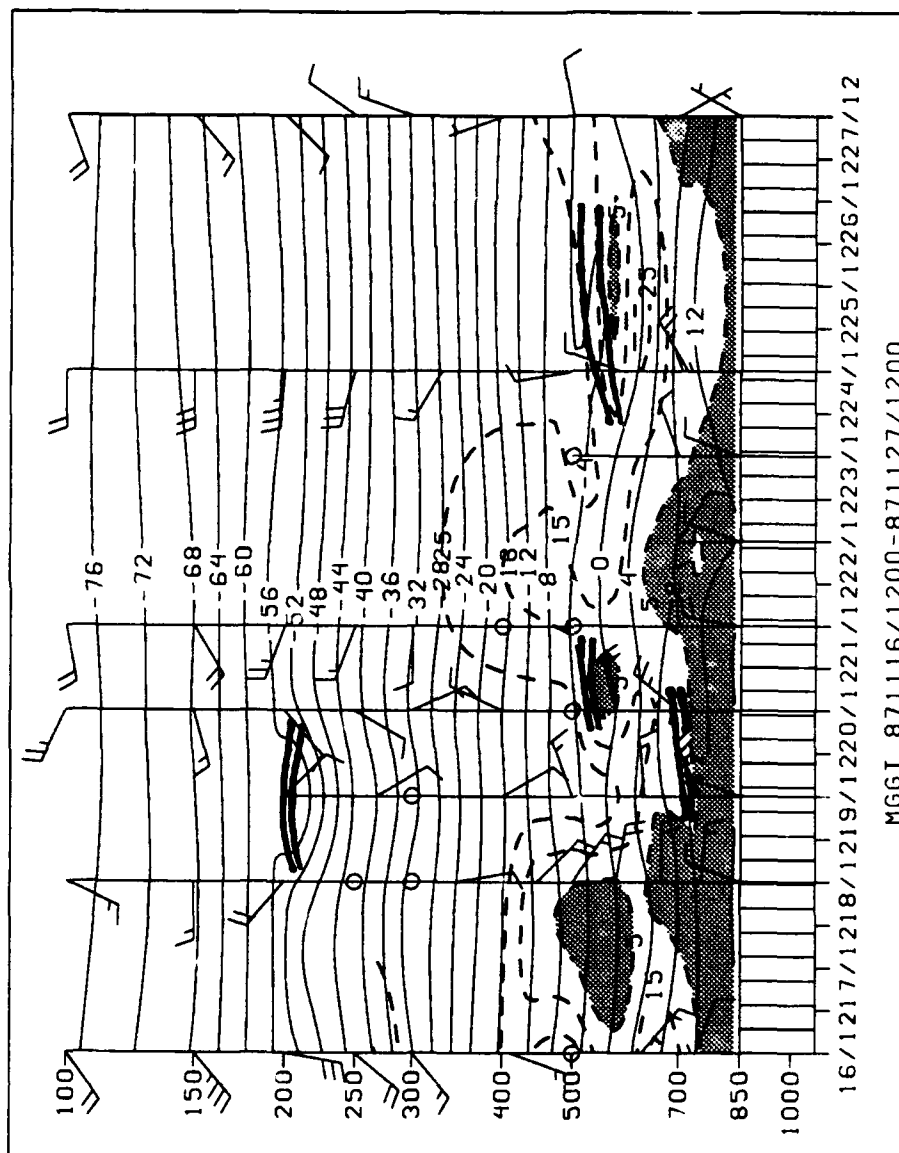


Figure 66. Vertical temporal cross section at Guatemala City, Guatemala from 16 November 1987, 1200 UTC to 27 November 1987, 1200 UTC. Isotherms (solid) are plotted at 4°C intervals and isodrosotherms (dashed) at 5°C, 15°C and 25°C. Also shown are areas with dew point depression less than or equal to 5°C (shaded), wind speed (kt) and direction, and inversion layers (heavy solid).

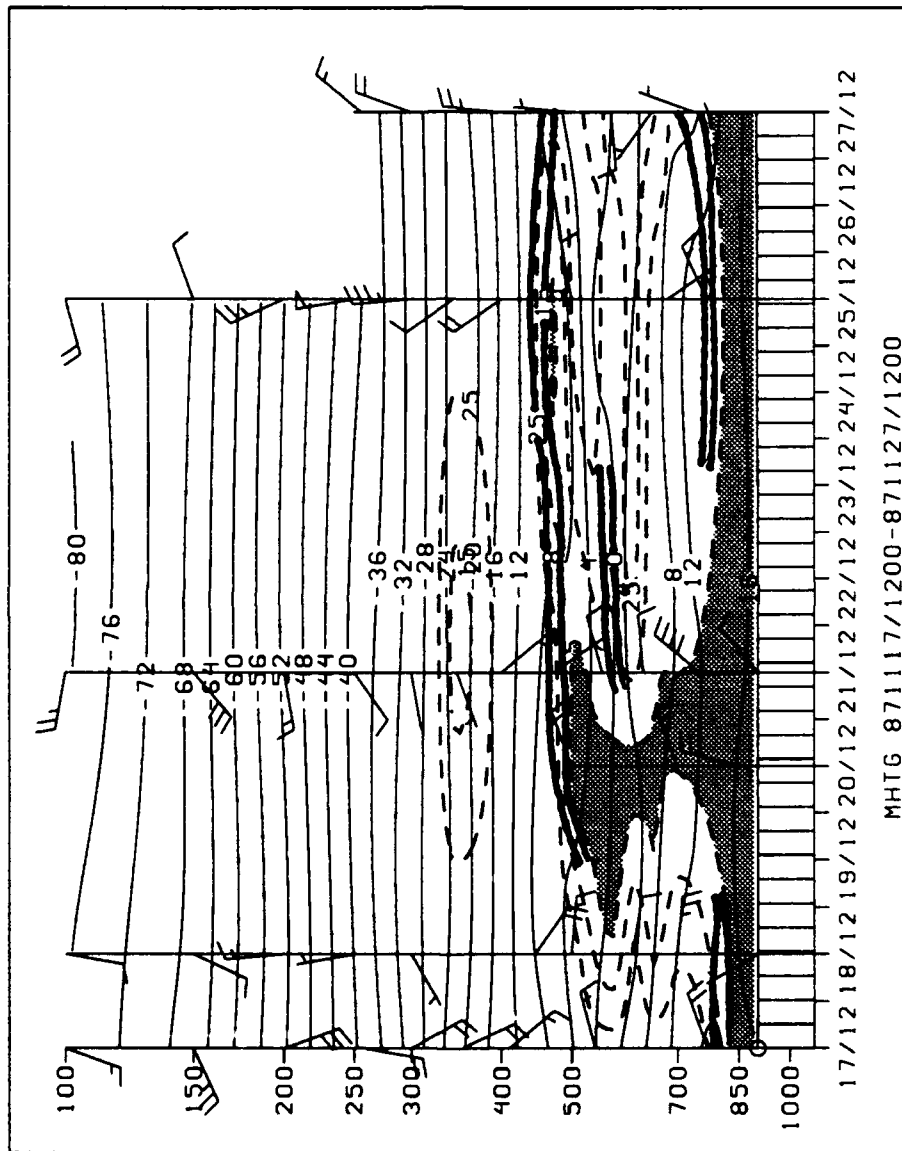


Figure 67. As in Fig. 66, except at Tegucigalpa, Honduras from 17 November 1987, 1200 UTC to 27 November 1987, 1200 UTC.

while westerly and northerly flow dominated above the inversion. A weak subsidence inversion was evident near 850 mb initially, with moist conditions confined below it. The moist layer expanded up to the trade wind inversion from 19-21 November. Although no surface observations were available at Tegucigalpa, this time frame corresponds to the days with rainfall at nearby Soto Cano AB. An interesting "split" frontal inversion was illustrated in this CACS event. The frontal inversion was initially analyzed near 650 mb on 21 November. By 25 November, the inversion was most prominent capping the moisture below 750 mb. It is possible that the two frontal inversions are actually one. However, missing data prevented a more accurate interpretation of the situation.

Moisture Fields

TPW fields and rain rates associated with this cold surge were discussed in detail in Chapter VI, Figs. 34-40.

Summary

This case illustrated the fact that many CACS events are initiated by a wave developing along an old frontal system. This was another moderate CACS, and appeared similar to the March 1984 case on GOES imagery. Surface variable response was similar to, but weaker than the March 1984 case. Funnelling effects may play an important role in the observed increase in wind speed after CACS onset in mountainous regions. The vertical structure of this cold surge did not weaken considerably, as frontal inversions were evident at both Belize City and Tegucigalpa. Evidence of convective activity in the Belize City cross section corresponded well to surface observations. Stratiform precipitation observed in central Honduras was reflected in the Tegucigalpa

cross section. A strong correlation was evident in the position of the relative TPW maximum, rain rate observations, and the position of the surface front as observed both from satellite and the surface.

CASE 3: 25 JANUARY - 2 FEBRUARY 1988

Satellite Cloud Signatures

This was a very interesting case because the same frontal system was responsible for two cold surge events. Imagery from 23 January showed a cold front extending across western Cuba into the Gulf of Honduras (Fig. 68). Broken to overcast low-level cloud cover was evident along the entire Mexican Gulf coast and across Guatemala into extreme western Honduras, clearly indicating northeasterly flow behind the cold front. An upper-level wave was developing over the western Gulf of Mexico. The cold front had moved back into the central Gulf of Mexico by 24 January (Fig. 69) and the wave appeared to be strengthening along the Georgia and Alabama Gulf coast. Easterly low-level flow and nearly clear skies dominated Central America. By 25 January, the wave had intensified considerably and moved rapidly along the northeast U.S. coast (Fig. 70). The cold front had returned to Central America, now extending across southern Florida and western Cuba into central Honduras. Strong northerly flow was evident with broken to overcast stratus/stratocumulus throughout the Caribbean side of southern Mexico, northern Guatemala and western Honduras. A sea breeze over extreme eastern Honduras and along the Nicaragua Caribbean coast indicates that easterly flow was still dominating the remainder of Central America. A well defined frontal cloud band extended across central Cuba and along the Caribbean coast of Nicaragua on 26 January. Northerly low-level flow dominated Central America north of the Nicaragua / Costa Rica border. Evidence of easterly flow was apparent only over the southern

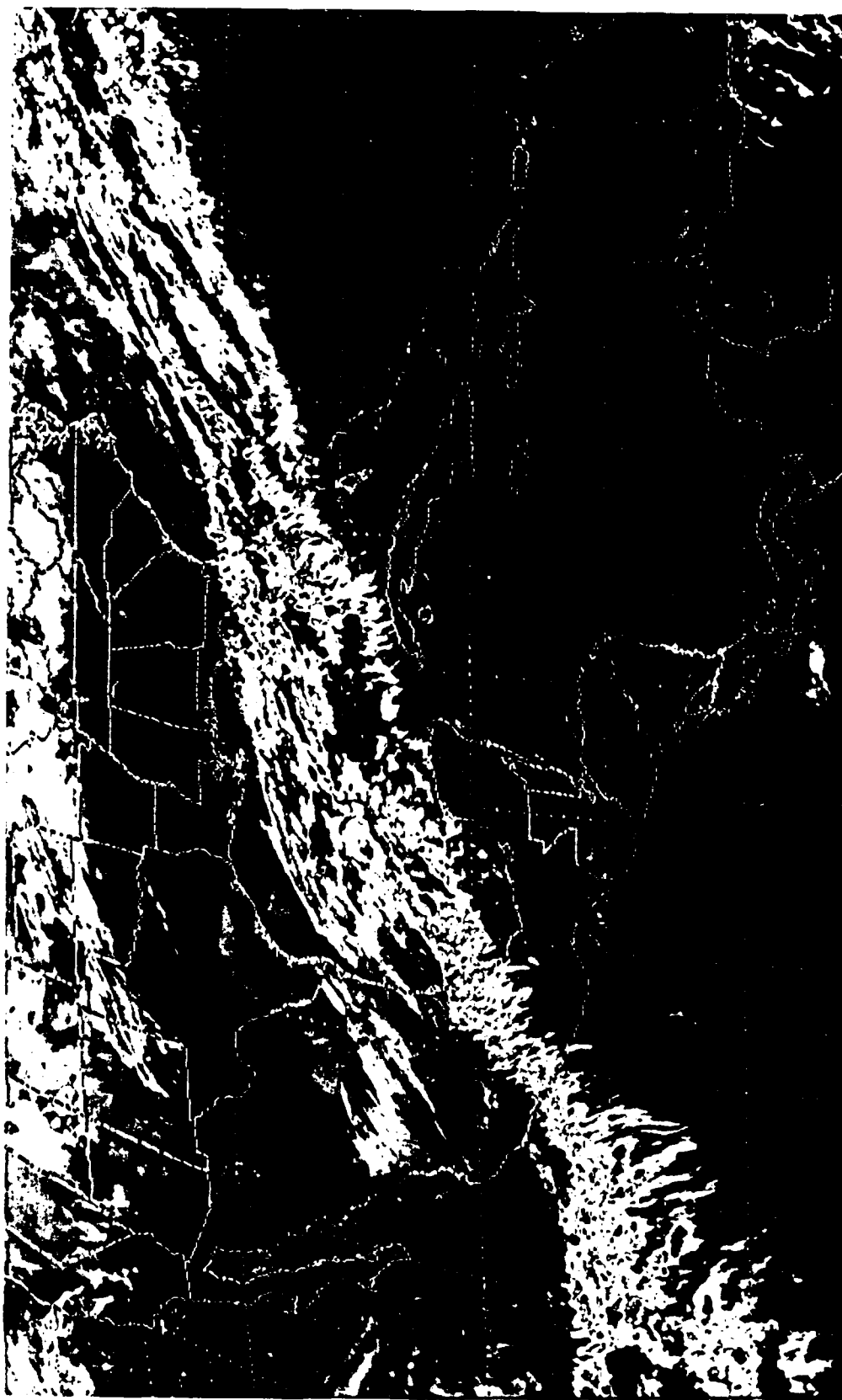


Figure 68. GOES IR satellite image with MB enhancement from 23 January 1988, 1901 UTC.

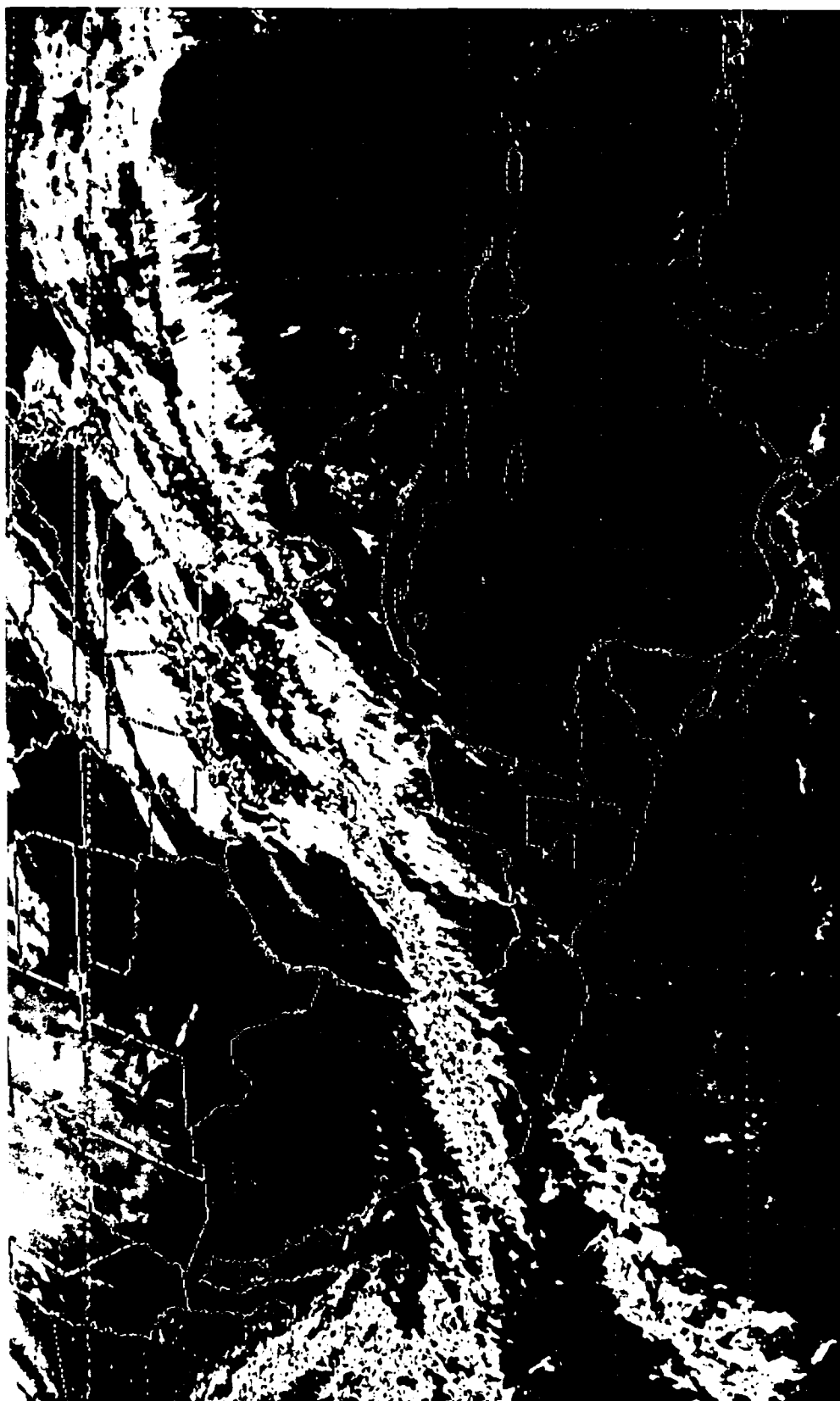


Figure 69. GOES IR satellite image with MB enhancement from 24 January 1988, 1831 UTC.

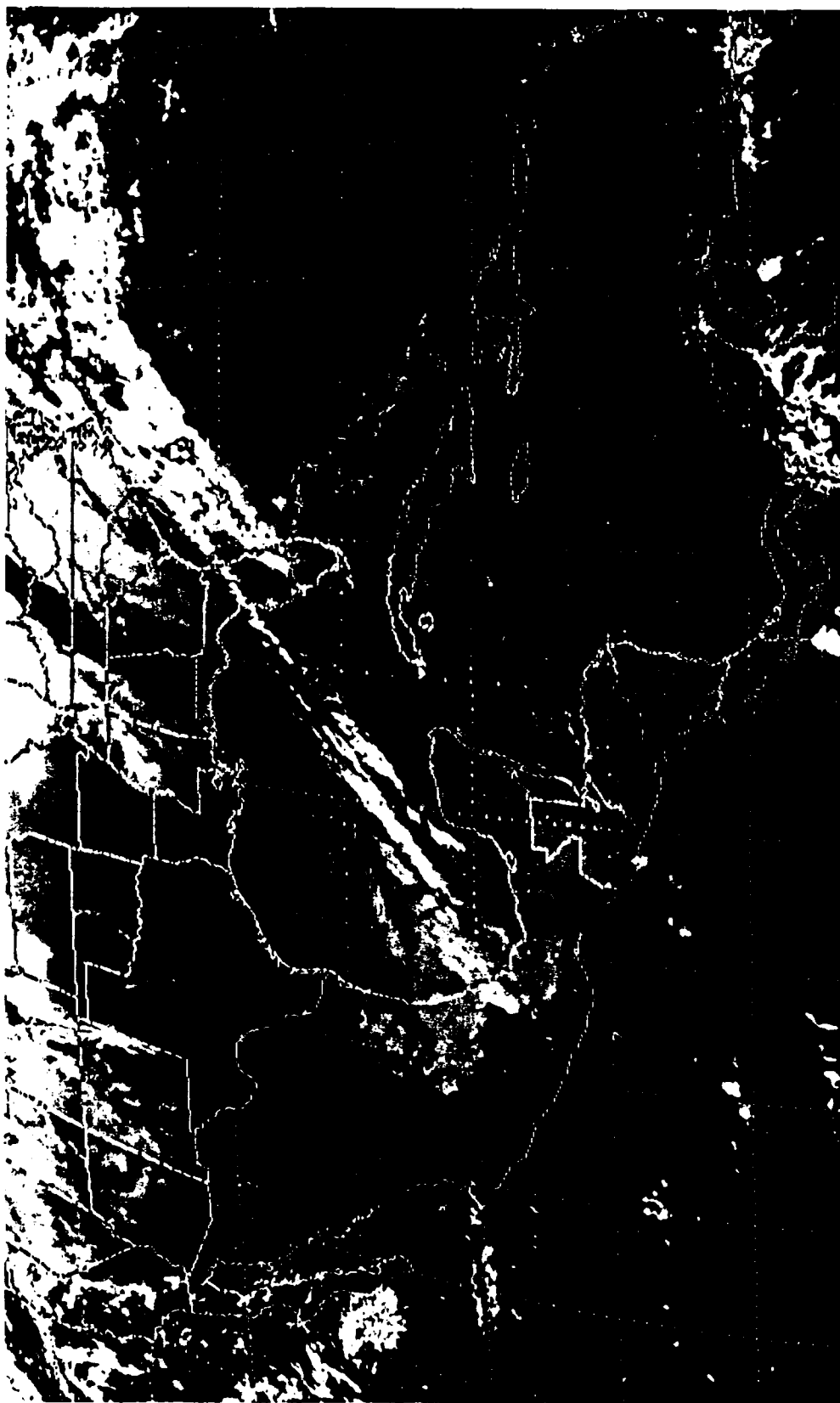


Figure 70. GOES IR satellite image with MB enhancement from 25 January 1988,
1831 UTC.

Caribbean. By 28 January, the cold surge had reached into extreme southern Costa Rica and western Panama, the maximum southward penetration of this CACS event (Fig. 71). Cloud lines extending from the eastern Florida coast across Cuba indicated very strong low-level northeasterly flow. Broken to overcast stratocumulus covered nearly all areas of the Central American Isthmus north and east of the continental divide, while nearly cloud free conditions were evident throughout southern Guatemala, El Salvador and western Nicaragua. The cold surge had weakened considerably by 30 January, however, evidence of northerly flow was still apparent in the cloud cover distribution from southern Mexico to northern Nicaragua. This pattern continued until 2 February, when easterly flow had clearly been reestablished over Central America (Fig. 72).

Surface Variables

This CACS event was much stronger than the March 1984 or November 1987 cold surge events. The two events combined for a total duration of 13 days, and the second cold surge penetrated to 8°N. Several reporting stations were added to the analysis, including Managua, Nicaragua, San Andres, Colombia, San Jose, Costa Rica, Bocas del Toro, Panama and David, Panama. Merida was not included in the analysis because of missing data. Surface variable trends were plotted from 20 January through 31 January, centered on the date of frontal passage at Belize City (25 January). Temperature and dew point data were not available for either station in Panama.

Daily maximum and minimum temperature both displayed definite CACS signatures at all stations, although drops in minimum temperature were not nearly as dramatic as in maximum temperature (Fig. 73). Additionally, all stations north of Tegucigalpa exhibited a well defined cold surge signal in response to the first event. The greatest drops in daily maximum temperature were again recorded at Soto Cano AB (17°C) and

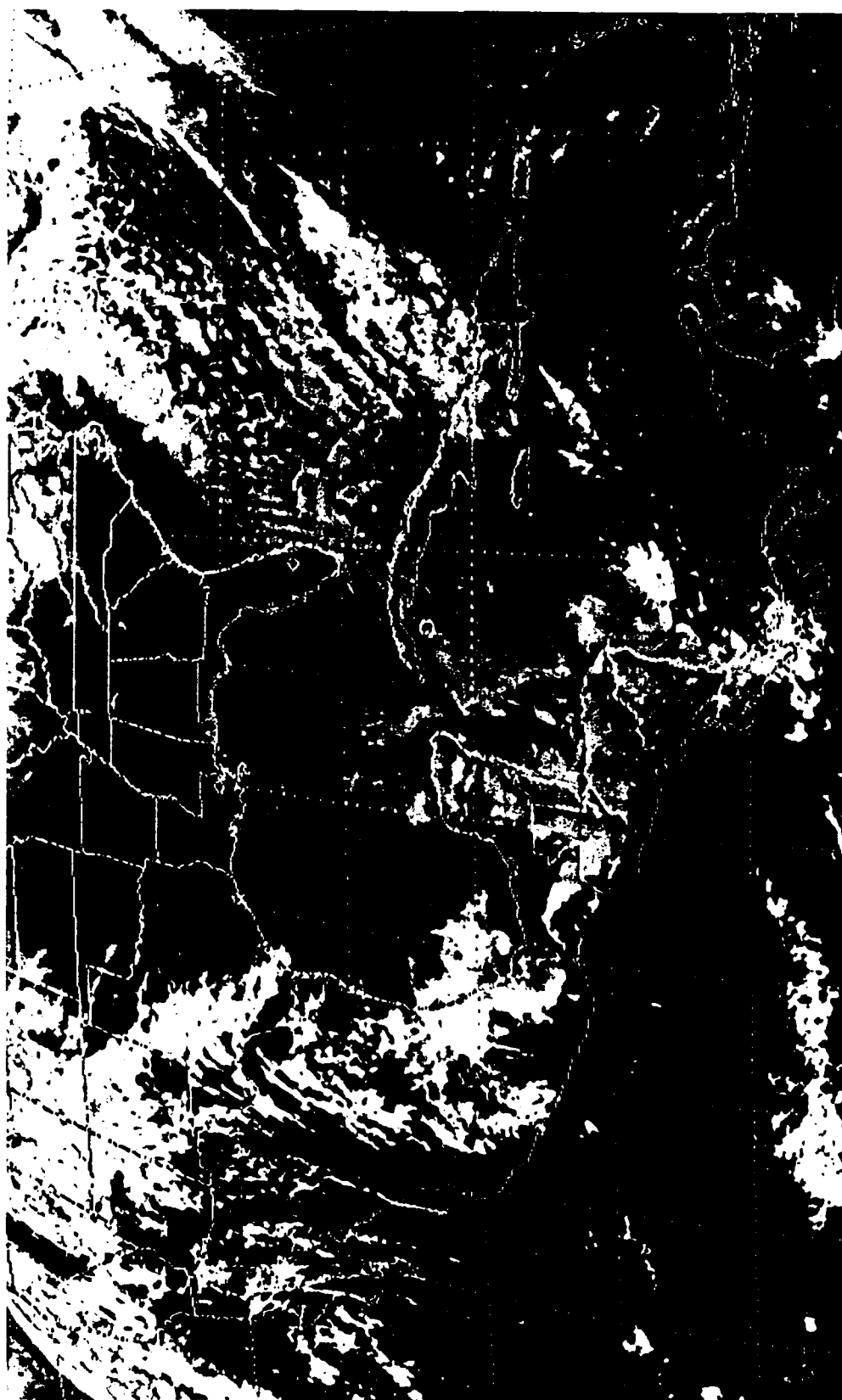


Figure 71. GOES IR satellite image with MB enhancement from 28 January 1988, 1831 UTC.

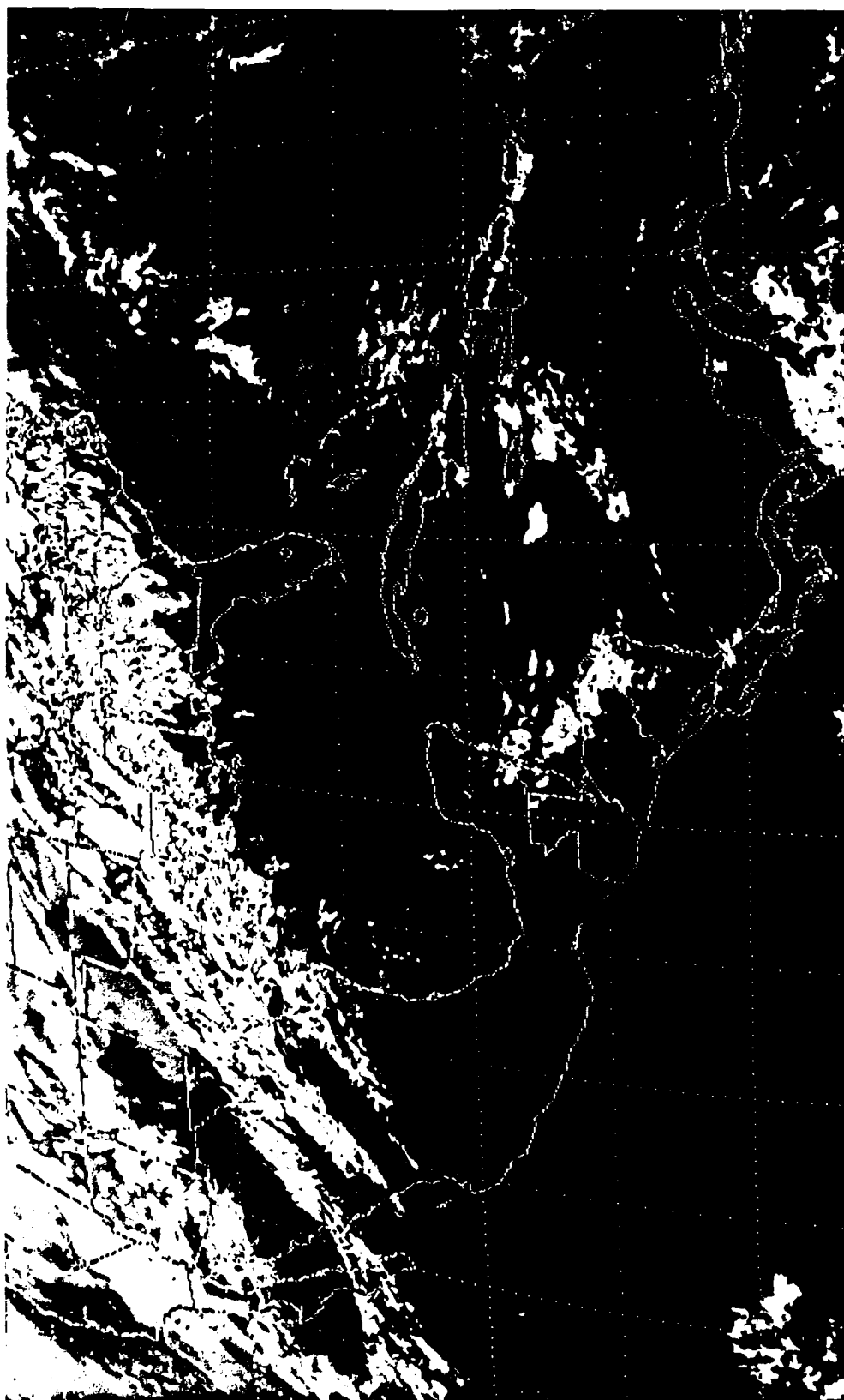


Figure 72. GOES IR satellite image with MB enhancement from 2 February 1988,
1831 UTC.

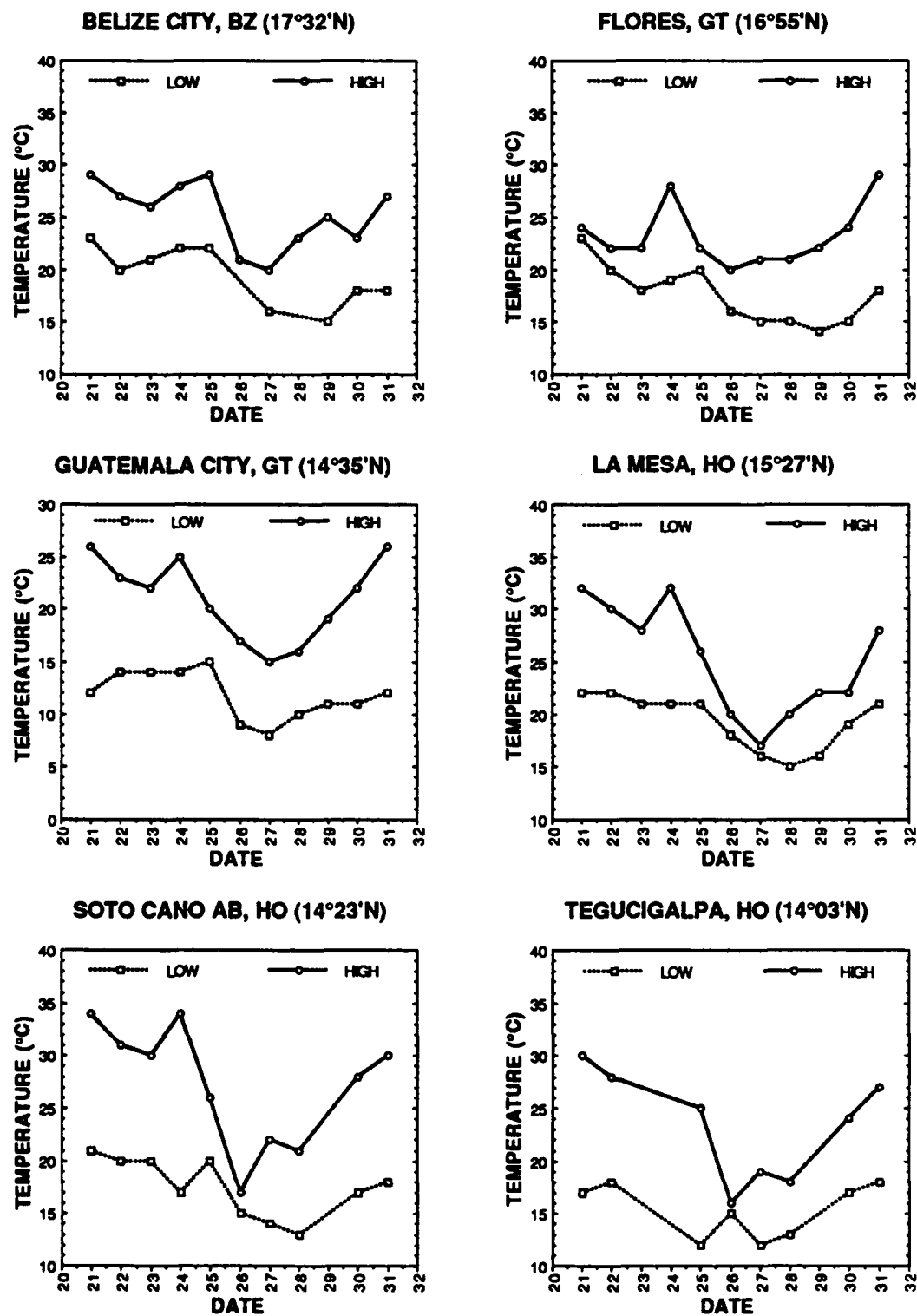


Figure 73. Daily maximum and minimum temperatures (°C) from 20-31 January 1988.

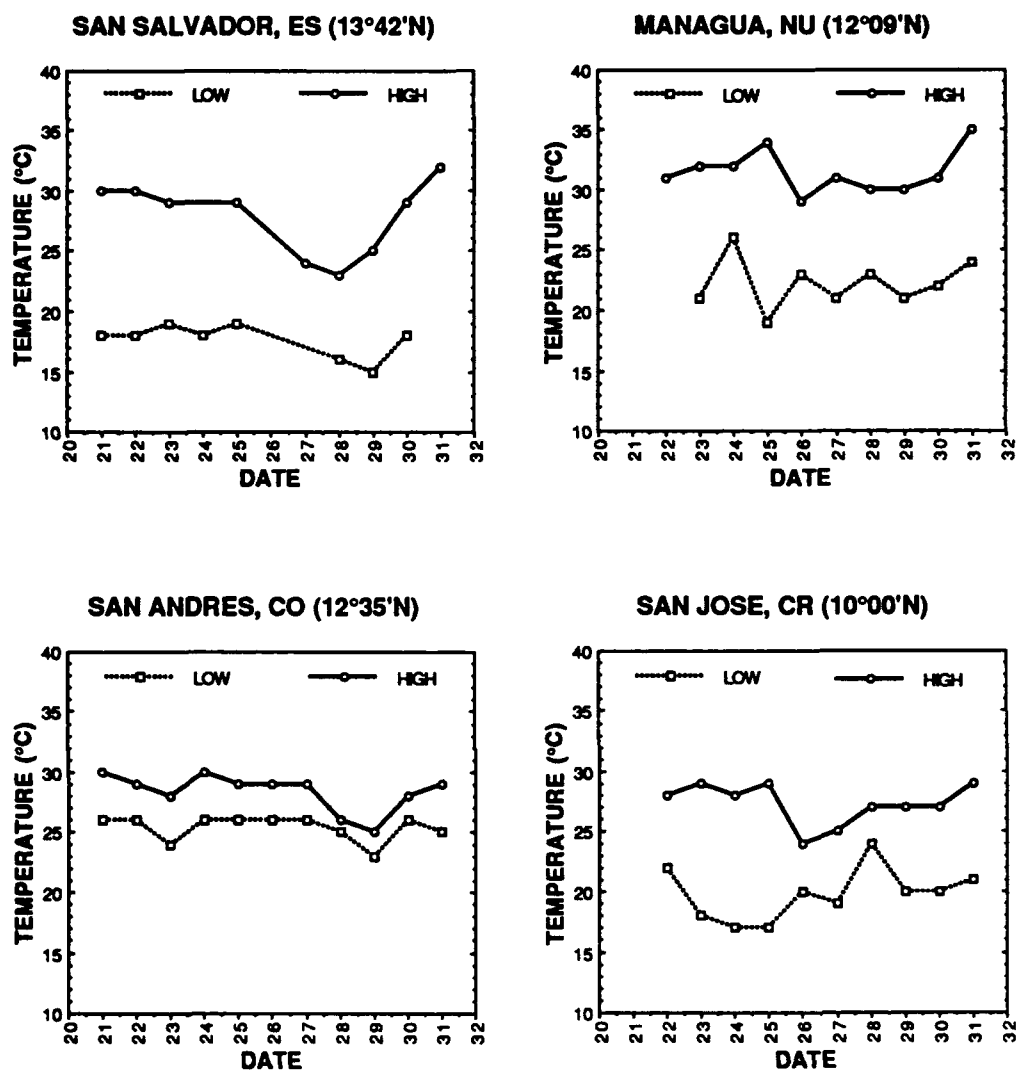


Figure 73. (Continued).

La Mesa (15°C). Temperature drops at the other stations ranged from 4°C at San Andres to 10°C at Guatemala City.

Significant drops in dew point were evident at all stations except San Andres and San Jose. (Fig. 74). Northern stations clearly displayed a stronger CACS signal than southern stations. The strongest decrease was noted at Belize City and Guatemala City where dew point dropped 11°C in the 48 h immediately after frontal passage. Dew point at Managua dropped from 20°C at 0000 UTC on 25 January to 15°C at 1200 UTC on 27 January. This may indicate that air mass modification during cold surge events had a greater influence on moisture than temperature, at least in this case.

Wind direction (Fig. 75) was not the variable with the best CACS signature during this event. Responses to the cold surge varied from station to station. At some stations, the cold surge response varied significantly from trends identified in the previous case studies. Easterly flow normally prevails at Flores prior to frontal passage, followed by a distinct shift to northerly flow after frontal passage. During this cold surge, wind direction at Flores oscillated randomly through most of the period. A similar pattern was noted at La Mesa. Very little CACS signal was evident at Managua or San Jose where wind directions remained easterly. Low-level flow is normally from the northwest at Bocas del Toro, but a short lived switch to northerly flow was evident at the time of frontal passage. The remaining stations all displayed a strong CACS signal, with either easterly flow or mountain valley breezed dominating before frontal passage followed by a shift to steady northerly flow.

Wind speed trends exhibited identifiable cold surge signatures at every station except Belize City and Flores (Fig. 76). Wind speed increases of 4 m/s to 10 m/s were typical immediately after frontal passage. The strongest signal was at San Andres, where wind speed increased from 2 m/s at 0000 UTC on 26 January to 18 m/s on 28 January. Wind

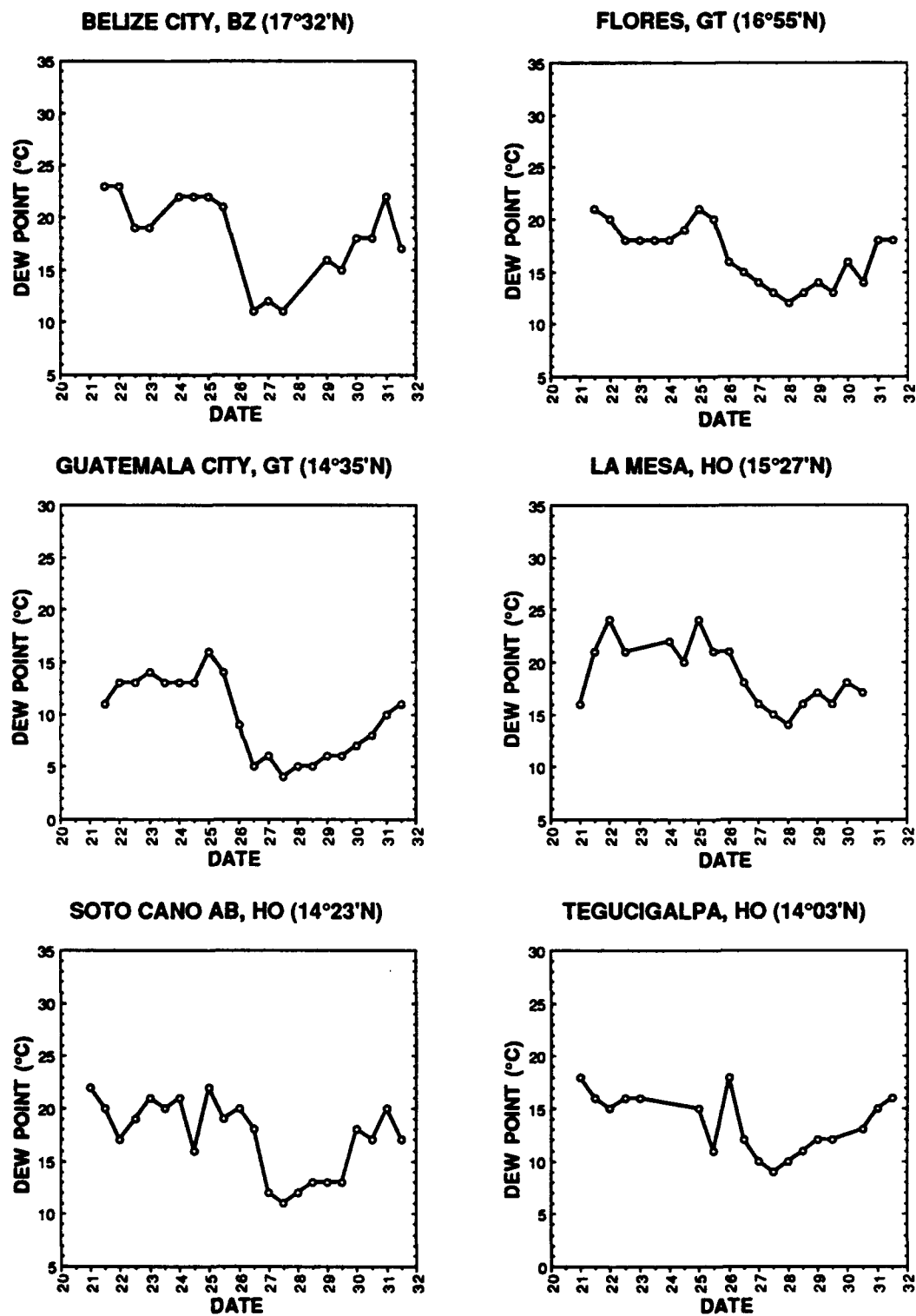


Figure 74. Dew point (°C) at 0000 UTC and 1200 UTC from 20-31 January 1988.

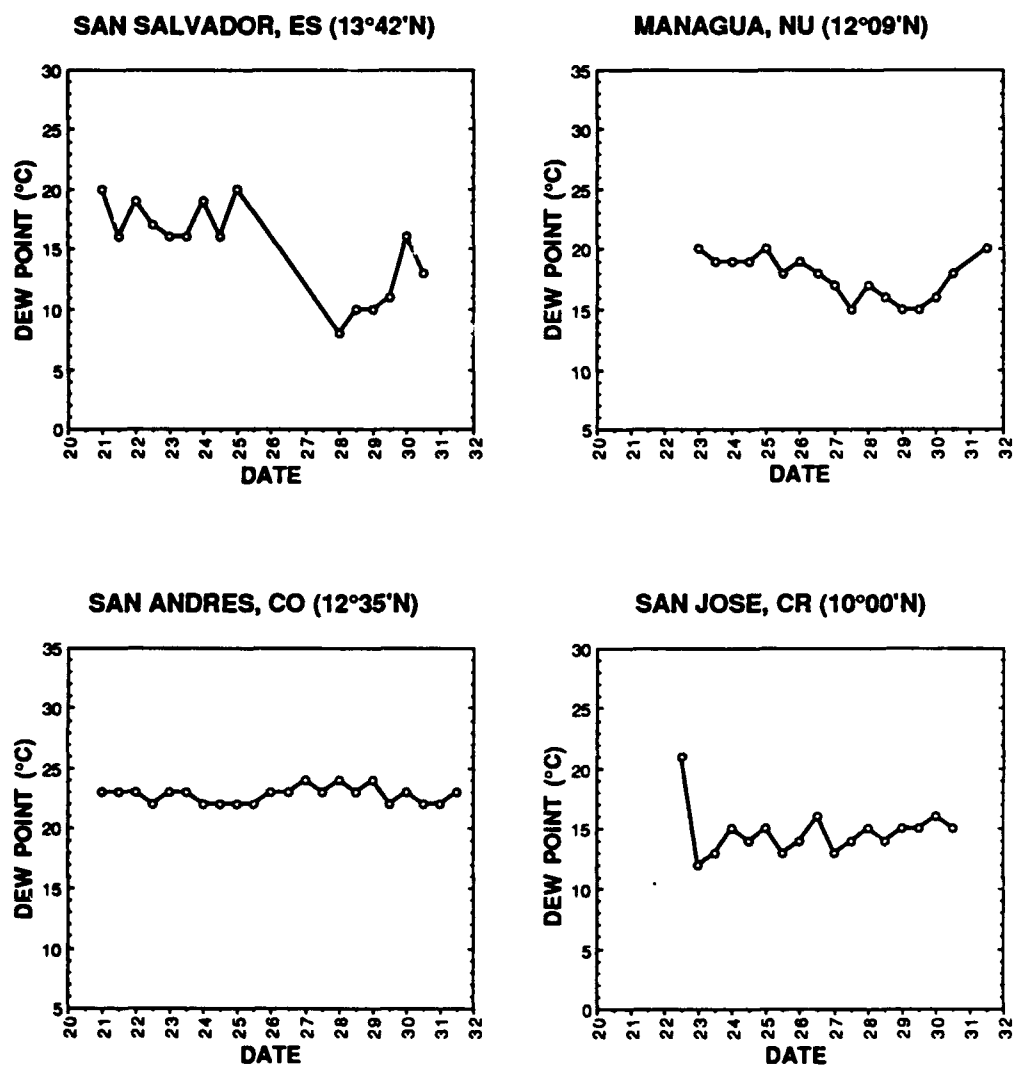


Figure 74. (Continued).

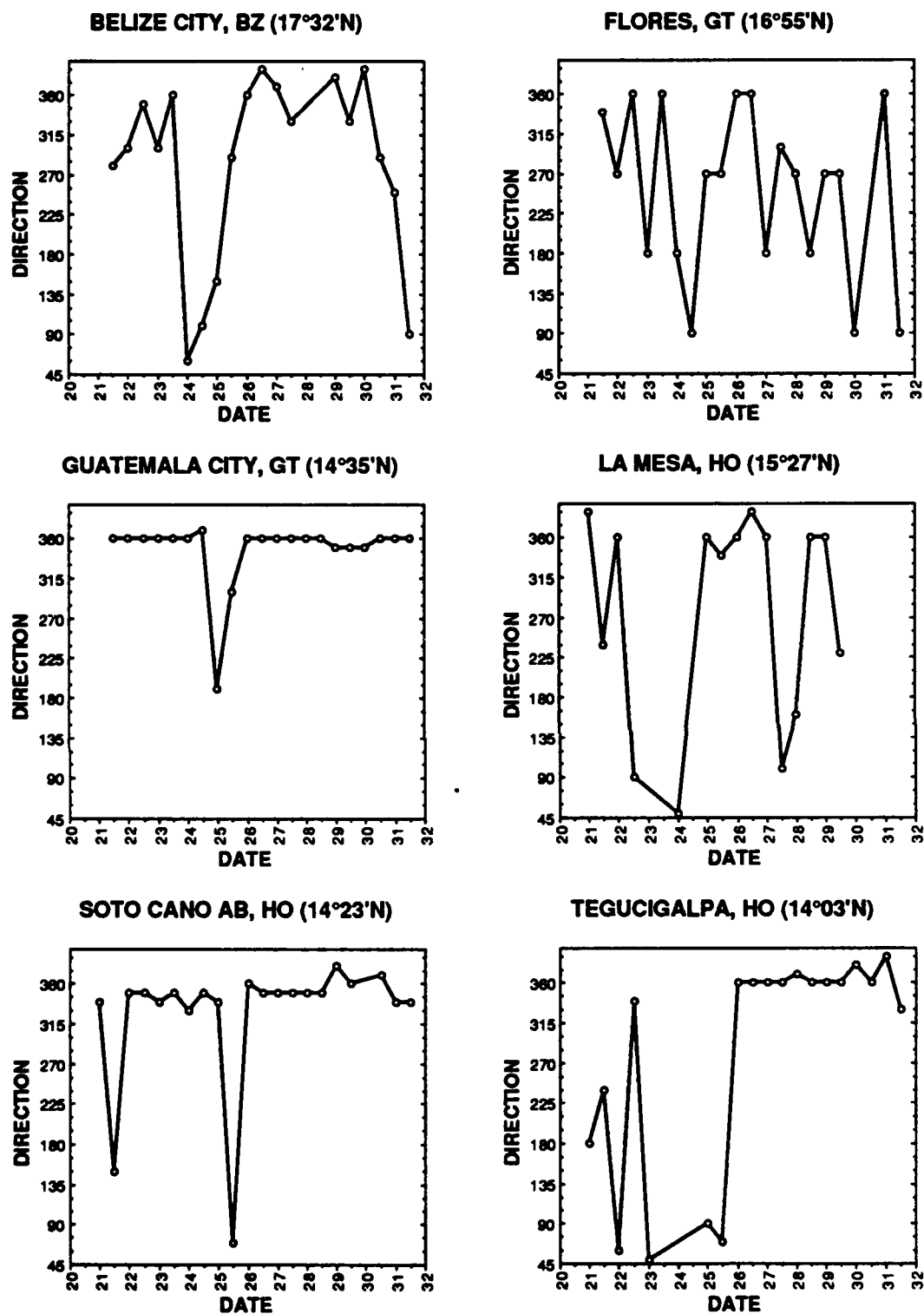


Figure 75. Wind direction at 0000 UTC and 1200 UTC from 20-31 January 1988.

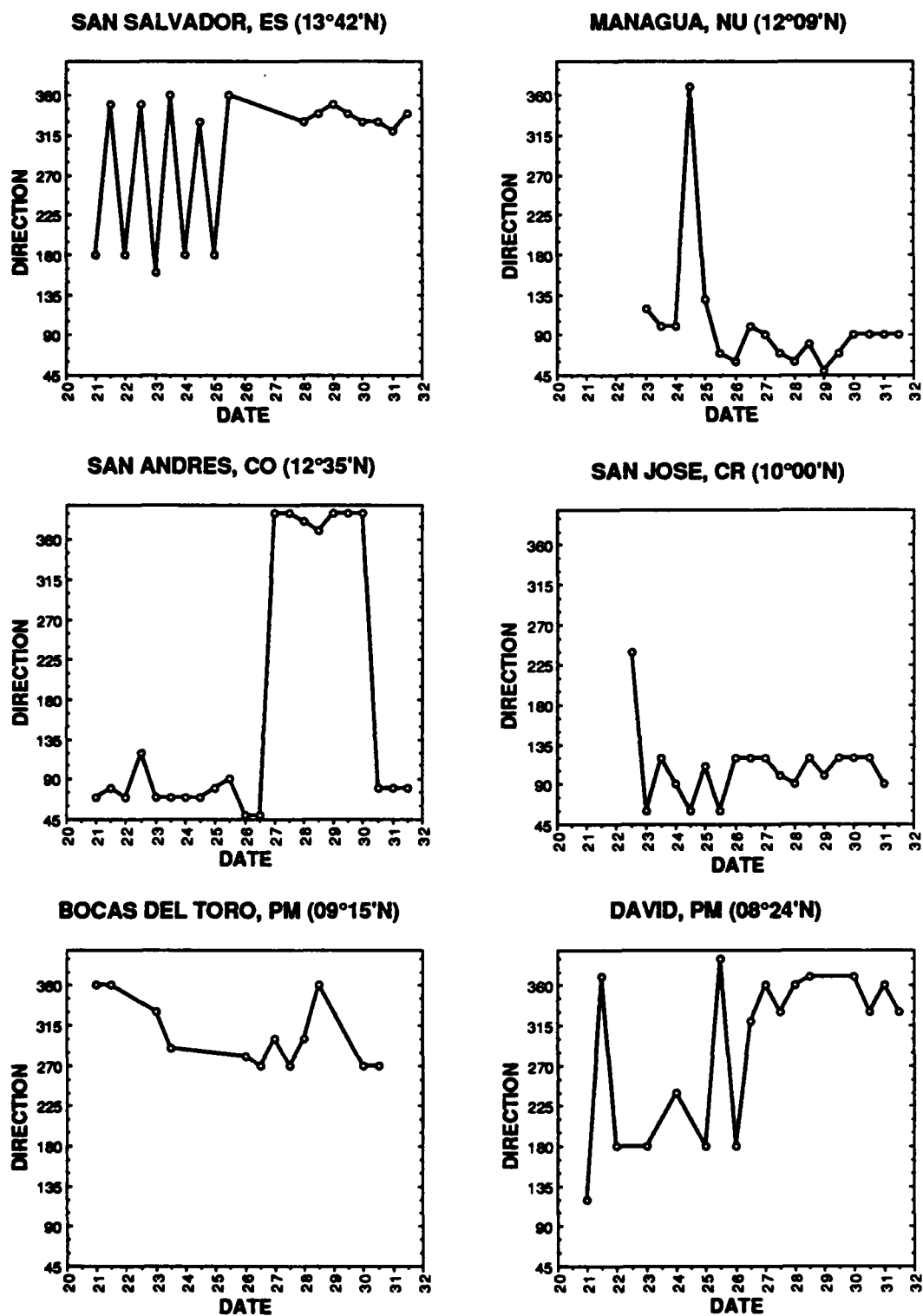


Figure 75. (Continued).

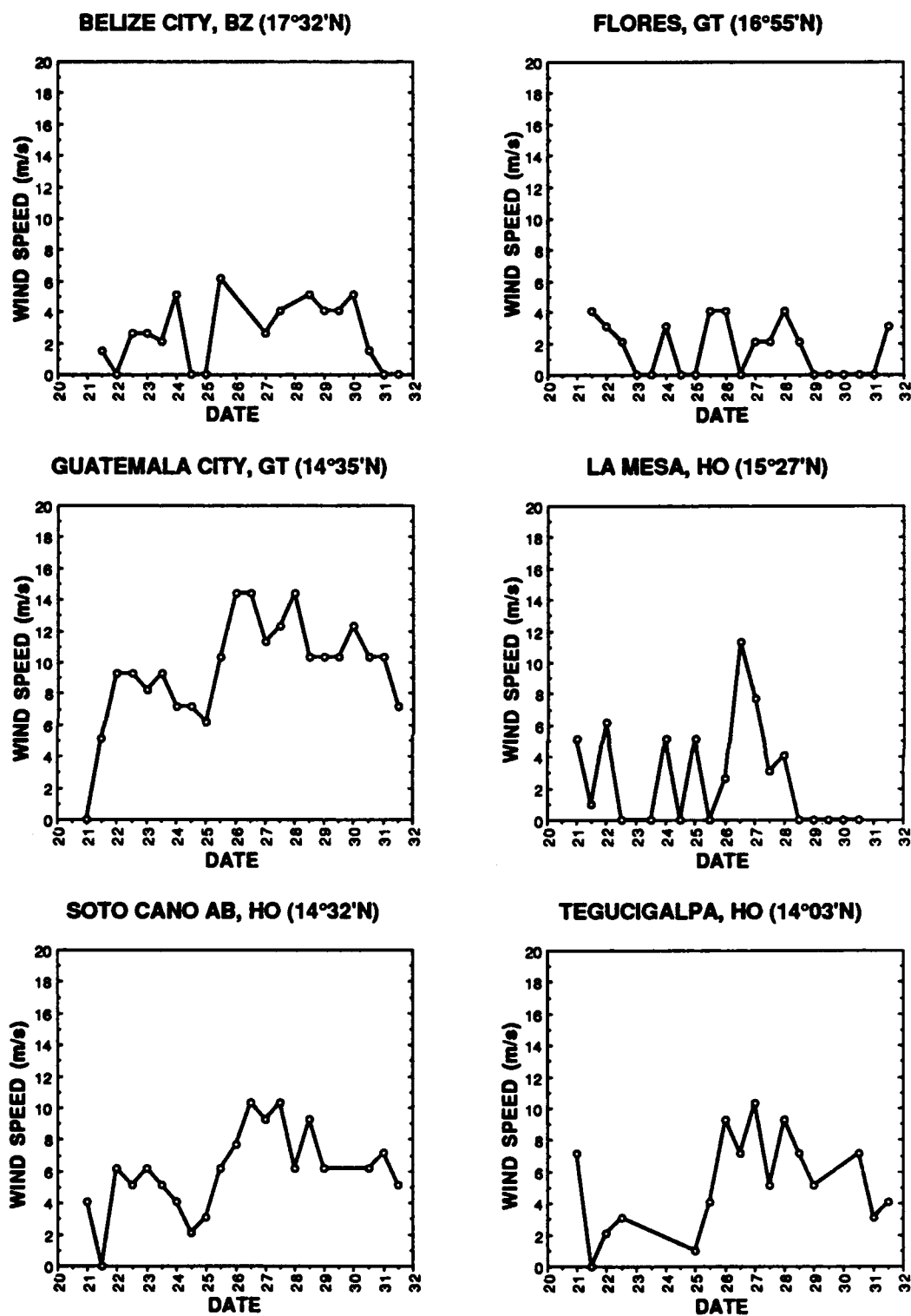


Figure 76. Wind speed (m/s) at 0000 UTC and 1800 UTC from 20-31 January 1988.

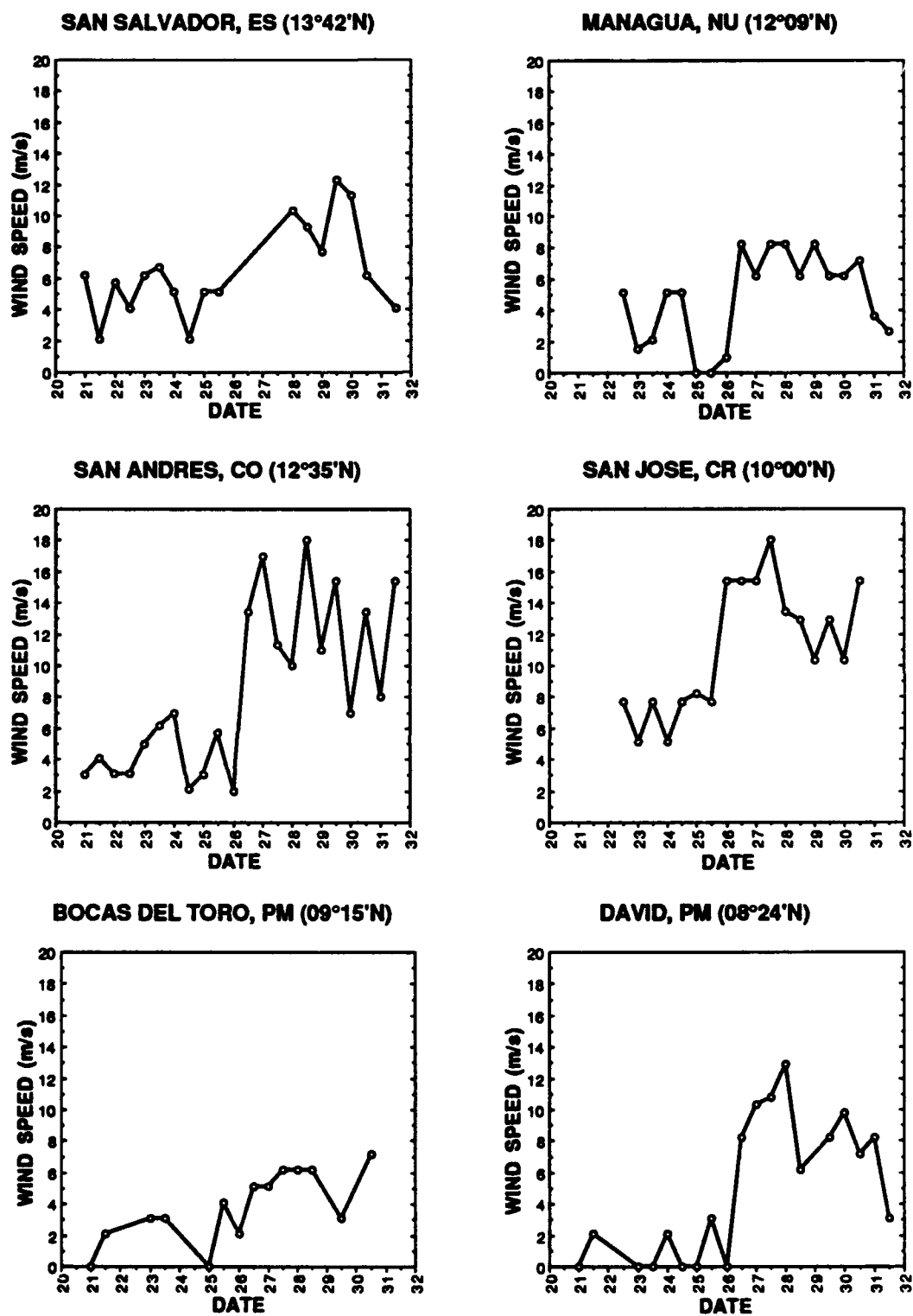


Figure 76. (Continued).

speed remained elevated through the remainder of the period. David, the southern most station, displayed a 12 m/s wind speed increase in the days after frontal passage.

Very distinct and consistent jumps in SLP were evident at all stations north of San Salvador during frontal passage (Fig 77). The greatest increase was at Flores, where pressure climbed 19.9 mb between 25 January at 0000 UTC and 27 January at 1500 UTC. Cold surge signals were evident, but very slight at the remaining stations.

A distinct CACS signature was apparent in cloud cover at every station except Flores, where skies remained cloudy and ceiling heights remained nearly constant through the entire period (Fig. 78). Every other station displayed a dramatic increase in cloud cover and/or decrease in ceiling height with frontal passage. Cloud ceilings at Bocas del Toro dropped from 3000 m to 300 m immediately after frontal passage and remained below 540 m through the duration of the cold surge. No cloud cover was reported at Tegucigalpa until after frontal passage. During the cold surge, cloud ceilings remained below 960 m. Even stations on the Pacific side of the continental divide, such as San Salvador and David, reported increases in cloud cover during this CACS event.

CACS induced precipitation varied widely from station to station (Fig. 79). San Salvador, Managua and David remained dry throughout the period, while Guatemala City recorded only 1 mm of rainfall. These stations are all on the Pacific side of the Central American Isthmus. Precipitation trends at all other stations displayed a definite CACS signature. Belize received 30 mm of rainfall during the cold surge, while Flores and San Andres recorded 37 mm and 76 mm respectively.

Vertical Structure

The Belize City time cross section was produced with 12-hourly upper air observations from 23 January at 0000 UTC through 27 January at 0000 UTC centered

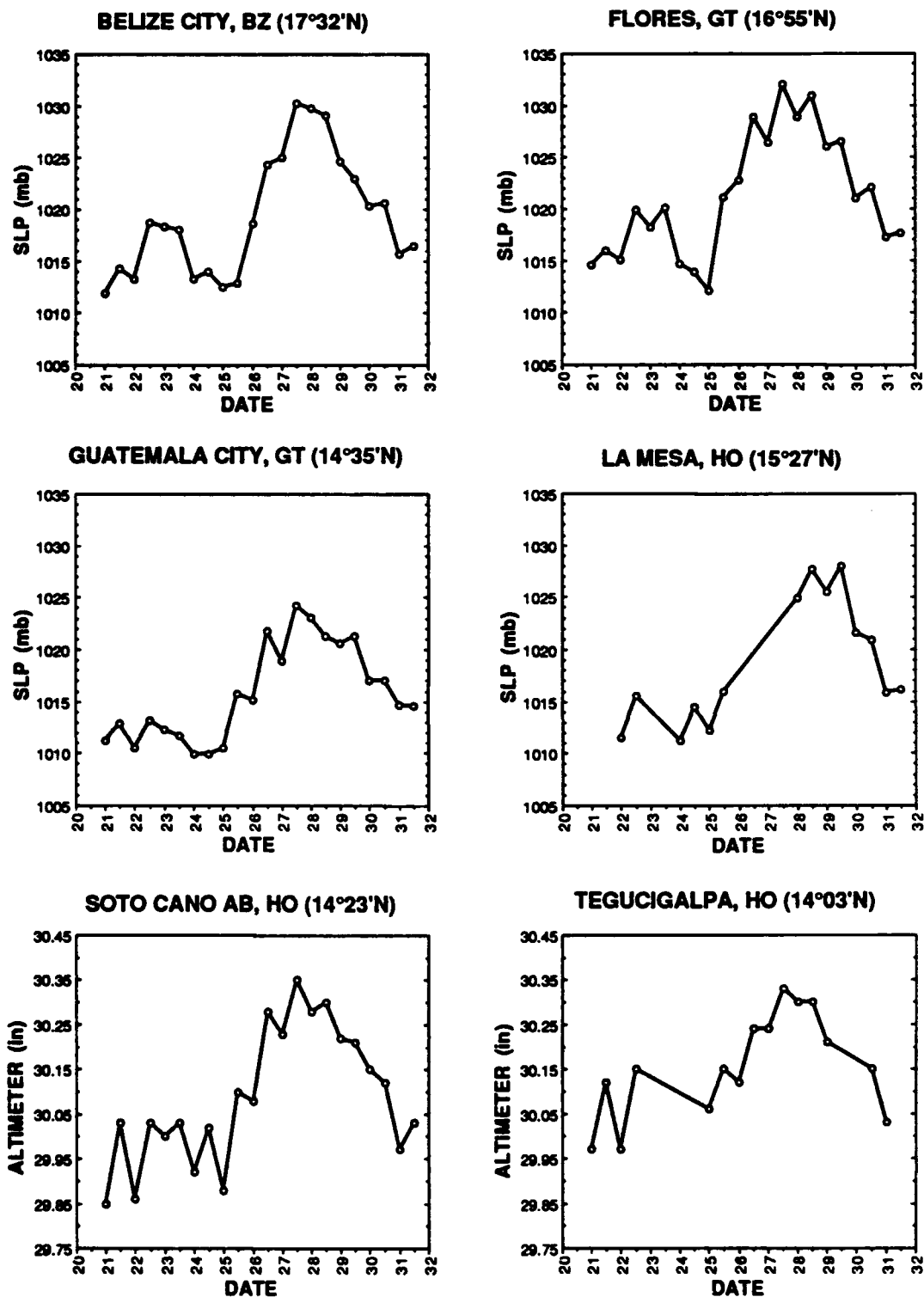


Figure 77. Sea level pressure (mb) or altimeter setting (in) at 0000 UTC and 1500 UTC from 20-31 January 1988.

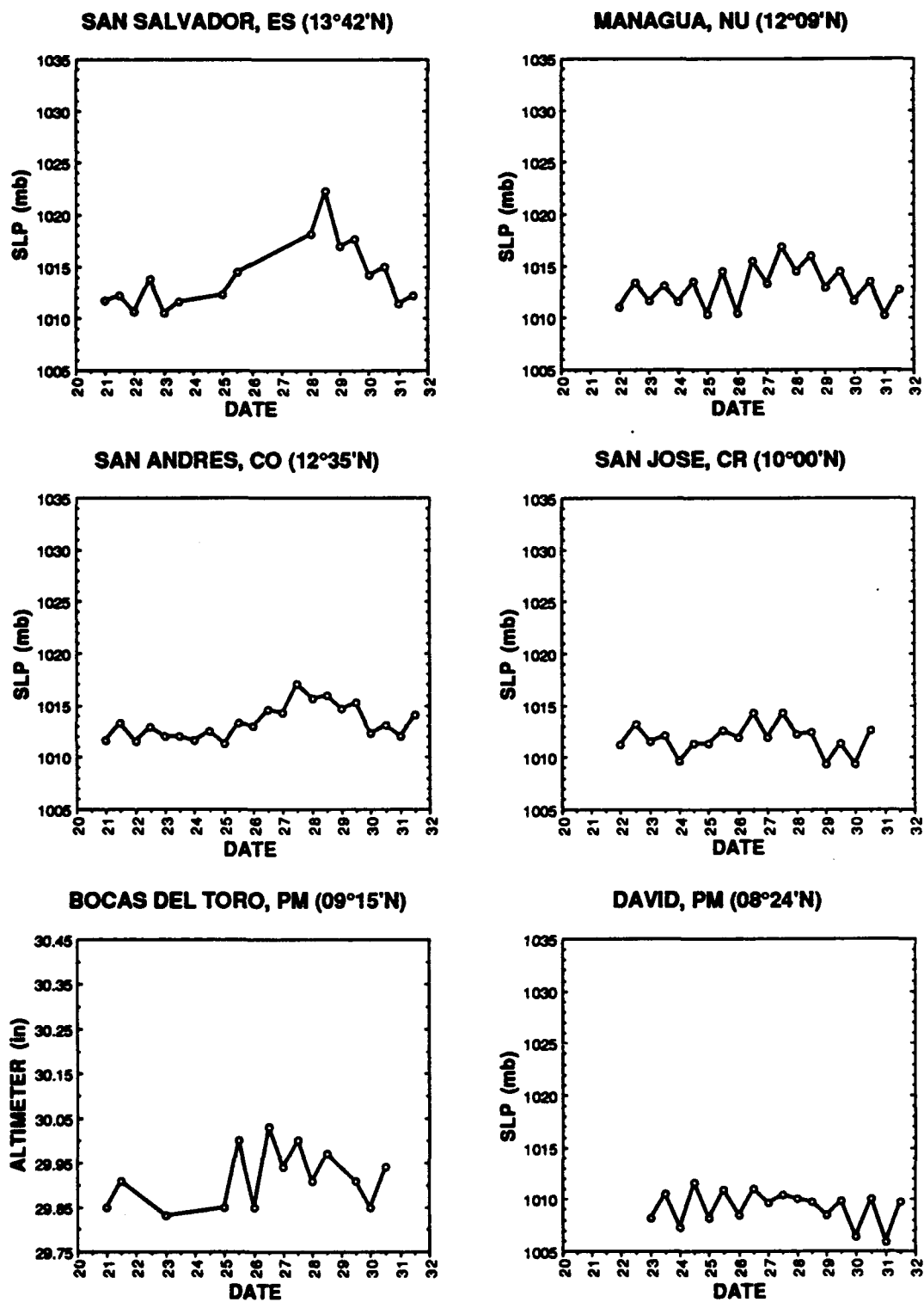


Figure 77. (Continued).

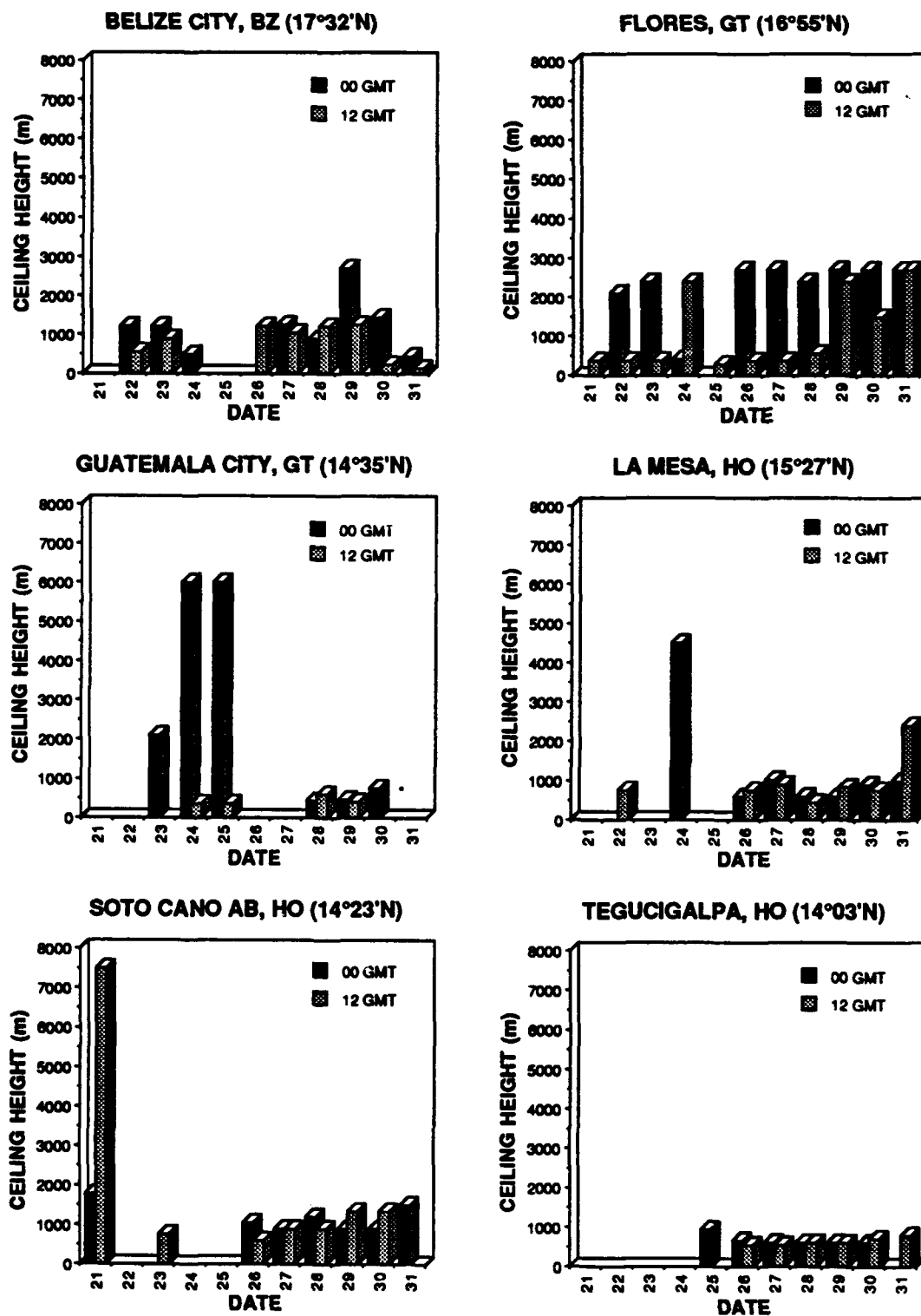


Figure 78. Cloud ceiling height (m) at 0000 UTC and 1200 UTC from 20-31 January 1988.

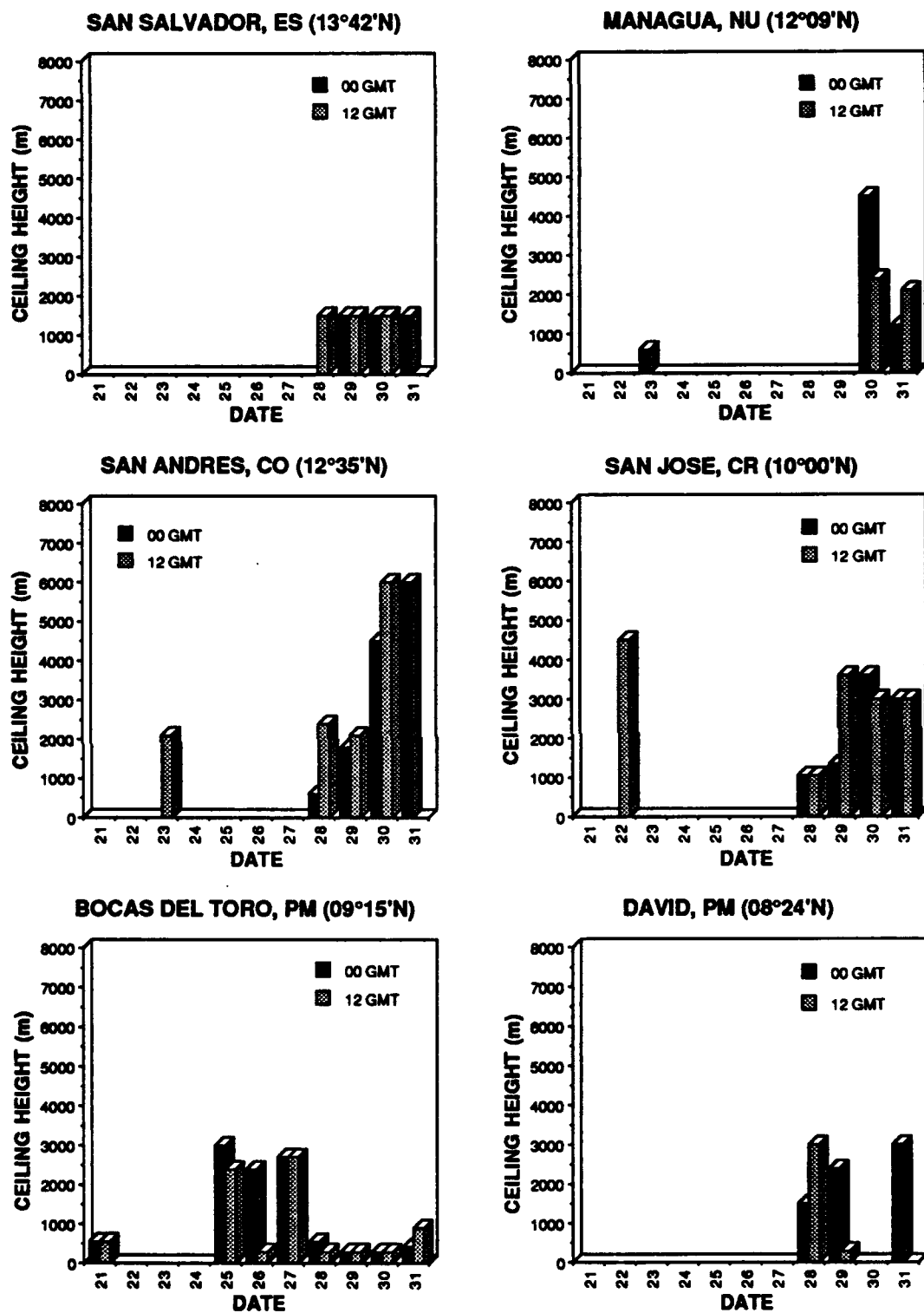


Figure 78. (Continued).

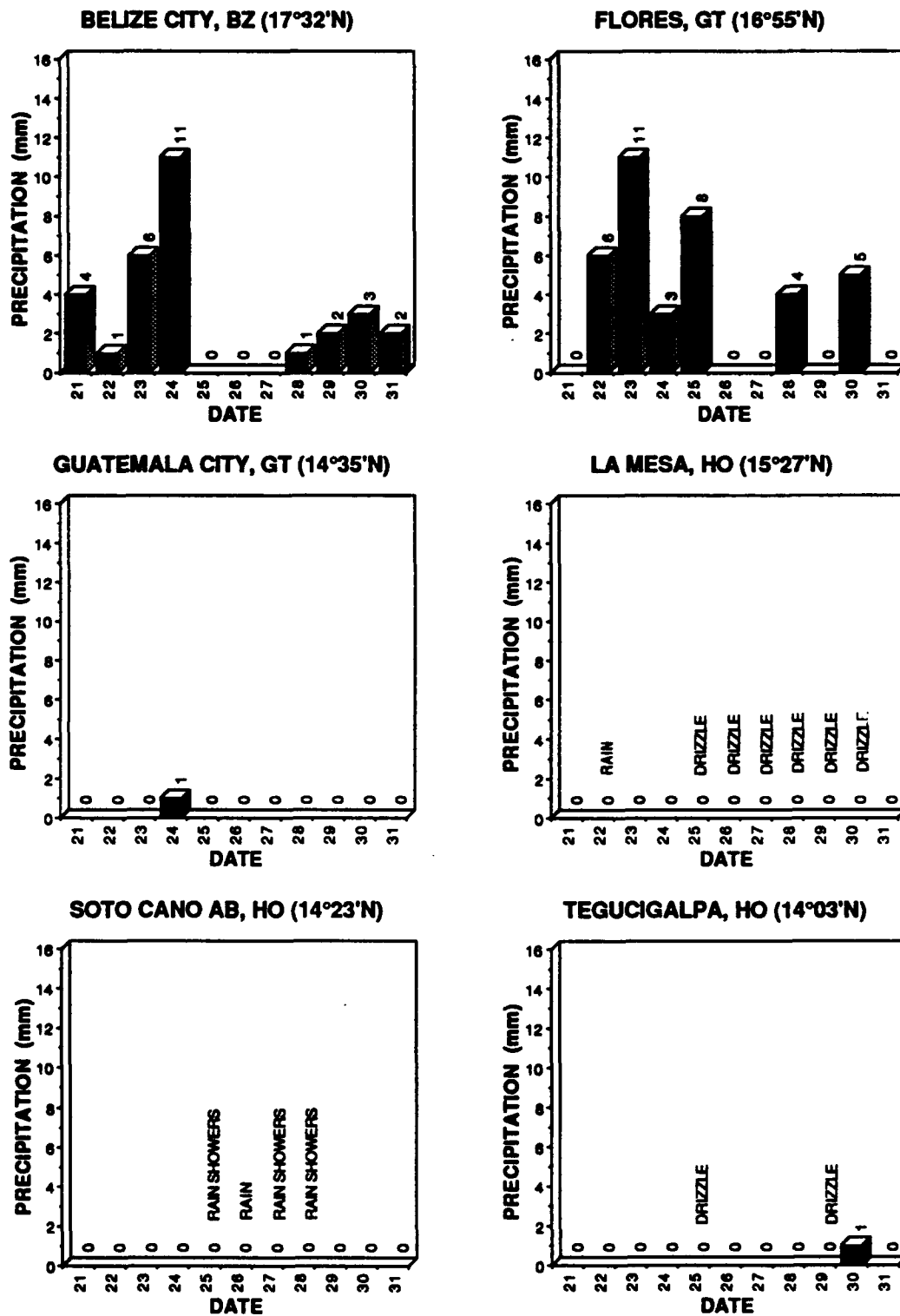


Figure 79. Daily precipitation (mm) from 20-31 January 1988.

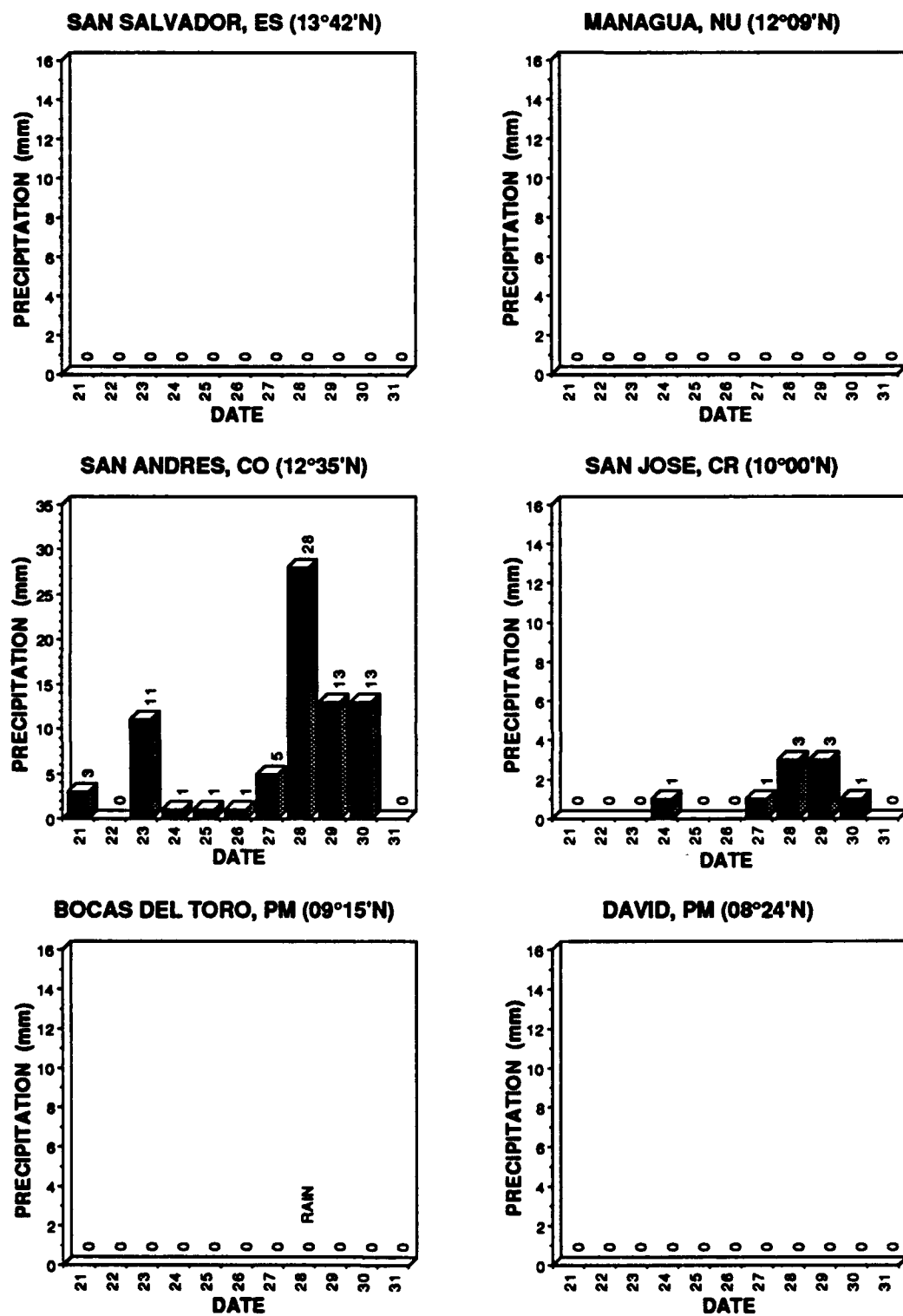


Figure 79. (Continued).

on the date of frontal passage (25 January). Observations from Tegucigalpa, San Andres and San Jose were only available at 1200 UTC. Cross sections were produced for each station using observations from 22 January through 31 January. Guatemala City was not included in this analysis because of missing data.

Both of the frontal passages during this cold surge event were evident in the Belize City cross section, corresponding well to both the satellite imagery and the surface observations. Initially, a frontal inversion was analyzed near 650 mb (Fig. 80). The cold front had moved north into the Gulf of Mexico by 24 January, and a strong subsidence inversion was evident capping moisture below 850 mb until 25 January. Another frontal inversion became apparent at the time of the second frontal passage and persisted between 700 mb and 650 mb through 27 January. Moisture was confined below this inversion. Northwest to northeast flow dominated up to 850 mb with both fronts, while southeast flow was evident only on 25 January. The prevailing winds were southwesterly above the frontal layer. While the atmosphere was generally stable throughout the period, stability increased dramatically after the second frontal passage.

Two major inversions were evident on the Tegucigalpa cross section (Fig. 81). The first was a subsidence inversion lasting from 22 January through 28 January near 700 mb. A frontal inversion was apparent near 750 mb from 25 January through 31 January. Areas of significant moisture were generally confined below these inversions. Strong cooling was also evident below the frontal inversion. Although winds below the inversions remained northerly through the period, flow up to 200 mb shifted from south-southeast to west-southwest and strengthened considerably after the frontal passage. The atmosphere remained stable through the entire period.

The cross section from San Andres indicated a pair of subsidence inversions dominating prior to frontal passage (Fig. 82). One of them capped moisture below 700

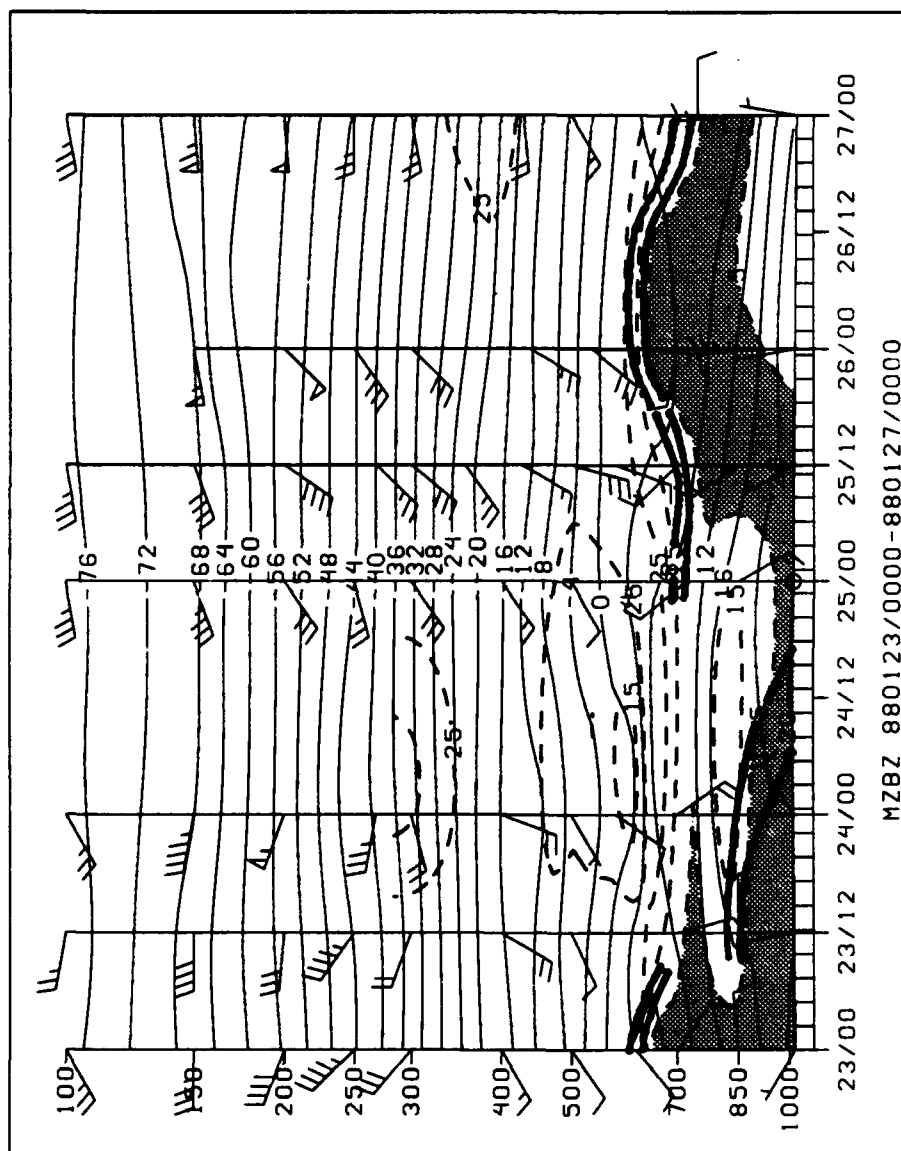


Figure 80. Vertical temporal cross section at Belize City, Belize from 23 January 1988, 0000 UTC to 27 January 1988, 0000 UTC. Isotherms (solid) are plotted at 4°C intervals and isodrosotherms (dashed) at 5°C, 15°C and 25°C. Also shown are areas with dew point depression less than or equal to 5°C (shaded), wind speed (kt) and direction, and inversion layers (heavy solid).

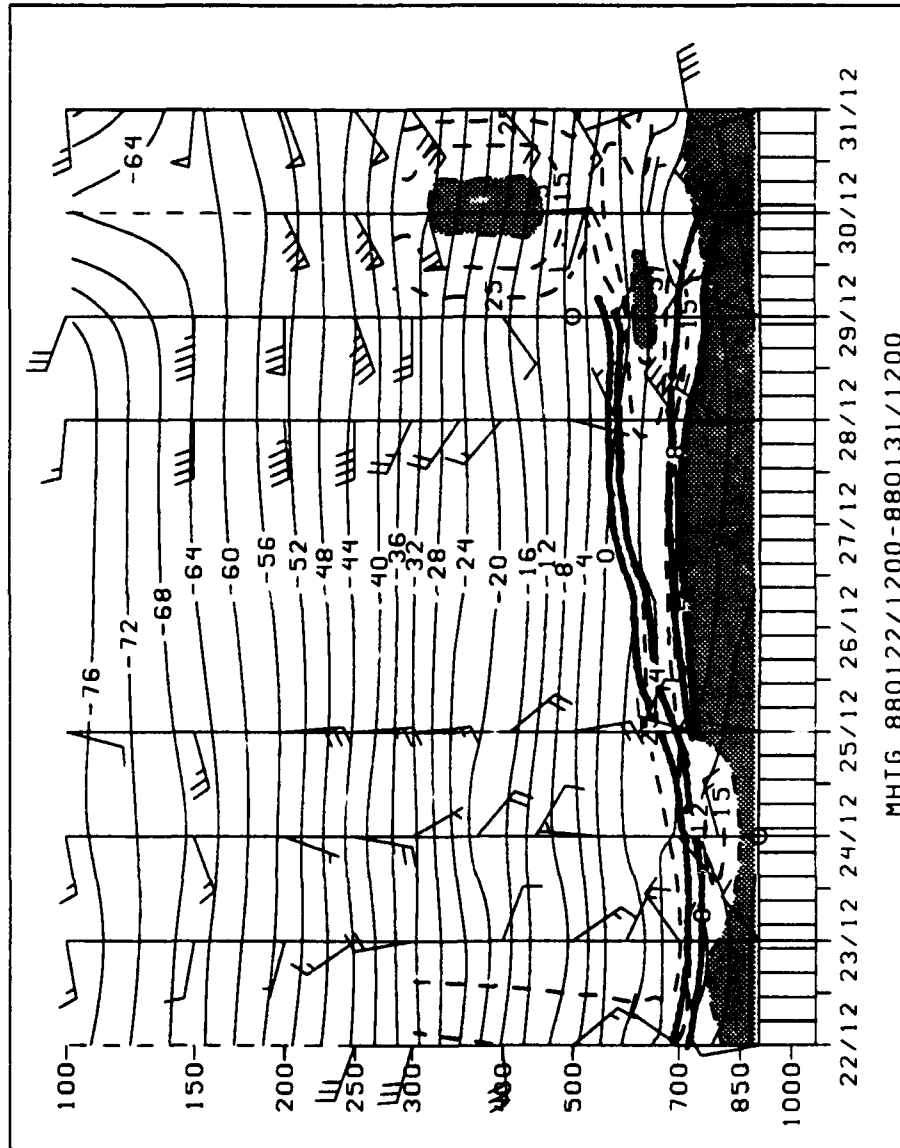


Figure 81. As in Fig. 80, except at Tegucigalpa, Honduras from 22 January 1988, 1200 UTC to 31 January 1988, 1200 UTC.

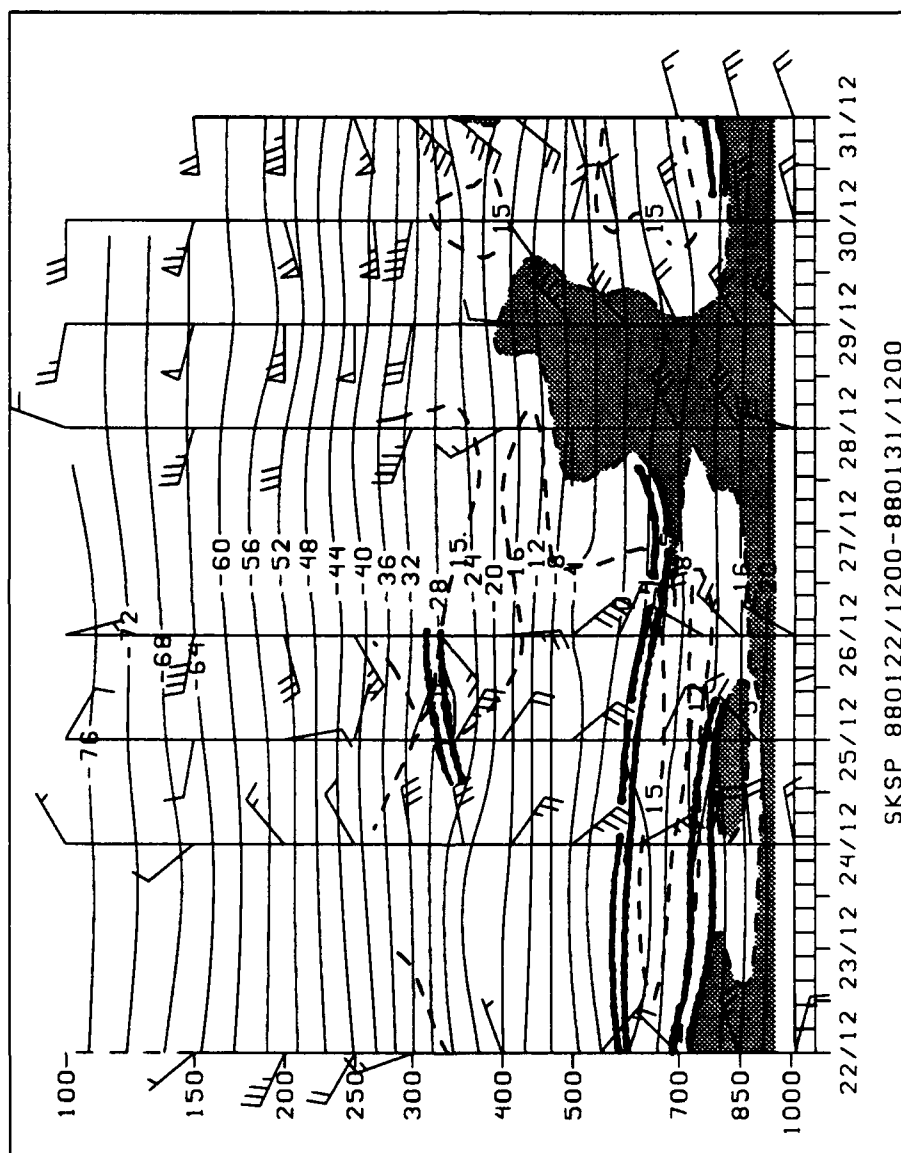


Figure 82. As in Fig. 80, except at San Andres, Colombia from 22 January 1988, 1200 UTC to 31 January 1988, 1200 UTC.

mb until 26 January. The stronger inversion was located near 600 mb and was apparently disrupted by frontal passage on 27 January. Moisture expanded up to approximately 400 mb after frontal passage, corresponding well to the San Andres precipitation pattern, and low-level wind flow indicated a slight turning to the north. As in the Tegucigalpa cross section, flow between 600 mb and 200 mb abruptly shifted from southeast to west-northwest and strengthened after the frontal passage. No frontal inversion was identified. The atmosphere remained generally stable through the period, although stability decreased gradually after frontal passage.

The San Jose cross section displayed few significant features, and little evidence of frontal passage at the surface except a 10 kt increase in the northeasterly flow (Fig. 83). A weak subsidence inversion was evident near 700 mb from 24-25 January. A pair of weak subsidence inversions were apparent toward the end of the period near 700 mb and 450 mb. The atmosphere remained stable throughout the period. The major evidence of change at San Jose was in the upper levels, where winds were weak (less than 30 kt) and variable before 26 January. After frontal passage, strong (40-75 kt) westerly flow dominated above 400 mb.

Moisture Fields

Estimates of TPW for this CACS event were similar to those described in the previous chapter. However, the moisture field in this case responded to two frontal passages instead of one. The relative TPW maximum corresponding to the first front extended across southern Florida and eastern Cuba into the Gulf of Honduras on 22 January (Fig. 84). TPW values in the Gulf of Mexico ranged from 15 kg/m² along the Texas coast to 30 kg/m² near the Yucatan Peninsula, while TPW in the relative maximum exceeded 45 kg/m². TPW was unusually low in the southern Atlantic,

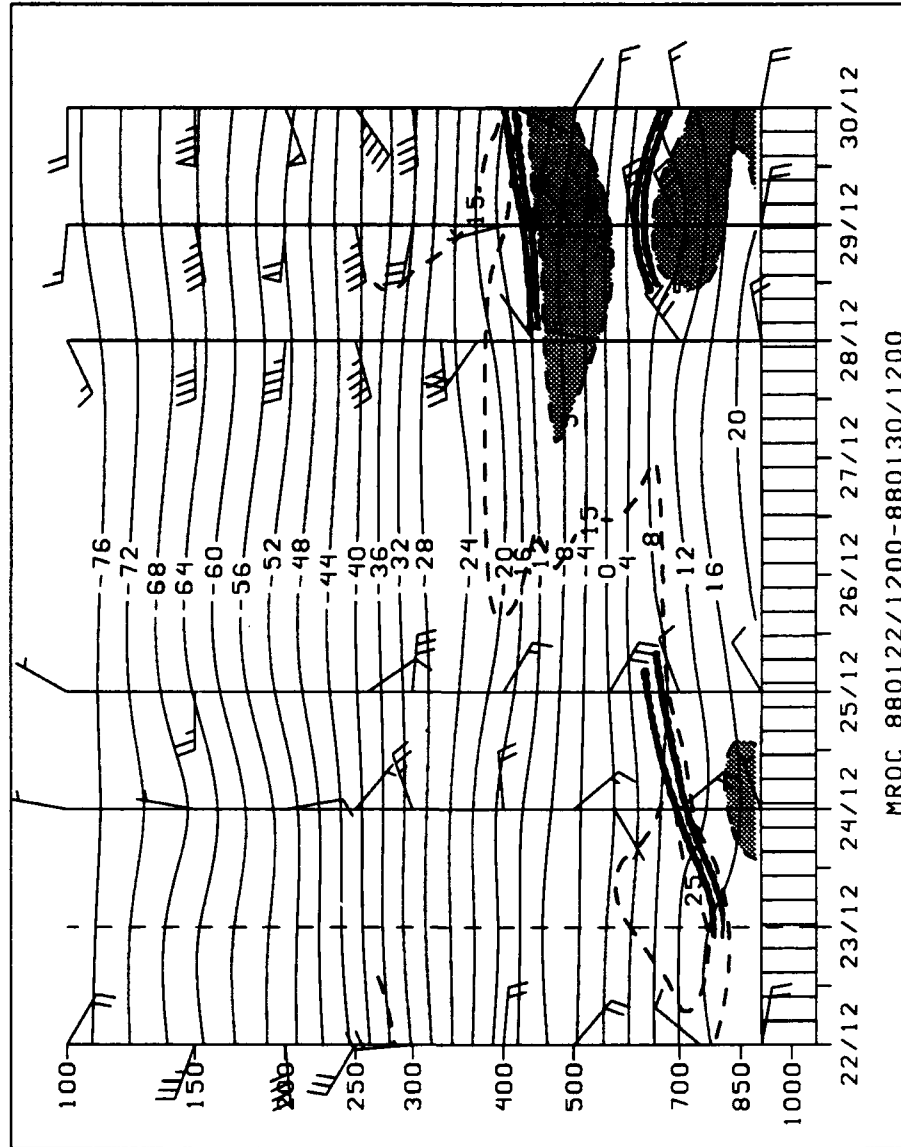


Figure 83. As in Fig. 80, except at San Jose, Costa Rica from 22 January 1988, 1200 UTC to 30 January 1988, 1200 UTC.

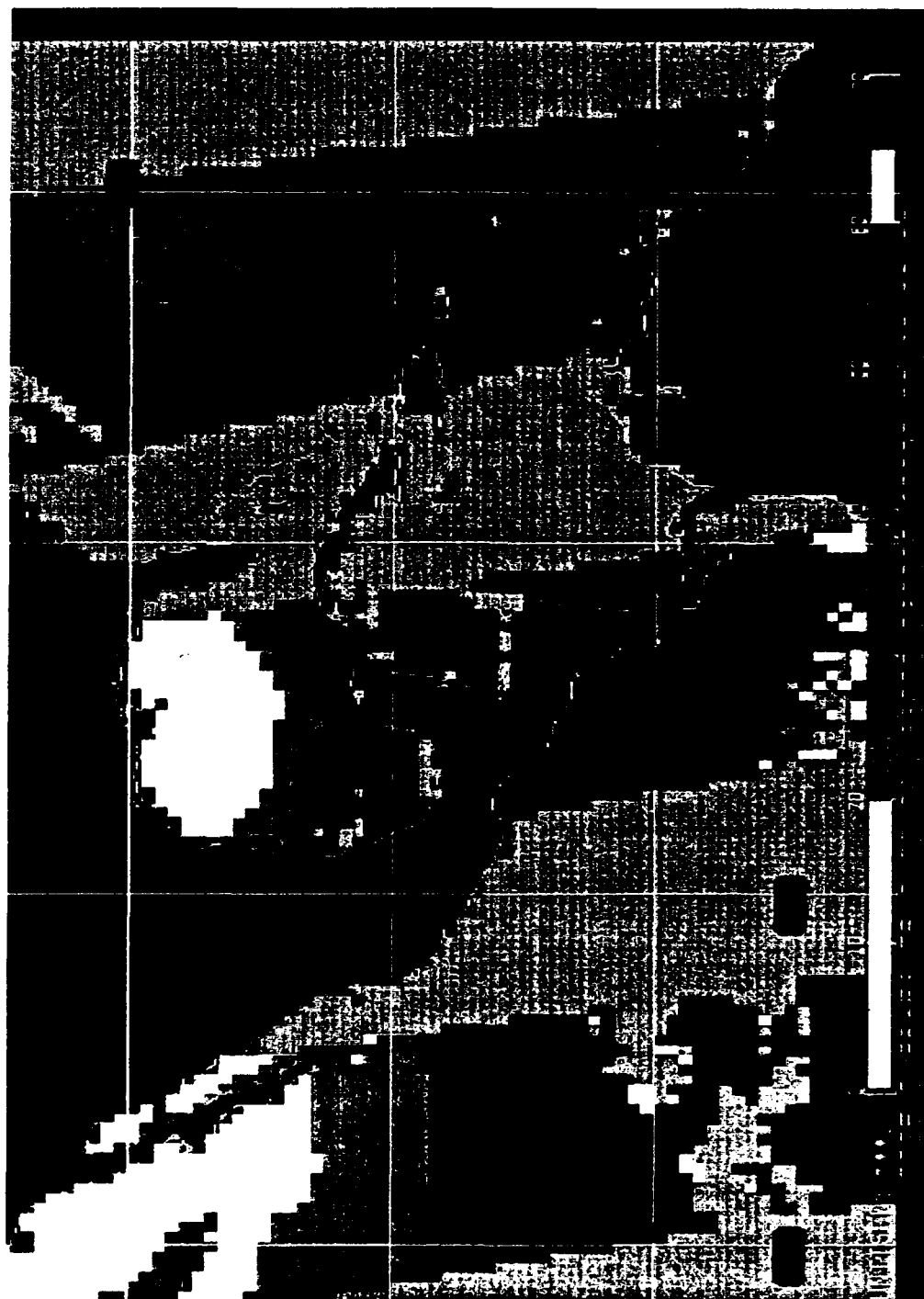


Figure 84. Total precipitable water (kg/m^2) field on 22 January 1988, 0600 UTC.

ranging from 25-40 kg/m². By 24 January, the relative TPW maximum had weakened to 40 kg/m², while a northward surge of TPW greater than 45 kg/m² was evident in the southern Gulf of Mexico (Fig. 85). More typical TPW values were returning to the southern Atlantic. The second cold surge had pushed into Central America by 27 January and TPW values in the Gulf of Mexico had decreased to 15-25 kg/m². The lowest TPW values (10 kg/m²) were located off the southeastern U.S. coast corresponding to the main focus of cold air advection. The relative TPW maximum which normally corresponds to the position of the surface front was not as distinct during the second portion of this cold surge. TPW values from 15-30 kg/m² had spread throughout the entire Gulf of Mexico and southern Atlantic by 29 January (Fig. 86) with the southern limit of the low TPW near 20°N. The relative TPW maximum was more defined, extending across Hispanola toward southern Central America. By 1 February, the relative TPW maximum had weakened, however, another surge of TPW greater than 45 kg/m² was apparent moving into the southern Gulf of Mexico in advance of the next cold surge.

Rain rate estimates for this CACS event, as with the other sample cold surges, were primarily confined to the vicinity of the surface fronts and along the northward facing coastlines of Central America. Rain rate values ranged from 0.5 mm/h to 4 mm/h, but were most commonly on the order of 1-2 mm/hr. Rain rates of 0.5-2 mm/h extended along the first surface front in the Gulf of Mexico on 21 January (Fig. 87). A more widespread area of precipitation was evident along the Gulf coast of southern Mexico. The second cold front had entered the Gulf by 25 January. Rain rates from 0.5 mm/h to 3 mm/h covered the northeastern portion of the Gulf and extended along the eastern U.S. coast. By 28 January (Fig. 88), rain rates of 0.5 mm/hr to greater than 4 mm/hr were evident along the surface front extending between Cuba and Haiti into western

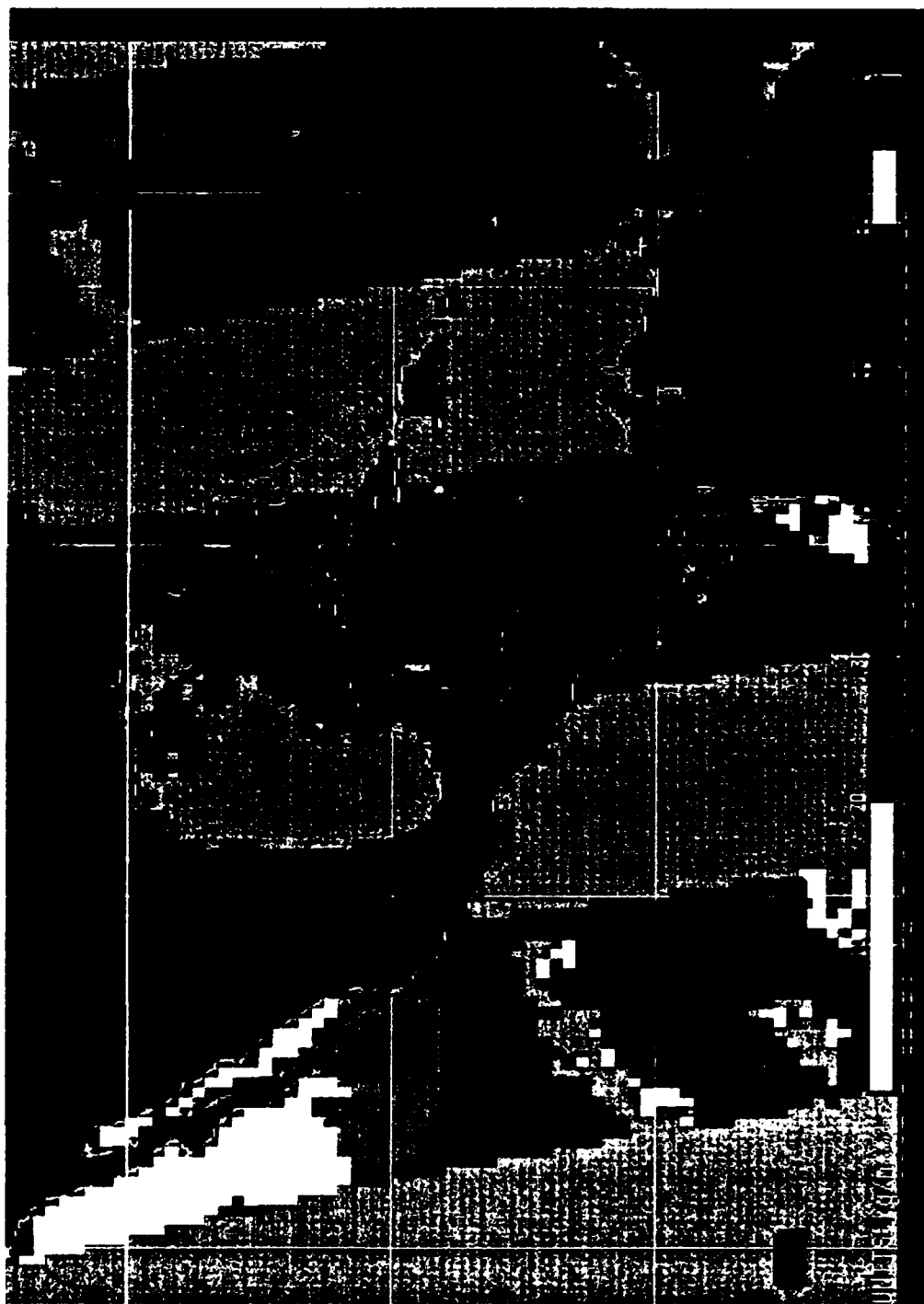


Figure 85. Total precipitable water (kg/m^2) field on 24 January 1988, 0600 UTC.



Figure 86. Total precipitable water (kg/m^2) field on 29 January 1988, 1800 UTC.

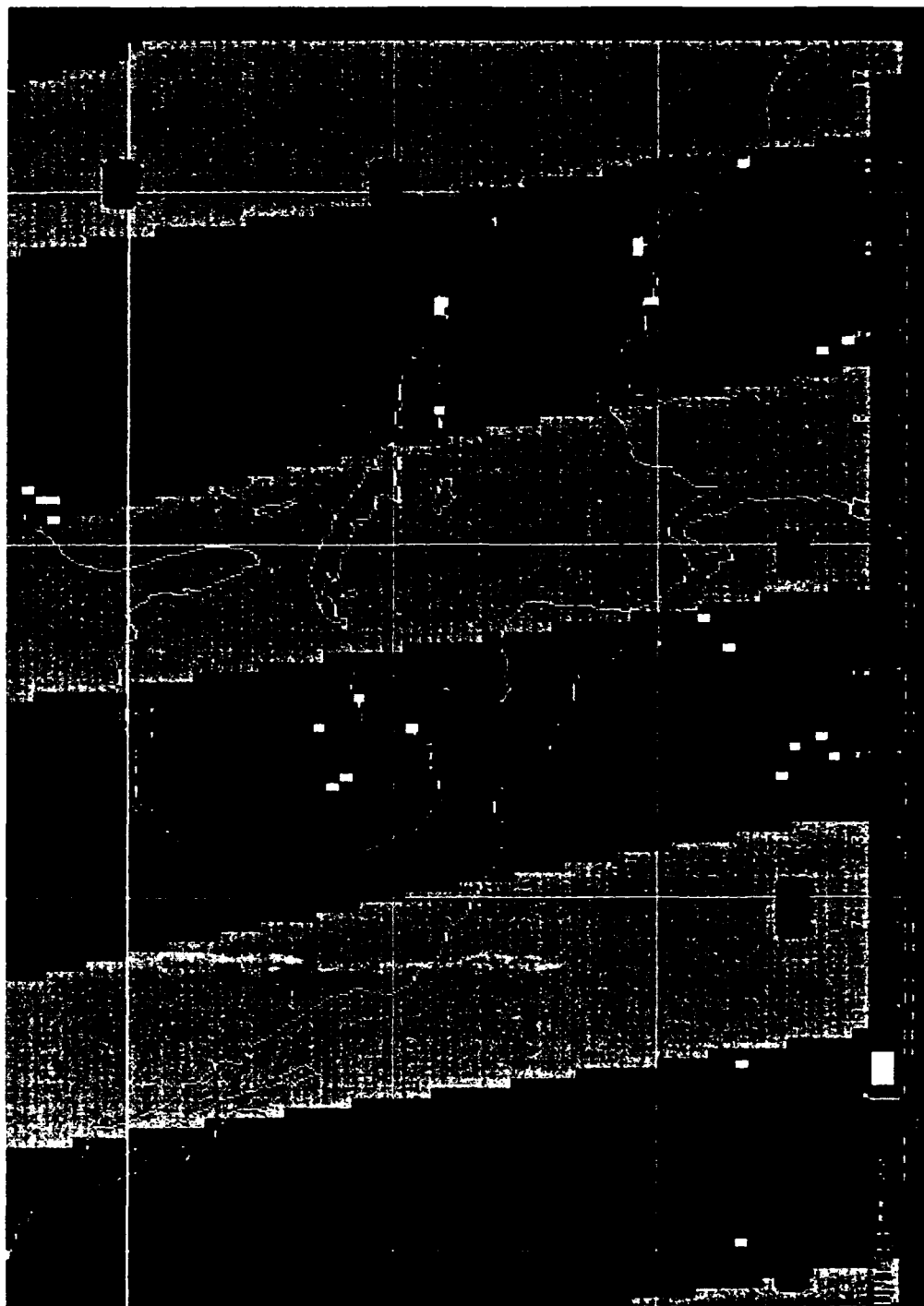


Figure 87. Rain rate (mm/h) on 21 January 1988, 0600 UTC.



Figure 88. Rain rate (mm/h) on 28 January 1988, 1800 UTC.

Panama. Rain rates along the front had weakened considerably by 30 January (Fig. 89). At the end of the cold surge, the most significant remaining area of precipitation was in response to orographic lifting along the northern Honduras coast, with rain rates ranging from 0.5 mm/h to greater than 4 mm/h.

This study is most concerned with the orographically forced precipitation along the Central American coast. Rain rate estimates were compared with the observed rainfall totals at Belize City, La Mesa and San Andres during the November 1987 and January 1988 cold surges. While these stations can not provide ground truth comparisons, they can provide a reasonable assessment of the accuracy of SSM/I rain rate estimates assuming the precipitation characteristics over water and along the coast are similar. For both cases, precipitation indicated by satellite underestimated the actual rainfall totals by nearly 35% at La Mesa and Belize. Results were slightly better at San Andres, where rainfall was underestimated by just over 25%.

Summary

This was a strong CACS, and it appeared much more impressive on GOES imagery. As in the November 1987 case, a wave developed along the front associated with the first cold surge, intensified, and initiated the second cold surge. The satellite analysis corresponded well to surface observations. The maximum southward penetration of the first cold surge was extreme northwestern Honduras. Both CACS events were evident in the surface observations at every station north of Tegucigalpa. Surface variable response to the second cold surge was similar, but more intense than the previous cases. Upper air observations also corresponded well with both satellite and surface observations, as both CACS events were evident on the Belize City cross section. Distinct frontal inversions were observed at both Belize City and Tegucigalpa, so the

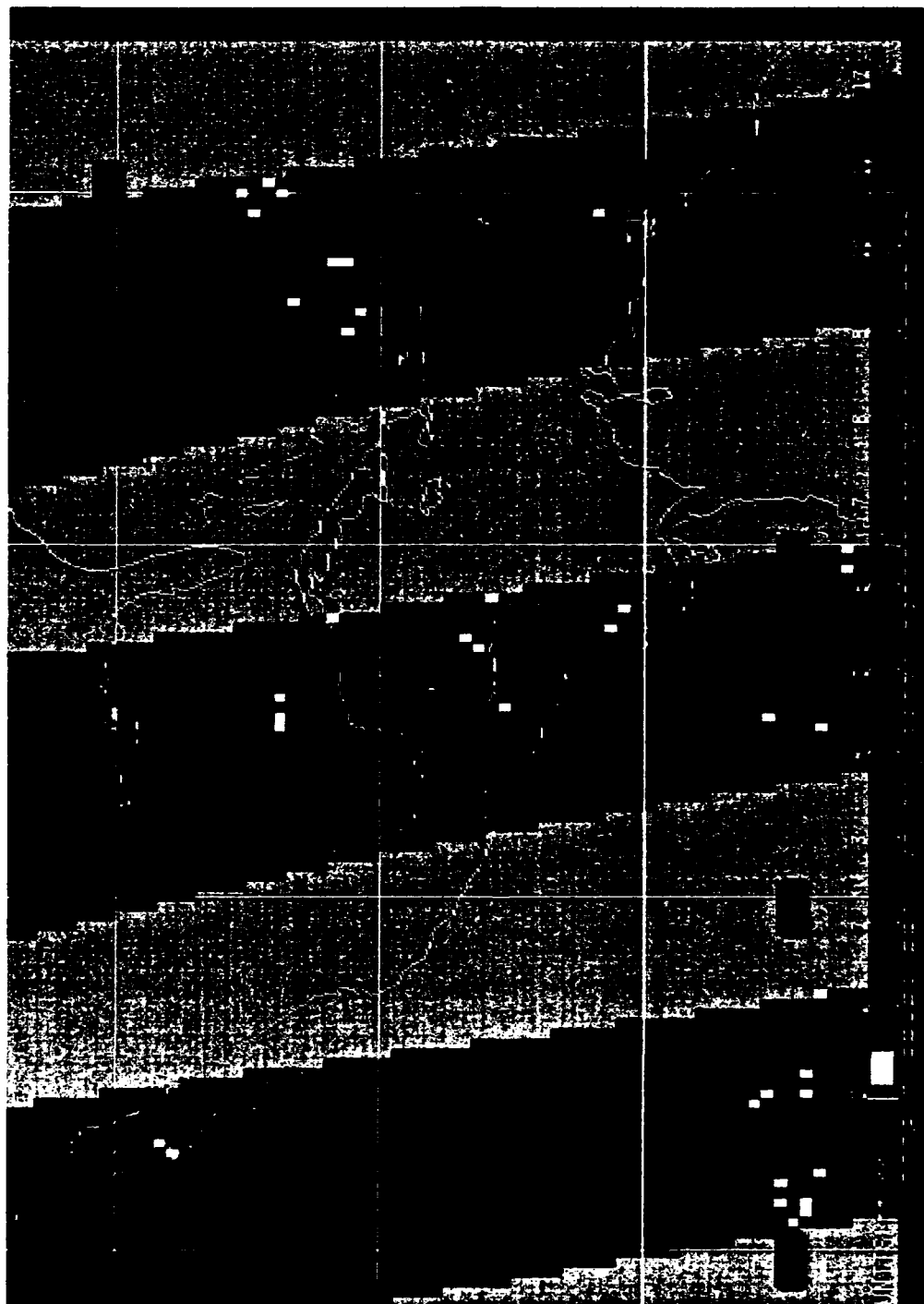


Figure 89. Rain rate (mm/h) on 30 January 1988, 0600 UTC.

vertical structure of the second cold surge remained in tact as least through southern Honduras. The trade wind inversion was apparent at both Tegucigalpa and San Andres prior to frontal passage. The main evidence of frontal passage at San Andres was the disruption of the trade wind inversion on 27 January. Again, primarily stratiform precipitation was indicated in the cross sections which corresponded well with surface rainfall observations. The evolution of TPW and rain rate were similar to the previous cases, and again corresponded well with both GOES, surface and upper air data.

COLD SURGE COMPARISON AND EVOLUTION

Cold Surge Comparison

This research was initially based on the assumption that the CACS was a similar phenomena to the EACS. The CACS definition was even modeled after established definitions of the EACS. Now that some of the climatology, structure and evolution of the CACS is known, an accurate comparison of the two events can be made.

The Central American and East Asian cold surges share many common features, the most obvious of which is topography. The Tibetan Plateau and the Rocky Mountains both provide a favorable setting for the buildup of vast pools of cold air, and act as a western boundary to assist in the equatorward penetration of the cold air (Hastenrath, 1988; Murakami, 1987). Both North America and East Asia have warm ocean currents along their eastern coast, the Gulf Stream and Kuroshio Current respectively. These currents correspond to areas of explosive cyclogenesis and maximum cyclogenesis frequency (Boyle and Chen, 1987). According to Lau and Lau (1984), these are the perfect breeding grounds for the development of intense cyclone-anticyclone pairs which typically accompany cold surges. Lau and Lau added that significant air mass modification occurs as the cold air mass behind the EACS passes over the South China

Sea. This parallels the role of the Gulf of Mexico in modifying the cold air mass associated with the CACS. Orographic lifting of the modified air mass often generates dense low-level cloud cover and persistent stratiform precipitation along the Caribbean coast of Central America during CACS events. A similar situation develops along the windward ranges of Taiwan, the Philippines, Vietnam and Borneo during the EACS (Ramage, 1971).

As similar as the CACS and EACS seem, two significant differences exist. The EACS often enhances low-level convergence producing deep cumulus convection and severe weather as it progresses equatorward (Lau and Lau, 1984). The CACS is relatively mild in comparison. The only severe weather occurs with strong winds or when stratiform rain persists long enough to generate flash flooding. Effects of the EACS have been tracked across the equator into the Southern Hemisphere. According to Johnson and Houze (1987), the EACS often leads to an increase in deep convection over Australia and may enhance the development of Southern Hemispheric tropical cyclones. The CACS, however, is apparently confined to the Northern Hemisphere by the Panamanian Isthmus and the mountains of northern Colombia.

CACS Termination

The end of a CACS event is signaled when east-northeast trade wind flow regains control over Central America. This can occur in several ways. The most common scenario occurs most often during weak or moderate cold surges when the southern end of the front undergoes frontolysis. As the parent cyclone moves farther into the Atlantic, the subtropical high builds back into the Caribbean and east-northeast trade wind flow replaces the north-northwest cold surge flow over Central America. This was evident in all 3 CACS cases. The tropical wave in the November 1987 case was

not the cause of CACS termination, it simply highlighted the fact that easterly flow had returned.

A similar scenario occurs during stronger cold surges. The only difference is that the southern end of the cold front maintains its identity and is forced back to the northwest over Central America as the subtropical high builds back into the Caribbean. Eventually, the parent cyclone and trailing cold front move off into the Atlantic and the trade winds again become dominant over Central America. This was evident in the CACS case described in Chapter V.

The least common scenario occurs during only the most intense cold surges. The cold front maintains its identity throughout the entire CACS event, sweeps through Central America, and continues on across the Caribbean and along the northern coast of South America. Northerly flow dominates the region until the Arctic high moves far enough into the Caribbean to restore easterly flow to Central America.

CACS Life Cycle

The information presented in this study is combined to illustrate the evolution of the typical synoptic scale features associated with a CACS. The CACS life cycle is summarized in four phases:

- a. Phase 1: Pre-CACS.
- b. Phase 2: CACS Onset.
- c. Phase 3: Mature CACS
- d. Phase 4: CACS Termination.

In the pre-CACS phase, easterly trade wind flow dominates Central America (Fig. 90). Scattered cumulus develop during the afternoon, primarily along coastal sea breezes, but the atmosphere is stable and the trade wind inversion prevents the

development of any significant convection. A weak cold front extends across the southeastern U.S., and a new wave is developing along the front near the Gulf coast. An upper level trough is evident over the eastern U.S. A tongue of TPW greater than 40 kg/m^2 is surging into the southern Gulf of Mexico north of the Yucatan Peninsula.

During the next day or two, the wave intensifies and moves rapidly northeast. The CACS onset phase is marked by a strong cold front extending from a mature cyclone along the central Atlantic coast of the U.S., into the southern Gulf of Mexico and across the northern Yucatan Peninsula (Fig. 91). Strong northerly flow behind the surface front is pushing cold air out across the Gulf of Mexico. The cold air is rapidly modified by the warm ocean surface producing streets of stratocumulus oriented in the direction of the wind flow over the Gulf of Mexico toward the surface front. The moisture is capped by a frontal inversion. Orographic lifting of the modified cold air is producing thick stratocumulus banked up against the Sierra Madres in eastern Mexico and stratiform precipitation along the Mexican Gulf coast. Rainshowers and thunderstorms are confined to a narrow band along and ahead of the surface front where the atmosphere is most unstable. The upper level trough has intensified, and the polar jet now extends into the Gulf of Mexico. The subtropical jet has also intensified. The subtropical high and trade wind inversion still dominate ahead of the surface front, with stable conditions and only scattered cloud cover across the majority of Central America. Low-level flow has become more southeasterly ahead of the front. TPW values over the northern Gulf of Mexico have dropped to near 20 kg/m^2 , marking the main focus of cold air advection. A relative TPW maximum of 40-50 kg/m^2 corresponds well to the position of the surface front.

Figure 92 depicts the mature phase of the CACS. The cyclone has continued to intensify over the last 24-36 h, and the cold front now extends NE-SW across the

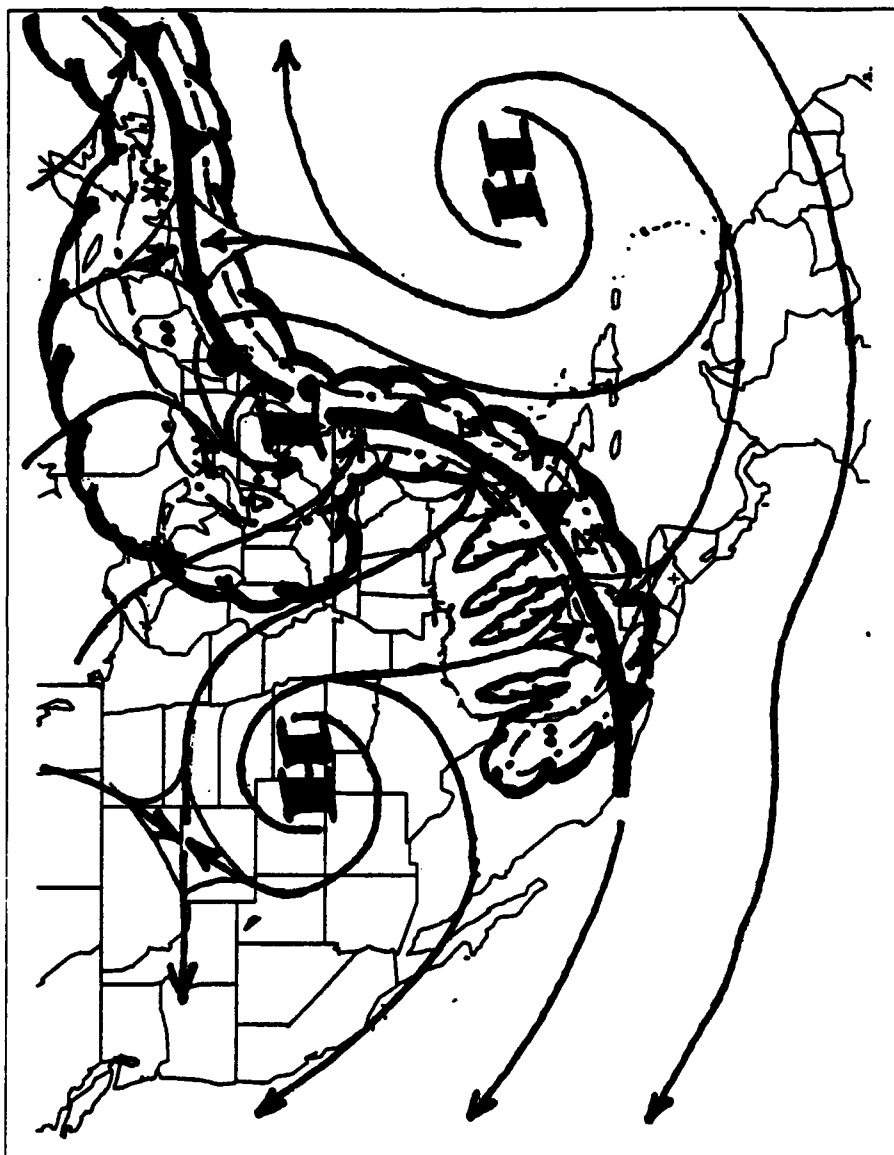


Figure 91. The Central American Cold Surge: Phase 2.

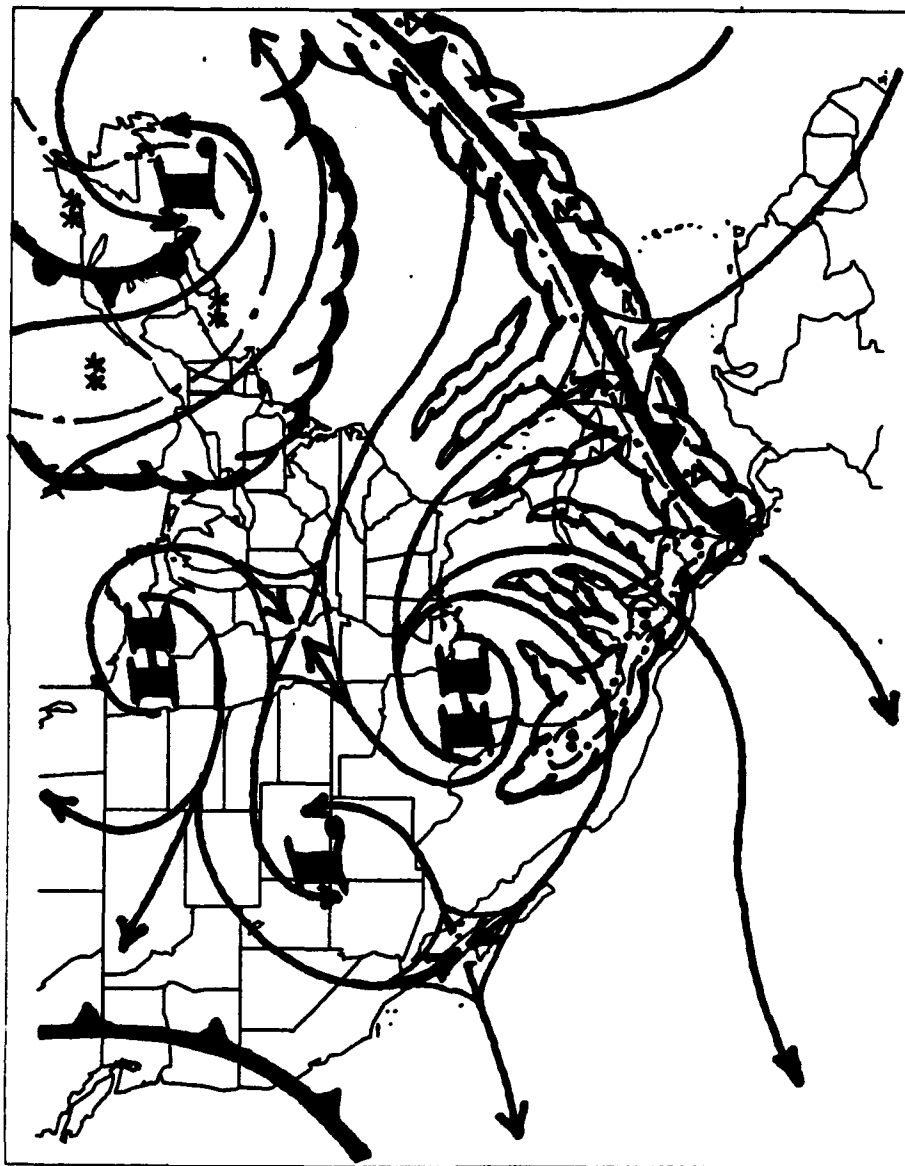


Figure 92. The Central American Cold Surge: Phase 3.

central Caribbean and into southern Central America. Strong north-northeasterly winds now dominate across the entire Gulf of Mexico, northern Caribbean and all areas of Central America north of the surface front. Cloud streets are still evident across the southern Gulf of Mexico into the Gulf of Honduras in the stable air behind the front. Thick stratocumulus is now evident banked up against the Caribbean side of the higher terrain features from central Mexico through Nicaragua, and orographic lifting of the modified cold air mass is generating stratiform precipitation especially across northern Honduras. All reporting stations behind the front on the Caribbean side of the Central American continental divide have experienced a drop in temperature and dew point, a wind shift to the north or northwest, an increase in wind speed, a sharp rise in SLP, an increase in cloud cover and decrease in cloud ceiling height, and light to moderate precipitation. Stable conditions and scattered cloud cover dominate on the Atlantic side of the continental divide. Rainshowers and thunderstorms are no longer occurring along the southern end of the cold front as the atmosphere is stable across the entire Central American and Caribbean region. The front has disrupted the trade wind inversion, but a weak frontal inversion is still evident. The subtropical jet is still strong. TPW values have dropped to near 20 kg/m^2 over the entire Gulf of Mexico and the relative TPW maximum still corresponds to the position of the surface front.

After three to four days, the southern end of the cold front weakens sufficiently to allow the subtropical high to build back into the Caribbean. East-northeast trade wind flow is re-established over Central America marking CACS termination (Fig. 93). Stable conditions and scattered cloud cover dominate the region, now under the trade wind inversion. A new cold front is moving across the central U.S., with a wave developing along the southern end of the front. TPW values have returned to their pre-CACS levels, but a surge of higher TPW values is evident moving into the southern

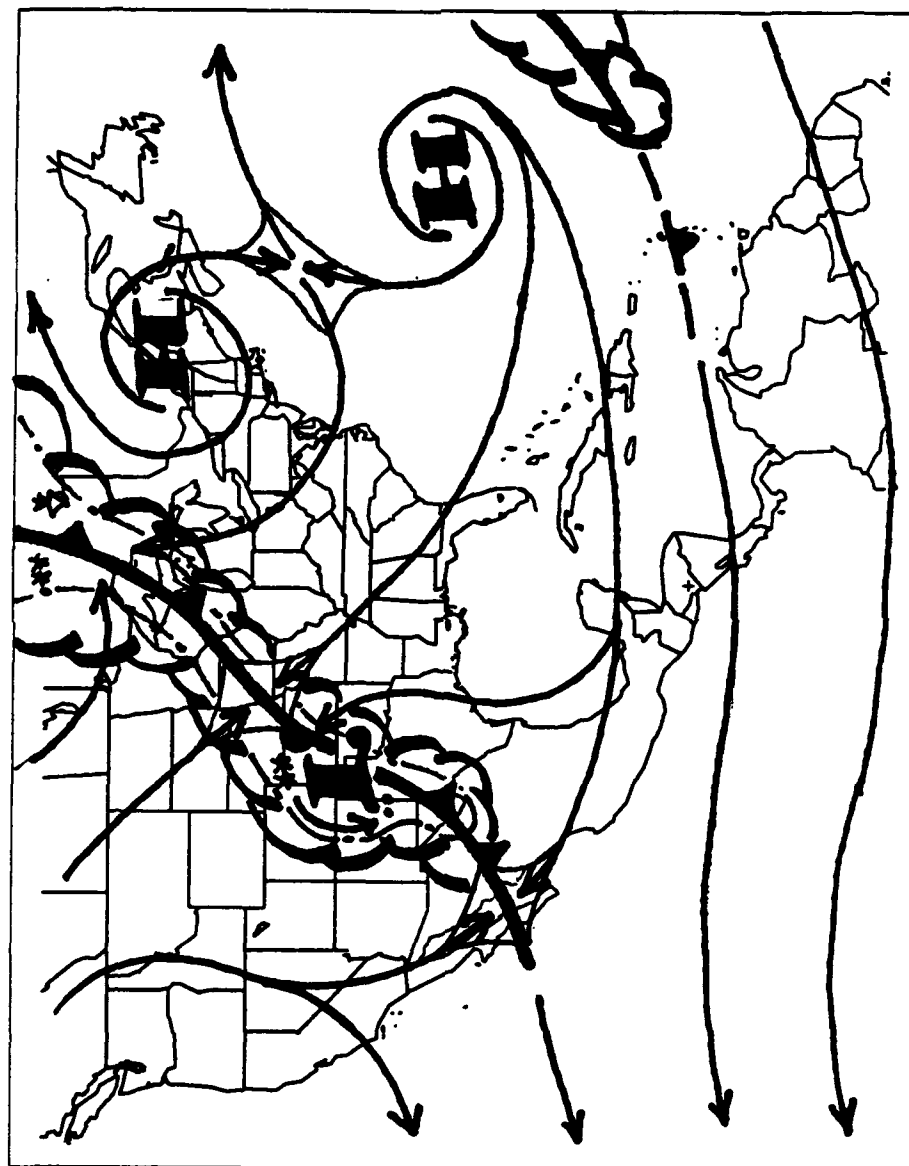


Figure 93. The Central American Cold Surge: Phase 4.

Gulf of Mexico in advance of the next CACS.

CHAPTER VIII

SUMMARY AND DISCUSSION

Several data sources were examined to quantify the occurrence and structure of cold surge events in Central America. Surface observations from Merida, Mexico and GOES satellite imagery were analyzed to construct a quantitative CACS definition. The definition was applied to an eleven winter season surface data base to determine the frequency and relative strength of CACS events. GOES imagery was analyzed to quantify the duration and southward penetration of CACS events.

Surface observations, upper air observations, and SSM/I and SMMR brightness temperature data were examined to quantify the horizontal, vertical and temporal structural characteristics of CACS events. Surface observations were analyzed to isolate and quantify the response of surface variables to CACS onset, and identify those variables most sensitive to CACS onset. Upper air observations were used to construct temporal cross sections and quantify the vertical structure of the pre- and post-CACS atmosphere. Satellite brightness temperatures were used to estimate TPW and rain rate. These products were analyzed to evaluate the temporal and spatial structure of the moisture field associated with CACS events.

Several typical and extreme cold surge events were studied in-depth to document the evolution and effects of CACS events as they progress through Central America. The climatology, structure and evolution of cold surge events were used to illustrate the life cycle of synoptic features associated with the CACS.

The main results of this study are summarized here. Two criteria were developed to define the CACS:

a. A decrease in daily maximum temperature greater than or equal to 4°C within 48 h at Merida, Mexico.

b. Northerly winds (300° - 030°) sustained for more than 24 h during the same period.

Based on this definition, North American cold fronts were found to penetrate into Central America at least 25% more frequently than was previously thought. CACS events occurred an average of 16 times annually. The minimum annual frequency was 11 events during the 1988-1989 winter season. The maximum annual frequency was 21 events during the 1982-1983 winter season. The monthly distribution of CACS events was found to be similar to the results of DiMego et al. (1976).

The mean temperature change associated with CACS onset at Merida, Mexico ranged from 4.7°C during the 1987-1988 winter season to 6.9°C during the 1983-1984 and 1987-1988 (El Nino) winter seasons. The maximum 48 h temperature change was 17°C during a CACS event in March 1989.

The mean CACS event duration ranged from 3.6 days during the 1982-1983 winter season to 6.3 days during the 1988-1989 winter season. The maximum duration was 13 days during a CACS event in October 1987.

The maximum southward penetration of North American cold fronts was found to be 7°N, approximately 200 km farther south than was previously known. The frequency of deep southward penetration was found to be over three times greater than current estimates. Over 76% of the CACS events studied penetrated south of 15°N, and 26% penetrated south of 10°N.

All surface variables at Belize City, Belize, except wind speed displayed a consistent and distinct CACS signature. A wind shift to the north, increase in cloud cover and decrease in cloud ceiling height, and sharp rise in sea level pressure were the most

distinct responses to frontal passage. Changes in temperature, dew point and precipitation were less pronounced. Cold surges generate 70-90% of Central America's winter season precipitation. Results were consistent with those of Horvath and Henry (1980).

The vertical structure of the pre-and post CACS atmosphere displayed unique features in each case studied. The most common feature was an increase in the depth of the moist layer after frontal passage.

The temporal and spatial TPW structure exhibited very distinct and consistent CACS signatures. TPW values greater than 45 kg/m² surged northward into the Gulf of Mexico immediately before the surface front entered the Gulf. TPW plummeted to below 20 kg/m² in the region of strongest cold air advection. The position of the surface front corresponded well to a relative TPW maximum through the duration of the cold surge.

The in-depth case studies yielded two important results. First, North American cold fronts can be easily and accurately tracked through Central America using satellite data and surface observations. Finally, CACS events can maintain a frontal temperature and density discontinuity throughout their life cycle, even into extreme southern Central America.

The objectives of this research were accomplished. A quantitative CACS definition was developed and the frequency, duration and meridional extent of the CACS was defined. The horizontal, vertical and temporal structural characteristics of the CACS were identified and quantified. The evolution of cold surge events progressing through Central America was documented.

Several recommendations for further study are presented here:

- Raw surface and upper air observations from Central America are not consistent and were often missing during CACS events. Therefore, alternative data sources such as satellite observations should be exploited whenever possible.
- A more detailed analysis of CACS events will be possible and should be attempted when the NMC extends its gridded data all the way to Panama.
- Examine the response of the general circulation to CACS events. Again, this will depend on the availability of appropriate data.
- Complete a study of CACS forecastability. A method for forecasting cold fronts into Honduras was developed by Brooks (1987), but is based on limited data and is relatively untested.

REFERENCES

- Anderson, R. K., and A. H. Smith, 1969: Application of Meteorological Satellite Data in Analysis and Forecasting. AWS/TR-212, Air Weather Service, Scott AFB, Illinois, 320 pp.
- Atkinson, G. D., 1971: Forecaster's Guide to Tropical Meteorology. AWS/TR-240, Air Weather Service, Scott AFB, Illinois, 347 pp.
- Boyle, J. S., and T. C. Chen, 1987: Synoptic aspects of the wintertime East Asian monsoon. *Monsoon Meteorology*, C.-P. Chang, and T.N. Krishnamurti, Eds., Oxford University Press, 125-160.
- Brooks, B. H., 1987: Forecasting the "Atemporalado" in Honduras. AWS/FM-87/001, Air Weather Service, Scott AFB, Illinois, 9 pp.
- Chapel, L. T., 1927: Winds and storms on the isthmus of Panama. *Mon. Wea. Rev.*, **55**, 519-530.
- DiMego, G. J., L. F. Bosart, and G. W. Enderson, 1976: An examination of the frequency and mean conditions surrounding frontal incursions into the Gulf of Mexico and Caribbean Sea. *Mon. Wea. Rev.*, **104**, 709-718.
- Fermor, J. H., 1971: The weather during northers at Kingston, Jamaica. *J. Trop. Geogr.*, **32**, 31-37.
- Fink, J. D., 1989: Tropical synoptic scale moisture fields observed from the Nimbus-7 SMMR. M.S. Thesis, Dept. of Meteorology, Texas A&M University, 74 pp.

- Garbel, M. A., 1947: *Tropical and Equatorial Meteorology*. Pitman, 237 pp.
- Guard, C. P., 1986: Local and Regional Influences on the Meteorology of Central America. AWS/FM-86/002, Air Weather Service, Scott AFB, Illinois, 23 pp.
- Hastenrath, S. L., 1967: Rainfall distribution and regime in Central America. *Arch. Meteor. Geophys. Bioklim.*, **B15**, 201-241.
- , 1988: *Climate and Circulation of the Tropics*. Reidel, 455 pp.
- Henry, W. K., 1979: Some aspects of the fate of cold fronts in the Gulf of Mexico. *Mon. Wea. Rev.*, **107**, 1078-1083.
- Hill, J. B., 1969: Temperature variability and synoptic cold fronts in the winter climate of Mexico. Climatological Research Series, No. 4, McGill University, Dept. of Geography, Montreal, 71 pp.
- Horvath, N. C., and W. K. Henry, 1980: Some aspects of cold fronts in Belize. *Nat. Wea. Dig.*, **5**, 25-32.
- Hurd, W. E., 1929: Northers in the Gulf of Tehuantepec. *Mon. Wea. Rev.*, **57**, 192-194.
- Huschke, R. E., Ed., 1959: *Glossary of Meteorology*. American Meteorological Society, 638 pp.
- Johnson, R. H., and R. A. Houze, 1987: Precipitating cloud systems of the Asian monsoon. *Monsoon Meteorology*, C.-P. Chang, and T.N. Krishnamurti, Eds., Oxford University Press, 298-353.

- Ladd, J. W., and W. K. Henry, 1980: An examination of some indicators of frontal passage in coastal Honduras. *Nat. Wea. Dig.*, **5**, 2-7.
- Lau, N. -C., and K. -M Lau, 1984: The structure and energetics of midlatitude disturbances accompanying cold-air outbreaks over East Asia. *Mon. Wea. Rev.*, **112**, 1309-1327.
- Murakami, T., 1987: Effects of the Tibetan Plateau. *Monsoon Meteorology*, C.-P. Chang, and T.N. Krishnamurti, Eds., Oxford University Press, 235-270.
- Palmer, C. E., C. W. Wise, L. J. Stempson, and G. H. Duncan, 1955: The Practical Aspect of Tropical Meteorology. AWS/TR-241 Vol. I, Air Weather Service, Scott AFB, Illinois, 195 pp.
- Parmenter, F. C., 1970: Picture of the month - A 'Tehuantepecer.' *Mon. Wea. Rev.*, **98**, 479.
- Pearson, D. C., M. Michel-Howel, C. S. Strager, and C. H. Larcomb, 1987: Seasons in Review: GOES Satellite Photos over Central America. 5WW/FM-87/006, 5th Weather Wing, Langley AFB, Virginia, 78 pp.
- Portig, W. H., 1958: Frontdurchgang in Mittlamerika. *Meteorologische Rundschau*, **11**, 112-116.
- , 1976: The climate of Central America. *World Survey of Climatology Volume 12*, W.Schwerdtfeger, Ed., Elsevier, 405-478.
- Ramage, C.S., 1971: *Monsoon Meteorology*. Academic Press, 296 pp.

- Schumann, T. E. W., and M. P. van Rooy, 1951: Frequency of fronts in the Northern Hemisphere. *Arch. Meteor. Geophys. Bioklim.*, **A4**, 87-97.
- Snow, J. W., 1976: The climate of northern South America. *World Survey of Climatology Volume 12*, W. Schwerdtfeger, Ed., Elsevier, 295-404.
- Whiteside, T. J., 1985: Central American Climatology. USAFETAC/TN-85/002, USAF Environmental Technical Applications Center, Scott AFB, Illinois, 154 pp.
- Wilheit, T. T., and A. T. C. Chang, 1980: An algorithm for retrieval of ocean surface and atmospheric parameters from the observations of the scanning multichannel microwave radiometer. *Radio Science*, **15**, 525-544.

APPENDIX A

INDIVIDUAL CACS EVENT STATISTICS

Table 3. CACS event statistics for the 1979-1980 winter season.

EVENT #	ONSET DATE	DURATION	MAXIMUM SOUTHERN INTRUSION	ΔT MERIDA, MEXICO
1	24 OCT 79	5 DAYS	13° N	N/A
2	1 NOV 79	3 DAYS	10° N	N/A
3	12 NOV 79	6 DAYS	14° N	5° C
4	28 NOV 79	8 DAYS	15° N	6° C
5	16 DEC 79	6 DAYS	9° N	7° C
6	25 DEC 79	3 DAYS	13° N	5° C
7	31 DEC 79	4 DAYS	11° N	4° C
8	4 JAN 80	4 DAYS	13° N	4° C
9	13 JAN 80	3 DAYS	16° N	4° C
10	23 JAN 80	2 DAYS	14° N	N/A
11	1 FEB 80	5 DAYS	8° N	10° C
12	10 FEB 80	3 DAYS	16° N	5° C
13	17 FEB 80	3 DAYS	13° N	12° C
14	25 FEB 80	3 DAYS	14° N	10° C
15	2 MAR 80	3 DAYS	8° N	12° C

Table 4. CACS event statistics for the 1980-1981 winter season.

EVENT #	ONSET DATE	DURATION	MAXIMUM SOUTHERN INTRUSION	ΔT MERIDA, MEXICO
1	3 OCT 80	9 DAYS	16° N	6° C
2	31 OCT 80	2 DAYS	19° N	4° C
3	18 NOV 80	3 DAYS	14° N	N/A
4	27 NOV 80	5 DAYS	13° N	9° C
5	12 DEC 80	3 DAYS	13° N	5° C
6	17 DEC 80	8 DAYS	8° N	4° C
7	26 DEC 80	5 DAYS	16° N	4° C
8	2 JAN 81	6 DAYS	10° N	N/A
9	11 JAN 81	5 DAYS	7° N	8° C
10	16 JAN 81	5 DAYS	7° N	4° C
11	21 JAN 81	6 DAYS	7° N	N/A
12	2 FEB 81	5 DAYS	10° N	7° C
13	11 FEB 81	5 DAYS	13° N	10° C
14	23 FEB 81	3 DAYS	16° N	N/A
15	16 MAR 81	2 DAYS	16° N	N/A
16	19 MAR 81	2 DAYS	11° N	N/A
17	22 MAR 81	2 DAYS	14° N	N/A

Table 5. CACS event statistics for the 1981-1982 winter season.

EVENT #	ONSET DATE	DURATION	MAXIMUM SOUTHERN INTRUSION	ΔT MERIDA, MEXICO
1	19 OCT 81	2 DAYS	16° N	8° C
2	6 NOV 81	2 DAYS	11° N	N/A
3	11 NOV 81	7 DAYS	10° N	N/A
4	21 NOV 81	2 DAYS	16° N	N/A
5	3 DEC 81	10 DAYS	7° N	4° C
6	15 DEC 81	2 DAYS	16° N	N/A
7	18 DEC 81	5 DAYS	8° N	4° C
8	4 JAN 82	2 DAYS	16° N	4° C
9	14 JAN 82	3 DAYS	13° N	14° C
10	25 JAN 82	6 DAYS	13° N	5° C
11	1 FEB 82	1 DAY	17° N	4° C
12	22 FEB 82	1 DAY	14° N	5° C
13	27 FEB 82	4 DAYS	13° N	6° C
14	7 MAR 82	3 DAYS	13° N	10° C

Table 6. CACS event statistics for the 1982-1983 winter season.

EVENT #	ONSET DATE	DURATION	MAXIMIM SOUTHERN INTRUSION	ΔT MERIDA, MEXICO
1	16 OCT 82	3 DAYS	16° N	5° C
2	4 NOV 82	8 DAYS	11° N	5° C
3	12 DEC 82	3 DAYS	14° N	8° C
4	16 DEC 82	6 DAYS	8° N	6° C
5	2 JAN 83	8 DAYS	14° N	7° C
6	11 JAN 83	11 DAYS	8° N	6° C
7	17 JAN 83	4 DAYS	14° N	4° C
8	20 JAN 83	11 DAYS	13° N	4° C
9	27 JAN 83	4 DAYS	10° N	N/A
10	2 FEB 83	3 DAYS	14° N	6° C
11	7 FEB 83	3 DAYS	14 N	4° C
12	10 FEB 83	6 DAYS	7° N	N/A
13	16 FEB 83	6 DAYS	11° N	7° C
14	23 FEB 83	3 DAYS	16° N	5° C
15	26 FEB 83	5 DAYS	11° N	N/A
16	8 MAR 83	N/A	N/A	7° C
17	11 MAR 83	N/A	N/A	6° C
18	15 MAR 83	N/A	N/A	4° C
19	21 MAR 83	N/A	N/A	8° C
20	28 MAR 83	N/A	N/A	7° C
21	31 MAR 83	N/A	N/A	N/A

Table 7. CACS event statistics for the 1983-1984 winter season.

EVENT #	ONSET DATE	DURATION	MAXIMUM SOUTHERN INTRUSION	ΔT MERIDA, MEXICO
1	1 OCT 83	10 DAYS	16° N	N/A
2	23 OCT 83	7 DAYS	14° N	8° C
3	11 NOV 83	4 DAYS	14° N	4° C
4	16 NOV 83	4 DAYS	14° N	5° C
5	25 NOV 83	2 DAYS	17° N	6° C
6	7 DEC 83	2 DAYS	19° N	5° C
7	12 DEC 83	2 DAYS	16° N	4° C
8	15 DEC 83	2 DAYS	17° N	4° C
9	25 DEC 83	4 DAYS	11° N	8° C
10	29 DEC 83	12 DAYS	7° N	5° C
11	10 JAN 84	7 DAYS	13° N	7° C
12	19 JAN 84	4 DAYS	14° N	10° C
13	27 JAN 84	4 DAYS	16° N	7° C
14	4 FEB 84	8 DAYS	13° N	7° C
15	14 FEB 84	1 DAY	14° N	N/A
16	21 FEB 84	4 DAYS	16° N	8° C
17	27 FEB 84	7 DAYS	8° N	8° C
18	6 MAR 84	6 DAYS	13° N	12° C
19	20 MAR 84	2 DAYS	13° N	9° C
20	28 MAR 84	3 DAYS	15° N	9° C

Table 8. CACS event statistics for the 1984-1985 winter season.

EVENT #	ONSET DATE	DURATION	MAXIMUM SOUTHERN INTRUSION	ΔT MERIDA, MEXICO
1	1 OCT 84	3 DAYS	13° N	N/A
2	6 NOV 84	3 DAYS	8° N	4° C
3	12 NOV 84	5 DAYS	12° N	4° C
4	20 NOV 84	5 DAYS	7° N	8° C
5	7 DEC 84	5 DAYS	12° N	7° C
6	3 JAN 85	7 DAYS	8° N	11° C
7	19 JAN 85	7 DAYS	11° N	8° C
8	8 FEB 85	2 DAYS	15° N	5° C
9	11 FEB 85	6 DAYS	13° N	10° C
10	15 FEB 85	2 DAYS	9° N	5° C
11	17 MAR 85	4 DAYS	13° N	4° C
12	21 MAR 85	2 DAYS	16° N	5° C

Table 9. CACS event statistics for the 1985-1986 winter season.

EVENT #	ONSET DATE	DURATION	MAXIMUM SOUTHERN INTRUSION	ΔT MERIDA, MEXICO
1	3 NOV 85	7 DAYS	9° N	6° C
2	2 DEC 85	6 DAYS	16° N	4° C
3	14 DEC 85	6 DAYS	14° N	6° C
4	19 DEC 85	4 DAYS	16° N	4° C
5	25 DEC 85	4 DAYS	13° N	4° C
6	9 JAN 86	10 DAYS	7° N	6° C
7	19 JAN 86	4 DAYS	16° N	N/A
8	23 JAN 86	3 DAYS	13° N	N/A
9	26 JAN 86	5 DAYS	8° N	7° C
10	12 FEB 86	3 DAYS	14° N	4° C
11	24 FEB 86	4 DAYS	8° N	8° C
12	1 MAR 86	3 DYAS	8° N	N/A
13	21 MAR 86	10 DAYS	8° N	13° C

Table 10. CACS event statistics for the 1986-1987 winter season.

EVENT #	ONSET DATE	DURATION	MAXIMUM SOUTHERN INTRUSION	ΔT MERIDA, MEXICO
1	17 OCT 86	4 DAYS	14° N	4° C
2	27 OCT 86	5 DAYS	14° N	N/A
3	28 NOV 86	4 DAYS	12° N	5° C
4	2 DEC 86	7 DAYS	14° N	N/A
5	4 DEC 86	5 DAYS	11° N	N/A
6	12 DEC 86	2 DAYS	15° N	5° C
7	23 DEC 86	4 DAYS	15° N	5° C
8	27 DEC 86	3 DAYS	18° N	7° C
9	31 DEC 86	4 DAYS	8° N	N/A
10	4 JAN 87	6 DAYS	7° N	6° C
11	11 JAN 87	4 DAYS	14° N	7° C
12	19 JAN 87	2 DAYS	16° N	10° C
13	22 JAN 87	5 DAYS	8° N	6° C
14	25 JAN 87	7 DAYS	8° N	N/A
15	6 FEB 87	9 DAYS	7° N	9° C
16	16 FEB 87	4 DAYS	15° N	6° C
17	1 MAR 87	10 DAYS	13° N	5° C
18	12 MAR 87	4 DAYS	10° N	8° C
19	23 MAR 87	2 DAYS	18° N	5° C
20	30 MAR 87	6 DAYS	11° N	9° C

Table 11. CACS event statistics for the 1987-1988 winter season.

EVENT #	ONSET DATE	DURATION	MAXIMUM SOUTHERN INTRUSION	ΔT MERIDA, MEXICO
1	1 OCT 87	13 DAYS	14° N	N/A
2	28 OCT 87	6 DAYS	8° N	4° C
3	5 NOV 87	3 DAYS	16° N	4° C
4	10 NOV 87	5 DAYS	12° N	N/A
5	20 NOV 87	6 DAYS	14° N	4° C
6	30 NOV 87	8 DAYS	9° N	6° C
7	16 DEC 87	3 DAYS	14° N	N/A
8	29 DEC 87	5 DAYS	14° N	7° C
9	2 JAN 88	5 DAYS	14° N	4° C
10	9 JAN 88	5 DAYS	15° N	5° C
11	21 JAN 88	4 DAYS	14° N	5° C
12	25 JAN 88	9 DAYS	8° N	N/A
13	6 FEB 88	4 DAYS	14° N	N/A
14	11 FEB 88	4 DAYS	14° N	N/A
15	19 FEB 88	N/A	N/A	4° C
16	26 FEB 88	N/A	N/A	N/A
17	10 MAR 88	2 DAYS	14° N	N/A
18	14 MAR 88	6 DAYS	13° N	4° C
19	19 MAR 88	6 DAYS	13° N	N/A

Table 12. CACS event statistics for the 1988-1989 winter season.

EVENT #	ONSET DATE	DURATION	MAXIMUM SOUTHERN INTRUSION	ΔT MERIDA, MEXICO
1	8 OCT 88	11 DAYS	16° N	N/A
2	6 NOV 88	1 DAY	16° N	4° C
3	22 NOV 88	5 DAYS	12° N	5° C
4	28 NOV 88	11 DAYS	13° N	5° C
5	12 DEC 88	5 DAYS	13° N	7° C
6	16 DEC 88	6 DAYS	9° N	N/A
7	21 JAN 89	10 DAYS	13° N	6° C
8	9 FEB 89	4 DAYS	14° N	4° C
9	22 FEB 89	7 DAYS	7° N	11° C
10	6 MAR 89	7 DAYS	7° N	17° C
11	22 MAR 89	2 DAYS	15° N	4° C

Table 13. CACS event statistics for the 1989-1990 winter season.

EVENT #	ONSET DATE	DURATION	MAXIMUM SOUTHERN INTRUSION	ΔT MERIDA, MEXICO
1	19 OCT 89	8 DAYS	13° N	8° C
2	17 NOV 89	2 DAYS	20° N	4° C
3	24 NOV 89	1 DAY	20° N	4° C
4	30 NOV 89	8 DAYS	13° N	5° C
5	8 DEC 89	4 DAYS	10° N	N/A
6	13 DEC 89	3 DAYS	14° N	7° C
7	22 DEC 89	8 DAYS	7° N	15° C
8	9 JAN 90	1 DAY	20° N	6° C
9	12 JAN 90	4 DAYS	14° N	5° C
10	26 JAN 90	3 DAYS	18° N	8° C
11	5 FEB 90	2 DAYS	18° N	4° C
12	11 FEB 90	3 DAYS	14° N	5° C
13	23 FEB 90	6 DAYS	13° N	10° C
14	3 MAR 90	2 DAYS	14° N	4° C
15	17 MAR 90	8 DAYS	13° N	12° C

VITA

Captain Philip John Reding, son of Mr. and Mrs. James J. Reding, was born and raised in Monticello, Iowa. He graduated from Monticello Central High School in 1981. Phil attended Loras College in Dubuque, Iowa for two years, and went on to earn his B.S. in Meteorology at Iowa State University in 1986. Upon graduation, he was commissioned a Second Lieutenant in the United States Air Force.

Phil's first assignment was to Dyess AFB, Texas, where he served as Forecaster and SAC Wing Weather Officer to the 96th Bomb Wing. In July 1988, he was reassigned to Headquarters, United States Southern Command (USSOUTHCOM), Quarry Heights, Panama and served as Forecast Officer for the USSOUTHCOM Forecast Unit. His tour included participation in Operation JUST CAUSE, the restoration of democracy to the Republic of Panama. Phil later married the former Erika Alvarez-Vasquez of Panama City, Panama.

While in Panama, Phil was selected to pursue his Masters degree in meteorology through the Air Force Institute of Technology, and enrolled at Texas A&M University in August, 1990. His academic awards include membership in *Who's Who Among Students at American Universities and Colleges*, and the *Sigma Gamma Epsilon* and *Chi Epsilon Pi* honor societies.

Phil's permanent address is 643 Hillcrest Drive, Monticello, Iowa, 52310.

Color copies of all Total Precipitable Water (TPW) and Rain Rate figures are available at the following addresses:

Dr. James P. McGuirk
Department of Meteorology
College of Geosciences and Maritime Studies
Texas A&M University
College Station, TX 77843
(409) 845-4431

Capt Phil Reding
Det. 4, HQ AWS
Bldg. 91027
595 Independence Rd
Hurlburt Field, FL 32544-5618
Comm: (904) 884-5730
DSN: 579-5730

END